ВЕСТНИК ТРАНСПЛАНТОЛОГИИ И ИСКУССТВЕННЫХ ОРГАНОВ

VESTNIK TRANSPLANTOLOGII I ISKUSSTVENNYKH ORGANOV

RUSSIAN JOURNAL OF TRANSPLANTOLOGY AND ARTIFICIAL ORGANS

УЧРЕДИТЕЛЬ: ОБЩЕРОССИЙСКАЯ ОБЩЕСТВЕННАЯ ОРГАНИЗАЦИЯ ТРАНСПЛАНТОЛОГОВ «РОССИЙСКОЕ ТРАНСПЛАНТОЛОГИЧЕСКОЕ ОБЩЕСТВО»

THE OFFICIAL JOURNAL OF ALL-RUSSIAN PUBLIC ORGANIZATION OF TRANSPLANTOLOGISTS "RUSSIAN TRANSPLANT SOCIETY"

2024. Том XXVI. № 2

2024. Vol. XXVI. № 2

Научно-практический журнал основан в 1999 г.
Регистр. № 018616

Scientific and Practical Journal was founded in 1999
Reg. № 018616

Журнал «Вестник трансплантологии и искусственных органов» включен ВАК РФ в перечень российских рецензируемых научных изданий, в которых должны быть опубликованы результаты диссертационных работ

Журнал «Вестник трансплантологии и искусственных органов» включен ФГБУ «НМИЦ ТИО им. ак. В.И. Шумакова» Минздрава России в перечень российских рецензируемых научных изданий, в которых должны быть опубликованы основные результаты исследований в рамках диссертаций, представляемых к защите в диссертационный совет ФГБУ «НМИЦ ТИО им. ак. В.И. Шумакова» Минздрава России

Журнал «Вестник трансплантологии и искусственных органов» индексируется в Scopus и размещен на платформе Web of Science Core Collection: Emerging Science Citation Index

"Russian Journal of Transplantology and Artificial Organs" is included in the list of leading peer-reviewed scientific publication editions, produced in the Russian Federation and is recommended for publication of primary results of dissertation research

"Russian Journal of transplantology and artificial organs" is included by the Federal State Budgetary Institution "Shumakov National Medical Research Center of Transplantology and Artificial Organs" of the Ministry of Health of Russia in the list of Russian peer-reviewed scientific publications in which the main results of research should be published within the framework of dissertations submitted for defense to the dissertation council of Shumakov National Medical Research Center of Transplantology and Artificial Organs

"Russian Journal of Transplantology and Artificial Organs" is indexed in Scopus and in the Emerging Science Citation Index of the Web of Science Core Collection

ISSN 1995-1191

Адрес для корреспонденции:

Россия, 123182, Москва, ул. Щукинская, 1
Тел./факс +7 (499) 193 87 62
E-mail: vestniktranspl@gmail.com
Интернет-сайт журнала: http://journal.transpl.ru
Научная электронная библиотека: http://elibrary.ru

Address for correspondence:

1, Shchukinskaya st., Moscow 123182, Russia
Tel./Fax +7 (499) 193 87 62
E-mail: vestniktranspl@gmail.com
Journal's web site: http://journal.transpl.ru
Scientific eLibrary: http://elibrary.ru

Подписной индекс в каталоге почты России – ПН380

СОДЕРЖАНИЕ

CONTENTS

УЧЕБНИК «ТРАНСПЛАНТОЛОГИЯ И ИСКУССТВЕННЫЕ ОРГАНЫ»: ИЗДАНИЕ ВТОРОЕ, ПЕРЕРАБОТАННОЕ И ДОПОЛНЕННОЕ

Глубокоуважаемые коллеги!

В 2024 году увидит свет второе издание учебника «Трансплантология и искусственные органы». Первое издание учебника вышло в 2018 г., и его появление явилось значимой вехой в развитии как клинической медицины, так и высшего медицинского образования в нашей стране, обогатившегося еще одной новой дисциплиной в рамках специальности «лечебное дело».

Учебник подготовлен с учетом шестнадцатилетнего опыта преподавания этой дисциплины в ведущем медицинском вузе – Первом МГМУ им. И.М. Сеченова (Сеченовский университет), а также клинического и научного опыта ведущего трансплантологического центра нашей страны – ФГБУ «Национальный медицинский исследовательский центр трансплантологии и искусственных органов имени академика В.И. Шумакова» Минздрава России.

Трансплантология – быстро развивающаяся область клинической медицины. Структура и базовое содержание во втором издании учебника сохранены; актуализирована и дополнена информация с учетом произошедших за последние годы изменений. С каждым годом повышается доступность трансплантации жизненно важных органов как вида высокотехнологичной медицинской помощи. Число выполняемых в стране операций по трансплантации солидных органов за последние пять лет возросло на треть; центры трансплантации расположены в 38 субъектах РФ, в том числе в отдаленных регионах нашей страны. Клинические результаты трансплантации соответствуют уровню лучших мировых практик, с достижением полной физической и социальной реабилитации реципиентов, включая репродуктивную функцию и возможность рождения здоровых детей.

"TRANSPLANTOLOGY AND ARTIFICIAL ORGANS": SECOND EDITION, REVISED AND ENRICHED

Dear colleagues,

The second edition of the textbook "Transplantology and Artificial Organs" will be released in 2024. The first edition was published in 2018, marking a significant milestone in the development of both clinical medicine and higher medical education in our country, which was enriched with one more new discipline within the 'general medicine' specialty.

The textbook has been prepared taking into account our 16 years of experience in teaching this discipline at foremost medical university Sechenov University. The textbook also incorporates various clinical research experiences gained at Russia's leading transplant center, Shumakov National Medical Research Center of Transplantology and Artificial Organs, Moscow.

Transplantology is a rapidly developing field of clinical medicine. The second edition of the textbook has been revised and augmented to reflect changes that have occurred in recent years, while maintaining the structure and basic content. Transplantation of vital organs is increasingly becoming accessible every day as a type of high-tech healthcare. Over the past five years, the number of solid organ transplants performed in the nation has increased by one third; transplant centers can be found in 38 federal subjects of the Russian Federation, including in remote regions of our country. Clinical transplant outcomes at these centers so far are on par with the highest international standards. Organ recipients have been able to achieve full physical and social rehabilitation, including the ability to reproduce and have healthy children.

В связи с необходимостью постоянного увеличения числа трансплантаций органов в РФ, открытием новых трансплантологических центров подготовка врачей в области трансплантологии, а также получение знаний по трансплантологии и искусственным органам врачами различных специальностей имеют актуальное значение в системе высшего профессионального медицинского образования.

Авторы рассчитывают, что переработанное и дополненное второе издание учебника будет востребовано не только студентами, но также может оказать помощь в обучении молодых специалистов, врачей, ученых, аспирантов, так как содержит актуальную и полную информацию по основным разделам трансплантологии, искусственным органам, а также регенеративной медицине и созданию биоискусственных органов.

С уважением,
главный редактор
академик РАН С.В. Готье

Due to the need for a constant increase in the number of organ transplants in the Russian Federation, the establishment of new transplant centers, training of physicians in the field of transplantology, and acquisition of knowledge on transplantology and artificial organs by doctors of various specialties are all critically important in the higher professional medical education system.

The authors expect that the revised and supplemented second edition of the textbook will not only be in demand among students but also can assist in the training of young specialists, doctors, scientists, graduate students, as it contains current and comprehensive information on the key areas of transplantology, artificial organs, regenerative medicine and manufacture of bioartificial organs.

Sincerely,
Sergey Gautier,
Fellow, Russian Academy of Sciences
Editor-in-chief, Russian Journal
of Transplantology and Artificial Organs

DOI: 10.15825/1995-1191-2024-2-8-15

PREGNANCY AFTER KIDNEY TRANSPLANTATION: CLINICAL FEATURES, COMPLICATIONS AND OUTCOMES

E.I. Prokopenko[1, 2], I.G. Nikolskaya[2], A.V. Vatazin[1], F.F. Burumkulova[2], D.V. Gubina[1]

[1] Vladimirsky Moscow Regional Research and Clinical Institute, Moscow, Russian Federation
[2] Moscow Regional Research Institute of Obstetrics and Gynecology, Moscow, Russian Federation

Pregnancy after kidney transplantation (KT) has become more common, but the risk of complications and adverse obstetric outcomes in this group of women remains high. **Objective:** to study pregnancy complications and outcomes in kidney recipients and renal graft (RG) survival after childbirth. **Material and methods.** The study included 22 pregnancies in 20 women with RG (transplants performed in 2006–2020). The comparison group consisted of 20 healthy women who had 20 pregnancies. Frequency and nature of pregnancy complications, neonatal health indicators, and pregnancy outcomes were evaluated. Graft survival was compared in the main group and in a group of 102 women after KT who did not have pregnancies. **Results.** Compared with healthy women, RG recipients had a higher rate of preeclampsia (25% and 0%, $p = 0.047$), fetal growth restriction (30% and 0%, $p = 0.020$), gestational diabetes (40% and 5%, $p = 0.020$), asymptomatic bacteriuria (35% and 5%, $p = 0.044$), preterm birth (60% and 0%, $p < 0.001$), and cesarean section (70% and 10%, $p < 0.001$). Median gestational age and birth weight were significantly lower in women with RG: 36.0 [33.9; 37.4] vs. 38.9 [38.9; 39.6] weeks, $p < 0.001$, and 2405 [2023; 2958] *vs.* 3355 [3200; 3690] g, $p < 0.001$, respectively. The rate of favorable pregnancy outcomes after KT was 81.8%, or 90% when early pregnancy loss is excluded. Two children were found to have genetic diseases passed from the mother. Graft survival did not differ between RG recipients with and without pregnancy, $p = 0.272$. **Conclusions.** Pregnancy outcomes in patients with RG are generally favorable, pregnancy and childbirth do not affect graft survival. When planning pregnancy after KT, it is necessary to consider the risk of complications and the possibility of transmitting genetic disorders to offspring.

Keywords: kidney transplantation, immunosuppression, pregnancy, complications, pregnancy outcomes, renal graft survival.

INTRODUCTION

Kidney transplantation (KT) provides the highest level of medical and social rehabilitation for patients with stage 5 chronic kidney disease (CKD); it enables many renal graft (RG) patients, both men and women, to exercise reproductive function [1, 2].

Although the pregnancy rate in this cohort is several times lower than in the general population, incidents of pregnancy among patients of kidney transplants are becoming regular occurrences [3, 4]. In recent years, assisted reproductive technologies, including *in vitro* fertilization programs, have even been used in post-KT patients suffering from infertility [5, 6]. Nevertheless, despite a fairly high rate of live births (>70% in most studies), pregnancy in RG recipients is associated with increased risk of complications and adverse outcomes. For instance, in a 2019 meta-analysis, which included 6,712 pregnancies in 4,174 kidney transplant recipients, the rate of spontaneous miscarriage was 15.4%, 95% CI 13.8–17.2, stillbirth was 5.1%, 95% CI 4.0–6.5, and preeclampsia was 21.5%; 95% CI 18.5–24.9 (for comparison, the population incidence of preeclampsia is 2–5%), pregnancy-induced hypertension was 24.1%, 95% CI 18.1–31.5, cesarean section was 62.6%, 95% CI 57.6–67.3, preterm delivery 43.1%, 95% CI 38.7–47.6 [7]. Adverse pregnancy outcomes and complications have been shown to be associated with reduced RG function before conception, especially when combined with severe proteinuria [8, 9].

A critical issue is the possible impact of pregnancy and childbirth on RG function and survival. Both individual studies and a large meta-analysis featuring 43 studies showed that pregnancy have no significant influence on kidney graft survival, although the rate of serum creatinine elevation was slightly higher in the first 2 years after delivery compared with women who did not have pregnancies after KT [10, 11].

The aim of our study is to investigate pregnancy complications and outcomes in kidney transplant recipients, as well as graft survival after delivery.

MATERIALS AND METHODS

Our longitudinal observational study included the main group – 20 kidney transplant recipients (among them one woman with a kidney and pancreas transplant)

Corresponding author: Elena Prokopenko. Address: 61/2, Shchepkina str., Moscow, 129110, Russian Federation. Phone: (495) 681-55-85. E-mail: renalnephron@gmail.com

who had 22 pregnancies. The comparison group of pregnancy outcomes included 20 pregnancies in 20 healthy women; they did not differ from the post-KT pregnant women by age, body mass index, and number of pregnancies in medical history. A control group of 102 kidney recipients who had not become pregnant after KT and were comparable to the main group in terms of age, underlying disease (cause of end-stage chronic renal failure), and immunosuppressive therapy, was used to assess the effect of pregnancy and childbirth on renal graft survival.

Each pregnancy was treated as a separate case. Transplants were performed in 2006–2020 at different transplant centers. During pregnancy following KT, the patients were observed by a nephrologist and an obstetrician-gynecologist from the Moscow Regional Research Institute of Obstetrics and Gynecology.

All transplants were the first being performed on the patient. In 16 cases (80%), the KT was from a deceased donor (including kidney and pancreaticoduodenal complex transplantation), while 4 (20%) cases were transplantations from a living related donor. End-stage chronic renal failure was caused by the following: chronic glomerulonephritis (11 patients; 55%), congenital urinary anomalies (6; 30%), nephropathy of unknown origin (2 patients; 10%), and diabetic nephropathy resulting from type 1 diabetes (1; 5%). Mean age at the time of KT and at the time of delivery was 27.5 ± 6.7 years and 33.8 ± 5.5 years, respectively.

Twenty-one pregnancies were spontaneous, and one was achieved through *in vitro* fertilization. The first were 10 observed pregnancies, the second were 6, the third, fourth and fifth were 2 pregnancies each. At pregnancy onset, glomerular filtration rate (GFR) in the renal graft indicated stage 1 CKD in 5 (22.7%) cases, stage 2 in 9 cases (40.9%), stage 3 in 7 (31.8%), and stage 4 in a case (4.5%).

The patient with stage 4 CKD and creatinine level above 200 μmol/L before conception, according to Order 736 of the Ministry of Health and Social Development of the Russian Federation dated December 3, 2007, was indicated for early termination of pregnancy for medical reasons; however, the woman categorically insisted on prolonging the pregnancy and signed an official refusal to terminate it.

Another RG recipient, whose unplanned pregnancy occurred while taking teratogenic drug mycophenolate mofetil, was offered artificial abortion in the first trimester. She had a history of ischemic stroke with primary antiphospholipid syndrome, which sharply increased the risk of thrombotic complications during pregnancy. However, she also refused to terminate the pregnancy; the teratogenic drug was withdrawn in early gestation.

Artificial abortion at 20–21 weeks of gestation was offered to a woman whose second prenatal ultrasound screening revealed a serious fetal malformation – bilateral hydronephrosis with a high level of obstruction, suspected cystic dysplasia, and oligohydramnios, but the patient refused.

All pregnant women with a transplanted kidney were observed according to an individual protocol with the recommended frequency of visits to the doctor at least once every 2 weeks, self-monitoring of blood pressure (BP) and heart rate 4 times a day, monitoring of clinical blood count, daily proteinuria, serum creatinine at least once every 4 weeks in the first half of pregnancy and once every 14 days after the 20th week of gestation, urine microbiological examination at least once every 4 weeks, measuring tacrolimus/cyclosporine blood levels at least once every 2–3 weeks, kidney transplant ultrasound once every 6–8 weeks, fetal ultrasound with Doppler ultrasonography at least once every 4 weeks (more frequently if indicated) in the second half of pregnancy, determination of angiogenic coefficient sFlt-1/PlGF once every 4–5 weeks, use of global methods of assessing the hemostatic system – thromboelastography and thrombodynamics – if indicated. Daily blood pressure monitoring was done in addition to office standardized blood pressure measurements in case choosing antihypertensive therapy proved to be difficult. Current guidelines for the diagnosis of gestational diabetes mellitus (GDM) were followed [12].

In all patients after KT, mycophenolic acid medications were discontinued or replaced with azathioprine no later than 3 months before conception, considering their teratogenic and mutagenic effects, except for one case of unplanned pregnancy. ACE inhibitors, angiotensin receptor blockers, statins, urate-lowering medications (allopurinol, febuxostat), warfarin, direct oral anticoagulants, and other drugs that are prohibited for use during pregnancy were also discontinued at the planning stage.

During pregnancy, all RG recipients received corticosteroids in minimal doses (5–10 mg orally in terms of prednisolone) and a calcineurin inhibitor: tacrolimus was used in 17 (77.3%) cases, cyclosporine A in 5 out of 22 (22.7%). The third drug of the immunosuppressive therapy – azathioprine at a dose of 50 mg/day – was used in 12 out of 22 cases (54.5%). Any chronic hypertension was treated with drugs approved during pregnancy – methyldopa, dihydropyridine calcium channel blockers (long-acting nifedipine, amlodipine), selective beta-blockers (bisoprolol, nebivolol) – as monotherapy or in various combinations.

In patients with chronic hypertension, the target BP was considered 130/80–110/70 mmHg. All kidney recipients received folate, vitamin D (cholecalciferol), potassium iodide, and antiplatelet agents in pregnancy-recommended doses to prevent preeclampsia – acetylsalicylic acid 150 mg/day from the 13th to the 36th week of gestation (dipyridamole 225 mg/day in case of acetylsalicylic acid intolerance), and prophylactic doses of low-molecular-weight heparin throughout pregnancy

and 6–8 weeks postpartum to prevent thromboembolic and placenta-associated complications.

To treat anemia, oral or intravenous iron preparations were used; erythropoietin preparations were used in some cases of persistent anemia against the background of iron saturation and absence of folic acid and vitamin B_{12} deficiency.

The frequency and nature of pregnancy complications, neonatal health indicators, and pregnancy outcomes were assessed in women of both groups. An unfavorable outcome was considered to be artificial termination of a desired pregnancy early for medical reasons, antenatal, intranatal or postnatal fetal/newborn death, birth of a child with serious malformations or diseases leading to disability. A favorable obstetric outcome was defined as the birth of a live baby without significant developmental anomalies or hereditary diseases and the child's survival in the postpartum period.

Statistical data processing. Normally distributed values were presented as "mean ± standard deviation". Indicators with non-normal distribution were described as "median [first quartile; third quartile]"; qualitative indicators were presented in fractions (percent), or in absolute values. Indicators with distributions different from normal were compared using the Mann–Whitney U test for two independent samples. Fisher's exact test was used to assess the significance of differences in qualitative features (proportions in groups), and the Kaplan–Meier method was used to assess renal graft survival. The level of 0.05 was taken as the critical level of significance of differences.

RESULTS

The interval between child delivery and KT was quite significant – the median was 64.1 [49.5; 91.5] months, meaning that pregnancy occurred on average 5 years after transplantation. Compared to healthy women, pregnant women with transplanted kidneys had a significantly higher incidence of gestational complications, including preeclampsia, fetal growth restriction, GDM, anemia, and asymptomatic bacteriuria (ABU). Urinary tract infections were also more likely to occur (Table). Post-KT pregnancy had a higher incidence of both preterm birth in general (delivery before 37 weeks of gestation occurred in 60% of cases, 0% in the comparison group, $p < 0.001$) and delivery before 34 weeks of gestation (25% in the main group and 0% in the healthy group, $p = 0.047$). The reasons for premature birth were preeclampsia in 4 (33.3%) cases, signs of fetal distress (decompensated fetoplacental insufficiency) in 3 (25%), onset of labor in 2 (16.7%), prenatal amniotic fluid discharge in 1 (8.3%), progressive increase of proteinuria in 1 case, and reversible increase of serum creatinine in 1 case.

Patients with kidney transplants had significantly higher rates of surgical deliveries than healthy patients: the main group had 70% of caesarean sections, whereas the control group had 10%, or seven times less, $p < 0.001$.

Median delivery time, median absolute birth weight and percentile birth weight were significantly lower in the transplanted kidney group. Additionally, the children born required treatment in the intensive care unit more often.

There were no rejection crises or kidney graft losses during pregnancy. In addition to active urinary infection (which every fifth pregnant woman with a transplanted kidney had during pregnancy) and ABU, other infections

Table

Pregnancy complications and obstetric outcomes in women with a transplanted kidney and in healthy women

Indicator	Women after KT	Healthy women	p
Incidence of preeclampsia	5 (25%)	0 (0%)	0.047
Incidence of intrauterine growth restriction	6 (30%)	0 (0%)	0.020
Incidence of gestational diabetes mellitus	8 (40%)	1 (5%)	0.020
Incidence of anemia	17 (85%)	7 (35%)	0.003
Incidence of asymptomatic bacteriuria	7 (35%)	1 (5%)	0.044
Incidence of active urinary tract infection	4 (20%)	0 (0%)	0.106
Proportion of births before 37 weeks of gestation	12 (60%)	0 (0%)	<0.001
Proportion of births before 34 weeks of gestation	5 (25%)	0 (0%)	0.047
Rate of cesarean section	14 (70%)	2 (10%)	<0.001
Due date (weeks)*	36.0 [33.9; 37.4]	38.9 [38.9; 39.6]	<0.001
Children's body weight at birth (g)*	2405 [2023; 2958]	3355 [3200; 3690]	<0.001
Children's body weight at birth)%)*	45 [23; 58]	61 [42; 77]	0.045
Rate of newborn transfer to the ICU	9 (45%)	0 (0%)	0.001
Favorable pregnancy outcome**	18 (81.8%)	20 (100%)	0.109

Note: *, indicator is presented as median [Q1; Q3]; **, indicator is calculated for 22 cases (all pregnancies that occurred), all other indicators are calculated for 20 pregnancies that ended in childbirth.

were observed in this group during gestation: herpes simplex in 1 case, shingles, bacterial tonsillitis, acute bronchitis, and food poisoning in 1 case each. Two patients had mild COVID-19 during pregnancy, and one had asymptomatic COVID-19 infection (tested positive to nasopharyngeal swab test). The virus was detected to have replicative activity during pregnancy in one recipient with chronic hepatitis B infection; a hepatologist prescribed antiviral therapy – tenofovir alafenamide 25 mg/day – for the entire gestational period. In all, 11 out of 20 (55%) pregnancies that ended in childbirth had infectious complications.

Out of 22 pregnancies, 20 (90.9%) ended in childbirth, there were 2 (9.1%) cases of first trimester nondeveloping pregnancy. Live birth rate was 90.9%. One newborn girl with prenatally diagnosed serious urinary anomalies (parents refused to terminate pregnancy) and congenital renal failure died on day 3 of birth despite renal replacement therapy by peritoneal dialysis. The cause of death was pulmonary dysplasia. Another child (a girl) inherited from her mother a genetic disease – oral-facial-digital syndrome type I with an X-linked dominant inheritance – while no internal organ abnormalities were detected in the girl; the early adaptation period was generally favorable. Thus, despite the child surviving in the latter case, the pregnancy was classified as an unfavorable outcome; favorable outcomes were observed in 18 out of 22 (81.8%) pregnancies. If we do not take into account early pregnancy loss (before 13 weeks), which often occurs in the general population, the rate of favorable outcomes is 90% (18 out of 20 pregnancies that reached 20 weeks). Children born to mothers with a transplanted kidney grow and develop normally.

Separately, we studied the renal graft status at the current time point (December 2023) in patients who had a pregnancy and delivery (Fig. 1). Median follow-up time after delivery was 26.9 [13.2; 47.1] months. The majority (72.8%) of women continued to be followed up with a functioning RG, 18.2% of recipients left follow-up. One patient (4.5%) lost the graft and returned for dialysis 4 years after delivery, which resulted in a second unplanned pregnancy that became complicated by preeclampsia. One patient with a history of primary antiphospholipid syndrome and two strokes died with a functioning graft from a recurrent stroke 20 months after delivery with a favorable obstetric outcome.

We analyzed RG survival after delivery (Fig. 2). One-year graft survival rate after delivery was 100%, 2-year survival was 92.3%, and 5-year survival was 73.8%.

To evaluate the effect of pregnancy and delivery on RG survival (from the time of transplantation), we compared graft survival in the main group and in the control group (women with a transplanted kidney who had no pregnancies after KT) (Fig. 3).

It turned out that there was no significant difference in RG survival rate between the main and control groups, $p = 0.272$.

DISCUSSION

The rate of favorable pregnancy outcomes was high – 81.8% or 90% (when early losses are taken out of the picture). These rates are comparable with those arrived at by other researchers [1, 7, 8, 13], even though some of our patients were contraindicated to carry a pregnancy to term but refused to terminate it. The rates of preeclampsia, intrauterine growth restriction, preterm labor, and operative delivery were higher than in the general population, which is consistent with reports [7, 14, 15]. At the same time, average delivery time (36 [2023; 2958] weeks) and birth weight (2405 [2023; 2958] g) provided a favorable prognosis in most cases for newborn nursing.

The high incidence of GDM in our cohort of pregnant women – 40% – is noteworthy, which is higher than the 2–6% rate described in other studies on pregnancy complications after KT [7, 16]. Apparently, this difference is because we paid special attention to this pregnancy complication, taking into account the adverse effect of hyperglycemia on gestational outcomes, and we used modern diagnostic criteria, which may have contributed to improved GDM detection [12]. In all cases, it was early GDM, largely associated with the diabetogenic effect of immunosuppressive drugs – calcineurin inhibitors and corticosteroids.

Prevention and treatment of infectious complications play a significant role in achieving favorable pregnancy outcomes after KT. Incidence of these complications in

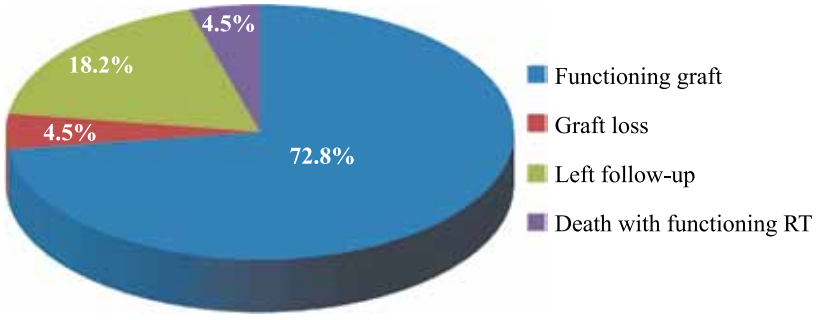

Fig. 1. Renal graft status after delivery

the pregnant women was quite high, 55%, but there were no severe infections. Urinary tract infection was the most common – in 7 out of 20 cases (35%) – and 4 pregnant women (20%) had both ABU and active infection. Active antibiotic treatment of all ABU episodes may have been important in preventing severe urinary infection.

In our study, there were no cases of acute graft rejection during pregnancy. This is probably due to the small size of our cohort. In a meta-analysis, the rate of rejection in pregnancy among 822 RG recipients was 9.4% (95% CI 6.4–13.7), which was comparable to the rate of rejection outside of pregnancy [7, 17]. Apparently, acute RG rejection is not a frequent pregnancy complication, especially with careful pharmacokinetic control and timely adjustment of immunosuppression, although the risk of rejection is still not zero, especially in the first 2–3 years after delivery.

It should be noted that most of the unfavorable outcomes occurred in unplanned pregnancies, when pregnancy was either contraindicated at all, or there were no clear contraindications but no pregravid preparation was carried out. A special problem is the possibility of the child inheriting a genetic disease from the mother. A patient with proven oral-facial-digital syndrome type I with an X-linked dominant inheritance and polycystic kidney disease, 50% risk of transmission regardless of sex, absolute mortality for male fetuses, was recommended (by a consilium with the participation of a geneticist) to get pregnant via IVF followed by preimplantation genetic testing in order to select female embryos with a favorable prognosis for the disease. However, the patient did not agree with the proposed tactics and became spontaneously pregnant, which resulted in transmission of the disease to the child. However, since the sex of the fetus

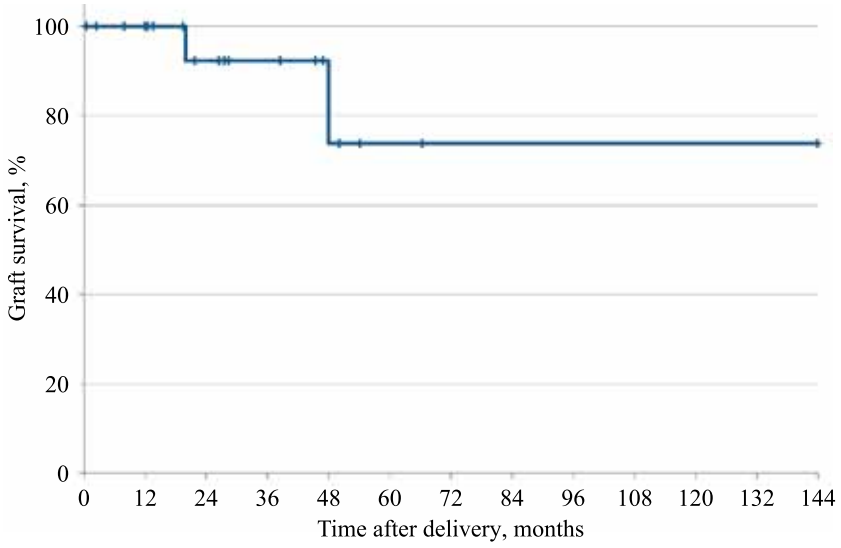

Fig. 2. Kidney graft survival after delivery

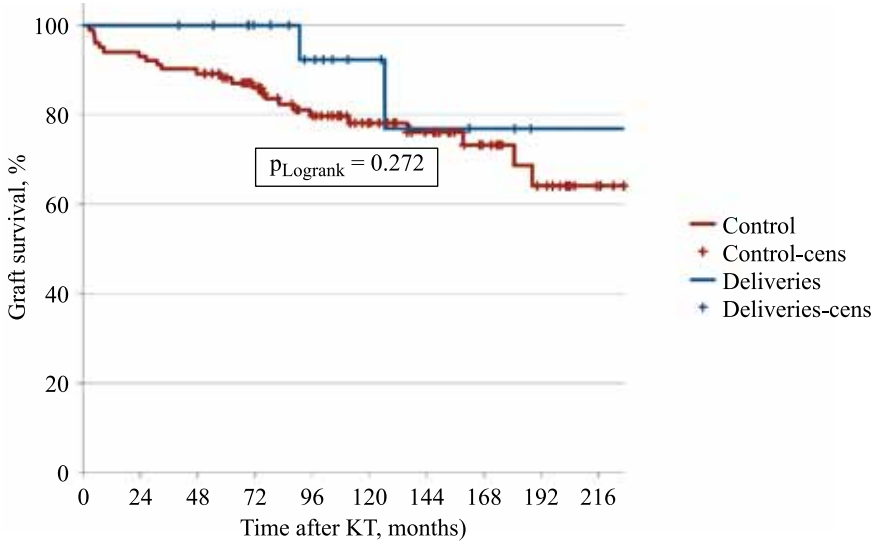

Fig. 3. Kidney graft survival (from the time of surgery) in women with and without pregnancy after transplantation

was female, there was no immediate threat to life during intrauterine development and in the neonatal period.

Another patient, who had not undergone pregravid preparation and came for a hospital appointment for the first time with pregnancy, was diagnosed with a urinary tract anomaly – neuromuscular dysplasia of both ureters, right-sided ureterohydronephrosis, and hypoplasia of the left kidney; the disease was not suspected to be hereditary in nature. The first fatal ultrasound screening detected no abnormalities, but at 20 weeks, the fetus was found to have a defect – bilateral hydronephrosis, high level of obstruction, suspected cystic renal dysplasia, and oligohydramnios. The parents refused to terminate the pregnancy and, unfortunately, the perinatal outcome was unfavorable. We cannot exclude the hereditary nature of the disease in this case, so the patient should undergo exome sequencing if she is planning a second pregnancy. In patients with CAKUT (congenital anomalies of the kidneys and urinary tracts) syndrome with bilateral lesions, monogenic anomalies can be detected in 22% of cases [18]. Thus, despite the relatively low frequency of hereditary diseases among pregnant women with RG, it is necessary to keep in mind the possible transmission of diseases to children and the advantages of using (in the presence of established mutations) modern assisted reproductive technologies.

When comparing graft survival in patients who carried a pregnancy and those who did not have pregnancies after KT, comparable in age, underlying disease, and nature of immunosuppression, no statistically significant differences were found; this does not contradict the finding from other researchers [10, 11]. However, given that pregnancy is usually allowed in patients with initially satisfactory RG function and without serious immunologic or non-immunologic complications, this comparison may not be entirely valid. To some extent, these 'advantages', when analyzing outcomes, may be offset by cases where pregnancies are unplanned in patients with non-ideal RG function or other contraindications to fertility and the woman insists on prolonging the pregnancy. Once again, we emphasize that in kidney transplant recipients, lack of pregnancy planning and pregravid preparation can have a negative impact on obstetric and nephrological outcomes.

CONCLUSION

Pregnancies can succeed in women who are kidney transplant recipients if there is careful selection of genetically healthy embryos, pregravid preparation and personalized management, despite their higher incidence of pregnancy complications compared to healthy women. When planning pregnancy after KT, one should keep in mind the possibility of transmitting hereditary diseases to the offspring: where there are no contraindications, IVF with preimplantation genetic testing and selection of genetically healthy embryos can be performed. Pregnancy after KT does not appear to have a significant effect on long-term graft survival, although further research on this is needed.

The authors declare no conflict of interest.

REFERENCES

1. *Chandra A, Midtvedt K, Åsberg A, Eide IA*. Immunosuppression and reproductive health after kidney transplantation. *Transplantation.* 2019; 103 (11): e325–e333. doi: 10.1097/TP.0000000000002903.
2. *Jesudason S, Williamson A, Huuskes B, Hewawasam E.* Parenthood with kidney failure: answering questions patients ask about pregnancy. *Kidney Int Rep.* 2022; 7 (7): 1477–1492. doi: 10.1016/j.ekir.2022.04.081.
3. *Gill JS, Zalunardo N, Rose C, Tonelli M.* The pregnancy rate and live birth rate in kidney transplant recipients. *Am J Transplant.* 2009; 9 (7): 1541–1549. doi: 10.1111/j.1600-6143.2009.02662.x.
4. *Salvadori M, Tsalouchos A.* Fertility and pregnancy in end stage kidney failure patients and after renal transplantation: an update. *Transplantology.* 2021; 2: 92–108. doi: 10.3390/transplantology2020010.
5. *Yaprak M, Doğru V, Sanhal CY, Özgür K, Erman M. In vitro* fertilization after renal transplantation: a single-center experience. *Transplant Proc.* 2019; 51 (4): 1089–1092. doi: 10.1016/j.transproceed.2019.01.105.
6. *Prokopenko EI, Guryeva VM, Petrukhin VA, Krasnopol'skaya KV, Burumkulova FF, Gubina DV*. IVF pregnancy after kidney transplantation: clinical case and literature review. *Russian Journal of Transplantology and Artificial Organs.* 2022; 24 (4): 15–23. doi: 10.15825/1995-1191-2022-4-15-23.
7. *Shah S, Venkatesan RL, Gupta A, Sanghavi MK, Welge J, Johansen R et al.* Pregnancy outcomes in women with kidney transplant: Metaanalysis and systematic review. *BMC Nephrol.* 2019; 20 (1): 24. doi: 10.1186/s12882-019-1213-5.
8. *Schwarz A, Schmitt R, Einecke G, Keller F, Bode U, Haller H, Guenter HH.* Graft function and pregnancy outcomes after kidney transplantation. *BMC Nephrol*. 2022; 23 (1): 27. doi: 10.1186/s12882-022-02665-2.
9. *Tangren J, Bathini L, Jeyakumar N, Dixon SN, Ray J, Wald R et al.* Pre-pregnancy eGFR and the risk of adverse maternal and fetal outcomes: a population-based study. *J Am Soc Nephrol.* 2023; 34 (4): 656–667. doi: 10.1681/ASN.0000000000000053.
10. *Kaatz R, Latartara E, Bachmann F, Lachmann N, Koch N, Zukunft B et al.* Pregnancy after kidney transplantation-impact of functional renal reserve, slope of eGFR before pregnancy, and intensity of immunosuppression on kidney function and maternal health. *J Clin Med.* 2023; 12 (4): 1545. doi: 10.3390/jcm12041545.
11. *Van Buren MC, Schellekens A, Groenhof TKJ, van Reekum F, van de Wetering J, Paauw ND, Lely AT.* Long-term graft survival and graft function following pregnancy in kidney transplant recipients: a systematic review and meta-analysis. *Transplantation.* 2020; 104 (8): 1675–1685. doi: 10.1097/TP.0000000000003026.

12. Standards of specialized diabetes care. Edited by I.I. Dedov, M.V. Shestakova, A.Yu. Mayorov. 11th Edition. M., 2023; 157. doi: 10.14341/DM13042.
13. *Gosselink ME, van Buren MC, Kooiman J, Groen H, Ganzevoort W, van Hamersvelt HW et al.* A nationwide Dutch cohort study shows relatively good pregnancy outcomes after kidney transplantation and finds risk factors for adverse outcomes. *Kidney Int.* 2022; 102 (4): 866–875. doi: 10.1016/j.kint.2022.06.006.
14. *Kovač D, Kovač L, Mertelj T, Steblovnik L.* Pregnancy after kidney transplantation. *Transplant Proc.* 2021; 53 (3): 1080–1084. doi: 10.1016/j.transproceed.2020.11.003.
15. *Mariano S, Guida JPS, Sousa MV, Parpinelli MA, Surita FG, Mazzali M, Costa ML.* Pregnancy among women with kidney transplantation: a 20-years single-center registry. *Rev Bras Ginecol Obstet.* 2019; 41 (7): 419–424. doi: 10.1055/s-0039-1688834.
16. *Devresse A, Jassogne C, Hubinont C, Debiève F, De Meyer M, Mourad M et al.* Pregnancy outcomes after kidney transplantation and long-term evolution of children: a single center experience. *Transplant Proc*. 2022; 54 (3): 652–657. doi: 10.1016/j.transproceed. 2022.01.019.
17. *Tanriover B, Jaikaransingh V, MacConmara MP, Parekh JR, Levea SL, Ariyamuthu VK et al.* Acute rejection rates and graft outcomes according to induction regimen among recipients of kidneys from deceased donors treated with tacrolimus and mycophenolate. *Clin J Am Soc Nephrol*. 2016; 11 (9): 1650–1661. doi: 10.2215/CJN.13171215.
18. *Riedhammer KM, Ćomić J, Tasic V, Putnik J, Abazi-Emini N, Paripovic A et al.* Exome sequencing in individuals with congenital anomalies of the kidney and urinary tract (CAKUT): a single-center experience. *Eur J Hum Genet.* 2023; 31 (6): 674–680. doi: 10.1038/s41431-023-01331-x.

The article was submitted to the journal on 11.01.2024

DOI: 10.15825/1995-1191-2024-2-16-27

TRANSJUGULAR INTRAHEPATIC PORTOSYSTEMIC SHUNT OR A COMBINATION OF NONSELECTIVE BETA-BLOCKERS AND ENDOSCOPIC VARICEAL LIGATION FOR PROPHYLAXIS OF BLEEDING IN WAITLISTED CIRRHOTIC PATIENTS

R.V. Korobka[1, 2], S.V. Gautier[3, 4], Yu.V. Khoronko[2], V.D. Pasechnikov[1, 5], N.G. Sapronova[2], I.A. Porshennikov[6, 7], M.V. Malevanny[1, 2], E.S. Pak[1, 2], D.V. Pasechnikov[5]

[1] Rostov Regional Clinical Hospital, Rostov-on-Don, Russian Federation
[2] Rostov State Medical University, Rostov-on-Don, Russian Federation
[3] Shumakov National Medical Research Center of Transplantology and Artificial Organs, Moscow, Russian Federation
[4] Sechenov University, Moscow, Russian Federation
[5] Stavropol State Medical University, Stavropol, Russian Federation
[6] Novosibirsk Regional Clinical Hospital, Novosibirsk, Russian Federation
[7] Novosibirsk State Medical University, Novosibirsk, Russian Federation

Objective: to substantiate the choice of an optimal method of preventing and reducing the risk of variceal bleeding (VB) and cardia in patients with decompensated cirrhosis who have been enlisted for liver transplantation (LT). **Materials and methods.** Patients with diuretic-resistant and diuretic-responsive ascites underwent prophylaxis for recurrent bleeding via transjugular intrahepatic portosystemic shunt (TIPS) or a combination of endoscopic variceal ligation (EVL) and nonselective beta-blockers (NSBB). **Results.** Leukocyte counts, Na levels, and Child–Turcotte–Pugh (CTP) liver disease class in patients with diuretic-resistant ascites had significant differences when comparing individuals who received EVL + NSBB or underwent TIPS. In diuretic-responsive patients, there were significant differences for blood platelet count, albumin and Na levels, and CTP class when comparing EVL + NSBB and TIPS groups. In diuretic-resistant patients, incidence of grade 2 varices in EVL + NSBB group was significantly higher than in TIPS. Incidence of grade 3 varices was significantly higher in TIPS patients than in EVL + NSBB cohort. In diuretic-responsive patients, incidence of grade 2 and 3 varices had no significant differences when comparing these indicators in both groups. The proportion of patients with CTP class B was significantly higher both in diuretic-resistant and diuretic-responsive patients with various methods of rebleeding prophylaxis. The proportions of CTP class C patients with both forms of ascites were significantly higher in EVL + NSBB group than in TIPS. During the LT wait period within 2 years from the start of bleeding prophylaxis in diuretic-resistant patients, 78.4% of patients who underwent TIPS implantation developed recurrent bleeding, 100% of EVL + NSBB group within the same time frame, developed recurrent bleeding. Using the Kaplan–Meier estimate with the Log-Rank test, we were able to establish that there is a significant difference between the proportions of patients with recurrent VB in EVL + NSBB or TIPS groups with both forms of ascites.

Keywords: liver transplant waiting list, ascites, recurrent VB, endoscopic variceal ligation, nonselective beta-blockers, TIPS implantation.

INTRODUCTION

VB is a life-threatening complication of portal hypertension, which is a marker of decompensated cirrhosis [1, 2] and high mortality [3]. The first episode of variceal hemorrhage occurs with a frequency exceeding 85% in patients with decompensated CKD [4]. In patients who recovered from the first bleeding episode, the risk of recurrent bleeding (RB) is 60% in the first year with a mortality of up to 33% [2]. Other publications report 30% of patients with a first episode of VB within the first two years [5]. The authors of the study found that after the first episode of VB, at least 60% of them are predisposed to RB with a mortality risk of 30% if they are not treated with secondary prophylaxis [6, 9]. But even, in case of secondary prophylaxis of bleeding with a combination of NSBB and EVL for VB in accordance with the guidelines of the American Association for the Study of Liver Diseases (AASLD) [2] and the Guidelines for the Management of Patients with portal hypertension – Baveno VI and Baveno VII [7, 8], RB risk within

Corresponding author: Victor Pasechnikov. Address: 21, Aviatsionnaya str., Stavropol, 355017, Russian Federation. Phone: (962) 447-75-13. E-mail: passetchnikov@mail.ru

2 years after the first episode increases from 29% to 57%, and the risk of death increases from 16% to 26% [10].

Increased hepatic venous pressure gradient (HVPG) of 20 mmHg or more is the main predictor of early RB and high mortality for acute rebleeding in cirrhotic patients awaiting LT [11, 12]. It has been shown that in patients awaiting LT, each 1 mmHg increase in HVPG increases the risk of death by 3% in a 19-month liver transplant waitlist (LTWL) stay [13].

As established by studies, EVL is not a measure to restrain an increase in HVPG during cirrhosis progression [11–13], and NSBB reduces HVPG level to a small extent (propranolol could only lower it by 10.1–23.2%, carvedilol by 18.6–27.7%) [14]. In addition, response to the use of propranolol or carvedilol in high HVPG has resulted in two categories of individuals: responders and non-responders [14–16], which reduces the efficacy of NSBB + EVL, which is well established in the primary prophylaxis of VB [17]. La Mura et al. [16] found that the incidence of primary or recurrent bleeding from esophageal varices within 1 year was 7% in responders of acute hemodynamic response to propranolol use, and 21% in non-responders.

Therefore, for patients with HVPG or portal pressure gradient (PPG) ≥25 mmHg, neither EVL, NSBB therapy, nor EVL + NSBB is effective in preventing VB when waiting for LT for 2 or more years [18].

In fact, an EVL plus NSBB, although considered the standard in prophylaxis of recurrent VB, has never been considered the only and indisputable strategy [19].

In recent years, the invasive TIPS procedure has become widespread, and many randomized controlled trials (RCTs) have confirmed that this technique is superior to other RB treatments. Nevertheless, it should be recognized that the use of TIPS has not improved patient survival rates significantly [10, 20].

Implantation of TIPS, while reducing HVPG or PPG, is thus the treatment of choice when first-line therapy (EVL + NSBB) is ineffective [21, 22]. Performing TIPS implantation after the second or third (and/or more) episodes of recurrent VB (especially if they recur at short intervals) is indicated in hemodynamically and clinically stable patients with optimal and manageable risk factors for complications of this procedure [23].

In most RCTs, patients were included in the study within 24 to 96 hours after bleeding occurred [24].

Studies comparing the efficacy of TIPS and EVL + NSBB in preventing recurrent VB are extremely rare [20, 23].

MATERIALS AND METHODS

The comparative retrospective study included 163 cases of patients with established VB awaiting LT between 2016 and 2023.

Inclusion criteria: Patients with diuretic-responsive and diuretic-resistant ascites, presence of one or more episodes of VB while in the liver transplant waiting list (LTWL), complete abstinence for at least 3 months (confirmed by addiction specialists) prior to inclusion in the LTWL for patients with alcohol-related cirrhosis, virus-related cirrhosis (hepatitis B virus (HBV) or hepatitis C virus (HCV)- associated etiology), cirrhosis of mixed etiology (virus-related and alcohol-related), and Child–Turcotte–Pugh (CTP) classes of cirrhosis.

Exclusion criteria: patients with hepatocellular cancer and other tumors accompanied by ascites, hepatic encephalopathy (HE) grade 2 and above, infectious diseases, portal vein thrombosis, contraindications to NSBB (bradyarrhythmia, bronchial asthma, obstructive pulmonary disease), and diabetes mellitus.

The patients included in the study were divided into two groups: group 1 consisted of 130 patients with diuretic-resistant ascites, group 2 included 33 patients with diuretic-responsive ascites. There were subgroups in both groups. In group 1: 1a had patients who received EVL plus NSBB (n = 77), 1b consisted of patients who underwent TIPS implantation (n = 53). Similarly, group 2 had subgroups: 2a was patients who received EVL plus NSBB (n = 9), 2b included patients who were implanted with TIPS (n = 24).

Demographic, clinical, and laboratory parameters were obtained from a permanent, continuously updated electronic database of patients who were under follow-up after their inclusion in the LTWL, after approval of the study by the Local Ethics Committee, Center for Surgery and Donation Coordination, Rostov Regional Clinical Hospital. Where patients' condition was stable, clinical and biochemical blood tests, hemostasis parameters, calculation of MELD-Na scores and CTP liver disease class, were repeated at 3-month intervals.

Where patients' condition were stable, abdominal ultrasound was performed every 6 months after the patients' initial examination.

In all patients, esophagogastroduodenoscopy (EGD) was performed to screen for varices with high risk of VB.

The Baveno VI [7] and World Gastroenterology Association (WGO) [24] guidelines served as a basis for identifying patients with varices requiring urgent therapy (medium and large size varices).

The criteria for diagnosing resistant ascites were as follows: diuretic resistance, decreased plasma Na levels (<125 mmol/L), increased fluid in the abdominal cavity (5–6 points on the CIRAS scale) [25]. The severity of diuretic-responsive ascites was determined according to the International Ascites Club criteria [26]. Mean arterial pressure (mAP) was determined by the formula: $mAP = (DP) + {}^{1}/_{3}(SP - DP)$, where SP is systolic pressure, and DP is diastolic pressure [27].

For the first-line therapy recommended by experts for prevention of recurrent esophageal hemorrhage [2, 7, 8], beta-1 blockers (propranolol, nadolol) and beta-1, beta-2, and alpha-1 adrenergic blocker (carvedilol) were used.

Propranolol was initiated at a starting dose of 40 mg/day, with a maximum dose of 240 mg/day. The starting dose of nadolol was 40 mg/day and the maximum was 80 mg/day. The starting dose of carvedilol was 6.25 mg/day and the maximum was 25 mg/day.

Drug doses were adjusted appropriately whenever there were changes in blood pressure (BP), heart rate (HR) and mAP.

Patients received diuretics, and paracentesis was performed in patients with diuretic-resistant ascites.

Patients with virus-related cirrhosis received antiviral therapy with nucleoside alternatives (HBV) and a combination of direct-acting antivirals (HCV) according to the guidelines for the treatment of LTWL patients [28].

EVL was performed using an EGD and a multi-band ligation system, starting at the gastroesophageal junction and continuing this procedure proximally. The number of rubber ligatures (2 to 4) was determined depending on the size of varices. In accordance with guidelines, obliteration of all varices meeting the criteria for emergency therapy [7, 24] was achieved through repeated EVL. Control EGD to monitor the obliteration was performed at 3-month intervals. Where there are recurrences (appearance of new varices), repeat EVL was performed.

TIPS implantation was performed in accordance with the guidelines for the treatment of decompensated cirrhosis [29, 30] under local anesthesia with intravenous sedation with analgesics. For implantation, we used a set of RUPS-100 instruments (Cook Medical®, USA), including Flexor Check-Flo introducer and curved Rösch catheter. After puncture of the right internal jugular vein (RIJV), under fluoroscopic control, a standard angiographic guidewire was advanced through the superior vena cava (SVC) and the atrial sinus into the inferior vena cava (IVC), placing its J-shaped end at a level slightly above the hepatic vein (HV) orifices. Flexor Check-Flo introducer with a curved Rösch catheter was passed through the guidewire and placed in the right hepatic vein (RHV) closer to its mouth. During surgical intervention, an intrahepatic conduit (tunnel) was formed from RHV to the portal vein (PV) right branch or bifurcation using a Rösch-Uchida needle and a balloon guided by a wire. After removal of the balloon, a stent-graft, which is a tubular metal mesh covered inside with a special sealed plastic – polytetrafluoroethylene (PTFE) – was implanted through the guidewire.

The obtained data were analyzed using statistical program IBM SPSS Statistics (version 23). Parameter analysis using the Kolmogorov–Smirnov test with the Lilliefors test for normality allowed us to determine the type of distribution of the obtained variables of the sample indicators (normal or non-normal distribution). In the case of normal distribution, variables were presented as arithmetic mean (M) with determination of standard deviation (SD); significance of differences between compared values was determined by Student's t-test. In the case of non-normal distribution, variables were expressed as median (Me) and interquartile range (IQR, interval between the 75th and 25th percentiles of the data). To determine the significance of differences between variables, the following nonparametric criteria were used: Wilcoxon test for pairwise comparisons of dependent variables, and Pearson's Chi-square for comparison of independent variables. The Mann–Whitney U test was used to compare samples with a small number of variables. Analysis of variance (ANOVA test) was also used. Analysis of frequencies of variables and their shares (%) was used when comparing qualitative parameters. The p value <0.05 was accepted as the criterion of statistical significance between compared parameters. The proportion of patients with RB in the compared groups, as well as the risk of verified event (bleeding) was determined by the Kaplan–Meier method. The significance of differences between compared curves was determined by calculating the logarithmic test [Log-Rank (Mantel-Cox)].

RESULTS

Table 1 and Table 2 present demographic, clinical, and laboratory parameters, as well as MELD-Na scores in the groups of patients with diuretic-resistant and diuretic-responsive ascites, who were treated with EVL + NSBB therapy or underwent TIPS implantation during the LT wait period.

As can be seen from the tables presented, demographic and most of the laboratory and instrumental parameters of patients who received NSBB therapy plus EVL or underwent TIPS implantation in the diuretic-resistant and diuretic-responsive groups had no significant differences.

Exceptions were leukocyte count, Na level and CTP class in the diuretic-resistant group, which had significant differences when comparing subgroups 1a and 1b. Also, when comparing indicators in subgroups 2a and 2b in the non-resistant group, there were significant differences in terms of platelet count, albumin and Na levels, and CTP class.

Table 3 and Table 4 present data on gender composition as well as etiology of cirrhosis, CTP class, and severity of varices in patients treated with NSBB plus EVL or underwent TIPS implantation in the diuretic-resistant and diuretic-responsive groups.

As can be seen from Tables 3 and 4, decompensated virus-related cirrhosis prevailed in the compared subgroups. Table 3 shows that in waitlisted patients with diuretic-resistant ascites, the incidence of grade 2 varices in subgroup 1a (EVL + NSBB) was significantly higher than in subgroup 1b (TIPS implantation). At the same time, the incidence of grade 3 varices was significantly higher in subgroup 1b than in subgroup 1a. In diuretic-responsive ascites patients (Table 4), the incidence of grade 2 and 3 varices was not significantly different when comparing these parameters in subgroups 2a and

2b (who received EVL plus NSBB and underwent TIPS implantation, respectively).

When comparing the severity of liver injury according to CTP class A, it was not possible to conduct an analysis due to the absence of such patients in subgroups 1a and 2a (diuretic-resistant and diuretic-responsive ascites). The proportion of patients with CTP class B was significantly higher in both diuretic-resistant and diuretic-responsive patients (subgroups 1a and 1b, respectively). The proportions of patients with CTP grade C for both forms of ascites were significantly higher in subgroups 1a and 2a (EVL + NSBB) compared with subgroups 2a and 2b (TIPS implantation).

During the LT waiting period between 24 and 48 weeks of follow-up in the LTWL (2-year period from the start of bleeding prophylaxis), RB developed in 29 of 37 diuretic-resistant patients (78.4%) who underwent TIPS implantation. In contrast, all patients (100%) who

Table 1

Comparative characteristics of patients with diuretic-resistant ascites (group 1), who received NSBB + EVL or underwent TIPS implantation (normal and non-normal distribution)

Indicator	Subgroup 1a EVL + NSBB (n = 73) M ± SD	Subgroup 1b TIPS (n = 37) M ± SD	Statistical significance
Normal distribution (M ± SD)			
Age	48.82 ± 10.59	51.46 ± 10.67	0.22
Hemoglobin (g/L)	87.91 ± 11.68	87.00 ± 11.39	0.32
Leukocytes ($\times 10^9$/L)	3.38 ± 1.20	4.31 ± 1.68	0.01
Platelets ($\times 10^9$/L)	84.41 ± 44.15	109.73 ± 78.65	0.03
Plasma albumin (g/L)	29.85 ± 3.06	30.38 ± 2.76	0.38
MELD-Na	21.92 ± 3.09	20.76 ± 3.06	0.06
mAP (mmHg)	78.22 ± 20.65	79.35 ± 21.12	0.23
Non-normal distribution (Me; IQR)			
INR	1.90 (1.70–2.05)	1.900 (1.60–2.10)	0.45
Bilirubin (μmol/L)	81.0 (64.50–105.00)	74.0 (64.50–77.50)	0.07
Creatinine (μmol/L)	112.0 (97.0–127.00)	109.0 (101.5–121.00)	0.59
Na (mmol/L)	136.6 (135.0–138.5)	132.0 (129.5–135.5)	0.001
CTP (score)	2.00 (2.00–2.00)	11.00 (8.50–14.00)	0.001

Note: EVL, endoscopic variceal ligation; NSBB, nonselective beta-blockers; TIPS, transjugular intrahepatic portosystemic shunt; mAP, mean arterial pressure; INR, international normalized ratio; Na, sodium; CTP, Child–Turcotte–Pugh.

Table 2

Comparative characteristics of patients with non-resistant ascites (group 2), who received NSBB therapy plus EVL or underwent TIPS implantation (normal and non-normal distribution)

Indicator	Subgroup 2a EVL + NSBB (n = 16) M ± SD	Subgroup 2b TIPS (n = 18) M ± SD	Statistical significance
Normal distribution (M ± SD)			
Age	46.45 ± 7.98	48.50 ± 10.18	0.12
Hemoglobin (g/L)	88.91 ± 10.32	87.38 ± 9.63	0.17
Leukocytes ($\times 10^9$/L)	4.76 ± 1.51	4.96 ± 1.86	0.10
Platelets ($\times 10^9$/L)	80.17 ± 44.05	131.11 ± 52.15	0.04
Plasma albumin (g/L)	26.33 ± 5.20	31.61 ± 2.48	0.03
MELD-Na	21.30 ± 3.49	19.38 ± 2.28	0.13
mAP (mmHg)	79.67 ± 22.43	81.44 ± 23.42	0.19
Non-normal distribution (Me; IQR)			
INR	1.750 (1.475–2.00)	1.700 (1.375–1.950)	0.50
Bilirubin (μmol/L)	107.5 (42.50–652.50)	79.5 (57.0–161.25)	0.55
Creatinine (μmol/L)	99.0 (77.25–104.25)	98.0 (82.25–117.25)	0.64
Na (mmol/L)	136.0 (136.0–137.25)	132.0 (130.0–132.0)	0.001
CTP (score)	2.00 (2.00–2.00)	8.00 (7.00–9.00)	0.003

Note: EVL, endoscopic variceal ligation; NSBB, nonselective beta-blockers; TIPS, transjugular intrahepatic portosystemic shunt; mAP, mean arterial pressure; INR, international normalized ratio; Na, sodium; CTP, Child–Turcotte–Pugh.

received EVL plus NSBB developed RB within the same time frame.

Using the Kaplan–Meier method with the Log-Rank test, a significant difference (p = 0.023) was found between the proportions of patients with recurrent VB in the compared groups (Fig. 1).

Fig. 2 shows the diagram of the cumulative risk of RB in the compared groups. The cumulative risk of RB in the EVL + NSBB subgroup was two or more times higher than in the TIPS subgroup (significant difference using Log-Rank test = 0.023).

During the LT wait period between 24 and 48 weeks of follow-up in the LTWL (2 years from the start of bleeding prophylaxis), RB developed in 8 of 18 diuretic-responsive patients (44.4%) who underwent TIPS implantation.

In the EVL + NSBB subgroup, all patients (100%) developed RB within the same time frame.

Using the Kaplan–Meier method with determination of Log-Rank test, a significant difference (p = 0.049) was found between the proportions of patients who developed recurrent VB in the compared groups (Fig. 3).

Fig. 4 shows a diagram of the cumulative risk of RB in the compared groups. The cumulative risk of RB in the EVL + NSBB subgroup was one and a half times higher than in the TIPS subgroup (significant difference using Log-Rank test = 0.023).

DISCUSSION

Our study showed a high rate of RB in diuretic-resistant and diuretic-responsive patients waiting for LT for 24–48 weeks, who received prophylactic therapy with a combination of an invasive procedure – EVL + NSBB (first-line therapy) – or underwent TIPS implantation, considered as second-line therapy in modern guidelines [8]. Note that the first bleeding recurrences occurred in the first 8–10 weeks from the start of secondary prophylaxis for RB in both forms of ascites and both prophylaxis methods. However, as the waiting period for LT increased (>10 weeks from the start of prophylaxis), the proportion of patients with RB became significantly higher, reaching 100% in patients with both forms of ascites when first-line therapy was used, while the use of

Table 3

Comparative characteristics of clinical and gender parameters of patients with diuretic-resistant ascites, who received NSBB plus EVL or underwent TIPS implantation

Indicator	Subgroup 1a NSBB + EVL (n = 73) (%)	Subgroup 1b TIPS (n = 37) (%)	Statistical significance
Male	41 (56.2%)	21 (56.8%)	0.11
Virus-related cirrhosis	35 (48.0%)	19 (32.4%)	0.001
Alcohol-related cirrhosis	19 (26.0%)	9 (24.3%)	0.13
Other CKD etiologies	19 (26.0%)	9 (24.3%)	0.14
Esophageal varices, grade 2	19 (26.0%)	4 (10.8%)	0.001
Esophageal varices, grade 3	54 (74.0%)	33 (89.2%)	0.001
CTP class A	0	1 (2.7%)	–
CTP class B	6 (8.2%)	9 (24.3%)	0.001
CTP class C	67 (91.8%)	27 (73.0%)	0.04

Note: EVL, endoscopic variceal ligation; NSBB, nonselective beta-blockers; TIPS, transjugular intrahepatic portosystemic shunt; CKD, chronic kidney disease; CTP, Child–Turcotte–Pugh.

Table 4

Comparative characteristics of clinical and gender parameters of patients with diuretic-responsive ascites, who received NSBB plus EVL or underwent TIPS implantation

Indicator	Subgroup 2a EVL + NSBB (n = 16) (%)	Subgroup 2b TIPS (n = 18) (%)	Statistical significance
Male	12 (75.01%)	14 (77.7%)	0.16
Virus-related cirrhosis	12 (75.0%)	12 (66.7%)	0.03
Alcohol-related cirrhosis	6 (25.0%)	4 (22.2%)	0.22
Other CKD etiologies	0	2 (11.1%)	–
Esophageal varices, grade 2	2 (12.5%)	2 (11.1%)	0.23
Esophageal varices, grade 3	14 (87.5%)	16 (88.9%)	0.24
CTP class A	0	1 (13.5%)	–
CTP class B	5 (8.2%)	14 (18.9%)	0.001
CTP class C	11 (91.8%)	3 (67.6%)	0.008

second-line therapy gave a significantly lower incidence of RB by the end of follow-up for both forms of ascites.

We found only five published studies and one meta-analysis (when analyzing the PubMed database up to January 2024) that aimed to compare the efficacy of TIPS implantation or a combination of EVL and NSBB on the rate of RB in patients with decompensated cirrhosis.

The same results as in our study were obtained by Zhou et al. [31], who compared the efficacy and safety of TIPS implantation or a combination of EVL and NSBB (propranolol) for secondary prophylaxis of VB bleeding. The study showed that the proportion of patients without RB was higher in TIPS than in EVL + NSBB (93% and 62%, respectively, $p < 0.001$). The authors concluded that compared to the combination of EVL and

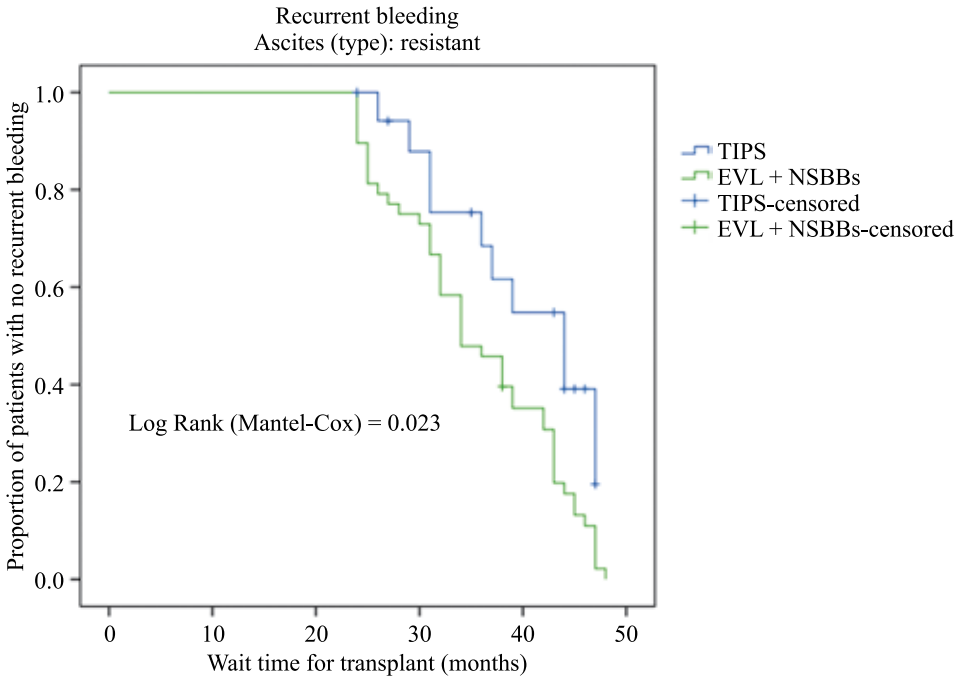

Fig. 1. Proportion of rebleeding patients with diuretic-resistant ascites, who underwent TIPS implantation or received NSBB + EVL (Kaplan–Meier method with Log-Rank test)

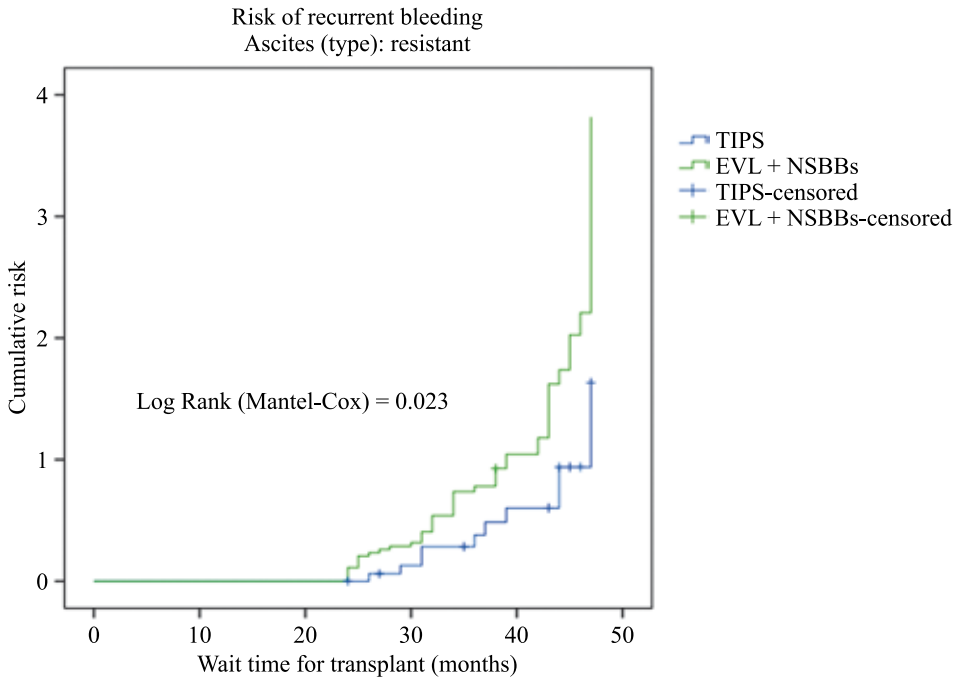

Fig. 2. Cumulative risk of recurrent bleeding in patients with resistant ascites who underwent TIPS implantation or received EVL + NSBB

NSBB, PTFE-covered TIPS could significantly reduce the variceal rebleeding rate in cirrhotic patients with HVPG≥20 mmHg.

Earlier studies comparing the efficacy of implantation of PTFE-covered TIPS and EVL + NSBB combination [10, 20, 32, 33] showed a significant difference between the former method and the latter in terms of RB prophylaxis. Importantly, the use of PTFE-covered TIPS did not increase the risk of patient mortality or the risk of HE.

Miao et al. [19] conducted a meta-analysis of RCTs to comparatively evaluate the efficacy of all proposed methods for prevention of re-therapy in patients with decompensated cirrhosis. Forty-eight trials with 4415 participants with cirrhosis and portal hypertension who had a history of recent variceal bleeding were included in the

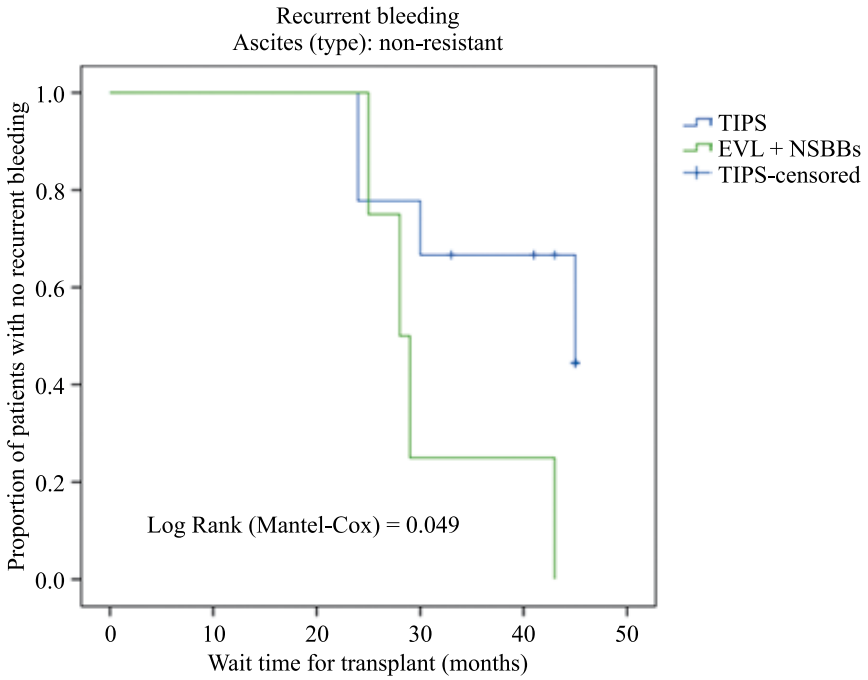

Fig. 3. Proportion of rebleeding patients with diuretic-responsive ascites, who underwent TIPS implantation or received NSBB + EVL (Kaplan–Meier method with Log-Rank test)

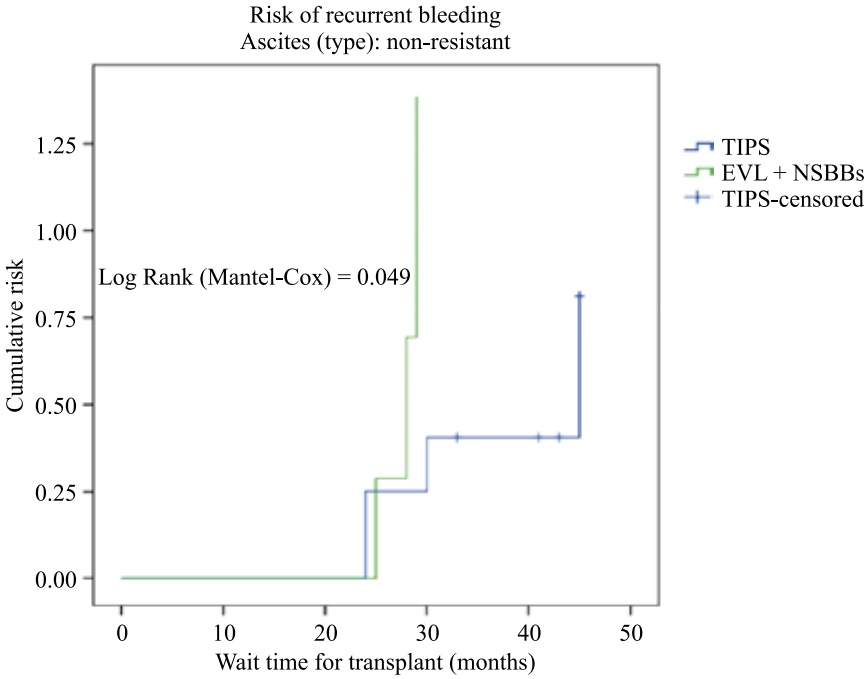

Fig. 4. Cumulative risk of recurrent bleeding in patients with diuretic-responsive ascites who underwent TIPS implantation or EVL + NSBB

meta-analysis. International databases, including EMBASE, PubMed, and Cochrane Database of Controlled Trials, were checked to identify relevant randomized controlled trials up to December 2019.

The authors of the meta-analysis concluded that NSBB + isosorbide mononitrate ranked significantly higher than NSBB + EVL (63.9% vs 49.6%, respectively) in reducing patient mortality. TIPS (98.8%) ranked higher than other treatments in reducing rebleeding but did not confer any survival benefit.

The risk of RB in our study was significantly higher in the EVL + NSBB subgroup than in the TIPS subgroup. Note that in our study, rebleeding occurred in diuretic-resistant and diuretic-responsive ascites patients, with high MELD-Na scores, as well as in a significant proportion of patients with grade 2 and 3 varices.

It is known that the main risk factor for recurrent variceal hemorrhage is elevated HVPG (≥20 mmHg) [11, 12, 33]. The increased proportion of patients with RB in both forms of ascites in those who received EVL plus NSBB in our study, compared with those who underwent TIPS implantation, is associated with higher HVPG while waiting for LT for 2 or more years. As found by Liu et al. [18], when HVPG or PPG ≥25 mmHg, neither EVL, NSBB therapy, nor EVL + NSBB provide reliable prophylaxis of recurrent variceal hemorrhage. A similar conclusion was reached by Zhang et al. [33] who showed that TIPS are more effective than NSBB (propranolol) + EVL in cirrhosis patients with high HVPG (≥20 mmHg).

In addition to HVPG ≥20 mmHg, other risk factors for RB in patients receiving NSBB plus EVL include ascites, HE, MELD score >12 [34], which is consistent with our study. Undoubtedly, the risk factors of re-bleeding should include medium- and high-grade esophageal varices that we identified in both forms of ascites. A study conducted by Irisawa et al. [35] showed that the size (diameter) of paraesophageal varices is a risk factor for RB.

How to reduce the risk of RB? Early use of TIPS implantation is the optimal strategy for rebleeding prophylaxis. The concept of "pre-emptive TIPS" was first introduced by Monescillo et al. [36], who showed that in patients with HVPG ≥20 mmHg, stent implantation in the first 24 hours after stabilization of the patient's condition against the background of the first bleeding provides better survival and lower rate of recurrent variceal hemorrhage than standard prophylactic therapy.

Ardevol et al. [34] confirmed this concept by showing that early use of TIPS after the first bleeding significantly reduces the risk of rebleeding.

Limitations of this approach include the need to measure HVPG to decide on the choice of prophylaxis for recurrent VB. This technique is not available in all medical centers, and its introduction may be considered as a prospect towards improving the diagnosis of portal hypertension and the choice of the method of prophylaxis of recurrent variceal hemorrhage with a long LT waiting period.

CONCLUSION

We found a high rate of rebleeding in both forms of ascites in patients awaiting LT within 24–48 weeks after inclusion in the LTWL.

Probable risk indicators for rebleeding in the patients are ascites, high MELD-Na score (≥19), and large (diameter) varices.

Prophylaxis of recurrent bleeding during the specified length of LTWL stay, while waiting for LT, is more effective with TIPS than with EVL + NSBB.

The authors declare no conflict of interest.

REFERENCES

1. *Liu L, Nie Y, Liu Q, Zhu X.* A Practical Model for Predicting Esophageal Variceal Rebleeding in Patients with Hepatitis B-Associated Cirrhosis. *Int J Clin Pract*. 2023 Aug 3; 2023: 9701841. doi: 10.1155/2023/9701841.
2. *Garcia-Tsao G, Abraldes JG, Berzigotti A, Bosch J.* Portal hypertensive bleeding in cirrhosis: Risk stratification, diagnosis, and management: 2016 practice guidance by the American Association for the study of liver diseases. *Hepatology* 2017; 65: 310–335. doi: 10.1002/hep.28906.
3. *Korobka VL, Pak ES, Shapovalov AM, Kostrykin MYu, Tkachev AV.* Analysis of four-year management of the waiting list for liver transplantation in Rostov region: prospects for reducing mortality of candidates listed for liver transplantation. *Medical Herald of the South of Russia*. 2019; 10 (3): 32–39. (In Russ.). doi: 10.21886/2219-8075-2019-10-3-32-39.
4. *Kovalak M, Lake J, Mattek N, Eisen G, Lieberman D, Zaman A*. Endoscopic screening for varices in cirrhotic patients: data from a national endoscopic database. *Gastrointest Endosc.* 2007 Jan; 65 (1): 82–88. PMID: 17185084. doi: 10.1016/j.gie.2006.08.023.
5. North Italian Endoscopic Club for the Study and Treatment of Esophageal Varices. Prediction of the first variceal hemorrhage in patients with cirrhosis of the liver and esophageal varices. A prospective multicenter study. *N Engl J Med*. 1988 Oct 13; 319 (15): 983–989. doi: 10.1056/NEJM198810133191505.
6. *Bosch J, García-Pagán JC*. Prevention of variceal rebleeding. *Lancet*. 2003 Mar 15; 361 (9361): 952–954. doi.org/10.1016/S0140-6736(03)12778-X.
7. *De Franchis R*. Expanding consensus in portal hypertension: Report of the Baveno VI Consensus Workshop: Stratifying risk and individualizing care for portal hypertension. *J Hepatol* 2015; 63: 743–752. doi: 10.1016/j.jhep.2015.05.022.
8. *De Franchis R, Bosch J, Garcia-Tsao G, Reiberger T, Ripoll C.* Baveno VII Faculty. Baveno VII – Renewing consensus in portal hypertension. *J Hepatol.* 2022; 76 (4): 959–974. doi: 10.1016/j.jhep.2021.12.022.
9. *Garcia-Tsao G, Bosch J.* Varices and Variceal Hemorrhage in Cirrhosis: A New View of an Old Problem.

Clin Gastroenterol Hepatol 2015; 13: 2109–2117. doi: 10.1016/j.cgh.2015.07.012.
10. *Lv Y, Qi X, He C, Wang Z, Yin Z, Niu J et al.* Covered TIPS versus endoscopic band ligation plus propranolol for the prevention of variceal rebleeding in cirrhotic patients with portal vein thrombosis: a randomised controlled trial. *Gut*. 2018 Dec; 67 (12): 2156–2168. doi: 10.1136/gutjnl-2017-314634.
11. *Abraldes JG, Villanueva C, Bañares R, Aracil C, Catalina MV, Garci A-Pagán JC, Bosch J.* Hepatic venous pressure gradient and prognosis in patients with acute variceal bleeding treated with pharmacologic and endoscopic therapy. *J Hepatol*. 2008 Feb; 48 (2): 229–236. doi: 10.1016/j.jhep.2007.10.008.
12. *Moitinho E, Escorsell A, Bandi JC, Salmerón JM, García-Pagán JC, Rodés J, Bosch J.* Prognostic value of early measurements of portal pressure in acute variceal bleeding. *Gastroenterology*. 1999 Sep; 117 (3): 626–631. PMID: 10464138. doi: 10.1016/s0016-5085(99)70455-5.
13. *Ripoll C, Bañares R, Rincón D, Catalina MV, Lo Iacono O, Salcedo M et al.* Influence of hepatic venous pressure gradient on the prediction of survival of patients with cirrhosis in the MELD Era. *Hepatology.* 2005 Oct; 42 (4): 793–801. doi: 10.1002/hep.20871.
14. *Sinagra E, Perricone G, D'Amico M, Tinè F, D'Amico G*. Systematic review with meta-analysis: the haemodynamic effects of carvedilol compared with propranolol for portal hypertension in cirrhosis. *Aliment Pharmacol Ther*. 2014 Mar; 39 (6): 557–568. doi: 10.1111/apt.12634.
15. *Hofer BS, Simbrunner B, Bauer DJM, Paternostro R, Schwabl P, Scheiner B et al.* Acute hemodynamic response to propranolol predicts bleeding and nonbleeding decompensation in patients with cirrhosis. *Hepatol Commun*. 2022 Sep; 6 (9): 2569–2580. doi: 10.1002/hep4.2021.
16. *La Mura V, Abraldes JG, Raffa S, Retto O, Berzigotti A, García-Pagán JC, Bosch J.* Prognostic value of acute hemodynamic response to i.v. propranolol in patients with cirrhosis and portal hypertension. *J Hepatol.* 2009 Aug; 51 (2): 279–287. Epub 2009 May 24. PMID: 19501930. doi: 10.1016/j.jhep.2009.04.015.
17. *Korobka VL, Pasechnikov VD, Korobka RV, Pak ES, Shapovalov AM.* Use of endoscopic band ligation alone and in combination with nonselective beta blockers for prevention of variceal bleeding in ascites patients on the liver transplant waiting list. *Russian Journal of Transplantology and Artificial Organs.* 2022; 24 (3): 42–50. [In Russ, English abstract]. doi: 10.15825/1995-1191-2022-3-42-50.
18. *Liu J, Shi Q, Xiao S, Zhou C, Zhou B, Yuan F et al.* Using transjugular intrahepatic portosystemic shunt as the first-line therapy in secondary prophylaxis of variceal hemorrhage. *J Gastroenterol Hepatol.* 2020 Feb; 35 (2): 278–283. Epub 2019 Jul 18. PMID: 31222830; PMCID: PMC7027763. doi: 10.1111/jgh.14761.
19. *Miao Z, Lu J, Yan J, Lu L, Ye B, Gu M.* Comparison of Therapies for Secondary Prophylaxis of Esophageal Variceal Bleeding in Cirrhosis: A Network Meta-analysis of Randomized Controlled Trials. *Clin Ther.* 2020 Jul; 42 (7): 1246–1275.e3. doi: 10.1016/j.clinthera.2020.04.014.
20. *Holster IL, Tjwa ET, Moelker A, Wils A, Hansen BE, Vermeijden JR et al.* Covered transjugular intrahepatic portosystemic shunt versus endoscopic therapy + β-blocker for prevention of variceal rebleeding. *Hepatology.* 2016 Feb; 63 (2): 581–589. Epub 2015 Dec 28. PMID: 26517576. doi: 10.1002/hep.28318.
21. *Rössle M.* TIPS: 25 years later. *J Hepatol*. 2013 Nov; 59 (5): 1081–1093. Epub 2013 Jun 25. PMID: 23811307. doi: 10.1016/j.jhep.2013.06.014.
22. *Boregowda U, Umapathy C, Halim N, Desai M, Nanjappa A, Arekapudi S et al.* Update on the management of gastrointestinal varices. *World J Gastrointest Pharmacol Ther.* 2019 Jan 21; 10 (1): 1–21. doi: 10.4292/wjgpt.v10.i1.1.
23. *Korsic S, Stabuc B, Skok P, Popovic P.* TIPS vs. endoscopic treatment for prevention of recurrent variceal bleeding: a long-term follow-up of 126 patients. *Radiol Oncol.* 2021 Jan 26; 55 (2): 164–171. doi: 10.2478/raon-2021-0006.
24. Esophageal Varices. Practice Guideline of World Gastroenterology Organisation. Available from: https://www.worldgastroenterology.org/UserFiles/file/guidelines/esophageal-varices-russian-2014.pdf.
25. *Gantzel RH, Aagaard NK, Vilstrup H, Watson H, Grønbaek H, Jepsen P.* Development and validation of the Cirrhotic Ascites Severity model-A patient-reported outcome-based model to predict 1-year mortality. *Hepatol Commun.* 2022 Nov; 6 (11): 3175–3185. doi: 10.1002/hep4.2065.
26. *Moore KP, Wong F, Gines P, Bernardi M, Ochs A, Salerno F et al.* The management of ascites in cirrhosis: report on the consensus conference of the International Ascites Club. *Hepatology.* 2003; 38 (1): 258–266. doi: 10.1053/jhep.2003.50315.
27. *DeMers D, Wachs D.* Physiology, Mean Arterial Pressure. [Updated 2023 Apr 10]. In: StatPearls [Internet]. Treasure Island (FL): StatPearls Publishing; 2023 Jan. Available from: https://www.ncbi.nlm.nih.gov/books/NBK538226.
28. *Khubutiya MSh, Voskanyan SE, Syutkin VE, Chulanov VP, Novruzbekov MS, Pasechnikov VD et al.* Recommendations for the prevention and treatment of hepatitis B and C infection in patients on the waiting list for liver transplantation and in liver transplant recipients. *Transplantologiya. The Russian Journal of Transplantation.* 2020; 12 (3): 231–244. [In Russ, English abstract]. doi: 10.23873/2074-0506-2020-12-3-231-244.
29. *Boike JR, Thomburg BG, Asrani SK, Fallon MB, Fortune BE, Izzy MJ et al.* North American Practice-Based Recommendations for Transjugular Intrahepatic Portosystemic Shunts in Portal Hypertension. *Clin Gastroenterol Hepatol.* 2022; 20 (8): 1636–1662.e36. PMID: 34274511 doi: 10.1016/j.cgh.2021.07.018.
30. *Büttner L, Aigner A, Pick L, Brittinger J, Stelb CJ, Böning G, Steitparth F*. 25 years of experience with transjugular intrahepatic portosystemic shunt (TIPS): changes in patient selection and procedural aspects. *Insights Ima-*

ging. 2022; 13 (1): 73. PMID: 35416547. doi: 10.1186/s13244-022-01216-5.

31. *Zhou Y, Zhang W, Zhang Z, Luo J, Gu J, Liu Q et al*. PTFE-covered TIPS is an effective treatment for secondary preventing variceal rebleeding in cirrhotic patients with high risks. *Eur J Gastroenterol Hepatol.* 2020 Sep; 32 (9): 1235–1243. PMID: 32744824; PMCID: PMC7423526. doi: 10.1097/MEG.0000000000001686.
32. *Sauerbruch T, Mengel M, Dollinger M, Zipprich A, Rössle M, Panther E et al*. Prevention of Rebleeding From Esophageal Varices in Patients With Cirrhosis Receiving Small-Diameter Stents Versus Hemodynamically Controlled Medical Therapy. *Gastroenterology.* 2015 Sep; 149 (3): 660–668.e1. Epub 2015 May 16. PMID: 25989386. doi: 10.1053/j.gastro.2015.05.011.
33. *Zhang M, Wang G, Zhao L, Wu Z, Zhang W, Zhang C.* Second prophylaxis of variceal bleeding in cirrhotic patients with a high HVPG. *Scand J Gastroenterol.* 2016 Dec; 51 (12): 1502–1506. Epub 2016 Jul 5. PMID: 27379704. doi: 10.1080/00365521.2016.1193218.
34. *Ardevol A, Alvarado-Tapias E, Garcia-Guix M, Brujats A, Gonzalez L, Hernández-Gea V et al.* Early rebleeding increases mortality of variecal bleeders on secondary prophylaxis with β-blockers and ligation. *Dig Liver Dis.* 2020 Sep; 52 (9): 1017–1025. Epub 2020 Jul 8. PMID: 32653417. doi: 10.1016/j.dld.2020.06.005.
35. *Irisawa A, Saito A, Obara K, Shibukawa G, Takagi T, Shishido H et al.* Endoscopic recurrence of esophageal varices is associated with the specific EUS abnormalities: severe periesophageal collateral veins and large perforating veins. *Gastrointest Endosc.* 2001 Jan; 53 (1): 77–84. PMID: 11154493. doi: 10.1067/mge.2001.108479.
36. *Monescillo A, Martínez-Lagares F, Ruiz-del-Arbol L, Sierra A, Guevara C, Jiménez E et al.* Influence of portal hypertension and its early decompression by TIPS placement on the outcome of variceal bleeding. *Hepatology.* 2004 Oct; 40 (4): 793–801. PMID: 15382120. doi: 10.1002/hep.20386.

The article was submitted to the journal on 09.02.2024

DOI: 10.15825/1995-1191-2024-2-28-33

ENDOSCOPIC FULL-THICKNESS RESECTION OF SIGMOID COLON CANCER IN A LIVER RECIPIENT

M.T. Bekov[1], A.R. Monakhov[1, 2], K.S. Smirnov[1], Ya.S. Yakunin[1], R.A. Latypov[1], D.O. Oleshkevich[1], O.M. Tsirulnikova[1, 2], S.V. Gautier[1, 2]

[1] Shumakov National Medical Research Center of Transplantology and Artificial Organs, Moscow, Russian Federation

[2] Sechenov University, Moscow, Russian Federation

Compared with the general population, solid organ transplant recipients have a higher cancer risk. This is mainly due to the use of immunosuppressive therapy. Colorectal cancer is one of the most common cancers in recipients. This paper presents the experience of endoscopic full-thickness resection (EFTR) of a sigmoid colon cancer in a liver recipient.

Keywords: solid organ transplantation, cancer morbidity, colorectal cancer, endoscopic full-thickness resection.

Organ transplantation is the operation of choice for terminal and irreversible organ failure, especially when the limit of conservative therapy has been exhausted [1]. In global practice, there is a persistent trend towards a higher number of vital organ transplants performed from both deceased and living related donors [2]. The number of regional centers in the Russian Federation, where transplantation is performed, is increasing every year. For instance, in 2022, organ transplants performed in Russia increased by 10.0% compared to 2021. In 2022, 2555 solid organ transplants were performed in Russia [3].

Solid organ recipients are at risk of malignant tumors [4]. This is largely due to the use of immunosuppressive drugs at preventing post-transplant immunologic complications [5].

Organ transplant recipients have a higher risk of developing colorectal cancer (CRC) than in the population [6]. In 2016, Safaeian et al. analyzed CRC incidence in solid organ recipients. The authors reviewed 790 CRC cases among 224,098 recipients of various organs. Recipients had elevated proximal CRC risk, while distal colon cancer was not increased, and rectal cancer was reduced compared to the general population.

According to multicenter analyses, CRC risk was significantly higher in lung recipients who were operated upon for cystic fibrosis [6–8].

Park et al. analyzed CRC incidence in kidney recipients [9]. The authors noted an elevated risk of colorectal adenomas and CRC in patients with Epstein–Barr virus and cytomegalovirus.

CRC incidence is significantly higher in liver transplant recipients with primary sclerosing cholangitis and with inflammatory bowel disease [10–11].

The outcome of 6,244 heart transplants was analyzed in a multicenter study by Sagastagoitia-Fornie et al. CRC was diagnosed in 116 recipients. The incidence of CRC increased from 56.6 per 100,000 person-years among under 45-year-olds to 436.4 per 100,000 person-years among over 64-year-olds [12].

Surgery is the main definitive treatment for CRC patients [13]. For early (stage 0–1) CRC, organ-preserving procedures like endoscopic mucosal resection with dissection in the submucosal layer is recommended.

Endoscopic full-thickness resection (EFTR) using a full-thickness resection device (FTRD) can replace surgical resection in some cases. The EFTR procedure is shown schematically in Fig. 1.

Andrisani et al. performed EFTR in 110 patients [14]. Main indications were: recurrent adenoma (39 cases), incomplete resection at endoscopic removal of tumor masses (26), non-lifting lesion (12), adenoma involving the appendix (2), subepithelial lesions (10 cases), suspected T1 carcinoma (16) and others. Mean size of specimens was 20 mm (range 6–42 mm). Residual disease was evident in only seven patients.

P. Aepli et al. reported the use of EFTR in 33 patients with colonic epithelial neoplasms [15]. Main indications were recurrent adenoma and nonlifting colorectal lesions. In 31 cases, complete removal of pathologic tissues was achieved. Three post-procedure bleedings and one perforation were seen.

CASE REPORT

Patient K., 54 years old, in August 2019 complained of general weakness, abdominal enlargement. In September 2019, bloody vomiting episodes and melena were noted. At the same time, toxic liver cirrhosis

Corresponding author: Maksat Bekov. Address: 1, Shchukinskaya str., Moscow, 123182, Russian Federation. Phone: (926) 399-49-75. E-mail: doctorbekov@gmail.com

(regular alcohol consumption every week, abstinence since 2019) with portal hypertension syndrome (ascitic syndrome, grade 3 esophageal varices (EV) according to N. Soehendra, K. Binmoeller) was diagnosed. Several laparocentesis sessions were performed, and a total of up to 30 liters of ascitic fluid were evacuated. Endoscopic variceal ligation (EVL) was performed in October 2019. The postoperative period was uneventful. The patient was diagnosed with extrinsic portal vein thrombosis in November 2019, for which apixaban therapy was administered at a dosage of 2.5 mg twice a day. In 2020, a second endoscopic ligation of grade 3 EV was performed, without complications. One month later, there were signs of progression of portal thrombosis which spread to the superior mesenteric vein. An increase in edematous-ascitic syndrome has been noted since December 2020.

In March 2021, the patient came to Shumakov National Medical Research Center of Transplantology and Artificial Organs. A comprehensive examination was performed, and the diagnosis was: cirrhosis of alimentary toxic genesis, decompensation, Child–Pugh class B, MELD-Na 12, complicated by portal hypertension syndrome (ascites, EV), hepatocellular failure (coagulopathy, hyperbilirubinemia, stage 1 hepatic encephalopathy) was established. The following concomitant diseases were diagnosed: type 2 diabetes mellitus; grade 2 arterial hypertension, risk 3; cholelithiasis with cholecystolithiasis. Due to the severity of the underlying disease and the futility of conservative therapy, liver transplantation (LT) was adopted as the definitive treatment method. The patient was added to the LT waiting list since there were no contraindications.

In April 2021, in preparation for LT, an outpatient colonoscopy was performed, which revealed adenomatous epithelial neoplasms of the colon and rectum. Preparation for the study was carried out with a Macrogol-based drug. The quality of preparation was evaluated as unsatisfactory (4 points on the Boston scale: left side (LS), 1; transverse colon (TS), 1; right side (RS), 2. Scheduled in-hospital endoscopic polypectomy was recommended. However, the patient refused hospitalization.

In July 2021, orthotopic LT from a deceased ABO-compatible donor was performed according to the classical technique. Immunosuppressive therapy was induced with basiliximab 20 mg and methylprednisolone 500 mg, followed by a reduction in methylprednisolone dosage and transition to oral administration with a daily dosage of 6 mg. The postoperative period was uneventful. On day 2, the second drug of the immunosuppressive therapy – Tacrolimus – was initiated, with gradual increase in target drug concentrations. Day 5 saw the start of mycophenolate mofetil at a dose of 1000 mg twice a day. The patient was discharged from the hospital on day 11 following LT under outpatient follow-up due to the situation having stabilized, the graft functioning satisfactorily, and there were no longer any reasons for further inpatient care.

There were regular visits for outpatient follow-up with clinical, laboratory and instrumental monitoring of the graft and general medical status. From August 2021, the patient was converted to prolonged-release tacrolimus with achievement of target drug concentrations in blood.

In December 2021, increased serum alpha-fetoprotein level (17.13 IU/mL) was noted. Diagnostic colonoscopy was performed in January 2022, which revealed: 3 epithelial masses of the ascending colon up to 6 mm in diameter, type 0-Is according to Paris classification, type 2 according to NICE classification; 3 epithelial masses of the transverse colon up to 6 mm in diameter, type 0-IIa

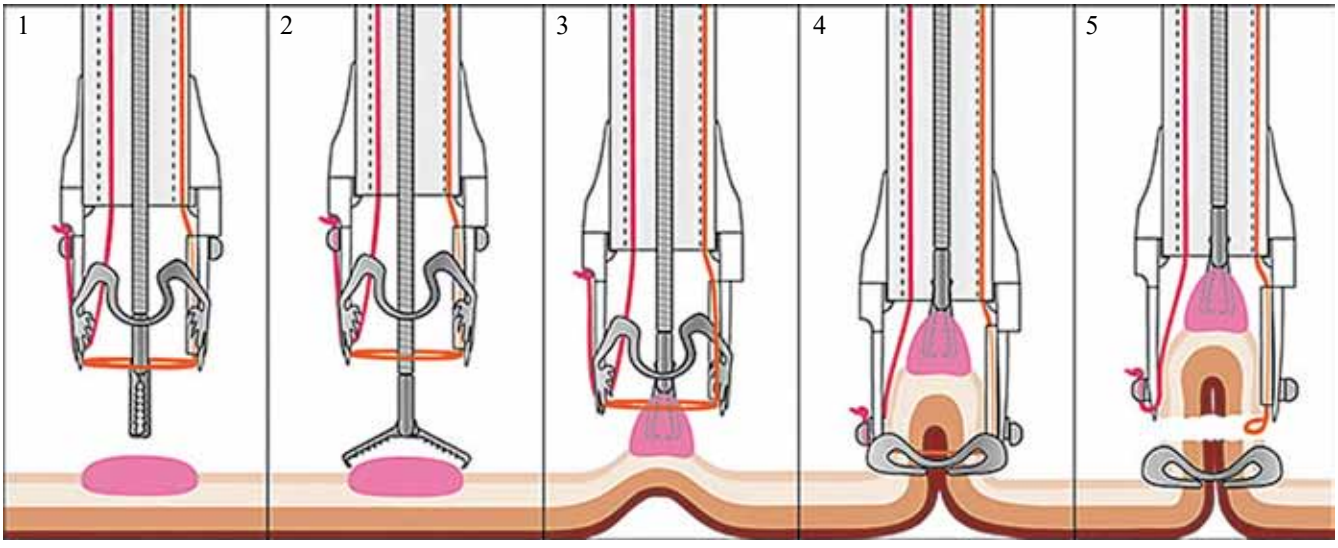

Fig. 1. The EFTR system is presented. 1, marking of the surgical intervention site; 2, grasping of the target tissue with a forceps; 3, retrieval of the target tissue within cap and fixation; 4, release of the clip; 5, closure of the snare and tissue incision using electrosurgery (source: www.ovesco.com)

according to Paris classification, type 2 according to NICE classification; two rectal epithelial masses up to 6 mm in diameter, type 0-Is according to Paris classification, type 2 according to NICE classification. Endoscopic cold snare polypectomy with subsequent histological examination was performed. Also, in the sigmoid colon, at 30–35 cm from the anus, a formation of up to 7–8 mm in diameter, type 0-IIa+IIc according to Paris classification, type 3 according to NICE classification, with central retraction was determined. The epithelial pattern was obliterated in some places; in the narrow band imaging (NBI) mode, curved multilobular vessels were detected (Fig. 2). Instrumental palpation revealed wall infiltration, but slight mobility remained during traction. A biopsy was taken. Also, the tumor was endoscopically marked with a Black Eye marker. Preparation for the study was carried out with a Macrogol-based agent with the addition of ascorbic acid. The quality of preparation was evaluated as satisfactory (6 points on the Boston scale: left side (LS), 2; transverse colon (TS), 2; right side (RS), 2.

Histological examination of the removed epithelial neoplasms revealed colonic tubular adenomas with mild dysplasia. The histologic picture of the epithelial neoplasm in the sigmoid colon was represented by a highly differentiated adenocarcinoma (low-grade).

Oncologic search was performed, including contrast-enhanced computed tomography of the brain, chest and abdominal cavity, esophagogastroduodenoscopy, and positron emission tomography. There were no signs of metastatic lesion. Taking into account the size of the tumor mass, absence of metastases, spread of the process (pT1N0M0, stage I), it was decided to perform EFTR of the sigmoid colon cancer.

In February 2022, in the operating room under intravenous sedation, EFTR of the sigmoid colon cancer was performed using the OTSC clipping system and Ovesco® endoscopic clips (Ovesco AG, Germany) (Olympus Evis Exera III video endoscopy system, CF-190L colonoscope (Olympus Corporation, Japan)). Using alligator biopsy forceps (Endo Stars LLC, Russia), the mass was retrieved within the device for clip application with grasping of the intestinal wall with unchanged mucosa. The next stage was application of Ovesco® clip within the healthy tissues. The epithelial formation was removed in ENDO CUT Q mode (effect 3, cutting width 1, cutting interval 6) (ERBE VIO 300D, Erbe Elektromedizin, Germany). The removed fragment was extracted from the intestinal lumen. No signs of residual tumor tissue were found during revision (Fig. 3).

Histological study revealed numerous colonic mucosa fragments with invasive growth of highly differentiated adenocarcinoma, moderate lymphocytic-leukocytic infiltration in the stroma. The resection margin was intact.

The postoperative period was uneventful. Following surgery, the patient was discharged from the hospital on day 7.

When performing control colonoscopy 6 months and 1 year 6 months after EFTR of a sigmoid colon cancer, no evidence of relapse was found (Fig. 4). At the time of writing, the follow-up period was 2 years.

CONCLUSION

Solid organ recipients have an increased risk of cancer, including CRC, especially with age and time since transplant. This statistical pattern is largely due to the use of immunosuppressive drugs for vital indications.

This patient cohort requires more thorough cancer screening. The gold standard for CRC screening is colonoscopy. The diagnostic value of this technique depends both on quality of preparation (including adherence to a specialized diet with the exclusion of fiber-rich foods),

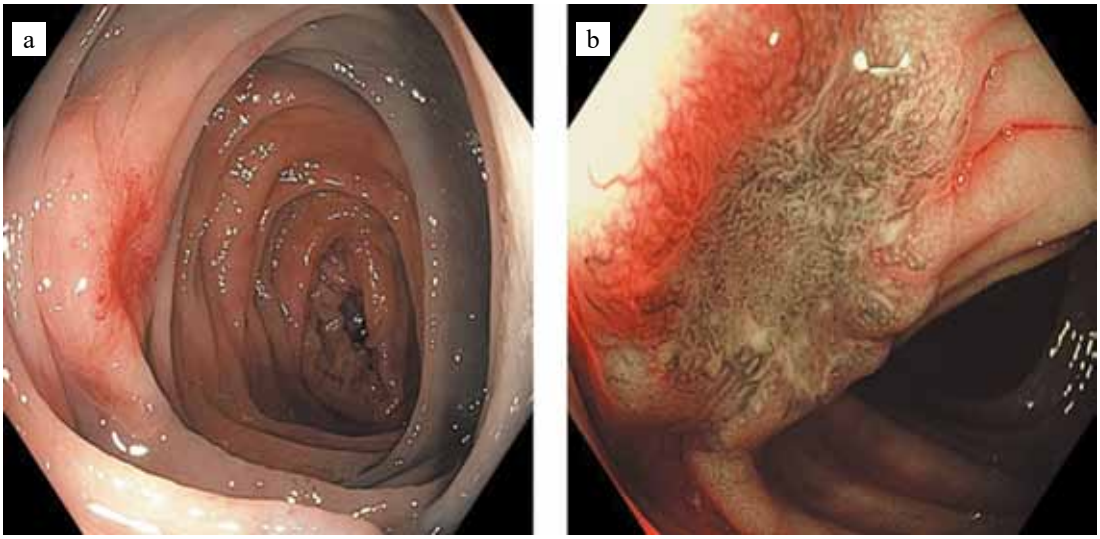

Fig. 2. Epithelial formation of the sigmoid colon: a, in white color; b, in narrow-spectral imaging mode, there is pronounced "neoangiogenesis", a sign of malignant growth

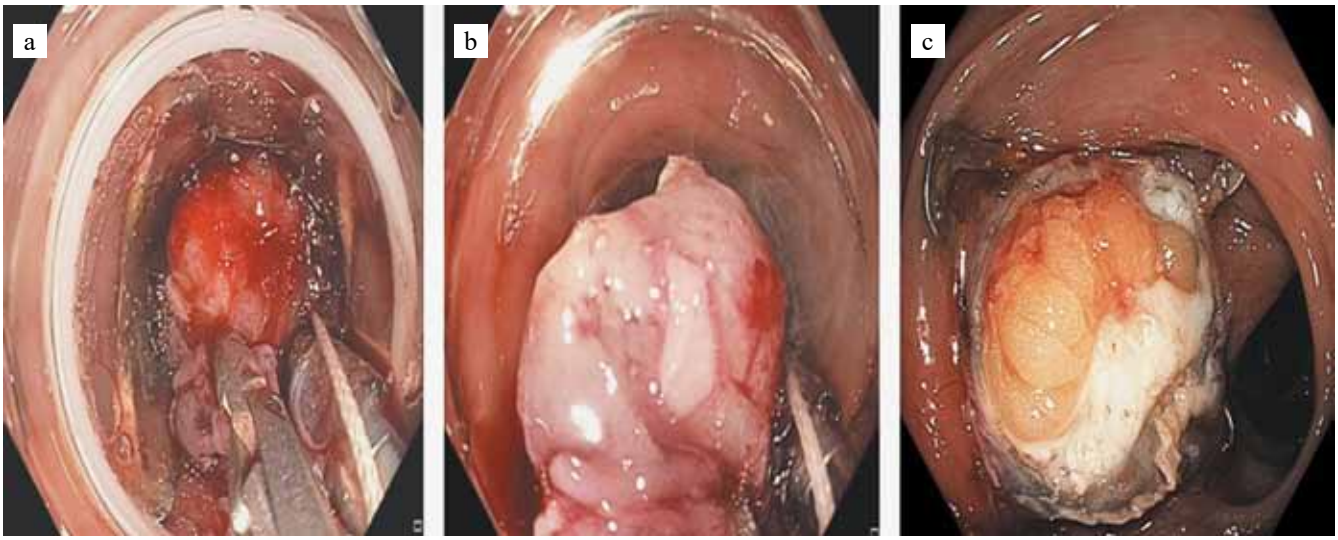

Fig. 3. Surgical intervention stages. a, grasping of the tumor tissue and retrieval within cap; b, fragment of the sigmoid colon wall resected using electrosurgery; c, revision after adenocarcinoma removal

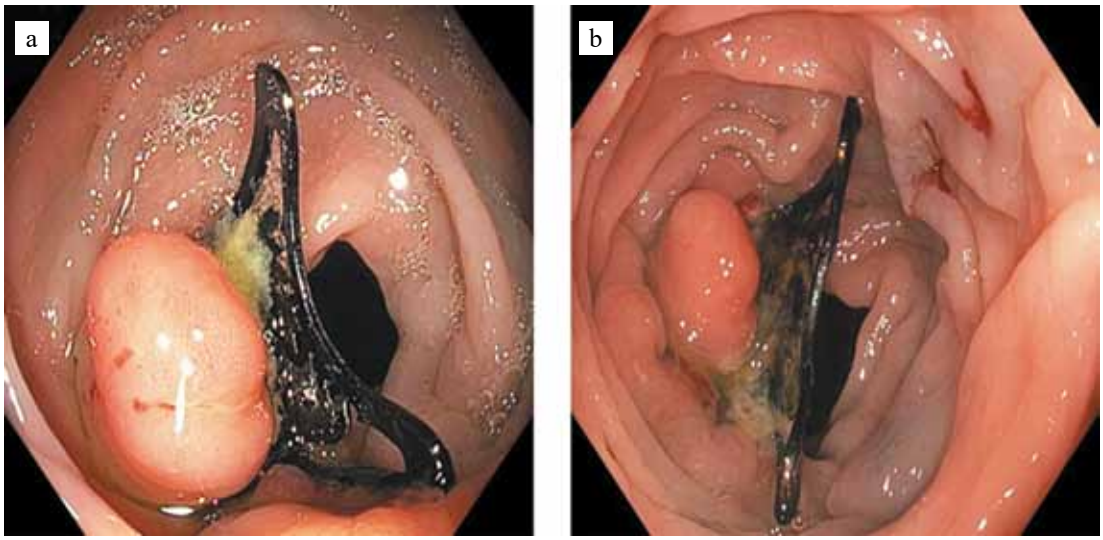

Fig. 4. Control colonoscopy after EFTR of sigmoid colon cancer: a, at 6 months; b, at 1 year 6 months (the clip is still in the intestinal lumen)

on split administration of Macrogol-based drugs, and on conducting an examination using expert-level equipment with a water-jet pump and carbon dioxide insufflator.

The use of EFTR of colonic epithelial neoplasms, if technically feasible and if there are no contraindications, may be an alternative to colon resection. EFTR can reduce the incidence of surgical complications, length of hospitalization, and can be considered in patients for whom abdominal surgery is contraindicated due to high anesthetic risks.

The authors declare no conflict of interest.

REFERENCES

1. Transplantologiya i iskusstvennye organy. Pod red. S.V. Gautier. M.: Laboratoriya znaniy, 2018; 319.
2. https://www.irodat.org [Internet]. International Registry In Organ Donation And Transplantation. Available from: https://www.irodat.org.
3. *Gautier SV, Khomyakov SM*. Organ donation and transplantation in the Russian Federation in 2022. 15th Report from the Registry of the Russian Transplant Society. *Russian Journal of Transplantology and Artificial Organs*. 2023; 25 (3): 8–30. https://doi.org/10.15825/1995-1191-2023-3-8-30.
4. *Buell JF, Gross TG, Woodle ES*. Malignancy after transplantation. *Transplantation*. 2005; 80 (2S): S254–S264. doi: 10.1097/01.tp.0000186382.81130.ba.
5. *Penn I.* Post-transplant malignancy: the role of immunosuppression. *Drug safety*. 2000; 23 (2): 101–113. doi: 10.2165/00002018-200023020-00002.
6. *Safaeian M, Robbins HA, Berndt SI, Lynch CF, Fraumeni JF Jr, Engels EA.* Risk of Colorectal Cancer After

Solid Organ Transplantation in the United States. *Am J Transplant*. 2016 Mar; 16 (3): 960–967. doi: 10.1111/ajt.13549.

7. *Meyer KC, Francois ML, Thomas HK, Radford KL, Hawes DS, Mack TL et al.* Colon cancer in lung transplant recipients with CF: increased risk and results of screening. *J Cyst Fibros*. 2011 Sep; 10 (5): 366–369. doi: 10.1016/j.jcf.2011.05.003.
8. *Merchea A, Shahjehan F, Croome KP, Cochuyt JJ, Li Z, Colibaseanu DT, Kasi PM.* Colorectal Cancer Characteristics and Outcomes after Solid Organ Transplantation. *J Oncol*. 2019 Feb 28; 2019: 5796108. doi: 10.1155/2019/5796108.
9. *Park JM, Choi MG, Kim SW, Chung IS, Yang CW, Kim YS et al.* Increased incidence of colorectal malignancies in renal transplant recipients: a case control study. *Am J Transplant*. 2010 Sep; 10 (9): 2043–2050. doi: 10.1111/j.1600-6143.2010.03231.x.
10. *Singh S, Edakkanambeth Varayil J, Loftus EV Jr, Talwalkar JA.* Incidence of colorectal cancer after liver transplantation for primary sclerosing cholangitis: a systematic review and meta-analysis. *Liver Transpl*. 2013 Dec; 19 (12): 1361–1369. doi: 10.1002/lt.23741.
11. *Silva MA, Jambulingam PS, Mirza DF.* Colorectal cancer after orthotopic liver transplantation. *Crit Rev Oncol Hematol*. 2005 Oct; 56 (1): 147–153. doi: 10.1016/j.critrevonc.2004.12.013.
12. *Sagastagoitia-Fornie M, Morán-Fernández L, Blázquez-Bermejo Z, Díaz-Molina B, Gómez-Bueno M, Almenar-Bonet L et al.* Incidence and Prognosis of Colorectal Cancer After Heart Transplantation: Data From the Spanish Post-Heart Transplant Tumor Registry. *Transpl Int*. 2023 May 19; 36: 11042. doi: 10.3389/ti.2023.11042.
13. *Fedyanin MYu, Achkasov SI, Bolotina LV, Gladkov OA, Glebovskaya VV, Gordeev SS i dr.* Prakticheskie rekomendatsii po lekarstvennomu lecheniyu raka obodochnoy kishki i rektosigmoidnogo soedineniya. *Zlokachestvennye opukholi*. 2021; 11 (3s2-1): 330–372. doi: 10.18027/2224-5057-2021-11-3s2-22.
14. *Andrisani G, Soriani P, Manno M, Pizzicannella M, Pugliese F, Mutignani M et al.* Colo-rectal endoscopic full-thickness resection (EFTR) with the over-the-scope device (FTRD®): A multicenter Italian experience. *Dig Liver Dis*. 2019 Mar; 51 (3): 375–381. doi: 10.1016/j.dld.2018.09.030.
15. *Aepli P, Criblez D, Baumeler S, Borovicka J, Frei R.* Endoscopic full thickness resection (EFTR) of colorectal neoplasms with the Full Thickness Resection Device (FTRD): Clinical experience from two tertiary referral centers in Switzerland. *United European Gastroenterol J*. 2018 Apr; 6 (3): 463–470. doi: 10.1177/2050640617728001.

The article was submitted to the journal on 12.02.2024

DOI: 10.15825/1995-1191-2024-2-34-41

AZYGOPORTAL DISCONNECTION OR A COMBINATION OF NON-SELECTIVE BETA-BLOCKERS AND ENDOSCOPIC VARICEAL LIGATION TO PREVENT RECURRENT BLEEDING IN PATIENTS WITH CIRRHOSIS AWAITING TRANSPLANTATION

R.V. Korobka[1, 2], S.V. Gautier[3, 4], Yu.V. Khoronko[2], V.D. Pasechnikov[1, 5], A.M. Shapovalov[1], M.V. Malevanny[1, 2], E.S. Pak[1, 2], D.V. Pasechnikov[5], E.V. Tadiyeva[1, 2]

[1] Rostov Regional Clinical Hospital, Rostov-on-Don, Russian Federation
[2] Rostov State Medical University, Rostov-on-Don, Russian Federation
[3] Shumakov National Medical Research Center of Transplantology and Artificial Organs, Moscow, Russian Federation
[4] Sechenov University, Moscow, Russian Federation
[5] Stavropol State Medical University, Stavropol, Russian Federation

Objective: to compare the efficacy of azygoportal disconnection (APD) surgery and a combination between endoscopic variceal ligation (EVL) and non-selective beta-blockers (NSBBs) in the prevention of recurrent variceal bleeding (RVB). To compare the incidence of gastric variceal bleeding (GVB) after these manipulations in patients with decompensated cirrhosis waitlisted for liver transplantation (LTx). **Materials and methods.** Patients with decompensated cirrhosis underwent RVB prophylaxis by APD surgery or by a combination of EVL and NSBBs. **Results.** There were no significant differences in clinical, laboratory, demographic parameters, MELD-Na and Child–Turcotte–Pugh (CTP) scores, and frequencies of medium- and large-sized varicose veins among subgroups of patients with different RVB prophylaxis methods Patients with decompensated cirrhosis who underwent APD surgery did not experience any RVB episodes during the LTx waiting period, which lasted two years from the start of bleeding prophylaxis. In the same period, RVB occurred in 100% of cases in the EVL plus NSBBs group. Using the Kaplan–Meier method with the Log-Rank test, a significant difference ($p = 0.0001$) was found between the proportions of non-RVB patients in the APD and EVL + NSBBs groups. In the meantime, 48.1% of patients who had APD surgery developed GVB, while 100% of cases in EVL + NSBBs group did not. The Kaplan–Meier method with the Log-Rank test revealed a significant difference ($p = 0.0001$) between the proportion of non-GVB patients in EVL + NSBBs and APD groups.

Keywords: liver transplant waiting list, recurrent variceal bleeding, gastric variceal bleeding, endoscopic variceal ligation, nonselective beta-blockers, azygoportal disconnection.

INTRODUCTION

The transition from compensated to decompensated cirrhosis, which is an indication for inclusion in the waiting list for liver transplantation (LTx) [1], is accompanied by clinically significant portal hypertension (CSPH), in which the leading cause of mortality among patients waiting for LTx is bleeding varicose veins [1–3]. It is known that after the first episode of bleeding esophageal varices, there is a high probability of recurrent variceal bleeding (RVB) within 2–3 days after the patient's condition has stabilized, reaching a frequency of up to 60% within a week, if no measures are taken to prevent this CSPH complication [4, 5]. It was found that secondary prophylaxis of RVB in this patient cohort does not eliminate the risk of development in 60% of patients within 1 year [6] and in 29–57% within two years after the first bleeding episode [7].

Experts from Baveno VII recommend "first-line therapy" to prevent RVB. This involves endoscopic variceal ligation (EVL) in combination with traditional nonselective beta-blockers (NSBBs) or carvedilol [1]. If EVL is contraindicated or there is an intolerance to drug therapy, any of the components of this combination may be used. The expert council recommends implantation of a transjugular intrahepatic portosystemic shunt (TIPS) as a second-line therapy [1].

Even though TIPS implantation is effective in reducing CSPH levels by preventing RVB, its use is considered as a step towards subsequent LTx because of RVB caused by stent block [8] and subsequent development of portosystemic hepatic encephalopathy (HE) [9].

Corresponding author: Victor Pasechnikov. Address: 21, Aviatsionnaya str., Stavropol, 355017, Russian Federation. Phone: (962) 447-75-13. E-mail: passetchnikov@mail.ru

Along with TIPS implantation, azygoportal disconnection (APD) surgery in various modifications has been proposed to prevent bleeding from the GDP [10, 11]. We have previously shown high efficacy of APD in the prevention of bleeding esophageal varices in patients awaiting LTx [12].

Objective: to compare the efficacy of APD surgery and a combination of EVL with NSBBs in the prevention of RVB. To compare the incidence of gastric variceal hemorrhage after these manipulations in patients with decompensated cirrhosis waitlisted for LTx.

MATERIALS AND METHODS

The comparative retrospective study included 177 patients with decompensated cirrhosis who were waiting for LT between 2016 and 2023 and had experienced at least one incident of bleeding varicose veins.

Inclusion criteria: patients with decompensated cirrhosis must have had at least one bleeding varicose vein during their stay on the liver transplant waitlist (LTWL); they must have had virus-related cirrhosis (HBV- or HCV-associated etiology), alcohol-related cirrhosis, or cirrhosis of mixed etiology (virus and alcohol); they must have completely abstained from alcohol for at least three months (confirmed by addiction specialists) prior to inclusion in the LTWL for patients with alcohol-related cirrhosis; they have Child–Turcotte–Pugh (CTP) classes B and C cirrhosis.

Exclusion criteria: hepatocellular cancer or other tumors, infectious diseases, portal vein thrombosis (PVT), contraindications to NSBBs (bradyarrhythmia, bronchial asthma, obstructive pulmonary disease), and diabetes mellitus.

The first group of patients included in the study consisted of 150 patients with a first bleeding episode who underwent EVL procedure in combination with NSBB administration. In cases where first-line therapy for prophylaxis of recurrent hemorrhage (endoscopic ligation in combination with non-selective beta-blockers) after stabilization of the patient's condition due to bleeding failed, 27 patients were routinely treated with APD.

All parameters included for subsequent analysis from a continuously updated electronic patient database (demographic, clinical and laboratory parameters) were obtained after approval of the study by the local ethics committee. Patient follow-up, including repeated studies of laboratory parameters, follow-up control of drug therapy, was carried out by specialists from the Center for Surgery and Donation Coordination, Rostov Regional Clinical Hospital.

When patients were enrolled in the LTWL, an examination was carried out on them, including laboratory and instrumental studies. These tests were repeated at 3-month intervals for stable patients (clinical and biochemical blood tests, haemostasis parameters, MELD-Na score and CTP score), and abdominal ultrasound was performed every 6 months. Whenever a patient's condition became unstable, laboratory and instrumental investigations were carried out as indicated.

In all patients, esophagogastroduodenoscopy (EGD) was performed to screen for varicose veins with high risk of bleeding (medium and large varicose veins) according to the Baveno VI Expert Committee [13] and World Gastroenterology Organisation (WGO) [14] guidelines.

The International Ascites Club (IAC) criteria were used to assess the severity of diuretic-responsive ascites [15]. The IAC criteria [15] and the CIRAS scale [16], which comprises clinical (no response to diuretic medication and increased volume of fluid in the abdominal cavity) and laboratory (plasma Na level <125 mmol/L) criteria, were used to diagnose diuretic-resistant ascites. For a score of 5–6 on this scale, diuretic-resistant ascites was considered well diagnosed [16].

Patients who responded to therapy received diuretics; patients with diuretic-resistant ascites underwent paracentesis.

After intravenous analgesia (sedation), EVL procedure was performed in a standard way using a varicose vein ligation kit and video esophagogastroduodenoscopy device. Varicose veins were ligated proximally, starting from the gastroesophageal junction. The number of rubber ligatures used varied from 2 to 4, depending on the size of the varicose veins. The EVL procedure was performed to obliterate all varicose veins fulfilling the criteria for emergency therapy [13, 14]. Repeated EGDs at 3-month intervals served as a control method, and if new varicose veins were found, the EVL procedure was repeated until the varicose veins were completely obliterated.

To perform APD surgery under total intravenous anesthesia, an upper midline laparotomy was carried out according to the standard technique. In order to adequately visualize the cardiac part of the stomach and the abdominal part of the esophagus, the gastroesophageal junction was lowered together with the fiber. The vagus nerve was isolated. Selective proximal vagotomy was performed. Mobilization of the stomach fundus and retroperitoneal part of the cardia with crossing of the vessels of the gastroesophageal ligament and branches of the left gastric artery and vein was performed. The abdominal part of the esophagus was isolated 6–8 cm above the lower esophageal sphincter with isolation, ligation and crossing of all collaterals, and then it was completely crossed at 2–3 cm from the esophageal-gastric recess. Using a linear stapler, we resected the part of the cardia facing the esophagus, 4–5 cm from the angle of His.

The second row of seromuscular sutures was used to reinforce the row of the machine stitch of the gastric stump. The stomach body was juxtaposed with the esophagus by moving its stump toward the liver. Next, a new ligamentous apparatus was formed by fixing the esophagus to the diaphragm legs with two ligamentous

sutures. The least vascularized zone was visually determined on the anterior wall of the stomach body, where a double-row esophagogastric anastomosis (EGA) was formed with a precision suture using PDS 5/0 monofilament. Then an anti-reflux cardia was formed: esophagus and EGA zone were wrapped with the stomach fundus, which was sutured and fixed with interrupted seromuscular sutures to the anterolateral surfaces of the esophagus and to the right and left diaphragm legs, closer to their thoracic part. Next, using single seromuscular sutures, the stomach fundus was fixed to the greater curvature and the anterior wall below the EGA, thus completing the formation of anti-reflux cardia.

The obtained data were analyzed using statistical software package IBM SPSS Statistics (version 23). Type of distribution of obtained variables of the studied samples was determined using the Kolmogorov–Smirnov test and the Lilliefors significance level. Where the variables are found to be of normal distribution, further analysis included calculation of arithmetic mean (M) and determination of standard deviation (SD). The significance of differences between compared variables was determined by Student's t test, using $p < 0.05$ as a criterion. The median (Me) with interquartile range (IQR, difference between the 25th and 75th percentiles) was used for further analysis of variables with non-normal distribution. The Wilcoxon test used for nonparametric analysis was used to determine the significance of differences in pairwise comparisons of dependent variables; Pearson's chi-squared test was used in comparisons of independent variables. The Mann–Whitney U test was used to compare variables in small sample sizes. ANOVA test was used for analysis of variance. Contingency tables were used in the analysis of qualitative parameters – frequencies of variables and their proportions (%); for small sample sizes, Fisher's exact test was used to assess the significance of the relationship between two variables.

The proportions of patients without RVB in the compared groups were determined by the Kaplan–Meier method. The significance of differences between the compared curves (patient proportions) was determined by calculating the log-rank test [Log-Rank (Mantel-Cox)].

RESULTS

Table 1 presents demographic, clinical, laboratory, and MELD-Na scores for the groups of patients who received NSBB therapy plus EVL or who underwent APD during the transplant waiting period.

Table 2 presents data on gender composition, as well as etiology of cirrhosis, CTP grade and severity of varicose veins in patients who received NSBB therapy plus EVL or who underwent APD surgery.

The compared groups (Table 1 and Table 2) were homogeneous in terms of demographic, clinical, and laboratory parameters, as well as in terms of MELD-Na scores, CTP classes B and C, and frequency of varicose veins of medium (grade 2) and large (grade 3) size.

All patients (100%) who underwent the EVL procedure in combination with receiving NSBBs developed RVB while waiting 2 years for LTx from the start of bleeding prophylaxis. Patients with decompensated cirrhosis who underwent APD surgery did not experience any RVB episodes during the LTx waiting period, which lasted two years from the beginning of bleeding prophylaxis.

Using the Kaplan–Meier method with the Log-Rank test, a significant difference ($p = 0.0001$) was found between the proportions of patients without RVB in the APD group and the NSBB + EVL group (Fig. 1).

Table 1

Comparative characteristics of EVL + NSBBs and APD patients (normal and non-normal distribution)

Indicator	EVL + NSBBs (n = 150) M ± SD	APD (n = 27) M ± SD	Statistical significance
Normal distribution (M ± SD)			
Age	49.76 ± 11.02	52.34 ± 10.89	p > 0.05
Hemoglobin (g/L)	89.96 ± 12.04	87.67 ± 11.99	p > 0.05
Leukocytes ($\times 10^9$/L)	3.46 ± 1.13	3.79 ± 1.75	p > 0.05
Platelets ($\times 10^9$/L)	89.35 ± 34.45	93.56 ± 42.23	p > 0.05
Plasma albumin (g/L)	31.12 ± 3.21	30.45 ± 2.89	p > 0.05
MELD-Na score	22.01 ± 3.11	21.92 ± 3.14	p > 0.05
Non-normal distribution (Me; IQR)			
INR	1.92 (1.65–2.10)	1.90 (1.62–2.12)	p > 0.05
Bilirubin (μmol/L)	86.5 (66.50–115.00)	84.0 (62.50–112.50)	p > 0.05
Creatinine (μmol/L)	110.2 (97.5–128.20)	109.4 (98.5–122.25)	p > 0.05
Na (mmol/L)	136.8 (132.0–140.5)	135.2 (128.5–142.5)	p > 0.05
CTP (points)	12.00 (8.00–14.50)	11.00 (8.50–14.00)	p > 0.05

Note: EVL, endoscopic variceal ligation; NSBBs, nonselective beta-blockers; APD, azygoportal disconnection; MELD-Na, Model for End-Stage Liver Disease-Sodium; INR, International normalized ratio; CTP, Child–Turcotte–Pugh; Na, sodium.

At the same time, bleeding from gastric varices occurred in 48.1% of APD patients, which was absent in 100% of EVL + NSBB patients. The Kaplan–Meier method with the Log-Rank test showed a significant difference ($p = 0.0001$) between the proportion of patients without bleeding gastric varices in the APD group or EVL + NSBB cohort (Fig. 2).

DISCUSSION

According to expert recommendations, secondary prophylaxis for RVB is performed through EVL in combination with traditional NSBBs or carvedilol (first-line therapy) [1]. Our study showed a high incidence of RVB in patients who waited for LTx for 24 months and were treated with secondary prophylaxis using first-line therapy (EVL + NSBBs). With this prophylaxis strategy, RVB started to develop from the first weeks of EVL in combination with NSBBs and continued up to 24 months (100% of cases). According to Garcia-Tsao et al. [6], the risk of developing RVB within a year is 60% despite bleeding prophylaxis.

It has been found that the main risk factor for RVB is higher hepatic venous pressure gradient (HVPG) [17]. Liu et al. [18] found that the main reason for the development of RVB was the increase in HVPG reaching high figures (≥25 mmHg). The authors of the study noted that neither EVL, nor NSBBs, nor an EVL + NSBBs combination provided reliable prophylaxis of RVB. This is quite understandable due to the following facts. Firstly, EVL has been found to have no effect on the increase in HVPG during CSPH progression [19], and secondly, NSBBs do not reduce HVPG as desired [20]. The in-

Table 2

Comparison of clinical and gender characteristics of EVL + NSBBs and APD patients

Indicator	EVL + NSBBs (n = 150) (%)	APD (n = 27) (%)	Statistical significance
Male gender	85 (56.6%)	15 (55.6%)	$p > 0.05$
Virus-related cirrhosis	72 (48.0%)	13 (48.1%)	$p > 0.05$
Alcohol-related cirrhosis	39 (26.0%)	8 (29.6%)	$p > 0.05$
Other causes of cirrhosis	39 (26.0%)	6 (22.3%)	$p > 0.05$
Esophageal varices, grade 2	40 (26.6%)	7 (25.9%)	$p > 0.05$
Esophageal varices, grade 3	110 (73.4%)	20 (74.1%)	$p > 0.05$
CTP class A	4 (2.7%)	1 (3.7%)	$p > 0.05$
CTP class B	37 (24.7%)	7 (25.9%)	$p > 0.05$
CTP class C	109 (72.6%)	19 (70.4%)	$p > 0.05$

Note: CTP, Child–Turcotte–Pugh; Na, sodium.

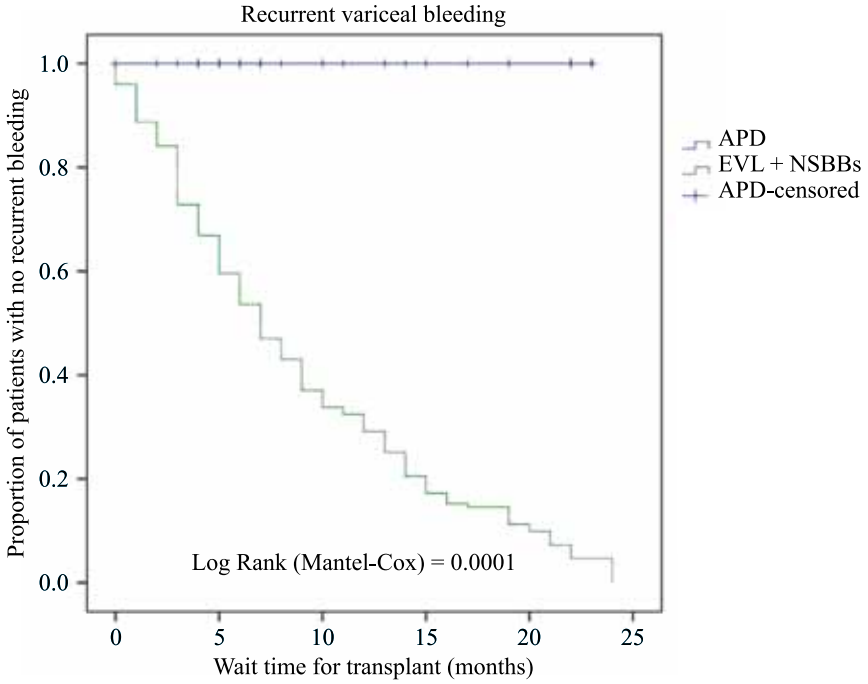

Fig. 1. Proportions of non-RVB patients who underwent APD surgery or received EVL + NSBB therapy (Kaplan–Meier method with Log-Rank test)

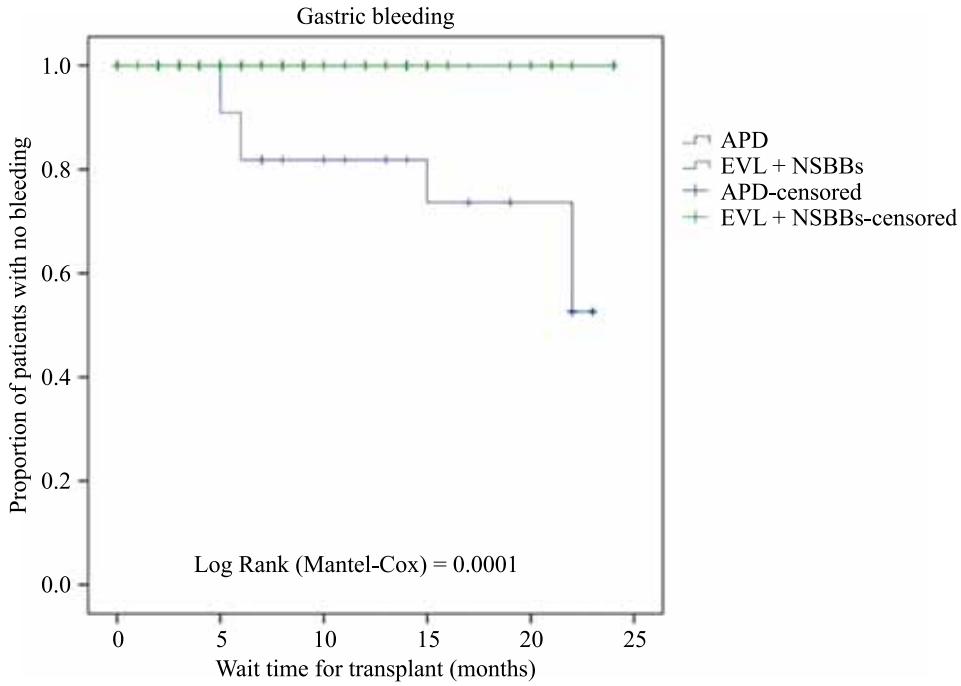

Fig. 2. Proportions of patients with no gastric variceal bleeding who underwent APD surgery or received EVL + NSBB therapy (Kaplan–Meier method with Log-Rank test)

significant level of HVPG reduction with propranolol (10.1–23.2%) and carvedilol (18.6–27.7%) [20] may be due to the lack of response to these drugs in some patients [20, 21].

We believe that the presence of responders and non-responders to NSBBs among patients with CSPH accounts for the reduced effectiveness of secondary prophylaxis of RVB using EVL in combination with beta-blocker administration. Incidence of re-bleeding in non-responders was found to be significantly higher than that in responders of acute hemodynamic response to propranolol use [22].

We discovered that individuals with decompensated cirrhosis who underwent APD surgery did not exhibit RVB during the two-year waiting period for LTx. APD was performed according to the original technique (Russian Federation patent, No 2412657 dated February 27, 2011) [11]. In the past, we have shown that this procedure can effectively prevent rebleeding and result in a three-year absence of recurrent bleeding [23].

However, despite the absence of RVB for 2 years, the present study did reveal the development of recurrent bleeding from gastric varices, which accounted for 48.1% of cases during the specified follow-up period. On the other hand, there was no evidence of gastric variceal hemorrhage associated with the use of EVL plus NSBBs in any case.

The difference in the incidence of gastric variceal bleeding for EVL plus NSBBs and for APD in our opinion is explained by the dynamics of HVPG after these invasive interventions. Abraldes et al. [19] found that EVL does not lead to higher HVPG, while Sinagra et al. [20] found a slight decrease in HVPG after propranolol or carvedilol therapy. Meanwhile, APD operation, disconnecting portocaval connections and reducing blood flow to esophageal varices, does not reduce HVPG and can be complicated by gastric variceal bleeding.

CONCLUSION

APD is an effective method of RVB prophylaxis when alternative treatment, including TIPS implantation or liver transplantation, is not possible.

After performing APD, repeated EGD is necessary for early detection of newly developed varicose veins in the stomach followed by an EVL procedure.

The authors declare no conflict of interest.

REFERENCES

1. *De Franchis R, Bosch J, Garcia-Tsao G, Reiberger T, Ripoll C; Baveno VII Faculty*. Baveno VII – Renewing consensus in portal hypertension. *J Hepatol*. 2022; 76 (4): 959–974. PMID: 35120736. doi: 10.1016/j.jhep.2021.12.022.
2. *Liu L, Nie Y, Liu Q, Zhu X.* A Practical Model for Predicting Esophageal Variceal Rebleeding in Patients with Hepatitis B-Associated Cirrhosis. *Int J Clin Pract.* 2023 Aug 3; 2023: 9701841. doi: 10.1155/2023/9701841.
3. *Korobka VL, Pak ES, Shapovalov AM, Kostrykin MYu, Tkachev AV.* Analysis of four-year management of the waiting list for liver transplantation in Rostov region: prospects for reducing mortality of candidates listed for liver transplantation. *Medical Herald of the South of Russia*. 2019; 10 (3): 32–39. [In Russ, English abstract]. doi: 10.21886/2219-8075-2019-10-3-32-39.

4. *Garcia-Tsao G, Bosch J.* Varices and Variceal Hemorrhage in Cirrhosis: A New View of an Old Problem. *Clin Gastroenterol Hepatol.* 2015; 13: 2109–2117. doi: 10.1016/j.cgh.2015.07.012.
5. *Asghar S, Mustafa J, Rehman HU, Farooq MK, Waheed MU, Shahid S.* Predictors Of Re-Bleeding After Oesophageal Variceal Banding In Cirrhotic Patients At 4 Weeks. *J Ayub Med Coll Abbottabad*. 2023 Feb-Mar; 35 (1): 99–103. PMID: 36849386.
6. *Garcia-Tsao G, Abraldes JG, Berzigotti A, Bosch J.* Portal hypertensive bleeding in cirrhosis: Risk stratification, diagnosis, and management: 2016 practice guidance by the American Association for the study of liver diseases. *Hepatology.* 2017; 65: 310–335. doi: 10.1002/hep.28906.
7. *Lv Y, Qi X, He C, Wang Z, Yin Z, Niu J et al*. Covered TIPS versus endoscopic band ligation plus propranolol for the prevention of variceal rebleeding in cirrhotic patients with portal vein thrombosis: a randomised controlled trial. *Gut*. 2018 Dec; 67 (12): 2156–2168. doi: 10.1136/gutjnl-2017-314634.
8. *Bucsics T, Schoder M, Goeschl N, Schwabl P, Mandorfer M, Diermayr M et al.* Rebleeding rates and survival after early transjugular intrahepatic portosystemic shunt (TIPS) in clinical practice. *Dig Liver Dis*. 2017 Dec; 49 (12): 1360–1367. doi: 10.1016/j.dld.2017.08.002.
9. *Bodzin AS, Baker TB.* Liver Transplantation Today: Where We Are Now and Where We Are Going. *Liver Transpl.* 2018 Oct; 24 (10): 1470–1475. doi: 10.1002/lt.25320.
10. *Nazyrov FG, Devyatov AV, Babadzhanov AKh, Salimov UR.* Evolution of Azigoportal DissociationTechnologies in Prevention of Bleedings of Portal Genesis. *Annaly khirurgicheskoy gepatologii = Annals of HPB surgery*. 2018; 23 (1): 65–73. [In Russ, English abstract]. doi: 10.16931/1995-5464.2018165-73.
11. *Korobka VL, Shapovalov AM, Danil'chuk OYa, Korobka RV*. Sposob khirurgicheskogo lecheniya i profilaktiki retsidiva krovotecheniy pri varikoznom rasshirenii ven pishchevoda i kardial'nogo otdela zheludka. Patent na izobretenie RU 2412657 C1, 27.02.2011. Zayavka № 2009128518/14 ot 23.07.2009.
12. *Korobka VL, Kostrykin MYu, Shapovalov AM.* Management of variceal bleeding in the liver transplant waiting list. *Russian Journal of Transplantology and Artificial Organs*. 2020; 22 (4): 58–64. [In Russ, English abstract]. doi: 10.15825/1995-1191-2020-4-58-64.
13. *De Franchis R; Baveno VI Faculty.* Expanding consensus in portal hypertension: Report of the Baveno VI Consensus Workshop: Stratifying risk and individualizing care for portal hypertension. *J Hepatol.* 2015; 63: 743–752. doi: 10.1016/j.jhep.2015.05.022.
14. Esophageal Varices. Practice Guideline of World Gastroenterology Organisation. Available at: https://www.worldgastroenterology.org/UserFiles/file/guidelines/esophageal-varices-russian-2014.pdf.
15. *Moore KP, Wong F, Gines P, Bernardi M, Ochs A, Salerno F et al.* The management of ascites in cirrhosis: report on the consensus conference of the International Ascites Club. *Hepatology.* 2003; 38 (1): 258–266. doi: 10.1053/jhep.2003.50315.
16. *Gantzel RH, Aagaard NK, Vilstrup H, Watson H, Grønbaek H, Jepsen P.* Development and validation of the Cirrhotic Ascites Severity model-A patient-reported outcome-based model to predict 1-year mortality. *Hepatol Commun.* 2022 Nov; 6 (11): 3175–3185. doi: 10.1002/hep4.2065.
17. *Zhang M, Wang G, Zhao L, Wu Z, Zhang W, Zhang C.* Second prophylaxis of variceal bleeding in cirrhotic patients with a high HVPG. *Scand J Gastroenterol*. 2016 Dec; 51 (12): 1502–1506. doi: 10.1080/00365521.2016.1193218.
18. *Liu J, Shi Q, Xiao S, Zhou C, Zhou B, Yuan F et al.* Using transjugular intrahepatic portosystemic shunt as the first-line therapy in secondary prophylaxis of variceal hemorrhage. *J Gastroenterol Hepatol.* 2020 Feb; 35 (2): 278–283. doi: 10.1111/jgh.14761.
19. *Abraldes JG, Villanueva C, Bañares R, Aracil C, Catalina MV, Garci A-Pagán JC, Bosch J; Spanish Cooperative Group for Portal Hypertension and Variceal Bleeding.* Hepatic venous pressure gradient and prognosis in patients with acute variceal bleeding treated with pharmacologic and endoscopic therapy. *J Hepatol.* 2008 Feb; 48 (2): 229–236. doi: 10.1016/j.jhep.2007.10.008.
20. *Sinagra E, Perricone G, D'Amico M, Tinè F, D'Amico G.* Systematic review with meta-analysis: the haemodynamic effects of carvedilol compared with propranolol for portal hypertension in cirrhosis. *Aliment Pharmacol Ther.* 2014 Mar; 39 (6): 557–568. doi: 10.1111/apt.12634.
21. *Hofer BS, Simbrunner B, Bauer DJM, Paternostro R, Schwabl P, Scheiner B et al.* Acute hemodynamic response to propranolol predicts bleeding and nonbleeding decompensation in patients with cirrhosis. *Hepatol Commun.* 2022 Sep; 6 (9): 2569–2580. doi: 10.1002/hep4.2021.
22. *La Mura V, Abraldes JG, Raffa S, Retto O, Berzigotti A, García-Pagán JC, Bosch J.* Prognostic value of acute hemodynamic response to i.v. propranolol in patients with cirrhosis and portal hypertension. *J Hepatol.* 2009 Aug; 51 (2): 279–287. Epub 2009 May 24. PMID: 19501930. doi: 10.1016/j.jhep.2009.04.015/.
23. *Shapovalov AM., Korobka VL., Cherkasov MF.* The method of surgical treatment and prophylaxis of bleeding from variceal of the esophagus and stomach. *Medical Herald of the South of Russia*. 2015; (3): 112–115. [In Russ, English abstract]. doi: 10.21886/2219-8075-2015-3-112-115.

The article was submitted to the journal on 11.04.2024

DOI: 10.15825/1995-1191-2024-2-42-47

CARDIAC ALLOGRAFT VASCULOPATHY: CURRENT REVIEW

B.L. Mironkov, D.D. Uvarova, N.N. Koloskova, Yu.V. Sapronova, I.I. Muminov, A.A. Yusova, S.A. Sakhovsky

Shumakov National Medical Research Center of Transplantology and Artificial Organs, Moscow, Russian Federation

Transplant coronary artery disease (TCAD) is one of the main causes of graft dysfunction and graft loss. Early diagnosis and treatment of cardiac allograft vasculopathy (CAV) can increase graft survival and improve the prognosis for heart transplant recipients. This review presents current data on the problem of CAV, its pathogenesis and the main factors influencing the course of this disease.

Keywords: cardiac allograft vasculopathy, heart transplantation.

About 6000 heart transplants are performed annually worldwide. In Russia, 308 heart transplants were performed in 2022, including 10 pediatric transplants [1]. Survival after heart transplantation is about 12.5 years [2 4]. Transplant coronary artery disease (TCAD) is a complex accelerated immune-inflammatory fibroproliferative disease of the transplant coronary bed. It is characterized by diffuse intimal hyperplasia in the early stages, which is followed by negative vascular remodeling. Ten percent of heart transplant recipients die within three years of receiving their transplant, with TCAD being the primary cause of death in these cases [3]. Recipients who experience rapidly progressive TCAD within the first year after transplantation have a significantly increased risk of death and/or retransplantation within 5 years.

The reasoning behind the prophylactic use of statins, immunosuppressants, and vigorous infection prevention against TCAD is based on current understanding of the pathophysiology of the disease [4].

TCAD RISK FACTORS

Immunological factors associated with TCAD are the initial link in the pathologic process. The interaction of "foreign" human leukocyte antigen (HLA) of allograft endothelial cells with the recipient's T lymphocytes initiates endothelial cell activation and inflammatory cell accumulation. This leads to production of cytokines (interleukins 2, 4, 5, and 6; interferon-gamma; tumor necrosis factor-alpha), proliferation, and activation of endothelial adhesion molecules. Activated macrophages accumulate in the intima and produce cytokines (interleukins 1 and 6, TNF-alpha) and growth factors. As a result, this causes smooth muscle cell migration into the intima, proliferation and deposition of the extracellular matrix. HLA class I antibodies promote endothelial and smooth muscle cell proliferation through activation of the mTOR pathway and induction of intracellular fibroblast growth factor receptor expression [5]. Even in the absence of pathogens, a variety of intracellular particles, including cytoplasm, mitochondria, and cell nuclei, which are also present in the extracellular matrix in transplanted organs, cause inflammatory processes [65]. Lin et al. showed the importance of this phenomenon by demonstrating that extracellular mitochondria are abundant in the blood of dead donor organs and that their abundance corresponds to rapid graft rejection [7]. Endothelial injury and activation induce the production of pro-inflammatory cytokines, chemokines and expression of adhesion molecules, which promotes immune cell recruitment and immune cell transmigration into the intima [8, 9].

Both innate and acquired immunity play an important role in both atherosclerosis and TCAD. Although the triggers of endothelial injury and endothelial dysfunction may differ in TCAD and atherosclerosis, once endothelial activation occurs, pathologic processes involved are similar in the two diseases.

Nonimmune factors associated with the risk of TCAD include advanced age (donors and recipients), male gender, infections, dyslipidemia, obesity, diabetes, coronary heart disease, cause of brain death in the donor, organ preservation and transportation conditions, surgical injury, and ischemia-reperfusion injury (IRI). Hyperlipidemia and insulin resistance are the most significant non-immune factors, occurring in 50–80% of heart transplant patients [10, 11].

An increased risk of TCAD has been linked to cytomegalovirus (CMV) infection [12]. By increasing the synthesis of nitric oxide synthase inhibitor, asymmetric dimethylarginine, CMV causes endothelial dysregulation and affects nitric oxide synthesis. The chemical similarity between CMV and endothelial cell surface may lead to cross-reactivity [7, 8]. However, recent studies have found no association between maximum intima-media thickening during the first year, assessed by intravascular

Corresponding author: Stepan Sakhovsky. Address: 1, Shchukinskaya str., Moscow, 123182, Russian Federation. Phone: (926) 636-00-31. E-mail: milifolium@gmail.com

ultrasound (IVUS), and CMV infection [13]. The cause of brain death in the donor is relevant to the success of transplantation. Brain death causes severe cardiac injury due to increased catecholamine production, endocrine and hemodynamic disorders leading to organ hypoperfusion and subsequent IRI after transplantation. In addition, the mechanism of donor brain death has a significant impact on heart transplant outcomes, with traumatic brain death being associated with decreased mortality, rejection, allograft vasculopathy, and transmissible atherosclerosis [14]. Based on observations at Shumakov National Medical Research Center of Transplantology and Artificial Organs, donor brain death was associated with higher probability of transmitting coronary atherosclerosis from older donors and donors with stroke [15]. IRI caused by surgical injury leads to production of large amounts of reactive oxygen species (ROS), which directly cause vascular injury and endothelial activation [16].

It should be noted that, in terms of pathological anatomy, TCAD has a variety of morphologic manifestations. Wei-hui Lu et al. published a study [17] that evaluated the pathologic anatomic findings in the explanted heart of patients who underwent retransplantation for graft dysfunction. The study reviewed archival records and microscopic sections of hearts surgically explanted from 64 patients: 54 adults (18 to 70 years old) and 10 children (3 to 15 years old). 54 adults (18 to 70 years) and 10 children (3 to 15 years). Vascular lesions were categorized as showing intimal fibromuscular hyperplasia, atherosclerosis and/or inflammation. A total of 75% of hearts had signs of acute cellular rejection, predominantly mild. Intramyocardial arteries showed primarily intimal fibromuscular hyperplasia and inflammation with no atheroma present. Lesions in the epicardial coronary arteries presented as intimal fibromuscular hyperplasia, atherosclerosis, and/or inflammation affecting one or more vascular layers (intima, media and adventitia). Severe TCAD with >75% luminal narrowing was seen in at least one vessel in all hearts. Two hearts had severe narrowing of the left main coronary artery. Nineteen arteries had luminal thrombus. All hearts had narrowing of smaller epicardial coronary arteries that were often severe. Atheromas were present in arteries of adults and children; thus, not all atheromas could be considered pre-existing prior to transplantation. Both arteries and veins showed intimal hyperplasia and inflammation.

Thus, TCAD is a pathologically multifaceted disorder that affects large and small epicardial coronary arteries of adults and children, with different types of lesions: intimal fibromuscular hyperplasia; atherosclerosis; and/or inflammation (vasculitis).

According to pathoanatomical studies conducted at Shumakov National Medical Research Center of Transplantology and Artificial Organs, cardiac allograft vasculopathy (CAV) in the proximal coronary arteries was a combination of accelerated atherosclerosis and chronic rejection [18–23].

But despite the many manifestations of TCAD, the current classification used is the one developed by the International Society for Heart and Lung Transplantation (ISHLT), which is based mainly on angiographic criteria (Table 1) [24].

TCAD and coronary atherosclerosis of native arteries have both common and different features. Moreover, the presence of different risk factors leads to different types of vascular lesions in cardiac allografts. For example, hyperlipidemia, diabetes, and smoking are risk factors common to atherosclerotic disease and TCAD. With these risk factors, graft vessels develop atherosclerotic-like lesions. On the other hand, alloantigen-dependent risk factors (number of anti-HLA antibodies, number of rejection episodes) and CMV infection are more likely to be associated with changes such as endotheliitis and arteritis [17].

Although some of the risk factors (donor organ IRI, donor age, organ quality, recipient age, donor brain death, major histocompatibility mismatch) are unique to TCAD, many are in addition to the others (hyperlipidemia, diabetes, oxidative stress, hypertension, cytokine modulation, inflammation, C-reactive protein [CRP], infections and other environmental factors, smoking) [8, 25, 26]. Comparative characteristics of these diseases are presented in Table 2.

Table 1

Classification system for angiographic features of TCAD

Severity	Angiographic criteria
ISHLT CAV0 (Not significant)	No detectable angiographic lesion.
ISHLT CAV1 (Mild)	Angiographic left main (LM) <50%, or primary vessel with maximum lesion of <70%, or any branch stenosis <70% (including diffuse narrowing) without allograft dysfunction.
ISHLT CAV2 (Moderate)	Angiographic LM <50%; a single primary vessel ≥70%, or isolated branch stenosis ≥70% in branches of 2 systems, without allograft dysfunction.
ISHLT CAV3 (Severe)	Angiographic LM ≥50%, or two or more primary vessels ≥70% stenosis, or isolated branch stenosis ≥70% in all 3 systems; or ISHLT CAV1 or CAV2 with allograft dysfunction (defined as LVEF ≤45% usually in the presence of regional wall motion abnormalities) or evidence of significant restrictive physiology.

Table 2

Comparative characteristics of TCAD and atherosclerosis

Sign	TCAD	Atherosclerosis
Vascular involvement	Epicardial and intramural coronary arteries are affected.	Large epicardial coronary arteries are affected.
	Diffuse and very extensive vascular lesions in combination with epicardial localization.	Proximal epicardial coronary arteries are largely affected. Intramyocardial vessels and arteries under muscle bridges are usually intact.
	Veins may also be involved.	Veins are never involved.
	The media may be either unaffected or almost completely replaced by fibrous tissue. As intimal lesion progresses, fibrosis of the media and adventitia also increases.	All the vascular wall layers are involved.
Nature of lesion	Diffuse, concentric intimal thickening.	Focal, eccentric proliferative and degenerative intimal lesions in the proximal coronary vessels.
	Varies from concentric, diffuse intimal lesions to widespread fibrofatty plaques with degeneration.	Predominantly fibrofatty plaques with necrotic depressions and progressively thinned fibrous cap.
Onset and progression of the disease	Initially manifested by smooth muscle cell proliferation into the intima and extracellular lipid accumulation.	Initially manifested by fatty streaks.
	Accelerated progression of intimal proliferation and luminal stenosis at the early stage of the disease with the development of foam cells.	Slow progression of the lesion (decades) is characteristic.
	Superficial endothelial erosion is uncommon but may be a rare finding.	Endothelial erosion is characteristic.
	Fibrous capsule thinning and plaque rupture are rare.	Thin fibrous capsule and plaque rupture are often observed in moderate to severe lesions.

Other factors influencing the course of vasculopathy: Increased platelet aggregation is a well-recognized risk factor for sudden cardiac death and myocardial infarction in heart transplant patients [1]. A study of over 200 heart transplant recipients found that early aspirin therapy was associated with a significant (68%) reduction in the risk of cardiovascular events [27].

Statins are well-known hypolipidemic and anti-inflammatory drugs [28]. A recent meta-analysis confirmed the beneficial effects of statins in reducing graft rejection and increasing survival in heart transplant recipients [28]. Fang et al. studied antioxidant therapy with vitamins C and E to prevent endothelial dysfunction in TCAD. The authors found that antioxidant therapy delayed TCAD [29]. Calcineurin inhibitors (cyclosporine, tacrolimus) have historically been the therapy of choice for maintenance immunosuppression [30]. The development of agents such as everolimus and sirolimus has expanded therapeutic options for TCAD. Everolimus has been shown to significantly reduce TCAD progression when combined with immunosuppressants (cyclosporine, tacrolimus) at year 1 after transplantation compared to when combined with mycophenolate and azathioprine. On the other hand, later initiation of everolimus therapy does not increase vasculopathy incidence. Sirolimus therapy resulted in decreased incidence of acute graft rejection and vasculopathy compared to calcineurin inhibitors. There is evidence that sirolimus can inhibit TCAD, even when initiated after disease onset [31]. These drugs, however, need further evaluation when combined with newer immunosuppressants such as tacrolimus [4, 17]. It should be noted that their use may be limited in some patients due to the high incidence of side effects, such as infections, pericardial effusion and delayed wound healing [31].

Unfortunately, these measures have had little impact on the 5- and 10-year incidence of TCAD over the last 20 years of follow-up (32–30% and 52–49%, respectively) [16]. Furthermore, for recipients who develop TCAD within 3 years after transplantation, the 5-year survival rate remains virtually the same as 20 years ago (28–22%) [16]. These statistics highlight how the need for more sensitive techniques for early TCAD detection severely limits therapy options for heart transplant recipients at this stage. This is because effective treatment to prevent or delay TCAD must be initiated as soon as feasible.

There have been recent studies to identify potential targets for immunologic treatment, mainly using monoclonal antibodies, to eventually replace existing therapeutic immunosuppressants [32]. The main goal of immunomodulation in the context of TCAD has been to inhibit or suppress predominantly T-cell activity against the allograft [4].

CONCLUSION

Transplant coronary artery disease is one of the main factors limiting graft survival. Due to its intricate origins and multifaceted nature, this condition requires further study on both immune contribution to the pathogenesis of vasculopathy and the classical factors of atherogene-

sis. Infectious agents (CMV) deserve special attention as early detection and influence on them can improve the prognosis for this patient cohort. Even though CAV manifests 3–5 years after heart transplantation, the first signs may appear in the first year, which in turn is an unfavorable predictor. This necessitates prompt modifications to immunosuppressive medication and closer observation of the disease's progression. Even though modern immunosuppressive medications, such as everolimus, cannot be used in every patient, incorporating them more frequently into treatment plans could help cardiac recipients have better outcomes. Correcting the classical atherosclerosis factors is another crucial aspect of treatment for heart transplant patients.

The authors declare no conflict of interest.

REFERENCES

1. *Gautier SV, Khomyakov SM*. Organ donation and transplantation in the Russian Federation in 2022. 15th Report from the Registry of the Russian Transplant Society. *Russian Journal of Transplantology and Artificial Organs*. 2023; 25 (3): 8–30. https://doi.org/10.15825/1995-1191-2023-3-8-30.
2. *Khush KK, Cherikh WS, Chambers DC, Harhay MO, Hayes D Jr, Hsich E* et al. The international thoracic organ transplant registry of the international society for heart and lung transplantation: thirty-sixth adult heart transplantation report – 2019. *J Heart Lung Transplant*. 2019; 38 (10): 1056–1066. doi: 10.1016/j.healun.2019.08.004.
3. *Shah KS, Kittleson MM, Kobashigawa JA*. Updates on Heart Transplantation. *Curr Heart Fail Rep*. 2019 Oct; 16 (5): 150–156. doi: 10.1007/s11897-019-00432-3.
4. *Shetty M, Chowdhury YS*. Heart Transplantation Allograft Vasculopathy. StatPearls [Internet]. Treasure Island (FL): StatPearls Publishing, 2023.
5. *Lee F, Nair V, Chih S.* Cardiac allograft vasculopathy: Insights on pathogenesis and therapy. *Clin Transplant*. 2020 Mar; 34 (3): e13794. doi: 10.1111/ctr.13794.
6. *Spitaleri G, Farrero Torres M, Sabatino M, Potena L.* The pharmaceutical management of cardiac allograft vasculopathy after heart transplantation. *Expert Opin Pharmacother*. 2020; 21 (11): 1367–1376.
7. *Spartalis M, Spartalis E, Siasos G.* Cardiac allograft vasculopathy after heart transplantation: Pathophysiology, detection approaches, prevention, and treatment management. *Trends Cardiovasc Med*. 2022 Aug; 32 (6): 333–338. doi: 10.1016/j.tcm.2021.07.002.
8. *Rahmani M, Cruz RP, Granville DJ, McManus BM.* Allograft vasculopathy versus atherosclerosis. Circ Res. 2006 Oct 13; 99 (8): 801–815. doi: 10.1161/01.RES.0000246086.93555.f3.
9. *Hu D, Yin C, Luo S, Habenicht AJR, Mohanta SK*. Vascular Smooth Muscle Cells Contribute to Atherosclerosis Immunity. *Front Immunol*. 2019 May 17; 10: 1101. doi: 10.3389/fimmu.2019.01101.
10. *Doulamis IP.* Editorial commentary: Cardiac allograft vasculopathy: Caveats and perspectives. *Trends Cardiovasc Med*. 2022; 32 (6): 339–340. doi: 10.1016/j.tcm.2021.07.007.
11. Bolezn' koronarnykh arteriy peresazhennogo serdtsa. Pod red. V.I. Shumakova. M.: MIA, 2008; 160. [Electronic resource]. https://www.centrmag.ru/catalog/product/bolezn-koronarnyh-arterij-peresazhennogo-serdca/ (accessed: 17.10.2023).
12. *Alyaydin E, Welp H, Reinecke H, Tuleta I.* Predisposing factors for late mortality in heart transplant patients. *Cardiol J*. 2021; 28 (5): 746–757. doi: 10.5603/CJ.a2020.0011.
13. *Guzik B, Szczepanek E, Niewiara Ł, Nosal M, Wierzbicki K, Krzanowski M et al.* Coronary revascularization after heart transplant – the search for prognostic factors. *Arch Med Sci*. 2020 Apr 18; 16 (4): 789–795. doi: 10.5114/aoms.2017.71847.
14. *Foroutan F, Alba AC, Guyatt G, Duero Posada J, Ng Fat Hing N, Arseneau E et al.* Predictors of 1-year mortality in heart transplant recipients: a systematic review and meta-analysis. *Heart*. 2018 Jan; 104 (2): 151–160. doi: 10.1136/heartjnl-2017-311435.
15. *Sakhovskiy SA, Izotov DA, Goncharova AYu, Koloskova NN, Mironkov BL.* Koronarnyy ateroskleroz donorskogo serdtsa. *Vserossiyskaya nauchno-prakticheskaya konferentsiya s mezhdunarodnym uchastiem "Kompleksnye problemy serdechno-sosudistykh zabolevaniy"*. 2021; S2: 166. https://cyberleninka.ru/article/n/koronarnyy-ateroskleroz-donorskogo-serdtsa (date of reference: 12.01.2024).
16. *Stehlik J, Kobashigawa J, Hunt SA, Reichenspurner H, Kirklin JK.* Honoring 50 Years of Clinical Heart Transplantation in Circulation: In-Depth State-of-the-Art Review. *Circulation*. 2018 Jan 2; 137 (1): 71–87. doi: 10.1161/CIRCULATIONAHA.117.029753.
17. *Lu WH, Palatnik K, Fishbein GA, Lai C, Levi DS, Perens G et al.* Diverse morphologic manifestations of cardiac allograft vasculopathy: a pathologic study of 64 allograft hearts. *J Heart Lung Transplant*. 2011 Sep; 30 (9): 1044–1050. doi: 10.1016/j.healun.2011.04.008.
18. *Mozheyko NP.* Patomorfologiya transplantirovannogo serdtsa: dis. … dokt. med. nauk. M., 2020; 171. [Electronic resource]. https://freereferats.ru/product_info.php?products_id=691983 (accessed: 17.10.2023).
19. *Muminov II, Koloskova NN, Poptsov VN, Zakharevich VM, Mozheiko NP, Sakhovsky SA, Shevchenko AO*. Experience of outpatient follow-up of heart transplant recipients at Shumakov center. *Russian Journal of Transplantology and Artificial Organs*. 2023; 25 (3): 68–75. https://doi.org/10.15825/1995-1191-2023-3-68-75.
20. *Sakhovskiy SA, Uvarova DD, Mironkov BL*. Techenie koronarnoy patologii u retsipientov serdtsa s gemodinamicheski ne znachimym transmissivnym ateroskleroz om. *Russian Journal of Transplantology and Artificial Organs*. 2023; 25 (S): 46.
21. *Sakhovsky SA, Koloskova NN, Izotov DA, Spirina EA, Goncharova AYu, Luchkin VM, Mironkov BL*. Life expectancy of heart recipients with donor-transmitted coronary atherosclerosis. *Russian Journal of Transplantology and Artificial Organs*. 2019; 21 (4): 14–19. https://doi.org/10.15825/1995-1191-2019-4-14-19.

22. *Chestukhin VV, Ostroumov EN, Tyunyaeva IYu, Zakharevich VM i dr.* Bolezn' koronarnykh arteriy peresazhennogo serdtsa. Vozmozhnosti diagnostiki i lecheniya. *Ocherki klinicheskoy transplantologii*. Pod red S.V. Gautier. M., 2009: 88–93.
23. *Gautier SV, Shevchenko AO, Poptsov VN.* Patsient s transplantirovannym serdtsem: rukovodstvo dlya vrachey po vedeniyu patsientov, perenesshikh transplantatsiyu serdtsa. M.–Tver': Triada, 2014; 144.
24. *Velleca A, Shullo MA, Dhital K, Azeka E, Colvin M, DePasquale E et al.* The International Society for Heart and Lung Transplantation (ISHLT) guidelines for the care of heart transplant recipients. *J Heart Lung Transplant*. 2023 May; 42 (5): e1–e141. doi: 10.1016/j.healun.2022.10.015.
25. *Raichlin E, Bae JH, Kushwaha SS, Lennon RJ, Prasad A, Rihal CS, Lerman A.* Inflammatory burden of cardiac allograft coronary atherosclerotic plaque is associated with early recurrent cellular rejection and predicts a higher risk of vasculopathy progression. *J Am Coll Cardiol*. 2009 Apr 14; 53 (15): 1279–1286. doi: 10.1016/j.jacc.2008.12.041.
26. *Pighi M, Gratta A, Marin F, Bellamoli M, Lunardi M, Fezzi S et al.* Cardiac allograft vasculopathy: Pathogenesis, diagnosis and therapy. *Transplant Rev (Orlando)*. 2020 Oct; 34 (4): 100569. doi: 10.1016/j.trre.2020.100569.
27. *Peled Y, Lavee J, Raichlin E, Katz M, Arad M, Kassif Y et al.* Early aspirin initiation following heart transplantation is associated with reduced risk of allograft vasculopathy during long-term follow-up. *Clin Transplant*. 2017 Dec; 31 (12). doi: 10.1111/ctr.13133.
28. *Vallakati A, Reddy S, Dunlap ME, Taylor DO.* Impact of Statin Use After Heart Transplantation: A Meta-Analysis. *Circ Heart Fail*. 2016 Oct; 9 (10): e003265. doi: 10.1161/CIRCHEARTFAILURE.116.003265.
29. *Fang JC, Kinlay S, Beltrame J, Hikiti H, Wainstein M, Behrendt D et al.* Effect of vitamins C and E on progression of transplant-associated arteriosclerosis: a randomised trial. *Lancet*. 2002 Mar 30; 359 (9312): 1108–1113. doi: 10.1016/S0140-6736(02)08154-0.
30. *Mallah SI, Atallah B, Moustafa F, Naguib M, El Hajj S, Bader F, Mehra MR.* Evidence-based pharmacotherapy for prevention and management of cardiac allograft vasculopathy. *Prog Cardiovasc Dis*. 2020 May-Jun; 63 (3): 194–209. doi: 10.1016/j.pcad.2020.03.007.
31. *Masetti M, Potena L, Nardozza M, Prestinenzi P, Taglieri N, Saia F et al.* Differential effect of everolimus on progression of early and late cardiac allograft vasculopathy in current clinical practice. *Am J Transplant*. 2013 May; 13 (5): 1217–1226. doi: 10.1111/ajt.12208.
32. *Bellumkonda L, Patel J.* Recent advances in the role of mammalian target of rapamycin inhibitors on cardiac allograft vasculopathy. *Clin Transplant*. 2020 Jan; 34 (1): e13769. doi: 10.1111/ctr.13769.

The article was submitted to the journal on 07.02.2024

DOI: 10.15825/1995-1191-2024-2-48-50

BRIDGE TO CANCER THERAPY IN PATIENTS WITH CHRONIC HEART FAILURE: IMPLANTATION OF A LEFT VENTRICULAR ASSIST DEVICE BEFORE SURGICAL TREATMENT OF GASTRIC CANCER

K.G. Ganaev[1], S.K. Kurbanov[1], E.E. Vlasova[1], E.V. Dzybinskaya[1], R.S. Latypov[1], K.V. Mershin[1], I.S. Stilidi[2], A.A. Shiryaev[1], R.S. Akchurin[1]

[1] National Medical Research Centre of Cardiology, Moscow, Russian Federation
[2] Blokhin Russian Cancer Research Center, Moscow, Russian Federation

The co-occurrence of chronic heart failure (CHF) and cancer is becoming more and more common as people live longer. The lack of a structured approach to the treatment of cancer patients with severe cardiovascular conditions is an essential issue. Up to 25% of cancer patients cannot be operated on for their main disease profile due to the presence of cardiovascular disease. This article describes a clinical case of successful treatment of a patient with two competing (prognosis-determining) diseases: end-stage heart failure and stomach cancer within the framework of a bridge-to-cancer strategy.

Keywords: chronic heart failure, mechanical circulatory support, bridge to cancer therapy.

INTRODUCTION

Cardiovascular diseases and cancer are the leading causes of death in the Russian Federation. Introduction of new methods of diagnosis and treatment, as well as increased life expectancy among the population naturally lead to higher numbers of patients with co-occurrence of heart failure (HF) and malignancies. Up to 25% of cancer patients cannot undergo cancer surgery due to the presence of cardiovascular disease. Patients with end-stage heart failure are at incredibly high risk of adverse outcomes in cancer treatment due to reduced myocardial contractile function and limited cardiac reserves.

Heart transplantation (HT) remains the gold standard treatment for end-stage HF. Meanwhile, cancer with a poor life prognosis is one of the contraindications to HT. Modern long-term mechanical left ventricular assist devices (LVADs) have shown improved survival and quality of life compared with optimal medical therapy and comparable survival to HT. LVAD therapy may be a valuable option for staged treatment of patients with operable cancer as part of a bridge-to-cancer treatment strategy.

The **aim** is to demonstrate a case of successful treatment of a patient with two competing (prognosis-determining) diseases: end-stage HF and gastric cancer as part of a bridge-to-cancer treatment strategy.

CLINICAL CASE

Patient P., 45 years old, with complaints of paroxysmal dyspnea. Family history: his mother died at the age of 46 years (dilated cardiomyopathy, DCM) and father at the age of 52 years (myocardial infarction). From medical history, we know that Hodgkin's lymphoma was detected at the age of 17; radiation therapy, chemotherapy in 1996–1997. PET/CT scans showed persistent remission. Dyspnea debuted in 2018 with gradual progression. He was examined in the same year and CAG was performed: no hemodynamically significant stenosis, diagnosed with DCM with the development of biventricular HF. He was admitted to the National Medical Research Centre of Cardiology in Moscow in September 2022. An examination was carried out, according to EchoCG data: end-diastolic volume (EDV) = 9.0 cm, ejection fraction (EF) = 20%, mitral regurgitation (MR) = grade 3, right ventricular EF = 53%, tricuspid annular plane systolic excursion (TAPSE) = 2.4 cm; coronary angiography (CAG): subtotal stenosis of the anterior descending artery (ADA) in the proximal segment; right heart catheterization (RHC): pulmonary artery pressure (systolic/diastolic/average) = 22/6/12 mmHg, cardiac index (CI) = 1.9 L/min·m^2, stroke volume (SV) = 63 mL, pulmonary vascular resistance (PVR) = 78 dyn/s/cm^{-5}.

Based on complaints, medical history and laboratory and instrumental examination, the following diagnosis was made: "Dilated cardiomyopathy. Acquired heart defect: moderate relative mitral valve regurgitation. Chronic heart failure with reduced ejection fraction, NYHA class I. Ischemic heart disease: grade 3 angina pectoris. Atherosclerosis of the aorta and coronary arteries (subtotal stenosis of the proximal segment of ADA), muscle bridge of the middle segment of ADA. Cardiac rhythm and conduction disorders: frequent ventricular

Corresponding author: Kamil Ganaev. Address: 15a, Akademika Chazova str., Moscow, 121552, Russian Federation. Phone: (999) 979-50-70. E-mail: dr_ganaev@mail.ru

extrasystole, short paroxysmal ventricular tachycardia; left anterior fascicular block. Concomitant: Stage 2 hodgkin's lymphoma with cervical submandibular lymph node involvement, radiotherapy (5 sessions) from 1996, chemotherapy (6 sessions) from 1997."

As part of additional examination, an esophagogastroduodenoscopy (EGD) was performed: an area of altered mucosa was detected along the anterior wall of the middle third and lower third of the stomach by infiltration type. Biopsy of the gastric mucosa area revealed "high grade" gastric dysplasia. The patient was consulted by an oncologist, and gastric cancer T3N2M0, stage IIIA was diagnosed based on examination results. The patient was indicated for definitive surgical intervention, however, such surgery is associated with extremely high risks of death against the background of end-stage HF. The patient was consulted at the transplant center: HT was contraindicated due to the presence of cancer with poor prognosis. It was decided to perform surgical treatment in two stages. The first stage (as part of the "bridge to cancer treatment" strategy) included implantation of a mechanical circulatory support device (Heartmate 3™ device) with one-stage coronary bypass (mammary-coronary bypass of the anterior descending artery). The second stage of definitive treatment of gastric cancer is planned.

In October 2022, the HeartMate 3™ LVAD was implanted. Postoperative echoCG parameters: EDV = 8.0 cm, MR = grade 2, systolic pulmonary artery pressure (SPAP) = 22 mmHg, CI = 2.7 L/min·m^2. System parameters: pump flow = 4.4, pump speed = 5200 rpm, PI = 4.0 pump power = 3.8. On day 4 after implantation, compensated HF was observed. The patient was discharged and sent to the second stage – definitive treatment of gastric cancer on day 21 after Heartmate 3™ implantation.

In December 2022, he was hospitalized at Blokhin Russian Cancer Research Center in Moscow, where he underwent surgery: gastrectomy, D2 lymph node dissection, splenectomy, distal pancreatectomy. The surgery was successful. Extubation and activation in standard periods. No signs of heart failure were observed with the implanted Heartmate 3™ device. The patient was discharged from the hospital on day 23 in a satisfactory condition after the operation. Postoperative follow-up period was 12 months. The patient is able to work, is active enough, and fully complies with all recommendations. The 6-minute walk distance (6MWD) was 402 meters. EQ-5D-5L parameters: mobility = 2, self-care = 2, usual activity = 2, pain/discomfort = 1, anxiety/depression = 2, VAS Health Perception = 75.

DISCUSSION

The use of modern mechanical circulatory support devices demonstrates high efficacy and safety in patients with end-stage CHF, comparable to 2-year heart transplant outcomes [1]. HeartMate 3™ implantation is considered as definitive therapy and as an alternative to HT. Given the limitations of HT in operable patients with malignant tumors, staged surgical treatment with implantation of a mechanical circulatory support device, in particular HeartMate 3™, followed by definitive treatment of cancer seems optimal.

There are very few articles in the literature and little experience with this therapy option available globally. Given that the supply cable is located in the anterior abdominal wall, it is crucial to draw attention to the technical difficulty of treating abdominal malignancies through surgery. In 2017, Nakamura et al. was the first to demonstrate the possibility of successful surgical intervention for gastric cancer with surgical access via laparotomy in a patient with an LVAD [2]. The following year, Zarbaliyev et al. published a similar paper describing a successful clinical case of gastrectomy for gastric cancer on day 20 following LVAD implantation [3].

In both cases reported in the literature, the malignancy was diagnosed after LVAD implantation. Confirmation of the cancer diagnosis during the preoperative period sets our case apart. We believe that the presence of operable malignancy could provide more justification for implantation of a mechanical circulatory support device. We expect that in the future, staged surgical intervention will be used more often in patients with end-stage CHF and operable malignancy and that clinical guidelines will codify this procedure for a certain patient cohort.

CONCLUSION

Our case demonstrates that cancer patients with end-stage HF, who are at a very high risk of dying, can benefit from phased surgical care. With an acceptable safety profile, the implantable HeartMate 3™ LVAD exhibits high immediate efficacy in supporting systemic hemodynamics. Surgical treatment of malignant tumors can be safely performed in the presence of LVAD as part of the "bridge-to-cancer treatment" strategy. This promising direction requires further research.

The authors declare no conflict of interest.

REFERENCES

1. *Lim S, Shaw S, Venkateswaran R Abu-Omar Y, Pettit S, Chue D*. HeartMate 3 Compared to Heart Transplant Outcomes in England. *J Heart Lung Transplant*. 2020; 39 (4), P. S15–S16. https://doi.org/10.1016/j.healun.2020.01.1138.
2. *Nakamura Y, Toda K, Nakamura T, Miyagawa S, Yoshikawa Y, Fukushima S et al.* Curative surgery for gastric cancer in a patient with an implantable left ventricular assist device. *J Artif Organs*. 2017 Jun; 20 (2): 170–173. doi: 10.1007/s10047-016-0944-3.
3. *Zarbaliyev E, Balkanay M, Sarsenov D*. Embracing the Future of Surgery: Gastric Cancer Resection Within One Month of Left Ventricular Assist Device Implantation. *Cureus*. 2018 Jun 23; 10 (6): e2868. doi: 10.7759/cureus.2868.

The article was submitted to the journal on 04.03.2024

DOI: 10.15825/1995-1191-2024-2-51-57

OPTIMAL STRATEGIES FOR PREVENTION OF ISCHEMIA-REPERFUSION INJURY IN HEART TRANSPLANTATION WITH PROLONGED COLD ISCHEMIA TIME (REVIEW)

A.V. Fomichev[1], G.B. Garmaev[1], M.O. Zhulkov[1], I.S. Zykov[1], A.G. Makaev[1], A.V. Protopopov[1], A.R. Tarkova[1], M.N. Murtazaliev[1], Ya.M. Smirnov[1], A.D. Limanskiy[1], A.V. Guseva[1], K.N. Kaldar[1], D.A. Sirota[1, 2]

[1] Meshalkin National Medical Research Center, Novosibirsk, Russian Federation
[2] Novosibirsk State Medical University, Novosibirsk, Russian Federation

The shortage of organs for transplant remains a major challenge in transplantology. Transporting donor organs over long distances increases cold ischemia time, which is a risk factor for ischemia-reperfusion injury (IRI). In the face of critical shortages, the method and timing of organ preservation are crucial in increasing the donor pool. This paper examines the approaches, benefits, and drawbacks of organ preservation techniques used around the world.

Keywords: cardioplegia, ischemia-reperfusion injury, heart transplantation, allograft.

INTRODUCTION

Gaps in the organization of organ donation currently remain the main problem of transplantology. Using unclaimed organs from distant locations is one solution to the critical organ shortage. he lengthy distances between donor bases and transplant facilities in interregional interactions, the predominant use of service vehicles or commercial aircraft for organ transportation, and the absence of "green corridors" are the hallmarks of the Russian organ donation system. As a consequence, long transportation and logistical challenges prolong the cold ischemia time [1].

Cardiac graft quality is inversely proportional to cold ischemia time, and the recommended maximum cold ischemia time for a donor heart is 240 minutes [2, 3]. Exceeding this safe threshold increases the risk of postoperative allograft dysfunction and death. This becomes especially relevant in heart transplantation from expanded criteria donors, as such a heart is most sensitive to the effects of ischemia. At the same time, the number of suboptimal donors in Russia is gradually increasing. Heart transplantation with prolonged cold ischemia is most typical for European countries, where the proportion of heart transplantations with ischemic time of more than 4 hours is over 40% [4].

During ischemia, decreased oxygen availability causes a shift from fatty acid metabolism to anaerobic glycolysis. The resulting lactic acidosis causes the extracellular pH to drop to 6.0–6.5. Continued acidosis results in activation of several transmembrane ion channels and receptors, each contributing to calcium overload, metabolic dysfunction, and ultimately cell death [5].

Ischemia-reperfusion injury (IRI) is the primary cause of donor graft dysfunction after prolonged transportation. Given the prohibitive risk of IRI and primary graft dysfunction with cold ischemia lasting more than 4 hours, there is an obvious necessity to enhance myocardial protection, but there is no consensus on the effectiveness of a particular method of preservation in prolonged ischemia of donor heart.

Currently in Russia, the standard heart preservation method is perfusion with Custodiol solution followed by static storage in a thermal container with ice and coolants; however, this is not able to fully protect the organ under conditions of prolonged ischemia [6]. Metabolism during cold cardioplegia does not stop under ischemic conditions; energy supply of metabolic processes occurs in anaerobic conditions, which leads to lactate accumulation and cardiomyocyte acidification, and metabolic acidosis occurs. In addition, histidine, one of the main components of Custodiol, has demonstrated some cytotoxic effects [7]. On the other hand, uncontrolled reduction in graft temperature to critical values and uneven cooling of the heart leads to impaired transmembrane transport of electrolytes, formation of free radicals that damage cardiomyocytes, as well as the process of tissue crystallization. Brain death causes a cascade of hormonal changes, changes in catecholamine levels, and release of inflammatory mediators (IL-1, IL-6, IL-8), resulting in hypotension and organ hypoperfusion. Appropriate handling of a brain-dead donor (conditioning) prior to

Corresponding author: Andrey Protopopov. Address: 15, Rechkunovskaya str., 630055, Novosibirsk, Russian Federation. Phone: (914) 708-39-79. E-mail: andrew-uss@yandex.ru

the withdrawal stage is equally critical because hypoperfusion and inflammatory response cause extra harm to the transplant even before IRI develops [2].

The increasing use of expanded criteria donors [1] – high inotropic therapy, over 55 years of age, myocardial hypertrophy, transmissible coronary atherosclerosis – also requires revision of the standard approach to heart transplant preservation.

Thus, the relevance of developing new strategies for graft transportation and preservation is obvious. Currently, various strategies have been described to further improve donor heart preservation results, including pharmacological, organizational and other methods that can significantly reduce IRI severity.

Analysis of known strategies for reducing the damaging effect of IRI during prolonged transportation of donor heart allows us to highlight several key aspects.

It is commonly known that when prolonged cold ischemia is anticipated, it is best to use hearts from young donors. An interesting observation was published by Kim et al [8]. When analyzing 43,304 heart transplantations, the scientists found that recipients of obese donor hearts experienced improved immediate and long-term outcomes when organ ischemic times exceeded 4 hours.

REPEATED INFUSION OF PRESERVATION SOLUTION

Several studies have shown that the use of repeated infusion of preservation solution (crystalloid, blood cardioplegia), which is given continuous retrograde or as terminal "hot shots", reduces organ ischemic injury, shortens intensive care stay, and improves early survival after transplantation [9]. The authors conclude that the technique is particularly relevant when using hearts from marginal donors and with prolonged cold graft ischemia. The history of research on the efficacy of repeated cardioplegia dates back to the 1990s, when the first prospective studies in this field were conducted.

Two studies used normothermic blood cardioplegia, administered immediately before the completion of aortic occlusion (terminal "hot shot") [10, 11]. The results of these studies showed that the use of blood cardioplegia was associated with a lower incidence of right ventricular failure, cardiac arrhythmias, and laboratory signs of ischemia (decreased levels of creatine kinase (CK), creatine kinase MB (CK-MB) in the early postoperative period. Twelve-year heart transplant outcomes demonstrated [12] that the use of blood cardioplegia is safe and results in comparable survival and prevalence of adverse events late after orthotopic heart transplantation. Encouraging results have also been obtained regarding the reduced incidence of chronic graft rejection and less prevalence of coronary artery disease in heart transplant patients after blood cardioplegia, but larger prospective studies in this area are needed to validate this hypothesis.

Two other studies used antegrade cold blood cardioplegia and an additional terminal "hot shot" with warm blood cardioplegic solution. Cold crystalloid cardioplegia was injected initially and cold blood cardioplegia (Buckberg) was infused every 30 minutes as soon as the graft arrived in the operating room [13]. No surface cooling was used. Warm blood cardioplegic reperfusion was administered before removal of the aortic clamp. Mean ischemic time was 158 minutes. The post-transplant need for catecholamines was tenfold lower in patients with warm blood cardioplegia reperfusion. Also, cytologic examination of the graft (after 7 days) showed a lower degree of ischemic lesions in this group of patients.

Some studies have been devoted to the use of continuous retrograde normothermic blood cardioplegia during donor heart implantation [14–16]. The results of these studies revealed that continuous normothermic blood cardioplegia can lead to less ischemic injury according to myocardial pathohistologic examination, while lower CK, CK-MB levels, more frequent recovery of spontaneous sinus rhythm, and lower duration of inotropic therapy were observed in groups using continuous blood cardioplegia technique.

A single-center retrospective study in Switzerland compared orthotopic heart transplant outcomes with (37 patients) and without additional cardioplegia (41 patients) [17]. The myocardial preservation protocol was standardized and included the infusion under low pressure of 2000 ml cold (4–8 °C) Celsior solution. In the study group, an additional single antegrade coronary infusion of 100 ml cardioplegic solution (Cardioplexol™, Laboratorium Dr G. Bichsel AG, Unterseen, Switzerland) was administered immediately before graft implantation. Cardioplexol™ is a ready-to-use solution based on potassium, magnesium, procaine and xylitol. The study group showed more frequent spontaneous restoration of sinus rhythm after aortic clamp removal and myocardial reperfusion, lower CK-MB/CK ratio, and shorter ICU and hospital stays.

Regarding immediate transplant outcomes, an analysis of available publications is favorable to the use of repeated or extra infusions of preservation solution, particularly when the preservation time is more than 240 minutes.

ISCHEMIC PRECONDITIONING AND POSTCONDITIONING

Because pharmacologic and ischemic preconditioning activate mitochondrial ATP-sensitive potassium channels, they may be useful cardioprotective methods [18]. Mozaffari et al. argue that the protective effect of ischemic preconditioning and postconditioning is linked to reduced IRI through regulation of the phosphatidylinositol-3 kinase (PI3K)/Akt pathway, which, in turn, leads to phosphorylation and inactivation of glycogen synthase

kinase-3β (GSK-3β), culminating in inhibition of the mitochondrial permeability transition pore. There have also been descriptions of mitochondrial KATP channels, which when activated, can confer cardioprotection.

The effect of preconditioning was demonstrated in a study on sheep orthotopic heart transplantation models. Preconditioning was achieved with brief (5 seconds) aortic occlusion followed by 10 minutes of reperfusion. The heart was then arrested with 1 liter of antegrade crystalloid cardioplegia, explanted, and placed in a transport cooler. Next, the heart was transplanted into a recipient sheep. The total ischemic time was 2 hours. The study showed that a single episode of preconditioning significantly reduced myocardial stunning and increased ATP level in tissues [19].

In another study, remote ischemic conditioning was used immediately after anesthesia induction (preconditioning) and 20 minutes after aortic declamping (postconditioning) [20]. The technique itself consists of applying four cycles of 5-min ischemia and 5-min reperfusion on the right upper limb by a cuff inflated to 200 mmHg, then the cuff was deflated. Patients in the control group underwent false cuffing of the right upper arm without inflation. Serum cardiac troponin I level was determined preoperatively and at 3, 6, 12, 24 hours after aortic declamping.

In summary, remote ischemic preconditioning and postconditioning reduced myocardial injury 6 hours after aortic clamping, but there was no evidence that this method could improve clinical outcomes. Preconditioning and postconditioning techniques in cardiac transplantation have been shown to reduce the severity of myocardial injury as measured by laboratory parameters, but no significant effect on clinical outcomes has been found. Available reports are based on a small number of patients, on retrospective analysis. A detailed study of the mechanism of the technique and further trials are needed.

PRESERVATION SOLUTIONS

As mentioned above, the standard cardiac preservation method is perfusion of the heart with a preservation solution followed by static storage in a refrigerator with ice and coolants. Despite notable disadvantages of HTK (Custodiol) solution, it remains the main preservation solution used in Russia both in heart transplantation and in cardiac surgery involving prolonged myocardial ischemia.

There are currently more than 167 different cardiac preservation solutions for heart transplantation. The most commonly used are histidine-tryptophan-ketoglutarate (HTK) solution, University of Wisconsin (UW) solution, and Celsior solution [21]. Due to the small number of heart transplants performed, there is a lack of high-quality randomized clinical trials to determine the effect of preservation fluids on graft function and survival. Such studies often lack the capacity to determine optimal regimens for the use of these preservation solutions.

Experimental studies provide conflicting results regarding the efficacy of different preservation solutions in preserving cardiac function during routine transportation with ice and coolants. According to some studies that compared UW with Celsior solution [22], UW demonstrated better survival at 30 and 90 days after transplantation. Recipients receiving suboptimal allografts, defined as donor age >50 years or ischemic duration >4 hours, had significantly increased mortality at 30 days and 1 year. The UW solution was also associated with better survival compared with the HTK solution. When HTK was compared with Celsior solution, there was no statistical difference in donor heart dysfunction and in-hospital mortality, with a mean ischemic time of 187.9 ± 52.6 minutes [23]. However, in multivariate analysis, a combination of recipient and donor age ≥60 years, intraoperative biventricular failure, and prior cardiac surgery were predictors of in-hospital mortality.

Four-hour preservation of porcine heart grafts obtained from beating and non-beating donor animals in Somah resulted in better cardiomyocyte and endothelial cell viability and higher expression levels of myocardial and endothelial proteins compared with controls. Better cardioprotection was observed after 5-hour preservation of porcine heart at about 21 °C compared to Celsior and UW.

The new Custodiol-N solution is an intracellular preservation solution that differs from HTK by its lower concentration of histidine, addition of amino acids glycine, alanine and arginine, N-acetyl-histidine partially replacing histidine, and aspartate and lactobionate replacing chloride. The superiority of Custodiol-N over HTK has been demonstrated in a rat model of heterotopic heart transplantation [24, 25]. Also, Custodiol-N showed significant benefit in a heart transplantation model in dogs after prolonged preservation for 8 and 12 hours. After heart transplantation in animals from the control group using conventional HTK, in no case was it possible to wean off from artificial circulation; in the Custodiol-N group, all animals were withdrawn from artificial circulation with stable hemodynamics [26]. According to the authors, the iron chelator LK614 played a key role in this mechanism by reducing the chelatable iron content in the myocardium. Thus, Custodiol-N, UW, Somah look preferable to conventional HTK with respect to long-term preservation.

A detailed analysis was performed by Minasyan et al. In their opinion, the possible methods of improving preservation methods in prolonged ischemia are by optimizing the composition of the preservation solution (PS), adding various active components to the PS (enhancing the buffer capacity and colloidal components), using polarizing PS, constant perfusion of donor heart, and low-temperature preservation [27]. The theory of

low-temperature preservation (<less than 0 degrees Celsius) using cryoprotectant protein looks interesting, considering some contradiction with the concept used in the Paragonix system [28]. However, standard cold transportation of donor hearts in a container with ice has several disadvantages, in particular, the lack of organ temperature control. A study on 186 organs showed that the average temperature of organs during transportation fell below +2 °C, and then below ±0 °C after 6 hours of transportation [29]. Preservation at this temperature may cause injury to the donor heart, especially if prolonged. It is known that there is damage to cardiomyocyte structures at a temperature <2 °C, irreversible diastolic dysfunction occurs at <1 °C, and protein denaturation at <0 °C.

The SherpaPak Cardiac Transport System (CTS) (Paragonix Technologies, MA, USA) has been developed, which involves uniform cooling with constant temperature from 4 °C to 8 °C, excluding any environmental influence, which prevents the risk of cold injury to the organ and further irreversible changes in myocardial cells. A decrease in post-heart transplant in-hospital mortality was demonstrated in a study group (Paragonix preservation) compared to standard "ice" preservation [30]. The Paragonix SherpaPak™ Cardiac Transport System demonstrates excellent results compared to standard cold preservation. It is necessary to study the system for cardiac preservation of >4 hours.

NORMOTHERMIC MACHINE PERFUSION OF DONOR HEART

The most promising technology for long transportation of donor organs is machine perfusion. Currently, the device for normothermic machine perfusion (NMP) of the heart manufactured by TransMedics Inc. (Andover, Massachusetts, USA) has the greatest clinical experience [31]. The prospective multicenter randomized PROCEED II study compared the NMP system with standard heart storage on ice. The 30-day patient survival rate was 94% in the machine perfusion group with a mean organ ischemia time of 5.4 hours and 97% in the control group. Short-term clinical results showed that the TransMedics Inc. organ care system was non-inferior to storing the graft in a refrigerator. Further studies demonstrated no differences in two-year survival or serious cardiac-related adverse events between the two groups [32].

In expanded criteria donors, the use of TransMedics Inc. normothermic perfusion systems has demonstrated a significant advantage over refrigerated allografts. The EXPAND-Heart study showed that expanded criteria hearts using NMP had a 30-day survival rate of 94% and a 6-month survival rate of 88%. The incidence of severe primary graft dysfunction was 11% [33]. There is also evidence of successful heart transplantation with an ischemia time of 611 minutes, which was performed using a normothermic myocardial perfusion system [34]. According to a study conducted in the USA, this machine perfusion system was more cost-effective than standard refrigerated graft storage [35]. The use of a normothermic perfusion system seems to be the most preferable and physiologic way to preserve the donor heart. The TransMedics system demonstrates good results for short- and long-distance transportation. The disadvantages of the system are determined by its weight/size characteristics and operating features, but its primary limiting factor is its exorbitant cost. Currently, normothermic cardiac perfusion is not used in Russia.

TECHNOLOGY OF THE FUTURE

Proton-activated acid-sensing ion channels (ASIC1a) are known to play a key role in IRI. Redd et al. demonstrated in an experimental rat model that the use of pharmacologic ASIC1a inhibitors derived from the venom of the Australian spider Hadronyche infensa (Hi1a) improves functional recovery of isolated rodent hearts after prolonged hypothermic ischemia. To evaluate the cardioprotective effect of ASIC1a inhibition in a donor heart preservation model, the scientists added a pharmacologic Hi1a inhibitor to Celsior solution, with an ischemia time of 8 hours. Coronary blood flow was then restored, and cardiac function assessed. Compared to the control group, hearts preserved with Hi1a supplementation showed a significant improvement in the recovery of aortic flow and cardiac output. These findings demonstrate that Hi1a has high cardioprotective activity against IRI in a clinically relevant model of donor heart preservation under long-term cold storage [5].

CONCLUSION

A detailed understanding of the pathophysiology of IRI and a fundamental approach are necessary when looking for an optimal method of preserving donor heart with prolonged cold ischemia. Available reports on this problem, with presumed prolonged cold ischemia, require that donors without associated risk factors be used, that any loss of time during transportation be avoided, and that repeated infusions of the preservative solution or blood cardioplegia be performed. There is an obvious urgent need to develop new Russian-made preserving solutions and to come up with new organ perfusion techniques.

The work was supported by a grant from the Russian Science Foundation (project 24-25-00352).

The authors declare no conflict of interest.

REFERENCES

1. *Fomichev AV, Poptsov VN, Sirota DA, Zhulkov MO, Edemskiy AG, Protopopov AV et al.* Mid-term and long-term outcomes following heart transplantation with pro-

longed cold ischemia. *Russian Journal of Transplantology and Artificial Organs*. 2023; 25 (1): 99–105. https://doi.org/10.15825/1995-1191-2023-1-99-105.
2. *Erasmus M, Neyrink A, Sabatino M, Potena L*. Heart allograft preservation: an arduous journey from the donor to the recipient. *Curr Opin Cardiol*. 2017; 32 (3): 292–300. https://doi.org/10.1097/hco.0000000000000395.
3. *Segovia J, Cosío MD, Barceló JM, Bueno MG, Pavía PG, Burgos R et al.* RADIAL: a novel primary graft failure risk score in heart transplantation. *J Heart Lung Transplant*. 2011; 30 (6): 644–651. https://doi.org/10.1016/j.healun.2011.01.721.
4. *Lund LH, Khush KK, Cherikh WS, Goldfarb S, Kucheryavaya AY, Levvey BJ et al.* The Registry of the International Society for Heart and Lung Transplantation: Thirty-fourth Adult Heart Transplantation Report – 2017; Focus Theme: Allograft ischemic time. *J Heart Lung Transplant*. 2017; 36 (10): 1037–1046. https://doi.org/10.1016/j.healun.2017.07.019.
5. *Redd MA, Scheuer SE, Saez NJ, Yoshikawa Y, Chiu HS, Gao L et al.* Therapeutic Inhibition of Acid-Sensing Ion Channel 1a Recovers Heart Function After Ischemia-Reperfusion Injury. *Circulation*. 2021; 144 (12): 947–960. https://doi.org/10.1161/cir.0000000000001020.
6. *Minasian SM, Galagudza MM, Dmitriev YV, Karpov AA, Vlasov TD.* Preservation of the donor heart: from basic science to clinical studies. *Interact Cardiovasc Thorac Surg*. 2015; 20 (4): 510–519. https://doi.org/10.1093/icvts/ivu432.
7. *Rauen U, Klempt S, De Groot H.* Histidine-induced injury to cultured liver cells, effects of histidine derivatives and of iron chelators. *Cell Mol Life Sci*. 2007; 64 (2): 192–205. https://doi.org/10.1007/s00018-006-6456-1.
8. *Kim ST, Helmers MR, Iyengar A, Han JJ, Patrick WL, Weingarten N D et al.* Interaction between donor obesity and prolonged donor ischemic time in heart transplantation. *J Cardiol*. 2022; 80 (4): 351–357. https://doi.org/10.1016/j.jjcc.2022.06.013.
9. *Ribeiro RVP, Friedrich JO, Ouzounian M, Yau T, Lee J, Yanagawa B.* Supplemental Cardioplegia During Donor Heart Implantation: A Systematic Review and Meta-Analysis. *Ann Thorac Surg*. 2020; 110 (2): 545–552. https://doi.org/10.1016/j.athoracsur.2019.10.094.
10. *Luciani GB, Faggian G, Montalbano G, Casali G, Forni A, Chiominto B, Mazzucco A.* Blood versus crystalloid cardioplegia for myocardial protection of donor hearts during transplantation: A prospective, randomized clinical trial. *J Thorac Cardiovasc Surg*. 1999; 118 (5): 787–795. https://doi.org/10.1016/s0022-5223(99)70047-4.
11. *Luciani GB, Faggian G, Forni A, Montalbano G, Chiominto B, Mazzucco A.* Myocardial protection during heart transplantation using blood cardioplegia. *Transplant Proc*. 1997; 29 (8): 3386–3388. https://doi.org/10.1016/s0041-1345(97)00950-0.
12. *Luciani GB, Forni A, Rigatelli G, Chiominto B, Cardaioli P, Mazzucco A, Faggian G.* Myocardial protection in heart transplantation using blood cardioplegia: 12-year outcome of a prospective randomized trial. *J Heart Lung Transplant*. 2011; 30 (1): 29–36. https://doi.org/10.1016/j.healun.2010.08.014.
13. *Soots G, Crepin F, Prat A, Gosselin B, Pol A, Moreau D, Devulder JP.* Cold blood cardioplegia and warm cardioplegic reperfusion in heart transplantation. *Eur J Cardiothorac Surg*. 1991; 5 (8): 400–404. https://doi.org/10.1016/1010-7940(91)90183-k.
14. *Carrier M, Leung TK, Solymoss BC, Cartier R, Leclerc Y, Pelletier LC.* Clinical trial of retrograde warm blood reperfusion versus standard cold topical irrigation of transplanted hearts. *Ann Thorac Surg*. 1996; 61 (5): 1310–1315. https://doi.org/10.1016/0003-4975(96)00075-6.
15. *Fiocchi R, Vernocchi A, Mammana C, Iamele L, Gamba A.* Continuous retrograde warm blood reperfusion reduces cardiac troponin I release after heart transplantation: a prospective randomized study. *Transpl Int*. 2000; 13 Suppl 1: S240–S244. https://doi.org/10.1111/j.1432-2277.2000.tb02027.x.
16. *Pradas G, Cuenca J, Juffe A.* Continuous warm reperfusion during heart transplantation. *J Thorac Cardiovasc Surg*. 1996; 111 (4): 784–790. https://doi.org/10.1016/s0022-5223(96)70338-0.
17. *Tevaearai Stahel HT, Unger D, Schmidli J, Gahl B, Englberger L, Kadner A et al.* Supplemental Cardioplegia Immediately before Graft Implantation may Improve Early Post-Transplantation Outcome. *Front Surg*. 2014; 1: 46. https://doi.org/10.3389/fsurg.2014.00046.
18. *Mozaffari MS, Liu JY, Abebe W, Baban B.* Mechanisms of load dependency of myocardial ischemia reperfusion injury. *Am J Cardiovasc Dis*. 2013; 3 (4): 180–196.
19. *Landymore RW, Bayes AJ, Murphy JT, Fris JH.* Preconditioning prevents myocardial stunning after cardiac transplantation. *Ann Thorac Surg*. 1998; 66 (6): 1953–1957. https://doi.org/10.1016/s0003-4975(98)00902-3.
20. *Wang G, Zhang Y, Yang L, Chen Y, Fang Z, Zhou H et al.* Cardioprotective effect of remote ischemic preconditioning with postconditioning on donor hearts in patients undergoing heart transplantation: A single-center, double-blind, randomized controlled trial. *BMC Anesthesiol*. 2019; 19 (1): 1–8. https://doi.org/10.21203/rs.2.182/v1.
21. *Carter KT, Lirette ST, Baran DA, Creswell LL, Panos AL, Cochran RP et al.* The Effect of Cardiac Preservation Solutions on Heart Transplant Survival. *J Surg Res*. 2019; 242: 157–165. https://doi.org/10.1016/j.jss.2019.04.041.
22. *George TJ, Arnaoutakis GJ, Beaty CA, Shah AS, Conte JV, Halushka MK.* A novel method of measuring cardiac preservation injury demonstrates University of Wisconsin solution is associated with less ischemic necrosis than Celsior in early cardiac allograft biopsy specimens. *J Heart Lung Transplant*. 2012; 31 (4): 410–418. https://doi.org/10.1016/j.healun.2011.11.023.
23. *Cannata A, Botta L, Colombo T, Russo CF, Taglieri C, Bruschi G et al.* Does the cardioplegic solution have an effect on early outcomes following heart transplantation? *Eur J Cardiothorac Surg*. 2012; 41 (4): e48–e52. https://doi.org/10.1093/ejcts/ezr321.
24. *Loganathan S, Radovits T, Hirschberg K, Korkmaz S, Koch A, Karck M, Szabó G*. Effects of Custodiol-N, a novel organ preservation solution, on ischemia/reperfusion injury. *J Thorac Cardiovasc Surg*. 2010; 139 (4): 1048–1056. https://doi.org/10.1016/j.jtcvs.2009.09.034.

25. *Mohr A, Brockmann JG, Becker F.* HTK-N: Modified Histidine-Tryptophan-Ketoglutarate Solution-A Promising New Tool in Solid Organ Preservation. *Int J Mol Sci*. 2020; 21 (18): 1–16. https://doi.org/10.3390/ijms21186468.
26. *Szabó G, Loganathan S, Korkmaz-Icöz S, Balogh Á, Papp Z, Brlecic P et al.* Improvement of Left Ventricular Graft Function Using an Iron-Chelator-Supplemented Bretschneider Solution in a Canine Model of Orthotopic Heart Transplantation. *Int J Mol Sci*. 2022; 23 (13): 7453. https://doi.org/10.3390/ijms23137453.
27. *Minasian SM, Galagudza MM, Dmitriev YuV, Karpov AA, Bobrova EA, Krasichkov AS et al.* Donor heart preservation: history and current status in terms of translational medicine. *Regional blood circulation and microcirculation*. 2014; 13 (3): 4–16. (In Russ.). https://doi.org/10.24884/1682-6655-2014-13-3-4-16.
28. *Radakovic D, Karimli S, Penov K, Schade I, Hamouda K, Bening C et al.* First clinical experience with the novel cold storage SherpaPakTM system for donor heart transportation. *J Thorac Dis*. 2020; 12 (12): 7227–7235. https://doi.org/10.21037/jtd-20-1827.
29. *Horch DF, Mehlitz T, Laurich O, Abel A, Reuter S, Pratschke H et al.* Organ transport temperature box: Multicenter study on transport temperature of organs. *Transplant Proc*. 2002; 34 (6): 2320. https://doi.org/10.1016/s0041-1345(02)03253-0.
30. *Michel SG, LaMuraglia Ii GM, Madariaga ML, Anderson LM.* Innovative cold storage of donor organs using the Paragonix Sherpa Pak TM devices. *Heart Lung Vessel*. 2015; 7 (3): 246–255.
31. *Kothari P*. *Ex-Vivo* Preservation of Heart Allografts – An Overview of the Current State. *J Cardiovasc Dev Dis*. 2023; 10 (3): 105. https://doi.org/10.3390/jcdd10030105.
32. *Ardehali A, Esmailian F, Deng M, Soltesz E, Hsich E, Naka Y et al. Ex-vivo* perfusion of donor hearts for human heart transplantation (PROCEED II): a prospective, open-label, multicentre, randomised non-inferiority trial. *Lancet*. 2015; 385 (9987): 2577–2584. https://doi.org/10.1016/s0140-6736(15)60261-6.
33. *Ragalie WS, Ardehali A.* Current status of normothermic *ex-vivo* perfusion of cardiac allografts. *Curr Opin Organ Transplant*. 2020; 25 (3): 237–240. https://doi.org/10.1097/mot.0000000000000759.
34. *Stamp NL, Shah A, Vincent V, Wright B, Wood C, Pavey W et al.* Successful Heart Transplant after Ten Hours Out-of-body Time using the TransMedics Organ Care System. *Heart Lung Circ*. 2015; 24 (6): 611–613. https://doi.org/10.1016/j.hlc.2015.01.005.
35. *Voigt JD, Leacche M, Copeland H, Wolfe SB, Pham SM, Shudo Y et al.* Multicenter Registry Using Propensity Score Analysis to Compare a Novel Transport/Preservation System to Traditional Means on Postoperative Hospital Outcomes and Costs for Heart Transplant Patients. *ASAIO J*. 2023; 69 (4): 345–349. https://doi.org/10.1097/mat.0000000000001844.

The article was submitted to the journal on 21.02.2024

DOI: 10.15825/1995-1191-2024-2-58-62

MANAGEMENT AND OUTCOMES OF ANEURYSMS FOUND IN DECEASED DONOR LIVERS: A REVIEW OF PUBLISHED CASES

A. González De Godos, B. Pérez Saborido, M. Bailón Cuadrado, D. Pacheco Sánchez

Río Hortega University Hospital, Valladolid, Spain

Introduction. The organ shortage has prompted transplant surgeons to accept grafts from deceased donors, which can lead to complex reconstructions. The presence of an aneurysm can complicate the arterial anastomosis of the liver transplant, leading to postoperative vascular complications such as hepatic artery thrombosis or stenosis. **Objective:** to review reported cases of donor liver aneurysms and their management. **Materials and methods.** After an exhaustive literature search, only 4 published cases of liver transplants from grafts with aneurysms in their vascular territory have been found. **Results.** These vascular anomalies were corrected by vascular reconstructions and no postoperative arterial complications were observed. **Conclusion.** Although no particular arterial configuration precludes the use of a donor liver for transplant, more arterial complications can be anticipated with complex arterial reconstructions. However, properly managed arterial anomalies do not necessarily compromise graft outcome. Therefore, our review of the literature shows the possibility of using these organs for liver transplantation, which would otherwise be discarded.

Keywords: liver transplantation, hepatic aneurysm, extended criteria donor, vascular abnormalities.

INTRODUCTION

The organ shortage has prompted transplant surgeons to accept grafts from deceased donors with severe vascular anomalies that may require complex reconstructions [1]. Recognition and adequate reconstruction of such variants are essential in the evolution of liver transplantation, since alterations in arterial flow usually cause graft loss due to biliary and/or parenchymal ischemic complications. In the literature, arterial anomalies have been linked to an increased incidence of arterial complications. Most of these studies were based on a relatively small number of grafts and none have analyzed the effect of the techniques for managing these anomalies on post-transplant complications. The optimal treatment of these findings in the donor liver is also unclear [2].

The discrepancy between supply and demand and the increase in morbidity and mortality of patients on the waiting list has led to a search for alternatives to the standard pool of brain-dead organ donors. The most immediate source of organs capable of expanding the donor pool is that of donors with extended criteria, also called marginal donors. These, although not universally defined, include a wide range of donors with unfavorable characteristics, historically associated with worse graft and patient survival [advanced age, steatosis, hypernatremia, donor in asystole, etc.]. Asystole donation is associated with severe ischemia-reperfusion injury, which is responsible for delayed graft function and biliary ischemia. However, if carefully selected and matched to appropriate recipients, asystole donor livers can be used safely and effectively [3].

Aneurysms of the visceral arteries are rare entities that affect the celiac trunk, splenic, superior mesenteric or inferior mesenteric artery and their branches. The prevalence of visceral artery aneurysms is 0.1% to 2%. Depending on the size and location of the aneurysm, mortality from rupture ranges from 25% to 100%. The splenic artery is the most commonly affected artery (60%), followed by the hepatic artery (20% to 50%) [4].

The presence of an aneurysm can complicate the arterial anastomosis of the liver transplant, leading to postoperative vascular complications such as thrombosis or stenosis of the hepatic artery. Careful arterial reconstruction of this vascular anomaly can reduce this risk of vascular complications and make it possible to use a graft that would have been discarded [5].

We performed a review of the literature on published cases of aneurysms found in this donor vascular territory and their management.

MATERIALS AND METHODS

The search was carried out in several databases: Pubmed, Scopus, Cochrane library, EMBASE, SciELO and LILACS; and in all of them the same search criteria were followed. The following algorithm was used: "liver donor aneurysm". The search was conducted on August 2, 2023. Studies published in Spanish and English were

Corresponding author: Andrea González De Godos. Río Hortega University Hospital, Valladolid, Spain.
ORCID code: 0000-0003-2402-5483. Address: Calle Dulzaina, 2, 47012 Valladolid (Spain).
Phone: +34 711749153. E-mail: agonzalezdeg@saludcastillayleon.es

included. All publications that did not deal with donor liver aneurysms were discarded. No filters of any kind (text availability, article type, publication date, …) were applied After reviewing the literature, 4 published cases were found.

RESULTS

In the first case described in 2012, a celiac trunk aneurysm (1.7 cm of transverse diameter) was found during the back-table surgery. The whole liver transplantation was performed to re-transplant a 43-year-old woman with end-stage liver disease (MELD score 30) that was caused by chronic rejection. The Model for End-Stage Liver Disease (MELD) is an objective and easily reproducible prognostic index of mortality based on three simple analytical variables: bilirubin, serum creatinine and the prothrombin time/International Normalized Ratio (INR) of protrombine time. The implementation of MELD as an organ allocation system has reduced mortality on the waiting list without affecting post-transplantation survival. A heterologous segmental hepatic arterial graft was used to guarantee optimal arterial flow. The hepatic artery was sewn end-to-end to the common hepatic artery and subsequently during the implantation the end of the donor common hepatic artery was sewn end-to-end to the native common hepatic artery of the recipient. The recipient is alive and well 6 months later, without any vascular or biliary complications [6].

In the second case described in 2015, a Michels type V variant was verified with a left accessory hepatic artery arising from an aneurysm of the left gastric artery of 2.3 × 2.3 cm and a second aneurysm of the common hepatic artery of 2.7 × 2.5 cm. At the bench-time, it was created a main common arterial trunk using four vascular sutures: the left hepatic artery (elongation) to a tubular splenic patch; the splenic patch to the gastric stump of the spleno-gastric carrefour; the splenic side of the carrefour to the right hepatic artery; the spleno-gastric carrefour to a mesenteric patch in order to obtain a good arterial stump for the anastomosis in the recipient. The new common arterial trunk (graft) was sutured to the common hepatic artery at the gastro-duodenal origin and the left accessory hepatic artery to the homologous branch of the recipient. After 36 months of follow-up, the patient was in good conditions with normal biochemistry. Contrast-enhanced computerized tomography 3D reconstruction showed arterial patency without any stricture and/or kinking of the reconstructed arteries [1].

In the third case described in 2020, computerized tomography demonstrated a proper hepatic artery aneurysm of 64 × 49 mm in diameter, which extended to the origin of the right and left hepatic arteries; the common hepatic artery arose from the superior mesenteric artery. At back table it was resected the aneurysm and reconstructed the left and right hepatic arteries on a vascular graft obtained from the donor's distal tract of the superior mesenteric artery. All collaterals of the mesenteric graft were accurately ligated, apart from the ileocolic bifurcation, which was used for the anastomosis. Liver transplant was performed using the piggy-back technique without venovenous bypass. For arterialization, it was anastomosed the mesenteric graft to the recipient's hepatic artery at the origin of the gastroduodenal artery. The postoperative course was uneventful, and no complications were observed after a total follow-up of 6 months [7].

In the fourth case described in 2021, it was identified a celiac artery aneurysm (CAA) 18 mm in diameter, with the common hepatic, splenic, and left gastric arteries originating from the aneurysm. The recipient's proper hepatic artery was dissected down to the level of the hepatic artery bifurcation to create the anastomosis. The donor's hepatic artery was divided away from the aneurysmal dilatation to the level of the common hepatic artery. The hepatic artery reconstruction was performed in an end-to-end fashion using a Carrel patch from the recipient's proper hepatic artery bifurcation to donor's common hepatic artery. Since discharge, the recipient had had 2 episodes of colestasis, which were managed by endoscopic retrograde cholangiopancreatography with sphincterectomy, dilation, and stent placement. The flow through the arterial anastomosis has demonstrated optimal post-operative flow patterns since transplant [5].

Summary of cases (Table)

Reconstruction scheme (Fig.)

DISCUSSION

Liver transplantation represents the treatment of choice for patients with end-stage liver disease and in recent years there have been improvements in immunosuppressive regimens, preservation solutions, anesthesia, surgical techniques, donor and recipient selection, and antibiotic therapy; however, the availability of liver grafts remains scarce [6].

The increasing median age of deceased donors and the increasing frequency of serious vascular anomalies today encourages transplant centers to be ready to manage such variations and vascular problems successfully [1].

Today professionals are forced to use the group of extended criteria donors (ECD) as a logical consequence of donor scarcity and significant changes in the socioeconomic and healthcare fronts and new development in the field of medicine. Consequently, the number of potentially younger organ donors has decreased and many centres in Europe report on an increasing median donor age in their population. ECD grafts are thought to be of lower than average quality, associated with poor posttransplant outcomes or an increase in disease transmission. Grafts, however, can be used safely through

careful selection of both donor and recipient risks. Although there is no precise definition for what constitutes an ECD liver, frequently cited characteristics are listed: advanced age; macrovesicular steatosis; donation after cardiac death (DCD); organ dysfunction at procurement; cause of death: anoxia, cerebrovascular accident; disease transmisión: Hepatitis B virus, Hepatitis C virus, CDC high-risk donors, HIV positive, extrahepatic malignancy, cold ischemia time (CIT) greater than 12 hours [8]. In short, careful donor and recipient selection remains crucial to optimize outcome after liver transplantation from ECD [9].

Despite the success demonstrated with liver transplantation, vascular complications remain the Achilles heel of the intervention. They usually occur at the anastomotic site, with thrombosis, hepatic artery stenosis, and other vascular complications associated with high morbidity and mortality. These complications can cause endothelial necrosis, necrosis of the biliary tree, or even loss of the graft, which would require a new transplant. Vascular variations or anomalies that require complex vascular reconstructions predispose to technical mistakes and the risk of vascular complications [1].

The presence of an aneurysm in a donor liver can complicate vascular reconstruction, distorting the arterial supply of the graft [5]. Our review of the literature on liver donor aneurysms shows only 4 case reports and data on the long-term outcomes of these grafts are sparse, illustrating the apprehension of transplant surgeons about using these grafts, which have the potential to achieve good results.

Although it is true that there were no significant complications in the reported cases, it must be taken into account that the follow-up period is short. A reconstruction as complex as the one mentioned by V. Tondolo (2015) [1], has a high rate of vascular complications and it would be necessary to consider whether this risk compensates the benefit of the transplant. Furthermore, the donor-recipient combination must be taken into account, since a patient in need of retransplantation, for example, may not be the best option for this type of donor. On the other hand, in the cases reported by F. Di Francesco (2012) [6] and O. Slivca (2021) [5], the need for arterial reconstruction would have to be considered if other options, such as the CHA-CHA anastomosis, were not possible. This option is not contemplated in the clinical case notification. Finally, we find the graft used in the case reported by De Carlis, R (2020) [7] interesting, although in our center we usually use the iliac bifurcation for this purpose.

Although there were no arterial complications in the studies analyzed, reconstruction involving multiple anastomoses significantly increases the risk. However, the incidence of chronic rejection and graft loss was similar in grafts with normal and abnormal arterial anatomy according to some studies [2].

It is essential that abnormalities in vessel wall integrity are evaluated in the operating room and infectious sources are excluded. The use of Doppler ultrasound in the immediate postoperative period allows early diagnosis of vascular complications and rapid treatment [5].

There are several strengths to this review. On the one hand, thorough literature search was conducted across multiple databases. On the other hand, discussion analyzes the risks/benefits of complex reconstructions versus discarding the grafts.

Our study was limited by a small sample size, given the few published cases of aneurysms in the liver of a deceased donor. Furthermore, this is not a comprehensive review, but rather a presentation of a problem in liver transplantation that can occur and the solutions that have been sought so far. Finally, more long-term follow-up on outcomes would be beneficial if available.

In summary, properly managed arterial anomalies do not necessarily compromise graft outcome. Although no particular arterial configuration precludes the use of a donor liver as a full or reduced graft, more arterial complications can be anticipated with complex arterial reconstructions [2]. More studies are needed to develop guidelines that advise on how to act in response to these findings in liver transplantation.

Table

Main characteristics of the cases described

Work	Location	Dimensions	Reconstruction	Anastomosis	Post-transplant complications
Di Francesco F. (2012)	Celiac trunk	1.7 cm (TD)	Heterologous segmental hepatic arterial graft	CHA-CHA	No
Tondolo V. (2015)	CHA LGA	2.7 × 2.5 cm 2.3 × 2.3 cm	Splenic patch, spleno-gastric carrefour, mesenteric patch	Graft-CHA/GDA	No
De Carlis R. (2020)	PHA	6.4 × 4.9 cm	Vascular graft from the donor's distal tract of the SMA	Graft-CHA/GDA	No
Slivca O. (2021)	Celiac trunk	1.8 cm (TD)	Carrel patch	CHA-PHA	Colestasis

Note. TD – transverse diameter; CHA – common hepatic artery; LGA – left gastric artery; SMA – superior mesenteric artery; GDA – gastroduodenal artery; PHA – proper hepatic artery.

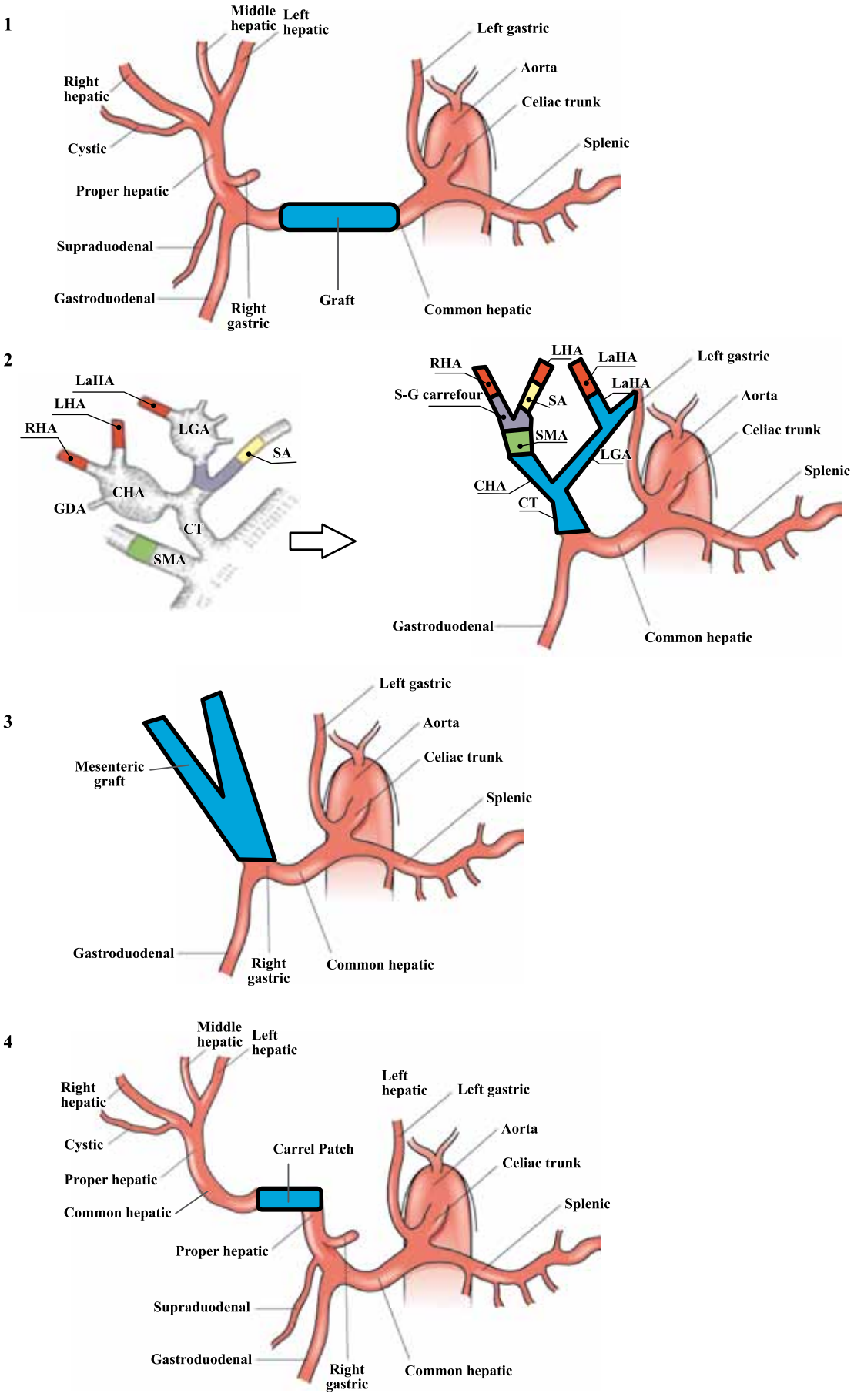

Fig. Reconstruction of the cases described. CHA – common hepatic artery; RHA – right hepatic artery; LHA – left hepatic artery; LGA – left gastric artery; GDA – gastroduodenal artery; SMA – superior mesenteric artery; LaHA – left accessory hepatic artery; SA – splenic artery; CT – celiac trunk; S-G carrefour – spleno-gastric carrefour

CONCLUSION

The presence of an aneurysm in the vascular territory of the liver donor should not be an absolute contraindication for its use as a liver graft. Although vascular anomalies and complex reconstructions may be associated with a higher risk of complications, our review of the literature shows the possibility of using these organs for liver transplantation. Anyway, further studies are necessary for more substantial conclusions.

Ethical responsibilities: *this study has no ethical considerations as it is a review.*

Funding: *this research has not received specific support from public sector agencies, the commercial sector or non-profit entities.*

The authors declare no conflict of interest.

REFERENCES

1. *Tondolo V, Manzoni A, Zamboni F.* A liver donor with double hepatic artery aneurysm: a saved graft. *Hepatobiliary Pancreat Dis Int*. agosto de 2015; 14 (4): 443–445. doi: 10.1016/s1499-3872(14)60325-8.
2. *Soin AS, Friend PJ, Rasmussen A, Saxena R, Tokat Y, Alexander GJ, et al.* Donor arterial variations in liver transplantation: management and outcome of 527 consecutive grafts. *Br J Surg*. mayo de 1996; 83 (5): 637–641. doi: 10.1002/bjs.1800830515.
3. European Association for the Study of the Liver. Electronic address: easloffice@easloffice.eu. EASL Clinical Practice Guidelines: Liver transplantation. *J Hepatol*. febrero de 2016; 64 (2): 433–485. doi: 10.1016/j.jhep.2015.10.006.
4. *James C. Stanley, Dawn M. Coleman y Jonathan L.* Eliason. Cirugía vascular y endovascular [Internet]. 9ª. Elsevier España; 2020 [cited August 2, 2023]. 687–699 p. Available in: https://www.clinicalkey.es/#!/content/book/3-s2.0-B9780323402323001291?scrollTo=%23hl0000082.
5. *Slivca O, Olowofela AS, Serrano OK, Pruett TL.* Maximizing Deceased-Donor Allograft Utilization: Management of a Celiac Artery Aneurysm in a Deceased-Donor Liver. *Exp Clin Transplant*. octubre de 2021; 19 (10): 1103–1105. doi: 10.6002/ect.2019.0023.
6. *Di Francesco F, Pagano D, Echeverri G, De Martino M, Spada M, Gridelli BG, et al.* Selective use of extended criteria deceased liver donors with anatomic variations. *Ann Transplant*. 31 de diciembre de 2012; 17 (4): 140–143. doi: 10.12659/aot.883705.
7. *De Carlis R, Andorno E, Buscemi V, Lauterio A, Diviacco P, Di Sandro S, et al.* Successful Transplant of a Liver Graft After Giant Hepatic Artery Aneurysm Resection and Reconstruction. *Exp Clin Transplant*. agosto de 2020; 18 (4): 522–525. doi: 10.6002/ect.2019.0028.
8. *Vodkin I, Kuo A.* Extended Criteria Donors in Liver Transplantation. *Clin Liver Dis*. mayo de 2017; 21 (2): 289–301. doi: 10.1016/j.cld.2016.12.004.
9. *Dasari BVM, Schlegel A, Mergental H, Perera MTPR.* The use of old donors in liver transplantation. *Best Pract Res Clin Gastroenterol*. abril de 2017; 31 (2): 211–217. doi: 10.1016/j.bpg.2017.03.002.

The article was submitted to the journal on 27.12.2023

DOI: 10.15825/1995-1191-2024-2-63-72

HYPOTHERMIC OXYGENATED PERFUSION IN LIVER TRANSPLANTATION FROM EXPANDED CRITERIA DONORS

A.V. Shabunin[1, 2], O.B. Loran[1, 2], D.Yu. Pushkar[1], E.I. Veliev[1], M.G. Minina[1, 3], P.A. Drozdov[1, 2], S.A. Astapovich[1], E.A. Lidzhieva[2]

[1] Botkin Hospital, Moscow, Russian Federation
[2] Russian Medical Academy of Postgraduate Education, Moscow, Russian Federation
[3] Shumakov National Medical Research Center of Transplantology and Artificial Organs, Moscow, Russian Federation

Objective: to improve the outcomes of liver transplantation (LTx) from expanded criteria donors (ECDs) through hypothermic oxygenated machine perfusion (HOPE). **Material and methods.** The study included 63 cases of LTx from suboptimal brain-dead donors. Group I (control) consisted of 34 persons in which liver transplant was preserved only by static cold storage (SCS), while group II (main) comprised 29 cases where *ex situ* HOPE was used after static preservation. We evaluated the efficacy and safety of the latter in a comparative clinical study and by studying ultrastructural changes in the liver using electron microscopy. **Results.** No statistically significant differences between the groups in terms of baseline characteristics of donors, recipients and several perioperative parameters ($p > 0.05$) were obtained. Peak aspartate aminotransferase (AST) and alanine aminotransferase (ALT) levels in the first week after transplantation were 1,052 (IQR: 712–1,842) U/L and 1,213 (IQR: 613–2,032) U/L in the HOPE group, and 1,943 (IQR: 1,294–5,214) U/L and 2,318 (IQR: 1,032–6,219) U/L in the SCS group (control). The levels were statistically significantly lower ($p = 0.002$ and $p < 0.001$, respectively). Median comprehensive complication index (CCI) in the main and control groups was 0 (IQR: 0–22.6) and 27.6 (IQR: 0–100) respectively. The differences were statistically significant ($p = 0.001$). Similarly, statistically significant differences were noted in terms of recipient time in the intensive care unit (ICU) and overall length of hospital stay ($p = 0.042$ and $p = 0.028$) – they were less in the HOPE group. Electron microscopy evaluation of the morphology of liver grafts revealed that hepatocytes sustained less injury during HOPE. **Conclusion.** *Ex situ* HOPE is a safe and effective way of preserving liver transplants. Its use in LTx from expanded criteria donors can lessen the severity of ischemia-reperfusion injury (IRI) in the organ and enable additional assessment of the suitability of an organ for transplantation.

Keywords: liver transplantation, preservation, expanded criteria donors.

INTRODUCTION

Liver transplantation (LTx) is currently the only definitive treatment for patients with end-stage liver disease. From Thomas Starzl's initial successful series of transplants in the 1960s to the present, this method has quickly expanded throughout the world and has become a routine clinical practice in many surgical centers. The availability of transplant care directly depends on donor resources, which is in short supply worldwide. This inevitably leads to a higher number of waitlisted candidates and increased waitlist mortality. According to a 2022 study by Eurotransplant, waitlist mortality reached 33.9% in 2022, essentially unchanged from outcomes a decade ago [1].

The use of expanded criteria donors (ECDs) is an effective way to increase the availability of LTx, but it is associated with increased risk of adverse effects in the postoperative period. It is known that grafts obtained from suboptimal donors are more susceptible to ischemic injury during preservation and subsequent reperfusion injury in the recipient's body [2]. Severe ischemia-reperfusion injury (IRI) causes early allograft dysfunction (EAD) [3]. According to the results of a large study from Mayo Clinic, the incidence of EAD was 26.5% and its development had a statistically significant impact on both immediate LTx outcomes and long-term recipient survival [4]. In some cases, EAD may be irreversible, which corresponds to primary graft nonfunction (PNF), with mortality exceeding 50% [5].

It is possible to reduce IRI severity in particular by improving graft preservation conditions. Perfusion methods of liver preservation from ECDs in comparison have already proved their advantage over static cold storage in many studies [6–8]. For instance, according to a multicenter randomized trial, the use of hypothermic oxygenated machine perfusion (HOPE) in LTx from ECDs reduces the risk of EAD, early postoperative complications, and duration of hospital stay [7]. Never-

Corresponding author: Pavel Drozdov. Address: 15/8, Brusilov str., Moscow, 117148, Russian Federation. Phone: (962) 985-04-41. E-mail: dc.drozdov@gmail.com

theless, introduction of perfusion technologies into the clinical practice of transplant programs is still limited. Only a few centers in the Russian Federation routinely perform machine perfusion preservation of donor organs.

Since 2020, Botkin Hospital has been introducing and actively using various perfusion techniques used for preservation of solid organs [9–11]. In this study, we have analyzed the first results of HOPE application in LTx from suboptimal brain-dead donors.

MATERIAL AND METHODS

The study is based on analysis of the outcomes of treatment of 63 liver recipients operated at Botkin Hospital from 2018 to 2023. In all cases, an isolated whole LTx from a brain-dead expanded criteria donor was performed. Donor data were classified into expanded criteria risk factors as proposed by Eurotransplant. These are:

- Donor age >65 years;
- ICU stay >7 days;
- Body mass index (BMI) >30 kg/m^2;
- Macrovesicular steatosis >40%;
- Sodium >155 mmol/L;
- ALT >105 U/L, AST >90 U/L;
- Total bilirubin >3 mg/dL.

Group characteristics

Group I (control group) included 34 cases in which liver graft was preserved only by static cold storage. The median age of recipients was 49 (IQR: 26–54) years, and median BMI was 24 (IQR: 21.0–32.0) kg/m^2. Among all recipients, 21 (61.7%) were males and 13 (38.2%) were females. Median MELD score was 16 (IQR: 14–19). Donor age was 54 (IQR: 31–66) years and BMI was 29 (IQR: 24.0–35.0) kg/m^2. Median time in ICU was 78 (IQR: 25.0–137.0) hours. Vasopressor therapy with norepinephrine was administered in all (100%) donors, among them 13 (34.7%) had the dose exceeding 1000 ng/kg/min or a second vasopressor was used. Median serum sodium level was 148 (IQR: 134–155) mmol/L, AST and ALT were 44.0 (IQR: 24.0–79.0) and 59.0 (IQR: 26.0–142) U/L, respectively. Mild steatosis (<40%) occurred in 10 (29.4%) and moderate (40–60%) in 24 (70.6%) liver transplants.

Group II (main group) included 29 recipients whose LTx was followed by HOPE after static storage. In 7 cases, classic HOPE was performed exclusively via the portal vein, in 22 cases dual HOPE was carried out both via the portal vein and via the hepatic artery. Median age of recipients was 51 (IQR: 32–59) years and BMI was 25 (IQR: 23.0–32.5). There were 16 males (55.2%) and 13 females (44.8%). Median MELD score was 17 (IQR: 14–20). Donor age was 58 (IQR: 31–67) years, BMI was 29 (IQR: 25.0–33.0) kg/m^2, and median ICU time was 86 (IQR: 34.0–122.0) hours, respectively. Vasopressor therapy was administered in all (100%) donors, among them 13 (44.8%) had a norepinephrine dose exceeding 1000 ng/kg/min or a second vasopressor was used. Median serum sodium level was 152 (IQR: 137–159) mmol/L, AST and ALT were 43.0 (IQR: 32.0–77.0) and 59.0 (IQR: 22.0–82.5) U/L, respectively. Express or routine histological examination showed that mild steatosis (<40%) occurred in 9 (31%) and moderate (40–60%) in 20 (69%) liver transplants. Detailed comparative characteristics of the groups are presented in Table 1.

Liver transplantation and postoperative period

Surgical interventions for liver removal from a deceased donor were performed using standard conventional technique. In all cases, organs were preserved using Bretschneider's solution (Custodiol HTK). Liver transplantation in all cases was performed with preservation of recipient inferior vena cava and caval reconstruction using the Belghiti technique. The recipient was managed in the postoperative period according to standard protocols in accordance with the National Clinical Guidelines. Basiliximab 20 mg was used as induction immunosuppressive therapy, administered intraoperatively and on day 4 after transplantation. Immediately before reperfusion, methylprednisolone was administered intravenously at 10 mg per kg of the recipient's weight, with subsequent reduction of the daily dose and complete withdrawal on day 4. For the majority of recipients, maintenance immunosuppression consisted of extended-release tacrolimus monotherapy, the target level of which was maintained within 7–10 ng/mL.

IRI intensity was determined by the highest level of transaminases in the first week after transplantation. EAD was defined according to the criteria stipulated by Olthoff et al. [3] with at least one of the following laboratory characteristics:

- Total bilirubin ≥10 mg/dL (171 μmol/L) on day 7 postoperatively;
- International normalized ratio (INR) ≥1.6 on day 7 postoperatively;
- ALT or AST >2000 IU/mL within the first week after surgery.

Ex situ hypothermic oxygenated machine perfusion

HOPE was carried out in the operating room of the transplant unit (according to the back-to-base technique) using a heart-lung machine. The liver graft was aseptically removed from the transport container into the container with Bretschneider's preservative solution (Custodiol HTK) cooled to 4–10 °C; the portal vein and graft artery were cannulated (Fig. 1, a). In the classic version, only the portal vein was cannulated (Fig. 1, b).

The perfusion procedure was performed by means of two roller pumps, two perfusion circuits and one oxygenator. The volumetric flow rates, determined by

operation of the roller pumps, were selected by the operator to maintain a perfusion pressure of 5 mmHg for the portal system and 25 mmHg for the arterial system. The effluent flowing through the inferior vena cava into the container where the graft was placed was taken into the perfusion system by two cannulas fixed at the bottom of the container. A schematic representation of the dual liver perfusion system is presented in Fig. 2.

Perfusate temperature remained within 10 °C throughout the entire procedure. Laboratory perfusion parameters were monitored every 30 minutes: acid-base balance (with partial pressure of oxygen PaO_2 determined), AST and ALT. The target PaO_2 of the perfusion solution was maintained at 400–600 mmHg.

During perfusion, the graft was treated before transplantation and its arteries were examined for leaks. Just before the graft was to be immersed into the wound, machine perfusion was terminated at the end of the hepatectomy stage.

Morphological assessment of liver grafts during preservation

We carried out an electron microscopic study in order to determine the intensity of liver cell damage at the ultrastructural level under ischemic conditions, depending

Table 1

Comparative analysis of liver transplant outcomes depending on preservation method

Indicator	Subgroup I.I (SCS) n = 34	Subgroup II.I (HOPE) n = 29	Significance (p value)
Recipient characteristics			
Recipient age (years)	49 (IQR: 26–54)	52 (IQR: 31–58)	0.32
Recipient male gender (n, %)	21 (61.7%)	15 (51.7%)	0.422
Recipient BMI (kg/m^2)	24 (IQR: 21.0–32.0)	22 (IQR: 21.0–34.0)	0.29
MELD	16 (IQR: 14–19)	17 (IQR: 13–19)	0.531
Donor characteristics			
Donor age (years)	54 (IQR: 31–66)	56 (IQR: 28–64)	0.357
Donor time in ICU (hours)	78 (IQR: 25.0–137.0)	86 (IQR: 32.0–166.0)	0.092
Donor BMI (kg/m^2)	29 (IQR: 24.0–35.0)	32 (IQR: 25.0–38.0)	0.252
Noradrenaline dose >1000 ng/mL or 2 vasopressors (n, %)	13 (34.7%)	7 (41.1%)	0.231
Na (mmol/L)	148 (IQR: 134–155)	142 (IQR: 135–154)	0.152
AST (U/L)	44.0 (IQR: 24.0–79.0)	47.0 (IQR: 24.0–78.0)	0.82
ALT (U/L)	59.0 (IQR: 26.0–142)	61.0 (IQR: 32.0–91.5)	0.139
Macrosteatosis >40%	24 (70.6%)	23 (79.3%)	0.564
Perioperative parameters			
Cold ischemia time (hours)	5.2 (IQR: 4.4–8.0)	5.7 (IQR: 4.3–7.8)	0.29
Static cold storage time (hours)	7.2 (IQR: 4.8–8.3)	2.5 (IQR: 1.5–4.5)	**0.012**
Operation duration (min)	6.8 (IQR: 5.5–7.5)	6.3 (IQR: 4.8–8.3)	0.457
Secondary warm ischemia time (min)	40 (IQR: 30–45)	35 (IQR: 35–45)	0.28
Biliary ischemia time (min)	40 (IQR: 35–45)	40 (IQR: 35–50)	0.93
Blood loss (mL)	1400 (IQR: 1100–2500)	1100 (IQR: 1000–2500)	0.21
Reinfusion (mL)	300 (IQR: 100–450)	250 (IQR: 50–450)	0.62
FFP transfusion (doses)	6 (IQR: 3–8)	4 (IQR: 2–7)	0.42
Erythrocyte suspension transfusion (doses)	1 (IQR: 0–3)	1 (IQR: 0–2)	0.652
Immediate liver transplant outcomes			
Length of stay in ICU (days)	5 (IQR: 3–9)	3 (IQR: 2–5)	**0.042**
Length of stay in hospital (days)	21 (IQR: 17–35)	15 (IQR: 12–24)	**0.028**
Peak AST level (U/L)	1052 (IQR: 712–1842)	1943 (IQR: 1294–5214)	**0.002**
Peak ALT level (U/L)	1213 (IQR: 613–2032)	2318 (IQR: 1032–6219)	**<0.001**
EAD (n, %)	21 (61.8%)	12 (41.3%)	0.106
Non-specific surgical complications (n, %)	11 (32.3%)	5 (9.4%)	**0.01**
Arterial thrombosis (n, %)	3 (8.9%)	1 (3.4%)	0.383
CCI	27.6 (IQR: 0–100)	0 (IQR: 0–22.6)	**<0.001**
Retransplantation (n, %)	1 (2.9%)	0	1
Mortality (n, %)	2 (5.9%)	0	0.495

Note. BMI, body mass index; ICU, intensive care unit; Na, sodium; AST, aspartate aminotransferase; ALT, alanine aminotransferase; FFP, fresh frozen plasma; EAD, early allograft dysfunction; CCI, comprehensive complication index.

on the preservation method. After graft delivery to the operating room, just before the beginning of machine perfusion, the first sample (1.1) was excised from the liver margin and fixed in formalin. At the same stage, a 2×2 cm fragment was excised from the liver and separately immersed in a cooled non-oxygenated preservative solution. Upon completion of machine perfusion preservation, the samples (1.2 and 1.3) were excised both from whole liver and from pre-cut fragments, which were under static cold storage conditions, and fixed in formalin. The sequence in which samples are taken for graft electron microscopy is presented in Fig. 3.

The immediate LTx outcomes depending on preservation method were analyzed by us in a comparative clinical study.

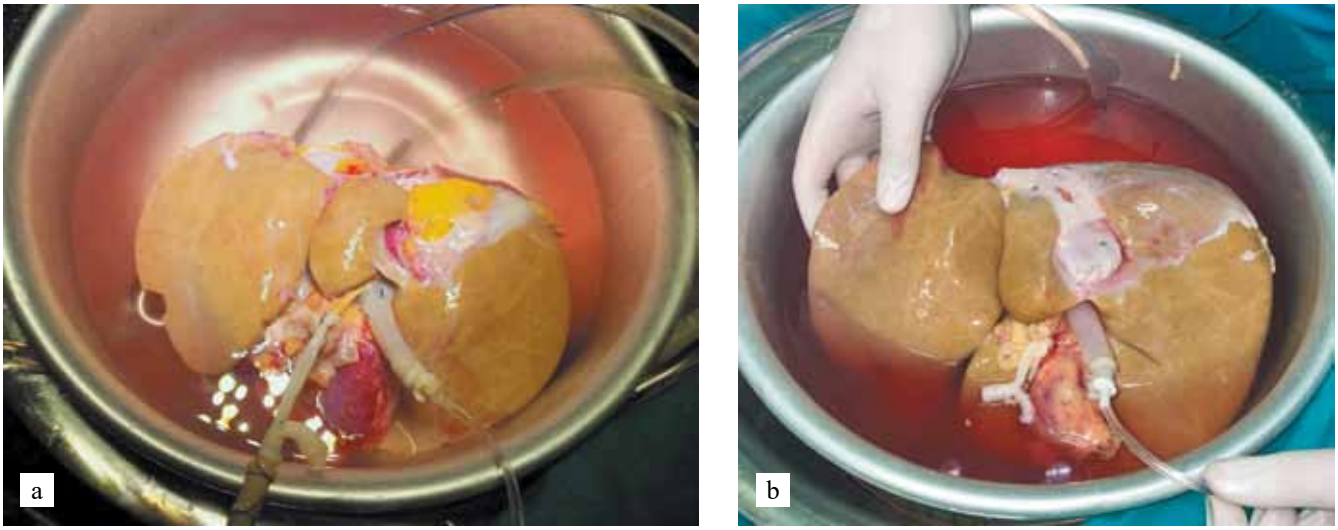

Fig. 1. Intraoperative photo: cannulation of the artery and portal vein of liver graft before the start of HOPE. a, dual perfusion of liver via the portal vein and hepatic artery; b, classic perfusion of liver via the portal vein

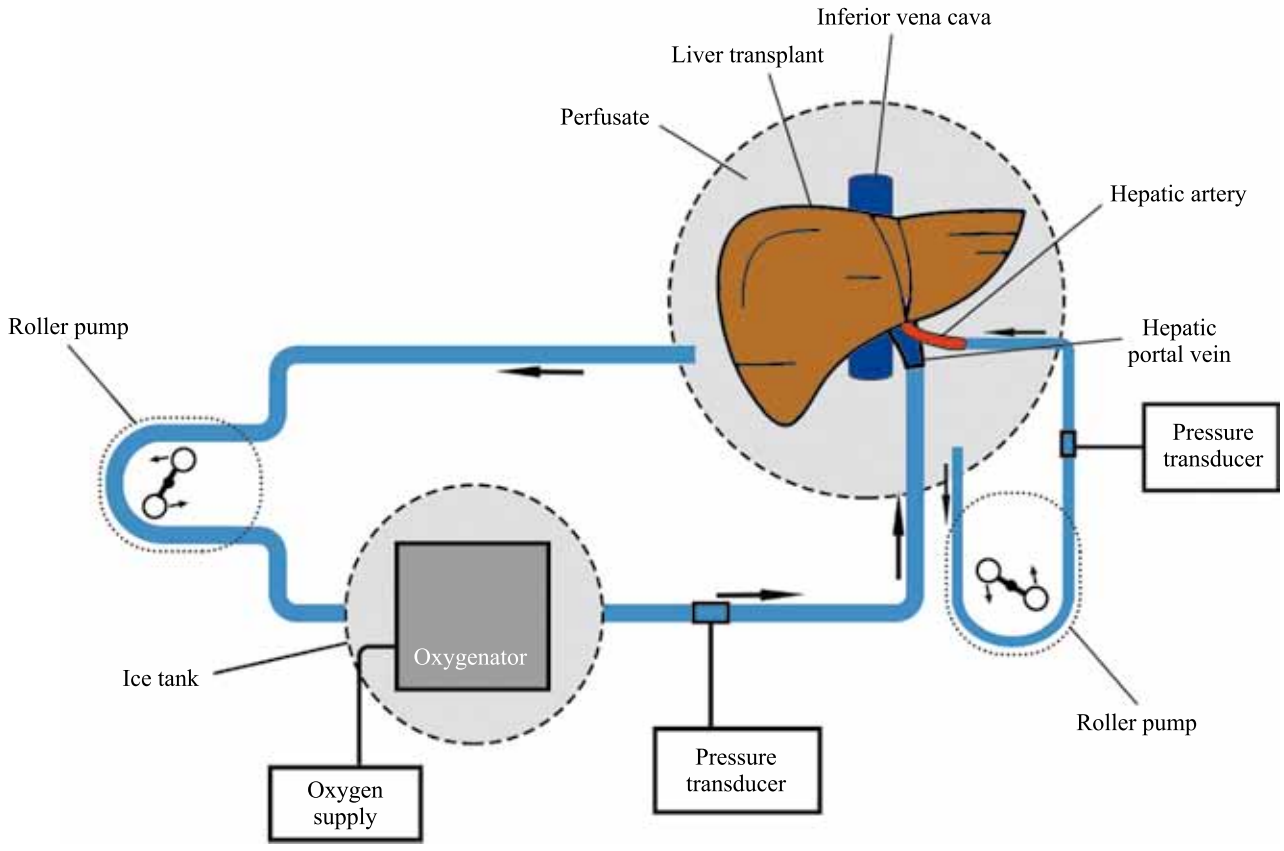

Fig. 2. Schematic representation of dual HOPE of the liver graft

Statistics

Statistical data processing and analysis were performed in the SPSS Statistics for Microsoft Windows 26 version (USA) program. Mann–Whitney U test was used to compare two groups of quantitative indicators due to the small sample size regardless of distribution. Categorical indicators were compared using Pearson's chi-squared test or Fisher's exact test. To determine the relationship between quantitative indicators, correlation analysis was performed with the determination of Spearman's rank correlation coefficient ρ and the closeness of the relationship using the Chaddock scale. Differences were considered statistically significant at $p < 0.05$.

RESULTS

Comparative analysis of liver transplant outcomes depending on preservation method

The groups were found to have no statistically significant differences in terms of baseline donor and recipient characteristics ($p > 0.05$). The total cold storage time did not differ between the groups: 5.2 (IQR: 4.4–8.0) vs. 5.4 (IQR: 4.2–7.3), ($p = 0.32$). There were no statistically significant differences in terms of total surgical intervention time, secondary warm ischemia time and biliary ischemia time ($p > 0.05$). Intraoperative blood loss and the need for blood transfusion also did not differ ($p > 0.05$).

Peak AST and ALT levels in the first week after transplantation in group II (HOPE) were 1052 (IQR: 712–1842) U/L and 1213 (IQR: 613–2032) U/L. In the control group, these values were 1943 (IQR: 1294–5214) U/L and 2318 (IQR: 1032–6219) U/L, which were statistically significantly lower than in the main group ($p = 0.002$ and $p < 0.001$, respectively). At the same time, no statistically significant differences were found in EAD incidence ($p = 0.106$). However, it was lower in the machine perfusion preservation group: 41.3% (12/29) vs. 61.8% (21/34). EAD was irreversible in two group I cases, which was considered as PNF, and resulted in early postoperative mortality of both recipients. In one case, retransplantation was performed for hepatic artery thrombosis. In group II, there was no postoperative mortality, PNF, or retransplantation.

Early postoperative complications were assessed by calculating comprehensive complication index (CCI) at the time of discharge. Median CCI was 0 (IQR: 0–22.6) in the main group, and 27.6 (IQR: 0–100) in the control group; the differences were statistically significant ($p = 0.001$). Similarly, statistically significant differences were recorded in terms of the time the recipient spent in the ICU and the total length of stay in the hospital ($p = 0.042$ and $p = 0.028$) – these parameters were less in the machine perfusion preservation group. A comparative analysis of LTx outcomes between the groups is presented in Table 1.

Influence of laboratory perfusion parameters on clinical outcomes of liver transplantation

In group II (HOPE), we also examined the impact of perfusate laboratory markers (AST and ALT), determined at 30 minutes, on early postoperative transplant outcomes in group II (HOPE). Median perfusate AST level was 589 (IQR: 272–1712) U/L, and ALT level was 482 (IQR: 214–1513). In the first week following transplantation, these levels exhibited statistically significant direct correlations with peak levels of these in the recipient's blood. In particular, perfusate AST levels at 30 minutes of perfusion correlated strongly with peak AST and ALT levels ($\rho = 0.723$ and $\rho = 0.712$, $p < 0.001$ and $p < 0.001$). Perfusate ALT level also had statistically significant relationships with blood transaminases, although not as strongly correlated ($\rho = 0$, 0.662 and $\rho = 0.389$, $p < 0.001$ and $p = 0.04$). Perfusate AST and ALT levels had no significant associations with total bilirubin level and INR value on day 7 after transplantation ($p > 0.05$). Length of ICU stay and total length of stay in the hospital were also not associated with perfusate transaminases ($p > 0.05$). The results are presented in Table 2.

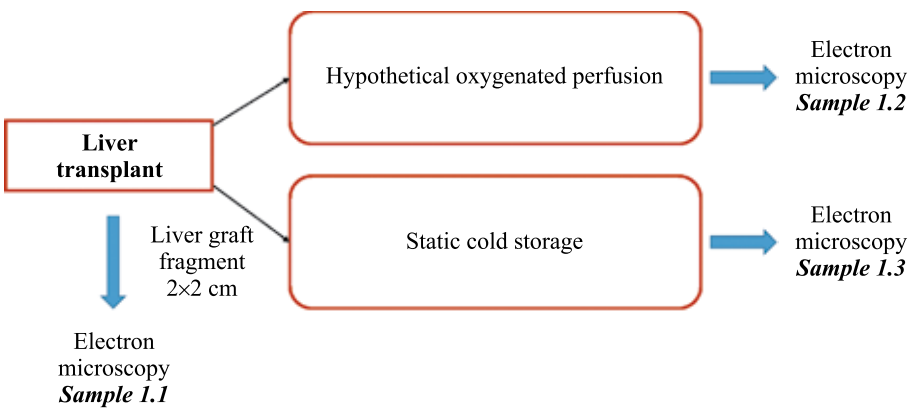

Fig. 3. Protocol for taking samples for liver graft electron microscopy

Morphological assessment of liver transplants depending on preservation method

Fig. 4, a shows an electron microscopy image of a hepatocyte fragment from sample 1.1 (liver before perfusion). Chromatin in the nucleus has a typical organization. The cytoplasm is filled with vesicles and mitochondria. The cristae in the granular endoplasmic reticulum are not dilated. The mitochondrial matrix is electronically dense, with few cristae. A similar picture was observed in sample 1.2 (liver after hypothermic oxygenated perfusion),

Table 2

Influence of laboratory perfusion parameters on immediate liver transplant outcomes

Indicators	Significance (p value)	Spearman's correlation coefficient ρ
AST level in the perfusate at 30 minutes of perfusion		
Peak AST level in the first week	**<0.001**	0.723
Peak ALT level in the first week	**<0.001**	0.712
INR on day 7	0.63	–
Total bilirubin on day 7	0.34	–
CCI	0.212	–
Length of stay in ICU	0.79	–
Length of stay in hospital	0.43	–
ALT level in the perfusate at 30 minutes of perfusion		
Peak AST level in the first week	**<0.001**	0.662
Peak ALT level in the first week	**0.04**	0.389
INR on day 7	0.74	–
Total bilirubin on day 7	0.82	–
CCI	0.65	–
Length of stay in ICU	0.29	–
Length of stay in hospital	0.72	

Note. AST, aspartate aminotransferase; ALT, alanine aminotransferase; INR, international normalized ratio; CCI, comprehensive complication index; ICU, intensive care unit.

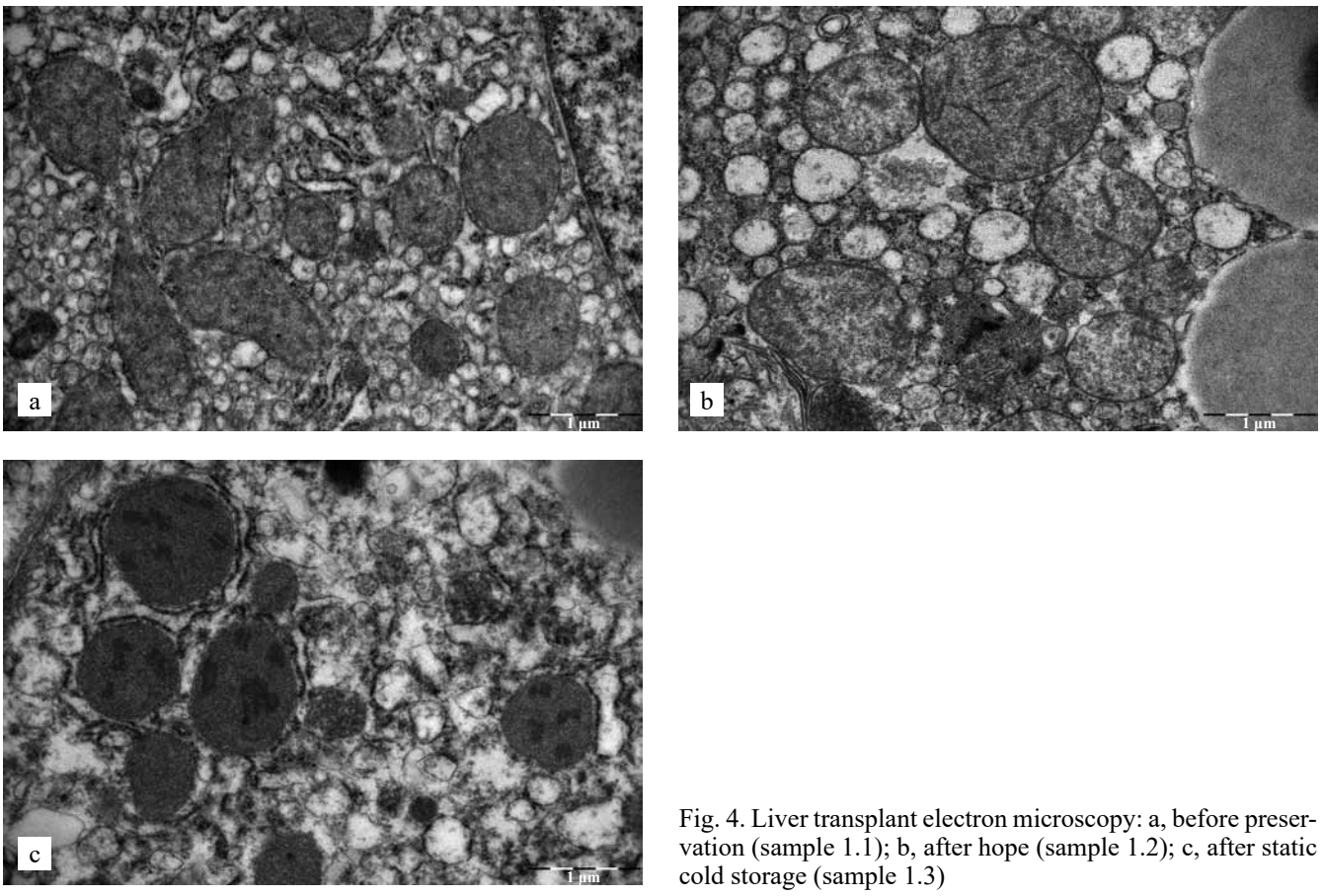

Fig. 4. Liver transplant electron microscopy: a, before preservation (sample 1.1); b, after hope (sample 1.2); c, after static cold storage (sample 1.3)

except for slight lucidity of the cytosol and swelling of the cristae in the granular endoplasmic reticulum. The ultrastructure of mitochondria is not altered (Fig. 4, b). On the contrary, during static liver preservation (sample 1.3), there were pronounced ultrastructural changes in the hepatocytes. The structure of the mitochondria underwent significant rearrangement, membrane stacks appeared and the granular endoplasmic reticulum swelled (Fig. 4, c).

DISCUSSION

The findings reported in this paper further support the association between LTx from ECDs and increased risk of EAD and its adverse effects. Thus, it is imperative to develop and implement technologies aimed at preventing IRI to the liver graft.

Machine perfusion preservation was introduced into the clinical practice of LTx just over 10 years ago, but many studies have already shown that it is superior to static cold storage. Guarrera et al. (2010) demonstrated that HOPE resulted in lower severity of reperfusion injury, lower incidence of EAD and shorter hospital stay [12]. Dutkowski et al. in 2014 published a successful experience of LTx from controlled non-heartbeating donors, in which HOPE had outcomes comparable to those after transplantation from a brain-dead donor [13]. In our study, the use of HOPE was also associated with better liver transplant outcomes in the early postoperative period. Compared to static storage, the degree of ischemic injury to the liver after perfusion was less significant, which was clearly confirmed by electron microscopy. The intensity of graft reperfusion injury, determined by peak transaminase levels during the first week, was statistically significantly lower in the machine perfusion preservation group than in the static preservation group ($p < 0.05$). We found no statistically significant reduction in EAD risk ($p = 0.106$). However, we attribute this to the small sample size. Meanwhile, CCI decreased significantly ($p = 0.001$), which characterizes the prevalence of postoperative complications, duration of recipient's stay in ICU ($p = 0.042$) and inpatient treatment ($p = 0.028$).

Apart from mitigating harm to the liver transplant during preservation, another advantage of HOPE was the ability to conduct further assessment of organ quality and suitability for transplantation. Thus, we found that perfusate transaminase levels at 30 minutes were directly correlated with those in the recipient's blood after transplantation ($p < 0.05$).

However, the predictive value of these indicators is limited as they did not show any correlation with immediate transplant outcomes. Nevertheless, we believe that it is advisable to determine the levels because the transplant team might decide not to proceed with transplantation if there are abnormally high AST and ALT levels in the perfusate since the risk of death is too high. Four such cases have led us to ultimately decide against transplantation due to abnormally high AST levels (>6000 U/L) in the effluent determined at 30 minutes after perfusion.

The results are consistent with global reports. In the aforementioned works by Guarrera and Dutkowski, perfusate transaminase levels likewise exhibited a statistically significant correlation with those in the recipient's blood during reperfusion, but they had no bearing on the recipient's prognosis [12–14]. Currently, many authors are searching for more accurate markers that can be determined during perfusion preservation for organ assessment. In particular, the determination of mitochondrial injury markers in the perfusion solution – such as FMN – has demonstrated high efficiency in assessing organ compatibility in several studies; nevertheless, further research is needed to confirm and validate this approach's wider application [14].

Even though machine perfusion preservation in LTx from suboptimal donors has been shown to be highly efficient, there are still a lot of unresolved technical issues around its use. For example, it is not completely known whether additional arterial perfusion of the graft (dual HOPE/DHOPE) or perfusion via the portal vein (classic HOPE) is adequate. DHOPE proponents contend that because bile ducts receive their supply exclusively from the hepatic artery, as opposed to hepatocytes, this approach may enable more effective perfusion of the biliary tree. Since post-transplant cholangiopathy is one of the most significant problems in LTx from marginal donors (in particular, non-heartbeating donors), prevention of IRI of the hepatic biliary system is very relevant. On the other hand, proponents of classic perfusion believe that the arterial bed can be adequately filled with perfusate due to retrograde current, and additional manipulations with the hepatic artery may lead to its injury and fatal complications.

To date, there are no clinical studies demonstrating the superiority of one method over the other, apart from an experimental work by de Vries et al. (2021), which demonstrated a 2-fold decrease in peak ALT levels in the perfusate ($p = 0.045$) and a lower peak lactate dehydrogenase in the bile ($p = 0.04$) of livers preserved by DHOPE in comparison with classic HOPE [15]. At the same time, none of the groups showed any microscopic sign of arterial injury. Although further clinical validation is still needed, we believe that extra arterial perfusion of the liver still offers a slightly higher potential efficacy than the classical approach. We believe that the danger of injury to the hepatic artery during the procedure is actually mitigated by the precise surgical technique used to deal with the hepatic artery and careful regulation of flow and pressure in the arterial perfusion system.

Thus, ex situ HOPE is a safe and effective liver transplant preservation technique. Its application in LTx from ECDs enables a more thorough evaluation of an organ's suitability for transplantation while also lessening the severity of IRI. This technique can improve LTx outcomes

in the postoperative period, while also safely increasing the availability of transplant care using suboptimal donors.

The authors declare no conflict of interest.

REFERENCES

1. Eurotransplant Annual Report 2022. [Internet] Available from: https://www.eurotransplant.org/statistics/annual-report/.
2. *Moysyuk YaG, Poptsov VN, Sushkov AI, Moysyuk LYa, Malinovskaya YuO, Belskikh LV*. Early liver allograft dysfunction: risk factors, clinical course and outcomes. *Transplantologiya. The Russian Journal of Transplantation*. 2016; (2): 16–28. [In Russ, English abstract].
3. *Olthoff KM, Kulik L, Samstein B, Kaminski M, Abecassis M, Emond J et al.* Validation of a current definition of early allograft dysfunction in liver transplant recipients and analysis of risk factors. *Liver Transpl*. 2010; 16 (8): 943–949. doi: 10.1002/lt.22091.
4. *Lee DD, Croome KP, Shalev JA, Musto KR, Sharma M, Keaveny AP et al.* Early allograft dysfunction after liver transplantation: an intermediate outcome measure for targeted improvements. *Ann Hepatol.* 2016; 15 (1): 53–60. doi: 10.5604/16652681.1184212.
5. *Hartog H, Hann A, Perera MTPR.* Primary Nonfunction of the Liver Allograft. *Transplantation.* 2022; 106 (1): 117–128. doi: 10.1097/TP.0000000000003682.
6. *Fedoruk DA, Kirkovsky LV, Sadovsky DN, Petrenko KI, Lebed' OA, Fedoruk AM et al.* Influence of hypothermic oxygenated machine perfusion on the degree of ischemic damage of ecd liver grafts. *Military medicine.* 2020; (2): 68–75. [In Russ, English abstract].
7. *Czigany Z, Pratschke J, Froněk J, Guba M, Schöning W, Raptis DA et al.* Hypothermic Oxygenated Machine Perfusion Reduces Early Allograft Injury and Improves Post-transplant Outcomes in Extended Criteria Donation Liver Transplantation From Donation After Brain Death: Results From a Multicenter Randomized Controlled Trial (HOPE ECD-DBD). *Ann Surg.* 2021; 274 (5): 705–712. doi: 10.1097/SLA.0000000000005110.
8. *Mugaanyi J, Dai L, Lu C, Mao S, Huang J, Lu C.* A Meta-Analysis and Systematic Review of Normothermic and Hypothermic Machine Perfusion in Liver Transplantation. *J Clin Med.* 2022; 12 (1): 235. doi: 10.3390/jcm12010235.
9. *Shabunin AV, Minina MG, Drozdov PA, Nesterenko IV, Makeev DA, Zhuravel OS et al.* Early experiments with hypothermic oxygenated machine perfusion of kidney grafts from extended criteria donors. *Russian Journal of Transplantology and Artificial Organs*. 2022; 24 (1): 143–150. doi: 10.15825/1995-1191-2022-1-143-150.
10. *Shabunin AV, Minina MG, Drozdov PA, Sevostianov VM, Nesterenko IV, Makeev DA et al.* Asystole kidney donation using automated chest compression system and hypothermic oxygenated machine perfusion (first experience in the Russian Federation). *Russian Journal of Transplantology and Artificial Organs*. 2022; 24 (2): 102–107. doi: 10.15825/1995-1191-2022-2-102-107.
11. *Shabunin AV, Minina MG, Drozdov PA, Miloserdov IA, Saydulaev DA, Sevostyanov VM et al.* Complex use of perfusion techniques in kidney transplantation from a donor with out-of-hospital cardiac arrest (clinical case). *Russian Journal of Transplantology and Artificial Organs*. 2023; 25 (3): 113–121. doi: 10.15825/1995-1191-2023-3-113-121.
12. *Guarrera JV, Henry SD, Samstein B, Odeh-Ramadan R, Kinkhabwala M, Goldstein MJ et al.* Hypothermic machine preservation in human liver transplantation: the first clinical series. *Am J Transplant*. 2010; 10 (2): 372–381. doi: 10.1111/j.1600-6143.2009.02932.x.
13. *Dutkowski P, Schlegel A, de Oliveira M, Mullhaupt B, Neff F, Clavien PA.* HOPE for human liver grafts obtained from donors after cardiac death. *J Hepatol.* 2014; 60: 765–772. doi: 10.1016/j.jhep.2013.11.023.
14. *Muller X, Schlegel A, Kron P, Eshmuminov D, Würdinger M, Meierhofer D et al.* Novel Real-time Prediction of Liver Graft Function During Hypothermic Oxygenated Machine Perfusion Before Liver Transplantation. *Ann Surg*. 2019; 270 (5): 783–790. doi: 10.1097/sla.0000000000003513.
15. *De Vries Y, Brüggenwirth IMA, Karangwa SA, von Meijenfeldt FA, van Leeuwen OB, Burlage LC et al.* Dual Versus Single Oxygenated Hypothermic Machine Perfusion of Porcine Livers: Impact on Hepatobiliary and Endothelial Cell Injury. *Transplant Direct.* 2021; 7 (9): e741. doi: 10.1097/TXD.0000000000001184.

The article was submitted to the journal on 21.01.2024

DOI: 10.15825/1995-1191-2024-2-73-81

HYPOTHERMIC MACHINE PERFUSION OF A DONOR KIDNEY USING AN EXPERIMENTAL DEXTRAN-40-BASED PRESERVATION SOLUTION AND ORTHOTOPIC TRANSPLANTATION (EXPERIMENTAL STUDY)

V.G. Shestakova[1], V.K. Bogdanov[2], R.D. Pavlov[1], V.M. Terekhov[1], A.S. Timanovsky[1], A.A. Zharikov[2], A.N. Shibaev[1, 3], N.V. Grudinin[2]

[1] Tver State Medical University, Tver, Russian Federation

[2] Shumakov National Medical Research Center of Transplantology and Artificial Organs, Moscow, Russian Federation

[3] Vladimirsky Moscow Regional Research and Clinical Institute, Moscow, Russian Federation

Objective: to evaluate the efficacy of hypothermic machine perfusion (HMP) of a donor kidney obtained from a non-heartbeating (NHB) donor, using an experimental dextran-40-based preservation solution, in subsequent orthotopic transplantation in a rabbit model. **Materials and methods.** Twenty grey giant rabbits weighing 2,500–3,100 g, divided into donors (n = 10) and recipients (n = 10), were used in the study. After obtaining kidney from an NHB donor, *ex vivo* HMP of the left donor kidney using a dextran-40-based preservation solution was performed and peripheral vascular resistance (PVR) parameters were measured. This was followed by bilateral nephrectomy and orthotopic transplantation. The follow-up period was 12 days. Creatinine levels, urea levels, and glomerular filtration rate (GFR) were measured during follow-up. **Results.** During *ex vivo* HMP of donor kidneys from NHBs, PVR dropped progressively from 1.90 ± 0.27 mmHg/mL/min to 0.72 ± 0.09 mmHg/mL/min at $p < 0.001$. In the early post-transplant period (during the first 2 days after implantation), creatinine and urea levels were moderately elevated compared to normal. Creatinine and urea levels were 91.07 ± 11.49 μmol/L at $p < 0.011$ and 9.09 ± 1.06 mmol/L at $p < 0.009$ on day 2, respectively, but by day 12, they reverted to physiologic values, which were 77.17 ± 10.19 μmol/L at $p < 0.019$ and 4.88 ± 0.54 mmol/L at $p < 0.022$, respectively. These findings were correlated with GFR values, which ranged from 26.29 to 26.74 mL/min/1.72 m^2 in mean values over the course of a 12-day follow-up period. **Conclusion.** *Ex vivo* HMP using dextran-40-based preservation solution has a positive effect on the kidney at 30 minutes of warm ischemia following asystole and achieves satisfactory graft function over 12 days of follow-up.

Keywords: transplantology, orthotopic kidney transplantation, ex vivo hypothermic kidney perfusion, dextran 40.

INTRODUCTION

Today, kidneys are the most commonly transplanted organ [1]. Kidney transplantation (KTx) is the treatment of choice for end-stage chronic kidney disease (CKD). However, before receiving a new organ, such patients must wait for a donor kidney while on renal replacement therapy (RRT). The number of people on RRT varies considerably from country to country. In Iceland, Norway and Australia, for example, there are about 100 people on RRT per million population. This figure is more than 300 per 100,000 in the USA and Taiwan. In Russia, about 50 people per million population go through this procedure per year [2]. The only definitive way to help such patients is by KTx [3].

Despite significant advances in transplantation of solid organs, especially the kidney, and better surgical techniques, issues surrounding the rehabilitation of donor organs from non-heartbeating (NHB) donors remain unresolved [3]. At present, the possibility of working with kidney transplants from suboptimal donors is a relevant direction of modern transplantology. Experimental study of new solutions and perfusion-preservation techniques is of considerable importance [4].

World literature presents many animal models for experimental studies. Each of the described models has advantages and disadvantages [5]. A rabbit animal model was chosen for the experimental study to evaluate the efficacy of hypothermic machine perfusion (HMP) of a left kidney transplant obtained from an NHB donor, using an experimental dextran-40-based preservation solution, with subsequent orthotopic transplantation.

The aim of this study is to evaluate the efficacy of HMP of a donor kidney, obtained from an NHB donor, using an experimental dextran-40-based preservation solution at subsequent orthotopic transplantation in a rabbit model.

Corresponding author: Vasily Terekhov. 4, Sovetskaya str., Tver, Tver Oblast, 170100, Russian Federation.
Phone: (904) 015-84-76. E-mail: terekhov-200002@mail.ru

MATERIALS AND METHODS

The study was conducted on male gray giant rabbits weighing 2,500–3,100 g (N = 20). All experimental animals were divided into two equal groups, donors (N = 10) and recipients (N = 10). The study was performed in accordance with the rules of laboratory practice in the Russian Federation: order No. 755 of the USSR Ministry of Health, dated August 12, 1977; order No. 267 of the Russian Ministry of Health, dated June 19, 2003; Law "On the Protection of Animals from Cruelty", dated December 1, 1999. Permission to conduct this study was obtained from the ethics committee at Tver State Medical University (protocol dated May 11, 2018).

The study was conducted according to the following protocol: effective circulatory arrest was simulated in the donor within 30 minutes after preliminary heparin injection, cold cardioplegia and removal of the left donor kidney, *ex vivo* HMP of donor kidney, orthotopic transplantation of left donor kidney to the recipient after preliminary bilateral nephrectomy. During the *ex vivo* HMP procedure using an experimental dextran-40-based preservation solution, peripheral vascular resistance (PVR) indicators were determined. In order to assess graft function, the animals were followed up in the postoperative period for 12 days. Immunosuppressive therapy with methylprednisolone was administered daily during the entire follow-up period and blood samples were taken to study biochemical parameters – markers of renal function. After the end of the follow-up period, the histologic material of the graft was taken, and the animal was withdrawn from the experiment.

Donor nephrectomy

For preoperative preparation, the donor animal was injected subcutaneously with Telazol 100 (Zoetis, Spain) 50 mg. Intravenous catheter Vasofix Certo 22 G (BBraun, Germany) was placed in the marginal ear vein. Atropine 0.2 mg and dexamethasone 2 mg intravenously were used for premedication. The animal was shaved and positioned on its back. Telazol 100 0.5 mL and Xyla (Interchemie, Netherlands) 0.5 mL (10 mg) were injected intravenously. A laparotomy was performed and the abdominal aorta and inferior vena cava with renal arteries and veins branching from them were visualized. The posterior leaflet of the parietal peritoneum was opened near the renal hilum, after which the left renal artery (RA) and left renal vein (RV) were isolated and mobilized. In addition to the renal vessels, the left ureter was also isolated and mobilized over a sufficient length (about 7–9 cm from the kidney). Next, heparin 5000 units was injected intravenously, the exposure time was 3 minutes. Next, a vascular clamp was placed on the main vessels above the renal arteries and 10 mL of 4% potassium chloride was injected intravenously to stop cardiac activity. After 30 minutes of exposure after asystole, a 20 G intravenous catheter was inserted through the aorta into the left RA, the left RV was crossed, and cold cardioplegia of the left kidney was initiated with 60 mL Custodiol 4 °C solution.

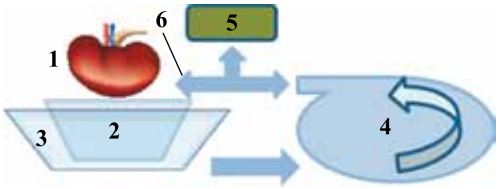

Fig. 1. Schematic diagram of the extracorporeal hypothermic perfusion device for *ex vivo* donor kidney preservation. 1, donor kidney; 2, organ reservoir with perfusate; 3, ice reservoir; 4, peristaltic pump; 5, invasive pressure measurement unit; 6, temperature sensor

Ex vivo HMP

The extracorporeal circuit was pre-assembled for *ex vivo* HMP of donor kidney. The perfusion circuit consisted of a stepper roller pump, an invasive pressure measurement unit, a temperature sensor, two containers (one for positioning the kidney transplant and the other for ice), perfusion lines and a perfusion cannula. A schematic representation of the extracorporeal circuit is shown in Fig. 1.

The perfusion circuit was filled with 100 mL of dextran-40-based solution 4 °C, and heparin 1000 IU was added. After cold cardioplegia preservation, a 20 G intravenous catheter was inserted into the RA of the left donor kidney, deaeration was performed and the perfusion line was connected to the catheter. The *ex vivo* HMP of the donor kidney was performed with pressure regulation. The target pressure was 30 mmHg, with acceptable ranges of 28 to 36 mmHg. The initial volumetric perfusion rate was 5 ± 1.1 mL/min with a gradual increase to 50 ± 15 mL/min over 30 minutes. PVR was an estimated index calculated by the formula: R = P/V, where R is resistance, P is pressure in mmHg, and V is volumetric perfusion rate in mL/min; this indicator reflects the compliance of the renal graft vascular bed, which was a predictor of renal function recovery after implantation. The procedure lasted for 240 minutes. At the end of hypothermic perfusion, we performed another cold cardioplegia using Custodiol solution.

Orthotopic transplantation of left donor kidney

After a preliminary 4-hour fast, the recipient animal was prepared for surgery. Induction of anesthesia was performed similarly to the donor stage. Vital functions of recipient animals were assessed by pulse oximetry (SpO_2 >90%, HR = 180–230/min), and respiratory movements were visually counted (HR >45/min). At laparotomy, bowel loops were removed to the right side and wrapped in sterile napkins pre-moistened with warmed

saline. After isolation and mobilization of recipient's renal vessels and isolation of ureters, heparin 100 units was injected intravenously, and bilateral nephrectomy was carried out. Blood flow through the RA and RV was stopped by applying bulldog clamps. The stumps of the vascular pedicle of the right kidney were sutured and tied with Prolene 5.0 suture material, the ureter was ligated caudally to the bladder with Prolene 5.0 suture material. The recipient's left RA and RV stumps were left sufficient for anastomosis, their length was 3–4 cm for RA and RV. First, end-to-end anastomosis was performed between the renal vein of the donor kidney and the recipient's left RV stump. The posterior wall was sutured with Prolene 6.0 suture material using continuous wraparound sutures, and the anterior wall was sutured with interrupted sutures. After venous anastomosis and checking the quality of venous suture hemostasis, an end-to-end arterial anastomosis was made between the RA of the donor kidney and the recipient's left RA stump using Prolene 7.0 suture material. The arteries were anastomosed using interrupted sutures. Before applying the last suture, deaeration was performed, the artery was treated with Lidocaine 2% to prevent vasospasm, methylprednisolone 20 mg was administered intravenously, and blood flow was started (Fig. 2).

Urine coming out of the ureteral stump after blood flow via the renal arteries was resumed was a sign that kidney function had recovered. Sixty minutes after the procedure started, Telazol 100 0.5 mL and Xyla 0.5 mL were injected intravenously to maintain anesthesia. Ureteral anastomosis was the last stage in the kidney transplant procedure. End-to-end ureteral anastomosis between the recipient's ureteral stump and the ureter coming from the donor kidney was performed using a stent – a 20 G IV catheter – and left inside the lumen. Four interrupted sutures were applied with Prolene 7.0 suture material evenly around the entire circumference of the ureter, after which the kidney was fixed to the renal bed with separate interrupted sutures between the fatty capsule of the kidney and the surrounding tissues. After kidney transplantation, the intestinal loops were placed back into the abdominal cavity and the wound was sutured layer-by-layer.

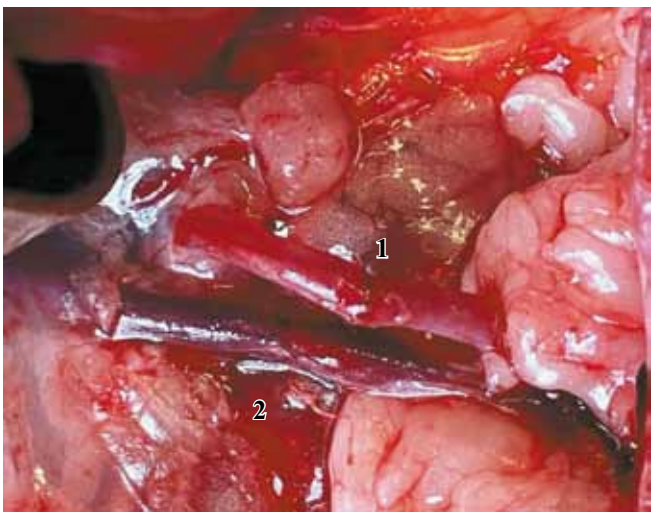

Fig. 2. Vascular anastomoses performed during donor kidney implantation. 1, renal artery anastomosis; 2, renal vein anastomosis

Material for histologic examination was collected on day 12 by routine excisional kidney biopsy, fixed in 10% neutral buffered formalin (Biovitrum, Russia), dehydrated in 8 changes of isopropanol, starting with 50% aqueous isopropanol, poured into Histomix paraffin medium (Biovitrum, Russia) using the ESD-2800 filling system (MedTekhnikaPoint, Russia). Thin paraffin sections, 4–6 μm thick, obtained on a semi-automatic rotary microtome ERM 3100 (Hestion, Australia) were stained with hematoxylin and eosin. Microscopic study of the obtained experimental material was performed using an Olympus CX21 microscope at low (100×), high (400×) magnifications and oil immersion (1000×). Microphotographs were obtained with a digital camera MC-10 (LOMO, Russia), the obtained images were processed in MCview software.

Statistical analysis was performed using the StatTech v. 3.1.10 program (developer StatTech LLC, Russia). Quantitative indicators were evaluated for conformity to normal distribution using the Shapiro–Wilk test (number of subjects less than 50). Quantitative indices having normal distribution were described using arithmetic mean (M) and standard deviations (SD), 95% confidence interval (95% CI) limits. One-way analysis of variance with repeated measures was used to compare three or more related groups on a normally distributed variable. Statistical significance of changes in the indicator over time was assessed using Pillai's Trace. Posterior analysis was performed using paired Student's t test with Holm correction. When comparing three or more dependent populations whose distribution differed from normal, the nonparametric Friedman test was used with post hoc comparisons using the Conover–Iman criterion with Holm correction. Results were considered statistically significant at $p < 0.05$.

RESULTS

Dynamics of changes in peripheral vascular resistance during hypothermic perfusion

During *ex vivo* HMP of the donor kidney, parameters such as RA pressure and volumetric flow rate, were recorded. Based on these parameters, an objective index – PVR, measured by an invasive method directly in the RA for 240 minutes – was calculated, which is depicted in Fig. 3.

In the PVR study, high values were recorded at the beginning of the procedure and after 30 minutes, which was reflected by values of 1.90 ± 0.27 mm Hg/mL/min, and

were a consequence of asystole preceding withdrawal for 30 minutes. However, by the end of the procedure, PVR values decreased and corresponded to physiologic values (0.72 ± 0.09 mmHg/mL/min) for experimental animals.

Dynamics of changes in biochemical parameters after transplantation

The main recorded biochemical indicators in the post-transplant period were creatinine (Fig. 4) and urea (Fig. 5) levels, as well as the calculated index – glomerular filtration rate (GFR), calculated according to the Schwartz formula: GFR = 36.5 X (length of the rabbit from head to tail in cm/serum creatinine in μmol/L), which is graphically depicted in Fig. 6.

Creatinine, as the main marker of renal function, reflected the excretory function of the graft in recipient animals. On the second day after transplantation, creatinine levels increased to 91.07 ± 11.49 μmol/L in all the animals. However, by the end of the follow-up period, the level did not exceed the limit values of physiologic norm – 77,17 ± 10,19 μmol/L in total. The nonlinearity of the graph of creatinine level fluctuations reflects the recipients' physiologic activity in the posttransplant period.

Changes in urea levels also reflected the state of excretory function of the graft. On the second follow-

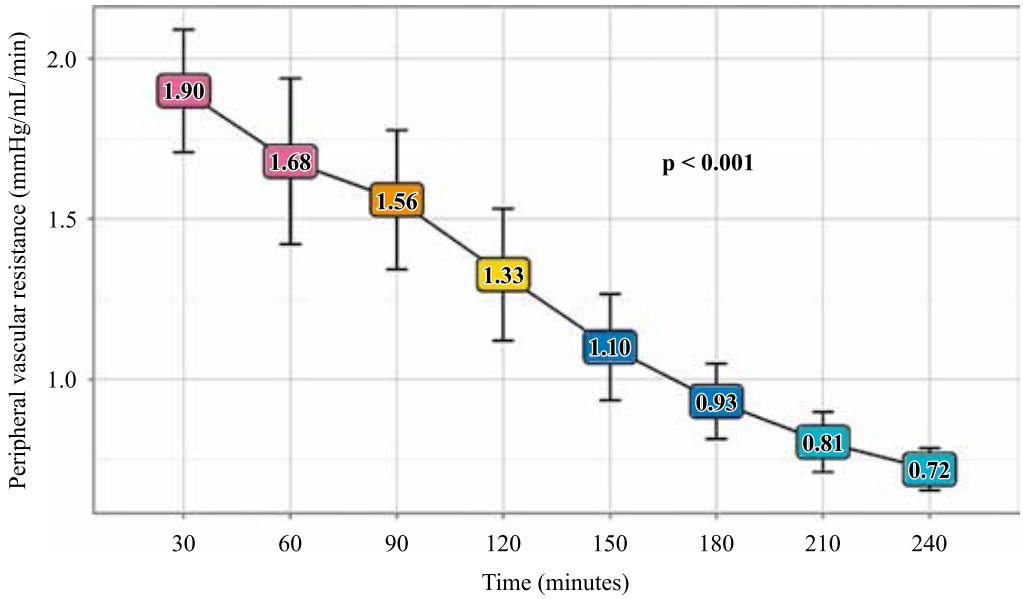

Fig. 3. Changes in peripheral vascular resistance during *ex vivo* hypothermic perfusion of donor kidney. The graph is represented by mean values, vertical lines denote standard deviations, p is statistical significance

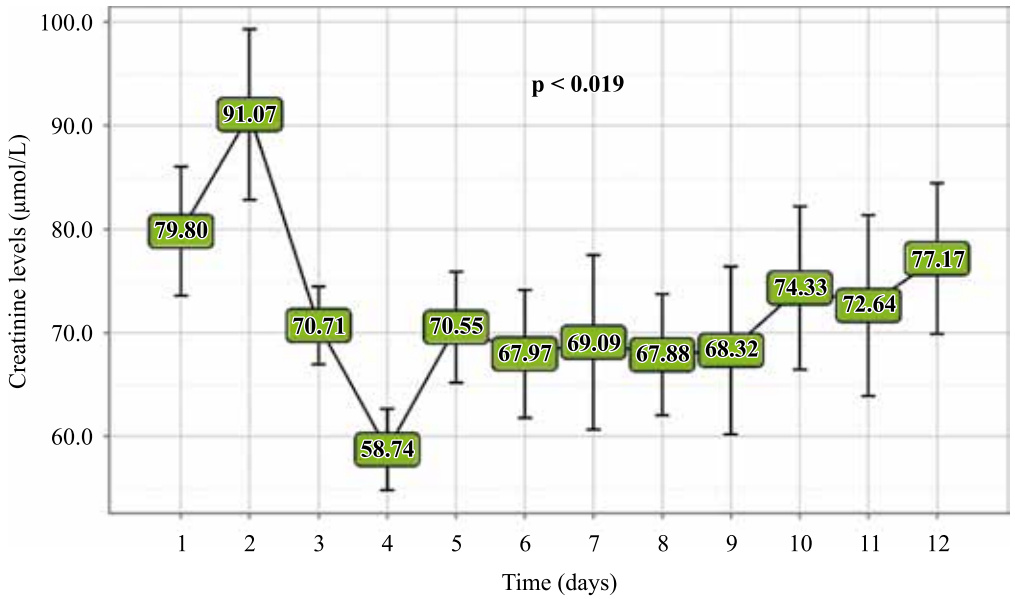

Fig. 4. Changes in creatinine levels after donor kidney transplantation in recipient animals. The graph is represented by mean values, vertical lines indicate standard deviations, p is statistical significance

up day, there was a peak in average urea levels up to 9.09 ± 1.06 mmol/L, which correlated with creatinine levels. However, the urea concentration curve was descending throughout the entire follow-up period, and on day 12, the indicators reached a physiologic norm, 4.88 ± 0.54 mmol/L.

GFR was an objective indicator of the functional status of the graft, adjusted for the small body surface area of the experimental animals. In the early post-transplant period, GFR varied from 26.29 to 29.18 mL/min/1.72 m^2 in mean values, and by the end of the follow-up period, the mean GFR value was 26.74 ml/min/1.72 m^2. Changes in GFR over 12 days did not go beyond the physiological norms of experimental animals.

Evaluation of biochemical parameters clearly demonstrate the preservation of excretory function of the transplant for 12 days, and the physiologic values of GFR suggest that the functional status of the donor kidney is satisfactory.

Post-transplant histological study

According to the histological study (Fig. 7) of 10 biopsy specimens obtained from recipient rabbits, morphological changes are represented by the presence of signs of dystrophic changes in the form of intracellular

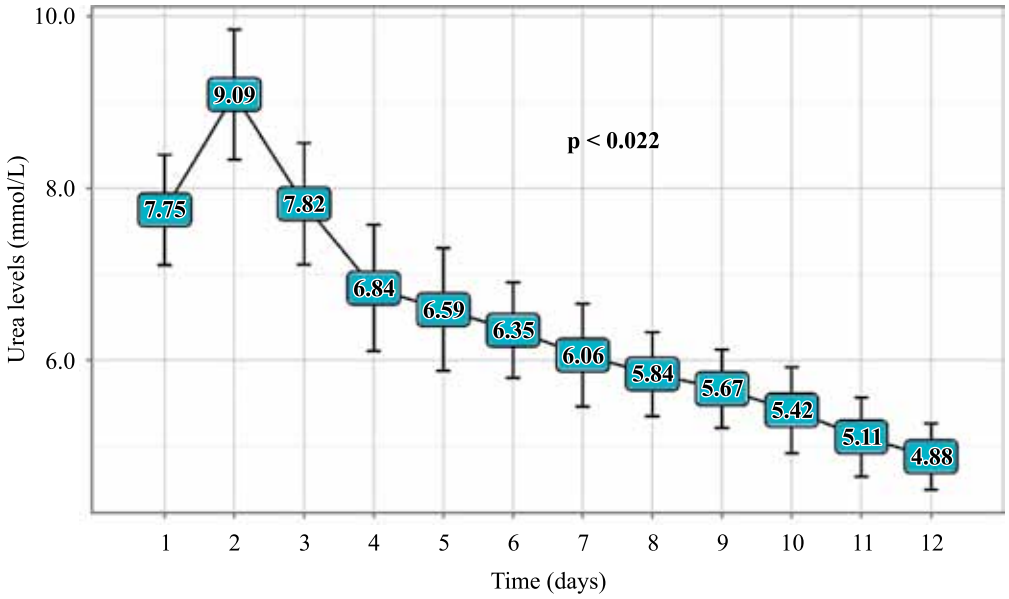

Fig. 5. Changes in urea levels after donor kidney transplantation in recipient animals. The graph is represented by mean values, vertical lines indicate standard deviations, p is statistical significance

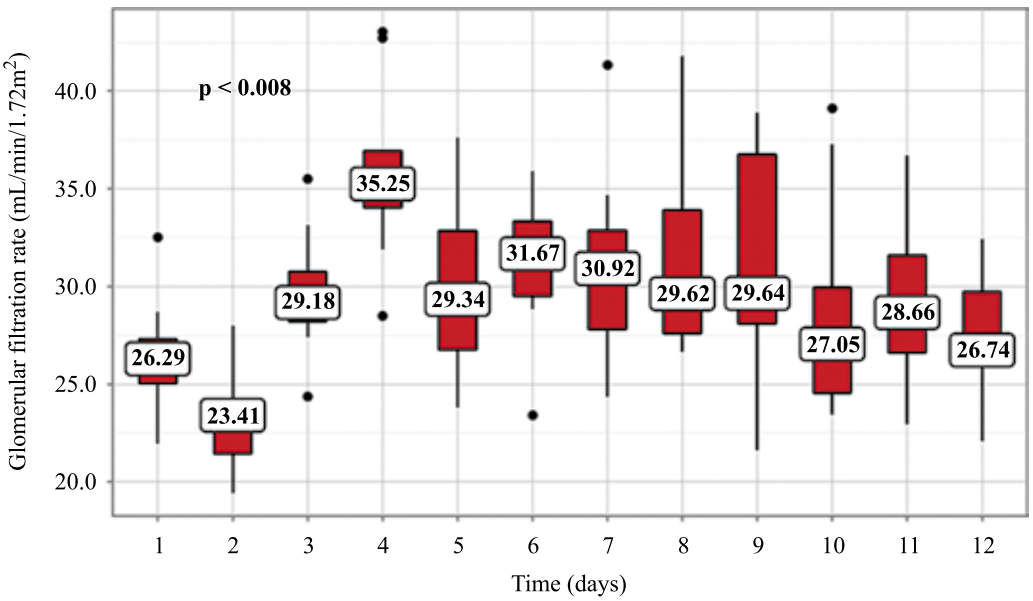

Fig. 6. GFR changes after donor kidney transplantation in recipient animals. The graph is represented by mean values, vertical lines denote standard deviations, p is statistical significance

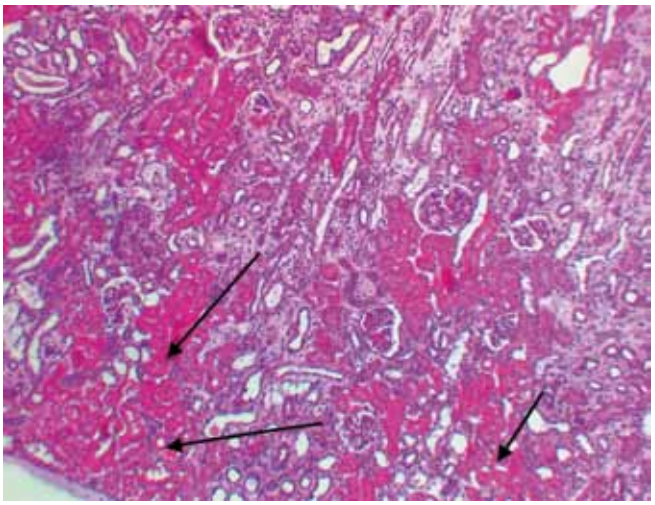

Fig. 7. Histological kidney tissue slide at 12 days after transplantation. Arrows indicate foci of renal tubule epithelium necrosis. H&E stain, magnification 100×

inclusions and diffuse foci of epithelial necrosis (marked by black arrows in the figure) of both proximal and distal tubules. Polymorphic cellular infiltration is also present, occupying from 10% to 25% of the parenchyma. The presence of signs of tubular atrophy in no more than 25% of the cortex indicates the onset of transplant glomerulopathy [7].

DISCUSSION

One possible path for modern transplantology is to enable the use of donor organs in cases of circulatory arrest [8]. *Ex vivo* perfusion of donor organs has allowed the donor pool to grow by over 25% to date, and this figure continues to rise annually. Thus, an experimental study of hypothermic perfusion, the influence of *ex vivo* perfusion technique, as well as subsequent clinical implementation will ensure a future increase in the number of transplants [9].

Investigation of new perfusion solutions is extremely important. Currently, the choice of perfusion agent for *ex vivo* hypothermic or normothermic machine perfusion remains an open debatable issue [10]. Despite the existing and implemented clinical protocols, an ideal perfusion agent has not been identified [11]. This study describes the use of a dextran-40-based preservation solution. Due to the high colloidal and rheological properties of dextran-40, as well as its moderate molecular size, this particular component has an advantage for use in *ex vivo* hypothermic perfusion of donor kidney. For example, Lindell et al. studied the effect of the commonly used potassium-rich hydroxyethyl starch (HES) – containing perfusion solutions for hypothermic perfusion of donor kidneys, Belzer MPS and UW Viaspan. Despite successful procedures, the results described moderate interstitial graft edema and moderate post-transplant changes [12]. In turn, because dextran-40 has the special ability to bind water molecules, it can prevent interstitial edema of donor kidney tissue during prolonged perfusion. Moreover, unlike albumin solutions and HES-containing agents, dextran molecules prevent the destruction of the renal structural unit without rupturing or occluding the nephron [13].

During *ex vivo* HMP of the donor kidney, high PVR values were observed, which was a consequence of a preliminary 30-minute asystole in the donor. Throughout the perfusion procedure, PVR decreased in all cases, and returned to normal at the end of perfusion, proving the efficacy of *ex vivo* HMP for rehabilitation of expanded criteria donor kidneys. After transplantation of such kidneys, physiologic indicators of biochemical markers of renal function were observed, not exceeding borderline values of the maximum permissible limits [14]. Graft function was preserved in all cases, which is evidence of the effectiveness of *ex vivo* HMP and correlates with the data obtained during perfusion.

CONCLUSION

In addition to demonstrating the preservation of the functional characteristics of the graft after transplantation in the rabbit experiment, the experimental study showed the admissibility of using a dextran-40-based preservation solution as a perfusion agent for *ex vivo* hypothermic machine perfusion of donor kidney. The findings of this work clearly indicate the need for a deeper investigation into the pathophysiological aspects of the effect of dextran-40-induced hypothermic perfusion on kidney graft, both in the early and the long-term postreperfusion periods.

The authors declare no conflict of interest.

REFERENCES

1. *Kabanova SA, Bogopol'skiy PM*. Kidney transplant: history, results and perspectives (The 50th anniversary of the first successful kidney transplant in Russia). *Journal of Transplantology*. 2015; 2: 55–56.
2. *Hill NR, Fatoba ST, Oke JL, Hirst JA, O'Callaghan CA, Lasserson DS, Hobbs FD.* Global Prevalence of Chronic Kidney Disease – A Systematic Review and Meta-Analysis. *PLoS One*. 2016; 11 (7): e0158765. doi: 10.1371/journal.pone.0158765.
3. *Tsai WC, Wu HY, Peng YS, Ko MJ, Wu MS, Hung KY et al.* Risk Factors for Development and Progression of Chronic Kidney Disease: A Systematic Review and Exploratory Meta-Analysis. *Medicine (Baltimore)*. 2016; 95 (11): e3013. doi: 10.1097/MD.0000000000003013.
4. *Gautier SV, Tsirulnikova OM, Pashkov IV, Oleshkevich DO, Filatov IA, Bogdanov VK et al*. Normothermic *ex vivo* perfusion of isolated lungs in an experiment using a russian-made perfusion system. *Russian Journal of Transplantology and Artificial Organs*. 2022; 24 (2): 94–101. https://doi.org/10.15825/1995-1191-2022-2-94-101.

5. *Gautier SV, Pashkov IV, Bogdanov VK, Oleshkevich DO, Bondarenko DM, Mozheiko NP et al*. Normothermic *ex vivo* lung perfusion using a developed solution followed by orthotopic left lung transplantation (experimental study). *Russian Journal of Transplantology and Artificial Organs*. 2023; 25 (2): 158–166. https://doi.org/10.15825/1995-1191-2023-2-158-166.
6. *Grudinin NV, Bogdanov VK, Sharapov MG, Bunenkov NS, Mozheiko NP, Goncharov RG et al*. Use of peroxiredoxin for preconditioning of heterotopic heart transplantation in a rat. *Russian Journal of Transplantology and Artificial Organs*. 2020; 22 (2): 158–164. https://doi.org/10.15825/1995-1191-2020-2-158-164.
7. *Suhanov AV.* Banff's Classificaton Of Renal Allograft Pathology. *Nephrology and Dialysis.* 2000; 2 (1–2): 58–62.
8. *Brat A, de Vries KM, van Heurn EWE, Huurman VAL, de Jongh W, Leuvenink HGD et al*. Hypothermic Machine Perfusion as a National Standard Preservation Method for Deceased Donor Kidneys. *Transplantation*. 2022 May; 106 (5): 1043–1050. doi: 10.1097/TP.0000000000003845.
9. *Peng P, Ding Z, He Y, Zhang J, Wang X, Yang Z*. Hypothermic Machine Perfusion Versus Static Cold Storage in Deceased Donor Kidney Transplantation: A Systematic Review and Meta-Analysis of Randomized Controlled Trials. *Artif Organs*. 2019 May; 43 (5): 478–489. doi: 10.1111/aor.13364. Epub 2018 Nov 9. PMID: 30282122.
10. *Simona MS, Alessandra V, Emanuela C, Elena T, Michela M, Fulvia G et al*. Evaluation of Oxidative Stress and Metabolic Profile in a Preclinical Kidney Transplantation Model According to Different Preservation Modalities. *Int J Mol Sci*. 2023 Jan 5; 24 (2): 1029. doi: 10.3390/ijms24021029. PMID: 36674540; PMCID: PMC9861050.
11. *Zulpaite R, Miknevicius P, Leber B, Strupas K, Stiegler P, Schemmer P. Ex-vivo* Kidney Machine Perfusion: Therapeutic Potential. *Front Med (Lausanne)*. 2021 Dec 24; 8: 808719. doi: 10.3389/fmed.2021.808719. PMID: 35004787; PMCID: PMC8741203.
12. *Lindell SL, Compagnon P, Mangino MJ, Southard JH*. UW Solution for Hypothermic Machine Perfusion of Warm Ischemic Kidneys. *Transplantation*. 2005 May 27; 79 (10): 1358–1361. doi: 10.1097/01.TP.0000159143.45022.F6.
13. *Elliott TR, Nicholson ML, Hosgood SA.* Normothermic kidney perfusion: An overview of protocols and strategies. *Am J Transplant*. 2021 Apr; 21 (4): 1382–1390. doi: 10.1111/ajt.16307. Epub 2020 Sep 25. PMID: 32897651.
14. *Campos Pamplona C, Moers C, Leuvenink HGD, van Leeuwen LL.* Expanding the Horizons of Pre-Transplant Renal Vascular Assessment Using *Ex Vivo* Perfusion. *Curr Issues Mol Biol*. 2023 Jun 29; 45 (7): 5437–5459. doi: 10.3390/cimb45070345. PMID: 37504261; PMCID: PMC10378498.

The article was submitted to the journal on 05.02.2024

DOI: 10.15825/1995-1191-2024-2-82-93

HYPERPARATHYROIDISM IN KIDNEY TRANSPLANT CANDIDATES AND POSTOPERATIVE PARATHYROID GLAND FUNCTION IN RECIPIENTS

O.N. Vetchinnikova

Vladimirsky Moscow Regional Research and Clinical Institute, Moscow, Russian Federation

Objective: to evaluate the effects of secondary hyperparathyroidism (HPT) in kidney transplantation (KT) candidates on recipients' parathyroid gland function in the first postoperative year. **Materials and methods.** The retrospective cohort study included 210 patients (103 women, 107 men, age 45 ± 9 years) with stage 5 chronic kidney disease (stage 5 CKD, including dialysis-dependent patients), who had undergone cadaveric KT. Biochemical screening before kidney transplantation and in the postoperative period at 3 and 12 months determined serum levels of parathyroid hormone (PTH), calcium, phosphorus, alkaline phosphatase activity, albumin and creatinine using standard methods. PTH levels of 130–595 pg/mL and ≤130 pg/mL were taken as the target level in the pre- and post-transplant periods, respectively. **Results.** Fifty-six KT candidates (group 1) had HPT and 154 (group 2) had the target PTH levels. PTH level was 897 (722; 1136) and 301 (229; 411) pg/mL, respectively, $p < 0.001$. PTH decreased in all recipients at 3 months after KT: by 595 (420; 812) in group 1 and 148 (77; 230) pg/mL in group 2, $p < 0.001$, to 254 (180; 455) and 150 (118; 212) pg/mL, respectively, $p < 0.001$; the target level was detected in 10.7% and 42.2% of recipients, respectively, $p < 0.001$. At 12 months, blood PTH was 171 (94; 239) pg/mL in group 1 and 112 (90; 135) pg/mL in group 2, $p = 0.004$; target level was found in 48.2% and 73.4% of recipients, respectively, $p < 0.001$. Kidney graft function was identical in both recipient groups: acute tubular necrosis in 41.1% and 54.5%; at 3 months, median glomerular filtration rates (GFR) of 60 and 65 mL/min (n.d.); at 12 months, 56 and 54 mL/min (n.d.). Post-transplant PTH levels correlated directly with preoperative levels in both groups and inversely with renal graft function in group 2 recipients. **Conclusion.** HPT in kidney transplant candidates is a major, graft function-independent predictor of excess PTH secretion in recipients, increasing the risk of persistent HPT 1.9-fold, one year after KT.

Keywords: kidney transplantation, parathyroid glands, secondary hyperparathyroidism, chronic kidney disease.

INTRODUCTION

Secondary hyperparathyroidism (HPT) is a common complication associated with CKD. HPT develops following a decline in renal function, which triggers a cascade of physiological and pathophysiological processes leading to excessive PTH release by parathyroid glands (PTG). HPT in CKD patients is a common condition, especially at the dialysis therapy stage. The disease is accompanied by damage to many organs and systems, it significantly worsens patient quality of life and increases mortality. Despite personalized approach and emergence of new medications, there are still challenges in treating secondary HPT [1–5].

Kidney transplantation (KT) is the treatment of choice for stage 5 CKD, and the number of such operations is increasing annually [6]. Patients with varying degrees of severity of secondary HPT among KT candidates have unavoidably resulted from the recent growth in the number of CKD patients, including the dialysis population with a high prevalence of secondary HPT, and the growing number of kidney transplants. A successful KT modifies HPT's trajectory, leading to either complete regression or persistence. The latter adversely affects clinical outcomes in kidney transplant recipients. Recent reports discuss various aspects of posttransplant HPT: risk factors, impact on renal graft function, quality of life and survival of patients [7–11].

The aim of this study was to evaluate the effects of secondary HPT in candidates awaiting KT on recipients' PTG function in the first postoperative year.

MATERIALS AND METHODS

The retrospective cohort single-center study included 210 patients with stage 5 CKD (including dialysis-dependent patients) who underwent cadaveric KT. Patient inclusion criteria: 1. presence of stage 5 CKD (including dialysis-dependent patients); 2. pre-KT PTH level ≥130 pg/mL; 3. successful primary KT not earlier than 12 months ago; 4. functioning kidney graft in the first postoperative year. Non-inclusion/exclusion criteria: 1. history of KT; 2. removal of kidney graft in the first

Corresponding author: Olga Vetchinnikova. Address: 61/2, Shchepkina str., Moscow, 129110, Russian Federation. Phone: (916) 532-49-00. E-mail: olg-vetchinnikova@yandex.ru

postoperative year; 3. parathyroidectomy prior to KT or in the first postoperative year.

The number of men and women included in the study was almost equal. The age of patients ranged from 19 to 70 years. Most patients suffered from various variants of non-diabetic kidney disease (91%). The predominant dialysis modality was hemodialysis. Duration of dialysis therapy ranged from 1 to 158 months; some patients were not placed on dialysis. All patients underwent cadaveric KT. Almost half of the patients had delayed renal graft function that required continuation of dialysis therapy (acute hemodialysis in 4 patients with pre-dialysis CKD). Duration of acute tubular necrosis ranged from 2 to 30 days (Table 1).

Biochemical examination was performed before KT and at 3 and 12 months postoperatively. Standard techniques were used to determine the serum levels of PTH, calcium, phosphorus, total alkaline phosphatase (ALP), albumin and creatinine. PTH levels of 130–585 pg/mL and ≤130 pg/mL were taken as the target level in the pre- and post-transplant period [12–15]. Estimated glomerular filtration rate (eGFR) was calculated using the Chronic Kidney Disease Epidemiology Collaboration (CKD-EPI) formula; CKD stages were stratified by eGFR level [16].

Table 1

Clinical characteristics of patients included in the study

Parameter	All patients (n = 210)
Men/women (n (%))	103/107 (49/51)
Age (years, M ± m)	45 ± 9
Body mass index	24.5 ± 3.5
Kidney disease	
Chronic glomerulonephritis (n (%))	94 (44.8)
Congenital nephrotic syndrome (n (%))	46 (21.9)
Chronic tubulointerstitial nephritis (n (%))	24 (11.4)
Diabetic kidney disease (n (%))	19 (9.0)
Kidney disease in systemic diseases (n (%))	10 (4.8)
Other (hypertensive nephrosclerosis, typical/atypical hemolytic uremic syndrome, kidney cancer, nephrolithiasis) (n (%))	17 (8.1)
Dialysis modality	
Hemodialysis (n (%))	145 (69.0)
Peritoneal dialysis (n (%))	34 (16.2)
Hemodialysis + peritoneal dialysis (n (%))	22 (10.5)
No dialysis (n (%))	9 (4.3)
Duration of dialysis therapy (months, [Me (Q1–Q3)])	19 (9; 35)
Kidney graft function	
Immediate (n (%))	107 (51.0)
Delayed (n (%))	103 (49.0)
Duration of acute tubular necrosis (day, [Me (Q1–Q3)]).	6 (3; 12)
Day of minimal blood creatinine recording after KT (day, [Me (Q1–Q3)])	7 (4; 13)

Statistical analysis of the material was performed using the GraphPad v.8.0.1 program. The form of distribution of characteristics was evaluated by the Kolmogorov–Smirnov test. Description of quantitative characteristics was presented in the form of arithmetic mean and standard deviation (M ± SD) in normal distribution, and in the form of median, 25% and 75% quartiles [Me (Q25–Q75)] in asymmetric distribution. Qualitative features were presented as absolute numbers (n) and proportions (%). The Mann–Whitney U test and Student t-test were used to compare quantitative data, while the chi-squared test was used for qualitative features. The strength of association between quantitative characteristics was assessed using Spearman's rank correlation coefficient. Relative risk (RR) with calculation of 95% confidence interval (95% CI) was used as a quantitative measure of effect when comparing relative indicators. The critical level of significance for testing statistical hypotheses in this study was taken to be 0.05.

RESULTS

Characteristics of traditional biochemical markers of secondary HPT in patients with stage 5 CKD (including dialysis-dependent patients) in the preoperative period is presented in Table 2.

PTH levels fluctuated widely (110–2500 pg/mL), and were outside the upper limit of the target interval in almost one third of patients. Serum phosphorus levels in most patients exceeded the reference values, while serum calcium levels were within target levels. Some patients had elevated blood alkaline phosphatase enzyme activity

Table 2

Traditional biochemical markers of HPT before kidney transplantation

Blood parameter	All patients (n = 210)
PTH (pg/mL [Me (Q1–Q3)])	400 (261; 620)
PTH 130–585 pg/mL (n (%))	154 (73.3)
PTH >585 pg/mL (n (%))	56 (26.7)
Phosphorus (mmol/L [Me (Q1–Q3)])	1.74 (1.44; 2.04)
Target level 0.87–1.49 mmol/L (n (%))	70 (33.3)
Hyperphosphatemia (>1.49 mmol/L (n (%)))	140 (66.7)
Hypophosphatemia (<0.87 mmol/L (n (%)))	0
Calcium (mmol/L, [Me (Q1–Q3)])	2.2 (2.3; 2.4)
Target level (2.1–2.6 mmol/L (n (%)))	193 (91.9)
Hypercalcemia (>2.6 mmol/L (n (%)))	9 (4.3)
Hypocalcemia (<2.1 mmol/L (n (%)))	8 (3.8)
Elevated blood AP levels (n (%))	19 (9.0)

Note. PTH, parathyroid hormone; AP, alkaline phosphatase.

(from one and a half to five times the upper limit of the reference interval).

Kidney transplant candidates were split into two groups based on their serum PTH levels. Group 1 included 56 patients with secondary HPT, and group 2 included 154 patients with target PTH levels. The clinical and laboratory characteristics of patient groups in the pre-transplant period are presented in Table 3. Group 1 patients received dialysis therapy for nearly 1.5 times as long. When analyzing routine biochemical markers of secondary HPT, these patients were found to be significantly more likely to have hyperphosphatemia, hypercalcemia and increased serum activity of alkaline phosphatase enzymes.

Three months after KT, PTH levels fell in all patients, fluctuating in the 80–1977 pg/mL range in group 1, and 10–535 pg/mL range in group 2 (Table 4, Fig. 1). The proportion of patients who achieved a PTH ≤130 pg/mL in group 1 was four times lower than in group 2, 10.7% and 42.2%, respectively. Pronounced changes were found in serum phosphorus, which reached normal or even low values in all recipients. The groups did not differ in absolute serum phosphorus levels, but patients with hypophosphatemia were slightly more frequent in group 1. Serum calcium levels remained stable; the incidence of hypercalcemia predominated in group 1 patients. The proportion of patients with increased ALP activity decreased 4-fold in group 1 and 3-fold in group 2; there was no intergroup difference in this parameter.

In the next 9 months, PTH levels further decreased from several to 670 pg/mL in 49 group 1 patients and from few to 221 pg/mL in 96 group 2 patients; the median was 81 (30; 145) and 25 (0; 61), respectively, $p < 0.001$; the remaining patients (7 in group 1 and 58 in group 2) had either an increase or no dynamics. All group 1 patients and 151 patients from group 2 generally showed decreased PTH levels of varying severity during the first postoperative year. This decrease was most pronounced in group 1 patients. At year 1 after the operation, the percentage of patients with the target PTH level was 1.5 times less than in group 2. The probability of normalization of PTG function in the first postoperative year was found to be significantly lower in renal transplant candidates with HPT compared with patients with the target range of pre-transplant serum PTH (Table 5).

Table 3

Clinical and laboratory characteristics of patient groups

Parameter	Patients		p
	Group 1 (n = 56)	Group 2 (n = 154)	
Men/women (n (%))	32/24 (57.1/42.9)	71/83 (46.1/53.9)	NS
Age (years (M ± m))	44 ± 10	45 ± 9	NS
Body mass index (kg^2/cm (M ± m))	24.6 ± 4.1	25.7 ± 4.7	NS
Chronic glomerulonephritis (n (%))	18 (32.1)	75 (48.7)	NS
Congenital nephrotic syndrome (n (%))	13 (23.2)	33 (21.4)	NS
Chronic tubulointerstitial nephritis (n (%))	8 (14.3)	16 (10.4)	NS
Diabetic kidney disease (n (%))	4 (7.1)	15 (9.7)	NS
Kidney disease in systemic diseases (n (%))	3 (5.4)	8 (5.2)	NS
Other (hypertensive nephrosclerosis, typical/atypical hemolytic uremic syndrome, kidney cancer, nephrolithiasis) (n (%))	10 (17.9)	7 (4.6)	0.004
Hemodialysis (n (%))	45 (80.4)	100 (64.9)	0.049
Peritoneal dialysis (n (%))	5 (8.9)	29 (18.8)	NS
Hemodialysis + peritoneal dialysis (n (%))	4 (7.1)	18 (11.7)	NS
No dialysis (n (%))	2 (3.6)	7 (4.6)	NS
Duration of dialysis therapy (months, [Me (Q1–Q3)])	26 (12; 44)	16 (8; 34)	0.009
Blood PTH, pg/mL [Me (Q1–Q3)]	897 (722; 1136)	301 (229; 411)	<0.001
Blood phosphorus, mmol/L [Me (Q1–Q3)]	1.92 (1.62; 2.31)	1.72 (1.42; 1.97)	<0.001
Target level (0.87–1.49 mmol/L) (n (%))	6 (10.7)	65 (42.2)	<0.001
Hyperphosphatemia (>1.49 mmol/L) (n (%))	50 (89.3)	89 (57.8)	<0.001
Hypophosphatemia (<0.87 mmol/L) (n (%))	0	0	NS
Calcium (total) blood, mmol/L [Me (Q1–Q3)]	2.3 (2.2; 2.5)	2.3 (2.2; 2.4)	NS
Target level (2.1–2.6 mmol/L) (n (%))	46 (82.1)	147 (95.5)	0.004
Hypercalcemia (>2.6 mmol/L) (n (%))	6 (10.8)	3 (1.9)	0.017
Hypocalcemia (<2.1 mmol/L) (n (%))	4 (7.1)	4 (2.6)	NS
Elevated blood AP levels (n (%))	12 (21.4)	7 (4.5)	<0.001

Note. PTH, parathyroid hormone; AP, alkaline phosphatase; p, statistical significance of differences between groups 1 and 2 parameters; NS, not significant.

Changes in serum phosphorus and calcium levels were minimal. Serum phosphorus in the majority of patients was within the reference range, a few patients in group 2 had hyperphosphatemia, while hypophosphatemia prevailed in group 1 patients. Serum calcium remained relatively stable throughout the entire follow-up

Table 4

Traditional biochemical markers of HPT in patients before KT, 3 and 12 months after KT

	Group 1 (n = 56)			Group 2 (n = 154)			p_1	p_2
	Pre-KT	3 months after KT	12 months after KT	Pre-KT	3 months after KT	12 months after KT		
Blood PTH, pg/mL [Me (Q1–Q3)]	897 (722; 1036)	254 (180; 455)*	171 (94; 239)** #	301 (229; 411)	150 (118; 212)*	112 (90; 135)** #	<0.001	0.004
ΔPTH (pg/mL)	0	595 (420; 812)	853 (705; 1178)	0	148 (77; 230)	196 (117; 340)	<0.001	0.001
Blood PTH ≤130 pg/mL (n (%))	0	6 (10.7)*	27 (48.2)**	0	65 (42.2)*	113 (73.4)** #	<0.001	<0.001
Blood phosphorus, mmol/L [Me (Q1–Q3)]	1.92 (1.62; 2.31)	0.97 (0.78; 1.21)*	0.94 (0.79; 1.05)#	1.72 (1.42; 1.97)	1.04 (0.91; 1.21)*	1.09 (0.99; 1.35)	NS	0.002
Hyperphosphatemia (>1.49 mmol/L) (n (%))	50 (89.3)	0*	0#	89 (57.8)	0*	6 (3.9)#	NS	NS
Hypophosphatemia (<0.87 mmol/L) (n (%))	0	18 (32.1)*	20 (35.7)#	0	29 (18.8)*	22 (14.3)#	0.051	0.001
Calcium (total) blood, mmol/L [Me (Q1–Q3)]	2.3 (2.2; 2.5)	2.5 (2.3; 2.6)	2.5 (2.4; 2.7)	2.3 (2.2; 2.4)	2.4 (2.3; 2.5)	2.4 (2.3; 2.5)	NS	NS
Hypercalcemia (>2.6 mmol/L) (n (%))	6 (10.8)	8 (12.7)	11 (19.6)	3 (1.9)	1 (0.7)	2 (1.3)	<0.001	<0.001
Hypocalcemia (<2.1 mmol/l) (n (%))	4 (7.1)	0	0	4 (2.6)	0	0	NS	NS
Elevated blood AP levels (n (%))	12 (21.4)	3 (4.8)*	5 (8.9)	7 (4.5)	2 (1.4)	1 (0.6)	NS	0.007

Note. PTH, parathyroid hormone; KT, kidney transplantation; ALP, alkaline phosphatase; *, differences are statistically significant between parameters before and 3 months after KT; **, differences statistically significant between parameters 3 and 12 months after KT; #, differences are statistically significant between parameters before and 12 months after KT; p_1, statistical significance of differences between groups 3 months after KT; p_2, statistical significance of differences between groups 12 months after KT; NS, not significant.

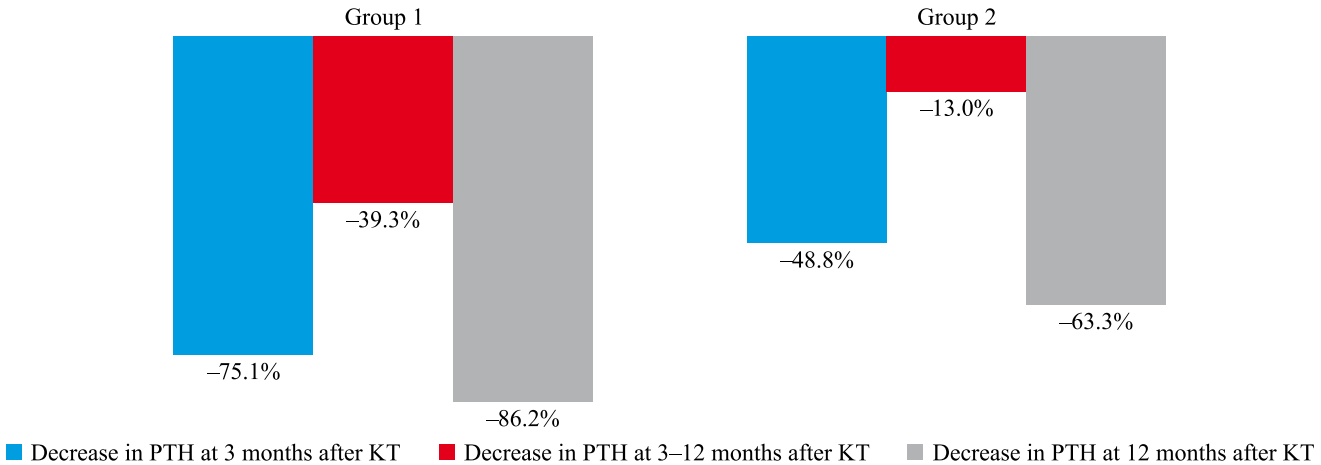

Fig. 1. Level of decrease in blood PTH levels in kidney transplant recipients during the first postoperative year. Differences between groups are statistically significant for each time interval; KT, kidney transplantation

time; hypercalcemia, as in the early postoperative period, was found more often in group 1 patients. Patients with increased ALP activity became more frequent in group 1.

When analyzing initial kidney graft function, differences between the groups was on duration of acute tubular necrosis only, which was longer in group 1 patients. The two remaining parameters – onset of kidney function and the day minimum serum creatinine level was detected – were identical. There were no differences in serum creatinine levels and eGFR between the groups at 3 or 12 months (Table 6). There were no intra- and intergroup differences in patient distribution by CKD stage (Fig. 2).

Table 7 presents data from correlation analysis for post-transplant PTH levels at 3 and 12 months.

In group 1 patients, postoperative PTH levels had a moderately close direct association with preoperative PTH levels and there was no such relationship with kid-

Table 5

Effect of HPT in KT candidates on normalization of parathyroid gland function in the first year after surgery

Factor	Normal thyroid function in the HPT group (n = 56)	Normal thyroid function in the no HPT group (n = 154)	Relative risk [95% CI]	p
At 3 months post KT	6 (10.7%)	65 (42.2%)	0.254 [0.116; 0.522]	<0.0001
At 1 year post KT	27 (48.2%)	113 (73.4%)	0.657 [0.480; 0.851]	0.0009

Table 6

Kidney graft function in the first year after surgery

Parameter	Patients		p_2
	Group 1 (n = 56)	Group 2 (n = 154)	
Initial kidney graft function Immediate (n (%)) Delayed (n (%))	 23 (41.1) 33 (58.9)	 84 (54.5) 70 (45.5)	 NS NS
Duration of acute tubular necrosis (days, [Me (Q1–Q3)])	7 (4; 15)	6 (3; 9)	0.034
Day of minimal blood creatinine recording after KT (day, [Me (Q1–Q3)])	7 (4; 18)	7 (4; 13)	NS
Blood creatinine at 3 months (μmol/L [Me (Q1–Q3)]) Blood creatinine after 12 months (μmol/L [Me (Q1–Q3)])	117 (88; 146) 123 (110; 146) $p_1 = 0.311$	110 (78; 124) 120 (96; 140) $p_2 = 0.019$	NS NS
eGFR at 3 months (mL/min) eGFR at 12 months (mL/min)	60 (46; 77) 56 (47; 63) $p_1 = 0.228$	65 (51; 88) 54 (46;70) $p_1 = 0.02$	NS NS
eGFR <60 mL/min at 3 months (n (%)) eGFR <60 mL/min at 12 months (n (%))	27 (48.2) 36 (64.3) $p_1 = 0.128$	74 (48.1) 94 (61.0%) $p_1 = 0.03$	NS NS

Note. eGFR, estimated glomerular filtration rate; p_1, statistical significance of differences between parameters at 3 and 12 months; p_2, statistical significance of differences between group 1 and 2 parameters; NS, not significant.

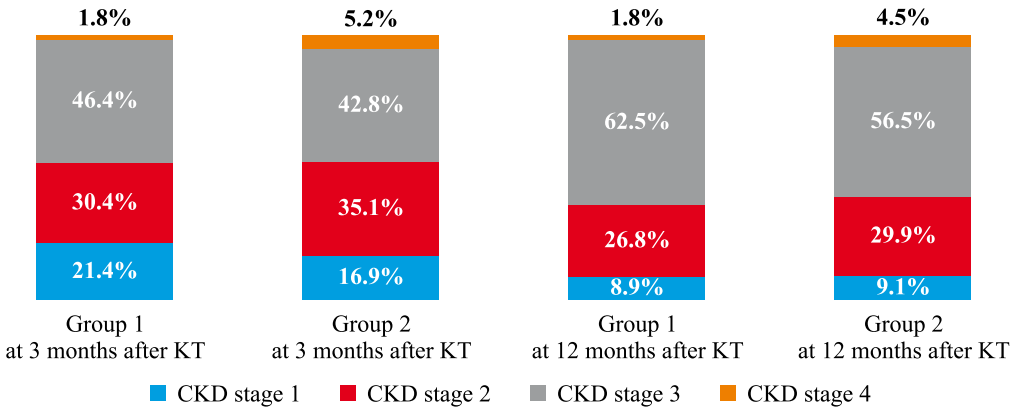

Fig. 2. Distribution of kidney transplant recipients by CKD severity. Differences between groups are not statistically significant for each time interval; KT, kidney transplantation

ney graft function at 3 months and by the end of the first postoperative year. In group 2 patients, there was also a direct correlation between post- and pre-transplant PTH levels, which was closer at 3 months following surgery. Unlike group 1 patients, this patient cohort showed a greater correlation between post-transplant PTH levels and renal graft function at 12 months of operation. In both groups, there was no association between post-transplant PTH levels and length of dialysis sessions.

DISCUSSION

Excessive synthesis and release of PTH is a natural reaction of PTG to various metabolic changes that develop in CKD patients – hypocalcemia, hyperphosphatemia, vitamin D deficiency, accumulation of fibroblast growth factor-23 in the blood, and others. Persistent excessive release of PTH with the formation of PTG hyperplasia leads to secondary HPT. Due to its prevalence, severe HPT often occurs in patients undergoing KT. In our study, 26.7% of such patients had pre-transplant PTH levels that persistently remained above 600 pg/mL.

Successful KT levels out the pathophysiological processes that lead to secondary HPT. It spontaneously normalizes PTG function within six months to a year, sometimes longer. However, this process does not occur in all patients; it may be absent in some patients due to formed structural changes in PTG [9, 17]. In general, among all the patients we observed, the incidence of post-transplant HPT at three months after surgery was 66.2% (89.3% in patients with previous HPT and 57.8% in patients without HPT); by the end of the first year, it decreased twofold, 33.3% (51.8% in patients with previous HPT and 26.6% in patients without HPT).

It has been widely shown that patients who have kidney transplants, including those who do not receive dialysis therapy, have a high incidence of HPT both in

Table 7

Correlation of PTH levels in KT recipients

Parameter	Group 1 (n = 56)		Group 2 (n = 154)	
	Post-KT PTH levels (pg/mL)			
	At 3 months	At 12 months	At 3 months	At 12 months
Pre-KT PTH levels (pg/mL)	r = 0.347 p = 0.009	r = 0.379 p = 0.005	r = 0.508 p < 0.001	r = 0.216 p = 0.007
Post-KT PTH levels at 3 months (pg/mL)	–	r = 0.542 p < 0.001	–	r = 0.581 p < 0.001
ΔPTH (0–3 months) (pg/mL)	r = –0.107 p = 0.433	r = 0.206 p = 0.134	r = –0.071 p = 0.386	r = 0.003 p = 0.971
ΔPTH (0–3 months) (%)	r = –0.780 p < 0.001	r = –0.293 p = 0.031	r = –0.516 p < 0.001	r = –0.019 p = 0.815
ΔPTH (0–12 months) (pg/mL)	–	r = –0.105 p = 0.449	–	r = –0.410 p < 0.001
ΔPTH (0–12 months) (%)	–	r = –0.399 p = 0.003	–	r = –0.509 p < 0.001
ΔPTH (3–12 months) (pg/mL)	–	r = 0.189 p = 0.162	–	r = –0.324 p < 0.001
ΔPTH (3–12 months) (%)	–	r = 0.114 p = 0.402	–	r = –0.699 p < 0.001
Duration of dialysis therapy (months)	r = –0.097 p = 0.478	r = 0.219 p = 0.104	r = 0.052 p = 0.523	r = –0.083 p = 0.306
Duration of acute tubular necrosis (days)	r = 0.318 p = 0.017	r = 0.440 p < 0.001	r = 0.134 p = 0.099	r = 0.047 p = 0.583
Minimum creatinine level (day)	r = 0.210 p = 0.124	r = –0.008 p = 0.952	r = 0.251 p = 0.002	r = 0.157 p = 0.062
Creatinine level at 3 months (μmol/L)	r = 0.201 p = 0.144	r = 0.163 p = 0.24	r = 0.186 p = 0.021	r = 0.246 p = 0.002
Creatinine level at 12 months (μmol/L)	–	r = –0.044 p = 0.749	–	r = 0.474 p < 0.001
eGFR at 3 months (mL/min)	r = –0.205 p = 0.129	r = –0.139 p = 0.308	r = –0.118 p = 0.146	r = –0.172 p = 0.033
eGFR at 12 months (mL/min)	–	r = 0.036 p = 0.799	–	r = –0.292 p < 0.001

Note. PTH, parathyroid hormone; ΔPTH, magnitude of parathyroid hormone reduction; eGFR, estimated glomerular filtration rate; NS, not significant.

the early and late periods following surgery [7, 17–19]. In our study, patients with preoperative secondary HPT had higher mean PTH levels at year following KT, and the percentage of patients with the target PTH levels was lower than in patients without HPT. However, group 1 patients had a significantly higher PTH reduction than group 2 patients. A similar pattern of dependence of HPT persistence after KT on preoperative PTH levels has been established by other teams of authors [8, 18–20].

It should be noted that in our study, we used the pre-transplant range of the target serum PTH level of 130–585 pg/mL (2–9 upper limits of the reference interval) proposed by international guidelines (Kidney Disease Improving Global Outcomes, KDIGO) and the post-transplant level of less than 130 pg/mL (2 upper limits of the reference interval) previously proposed by some authors [12–15]. At the same time, some recent foreign studies have used lower serum PTH levels as a diagnostic criterion for pre- and post-transplant HPT [18, 19]. This changes the data on HPT prevalence in kidney transplant candidates and recipients and complicates the process of comparing study findings.

Taken together, these data emphasize the importance of early diagnosis, prevention and adequate treatment of secondary HPT in kidney transplant candidates to prevent persistent post-transplant HPT. Timely detection of secondary HPT in CKD patients on the KT waitlist is ensured by dynamic examination of PTG function and associated mineral and bone metabolism parameters, especially since there are no early clinical manifestations of the disease. International guidelines (KDIGO) recommend aggressive treatment of severe HPT before KT and, if drug therapy is ineffective, parathyroidectomy (PTx), while the US National Kidney Foundation's Kidney Disease Outcomes Quality Initiative (KDOQI) and Russian national guidelines provide no information in this regard [21–23]. Several studies have demonstrated the benefits of performing PTx in patients with CKD and severe HPT prior to kidney transplantation. For instance, in comparison to patients receiving cinacalcet, these patients have better controllability of HPT, lower risk of tertiary HPT, lower post-transplant PTH levels and the less medical care, compared with patients receiving cinacalcet [24]. On the contrary, where PTx is performed, kidney graft function has been found to worsen in the postoperative period [25, 26].

Renal graft function, another risk factor for posttransplant HPT that has been established in multiple studies, was not entirely confirmed by this observation [27, 28]. Serum creatinine levels and eGFR were identical in both groups of patients over the course of the first year following surgery. Correlation analysis in patients with HPT before KT revealed no association between post-transplant PTH levels and renal graft function in the first postoperative year, whereas patients with target blood PTH levels before surgery showed such an association. This result may be due to the short follow-up period. It is very likely that longer follow-up could reveal a correlation between posttransplant PTH levels and renal graft function in patients with preoperative HPT.

Other risk factors for postoperative HPT have been established in some cases [7, 9, 18]. In our study as well as in a study by Sutton W. et al. [18], there was no evidence of an association between posttransplant serum PTH and duration of preoperative dialysis treatment, although some authors have pointed out that such a relationship exists [8, 20].

So, preoperative secondary HPT in patients with CKD is the predominant factor in excessive PTH secretion and persistent posttransplant HPT. The impact of the latter on KT outcomes is debated. A number of studies have reported a deterioration in quality of life and increased risk of mortality in recipients with HPT.

Studies on the association between posttransplant HPT and kidney graft function are of particular importance [10, 11, 17, 29–31]. A recently published study by Molinari et al. [7] demonstrated a close association between high PTH levels in the first year after KT and long-term kidney graft loss. The exact mechanism by which PTH damages kidney grafts is not entirely understood. Experimental studies suggest that it affects renal blood flow, i.e., dilation of supply and constriction of efferent arterioles, which leads to glomerular hyperfiltration [32].

A clinical observation in patients with transplanted kidney who underwent PTx in the early postoperative period found a decrease in effective renal blood flow and GFR, reflecting a close relationship between the hemodynamic effect of PTH and renal function [33]. The longer duration of acute tubular necrosis observed in our recipients with pre-operative HPT, with the same incidence in both groups, was most likely caused by the relationship between the hemodynamic effect of PTH and renal function. Another possible mechanism of progressive graft dysfunction on the background of postoperative HPT is renal vasoconstriction, impaired urine concentration, and renal resistance to vasopressin caused by hypercalcemia; in our study, such patients were orders of magnitude more numerous among those with pre-transplant HPT [34]. In addition, high serum PTH levels are involved in renal fibrosis, vascular calcification, immunodeficiency and anemia, which may also adversely affect renal graft function [35].

In addition to worsening renal graft function, HPT in recipients is accompanied by a high risk of bone fractures and all-cause mortality [10, 13]. Obtained results on the adverse effect of persistent HPT on the posttransplant period justify the expediency of monitoring PTH levels in kidney recipients in order to develop an algorithm for the prevention and treatment of this disease.

Limitations of this study include (1) retrospective design; (2) generalization of results from a single center;

and (3) analysis of only routine markers of mineral bone disease associated with CKD.

CONCLUSION

HPT is a common complication in CKD patients, occurring in kidney transplant candidates. The disease is the main graft function-independent predictor; it prevents patients' PTG function from normalizing in the first postoperative year. Early detection, prevention, and adequate treatment of secondary HPT should be prioritized while preparing kidney transplant candidates. In the follow-up of kidney transplant recipients, monitoring PTH levels is advised to prevent and treat posttransplant HPT.

The authors declare no conflict of interest.

REFERENCES

1. *Messa P, Alfieri CM.* Secondary and tertiary hyperparathyroidism. Brandi ML (ed): Parathyroid Disorders. Focusing on Unmet Needs. *Front Horm Res*. 2019; 51: 91–108. doi: 10.1159/000491041.
2. *Vetchinnikova ON.* Hyperparathyroidism and chronic kidney disease. Part 1. Features of pathogenesis, clinical manifestations, diagnostic strategy. Lecture. *Nephrology and Dialysis*. 2023; 25 (1): 36–56. doi: 10.28996/2618-9801-2023-1-36-56.
3. *Ermolenko VM, Volgina GV, Mikhaylova NA, Zemchenkov AYu, Ryasnyanskiy VYu, Vetchinnikova ON i dr*. Lechenie mineral'nykh i kostnykh narusheniy pri khronicheskoy bolezni pochek. *Nefrologiya. Klinicheskie rekomendatsii*. Pod red. E.M. Shilova, A.V. Smirnova, N.L. Kozlovskoy. M.: GEOTAR-Media, 2016: 687–709. (In Russ).
4. *Alfieri C, Regalia A, Zanoni F, Vettoretti S, Cozzolino M, Messa P*. The importance of adherence in the treatment of secondary hyperparathyroidism. *Blood Purif*. 2019; 47 (1-3): 37–44. doi: 10.1159/000492918.
5. *Ketteler M, Bover J, Mazzaferro S*. Treatment of secondary hyperparathyroidism in non-dialysis CKD: an appraisal 2022s. Nephrol Dial Transplant 2022; 0: 1–7. doi: 10.1093/ndt/gfac236.
6. *Gautier SV, Khomyakov SM*. Organ donation and transplantation in the Russian Federation in 2022. 15th Report from the Registry of the Russian Transplant Society. *Russian Journal of Transplantology and Artificial Organs*. 2023; XXV (3): 8–30. (In Russ., English abstract). doi: 10.15825/1995-1191-2023-3-8-30.
7. *Molinari P, Regalia A, Leoni A, Campise M, Cresseri D, Cicero E et al*. Impact of hyperparathyroidism and its different subtypes on long term graft outcome: a single Transplant Center cohort study. *Front Med (Lausanne)*. 2023; 10: 1221086. doi: 10.3389/fmed.2023.1221086.
8. *Yamamoto T, Tominaga Y, Okada M, Hiramitsu T, Tsujita M, Goto N et al*. Characteristics of persistent hyperparathyroidism after renal transplantation. *World J Surg*. 2016; 40 (3): 600–606. doi: 10.1007/s00268-015-3314-z. PMID: 26546189.
9. *Lou I, Foley D, Odorico SK, Leverson G, Schneider DF, Sippel R et al*. How well does renal transplantation cure hyperparathyroidism? *Ann Surg*. 2015; 262 (4): 653–659. doi: 10.1097/SLA.0000000000001431.
10. *Pihlstrøm H, Dahle DO, Mjoen G, Pilz S, Marz W, Abedini S et al*. Increased risk of all-cause mortality and renal graft loss in stable renal transplant recipients with hyperparathyroidism. *Transplantation*. 2015; 99 (2): 351–359. doi: 10.1097/tp.00000 00000000583.
11. *Okada M, Tominaga Y, Sato T, Tomosugi T, Futamura K, Hiramitsu T et al*. Elevated parathyroid hormone one year after kidney transplantation is an independent risk factor for graft loss even without hypercalcemia. *BMC Nephrol*. 2022; 23: 212. doi: 10.1186/S12882-022-02840-5.
12. KDIGO 2017. Clinical Practice Guideline Update for the Diagnosis, Evalution, Prevention and Treatment of Chronic Kidney Disease – Mineral and Bone Disorder (CKD-MBD). *Kidney Int*. 2017; 7 (1): 1–59.
13. *Perrin P, Caillard S, Javier RM, Braun L, Heibel F, Borni-Duval C et al*. Persistent hyperparathyroidism is a major risk factor for fractures in the five years after kidney transplantation. *Am J Transplant*. 2013; 13: 2653–2663. doi: 10.1111/ajt.12425.
14. *Bleskestad IH, Bergrem H, Leivestad T, Hartmann A, Gøransson LG*. Parathyroid hormone and clinical outcome in kidney transplant patients with optimal transplant function. *Clin Transplant*. 2014; 28: 479–486. doi: 10.1111/ctr12341.
15. *Evenepoel P, Claes K, Kuypers D, Maes B, Bammens B, Vanrenterghem Y*. Natural history of parathyroid function and calcium metabolism after kidney transplantation: A single-centre study. *Nephrol Dial Transplant*. 2004; 19: 1281–1287. doi: 10.1093/ndt/gfh128.
16. National kidney foundation. K/DOQI Clinical Practice Guidelines for Bone Metabolism and Disease in Chronic Kidney Disease. *Am J Kidney Dis*. 2003; 42 (Suppl. 3): S1–S202.
17. *Wang R, Price G, Disharoon M, Stidham G, McLeod M-C, McMullin JL et al*. Resolution of secondary hyperparathyroidism after kidney transplantation and the effect on graft survival. *Ann Surg*. 2023; 278 (3): 366–375. doi: 10.1097/SLA.0000000000005946.
18. *Sutton W, Chen X, Patel P, Karzai S, Prescott JD, Segev DL et al*. Prevalence and risk factors for tertiary hyperparathyroidism in kidney transplant recipients. *Surgery*. 2022; 171 (1): 69–76. doi: 10.1016/j.surg.2021.03.067.
19. *Okada M, Sato T, Hasegawa Y, Futamura K, Hiramitsu T, Ichimori T et al*. Persistent hyperparathyroidism after preemptive kidney transplantation. *Clin Exp Nephrol*. 2023; Jun 23. doi: 10.1007/s10157-023-02371-9.
20. *Kirnap NG, Kirnap M, Sayin B, Akdur A, Bascil Tutuncu N, Haberal M*. Risk factors and treatment options for persistent hyperparathyroidism after kidney transplantation. *Transplant Proc*. 2020; 52 (1): 157–161. doi: 10.1016/j.transproceed.2019.11.020.
21. *Chadban SJ, Ahn C, Axelrod DA, Foster BJ, Kasiske BL, Kher V et al*. KDIGO clinical practice guideline on the evaluation and management of candidates for kidney transplantation. *Transplantation*. 2020; 104 (4S1 Sup-

pl. 1): S11–S103. doi: 10.1097/TP.0000000000003136. PMID: 32301874.
22. *Puttarajappa CM, Schinstock CA, Wu CM, Leca N, Kumar V, Vasudev BS, Hariharan S*. KDOQI US commentary on the 2020 KDIGO clinical practice guideline on the evaluation and management of candidates for kidney transplantation. *Am J Kidney Dis*. 2021; 77 (6): 833–856. doi: 10.1053/j.ajkd.2020.11.017.
23. *Smirnov AV, Vatazin AV, Dobronravov VA, Bobkova IN, Vetchinnikova ON, Volgina GV et al*. Clinical recommendations. Chronic kidney disease (CKD). *Nephrology (Saint-Petersburg)*. 2021; 25 (5): 10–84. (In Russ.). doi: 10.36485/1561-6274-2021-25-5-10-84.
24. *Egan CE, Qazi M, Lee J, Lee-Saxton YJ, Greenberg JA, Beninato T et al*. Treatment of secondary hyperparathyroidism and posttransplant tertiary hyperparathyroidism. *J Surg Res*. 2023; 291: 330–335. doi: 10.1016/j.jss.2023.06.031.
25. *Jeon HJ, Kim YJ, Kwon HY, Koo TY, Baek SH, Kim HJ et al*. Impact of parathyroidectomy on allograft outcomes in kidney transplantation. *Transpl Int*. 2012; 25 (12): 1248–1256. doi: 10.1111/j.1432-2277.2012.01564.x.
26. *Littbarski SA, Kaltenborn A, Gwiasda J, Beneke J, Arelin V, Schwager Y et al*. Timing of parathyroidectomy in kidney transplant candidates with secondary hyperparathryroidism: Effect of pretransplant versus early or late post-transplant parathyroidectomy. *Surgery*. 2018; 163 (2): 373–380. doi: 10.1016/j.surg.2017.10.016.
27. *Alagoz S, Trabulus S*. Long-term evaluation of mineral metabolism after kidney transplantation. *Transplant Proc*. 2019; 51 (7): 2330–2333. doi: 10.1016/j.transproceed.2019.01.181.
28. *Kettler B, Scheffner I, Bräsen JH, Hallensleben M, Richter N, Heiringhoff KH et al*. Kidney graft survival of >25 years: a single center report including associated graft biopsy results. *Transpl Int*. 2019; 32 (12): 1277–1285. doi: 10.1111/tri.13469.
29. *Araujo MJCLN, Ramalho JAM, Elias RM, Jorgetti V, Nahas W, Custodio M et al*. Persistent hyperparathyroidism as a risk factor for long-term graft failure: the need to discuss indication for parathyroidectomy. *Surgery*. 2018; 163: 1144–1150. doi: 10.1016/j.surg.2017.12.010.
30. *Isakov O, Ghinea R, Beckerman P, Mor E, Riella LV, Hod T*. Early persistent hyperparathyroidism post-renal transplantation as a predictor of worse graft function and mortality after transplantation. *Clin Transpl*. 2020; 34: e14085. doi: 10.1111/ctr.14085.
31. *Tsai M-H, Chen M, Liou H-H, Lee T-S, Huang Y-C, Liu P-Y, Fang Y-W*. Impact of pre-transplant parathyroidectomy on graft survival: A comparative study of renal transplant patients (2005–2015). *Med Sci Monit*. 2023; 29: e940959. doi: 10.12659/MSM.940959.
32. *Massfelder T, Parekh N, Endlich K, Saussine C, Steinhausen M, Helwig JJ*. Effect of intrarenally infused parathyroid hormone-related protein on renal blood flow and glomerular filtration rate in the anaesthetized. *Br J Pharmacol*. 1996; 118: 1995–2000. doi: 10.1111/j.1476-5381.1996.tb15635.x.
33. *Schwarz A, Rustien G, Merkel S, Radermacher J, Haller H*. Decreased renal transplant function after parathyroidectomy. *Nephrol Dial Transplant*. 2007; 22: 584–591. doi: 10.1093/ndt/gfl583.
34. *Ruda JM, Hollenbeak CS, Stack BC Jr*. A systematic review of the diagnosis and treatment of primary hyperparathyroidism from 1995 to 2003. *Otolaryngol Head Neck Surg*. 2005; 132: 359–372. doi: 10.1016/j.otohns.2004.10.005.
35. *Duque EJ, Elias RM, Moysés RMA*. Parathyroid hormone: A uremic toxin. *Toxins*. 2020; 12: 189–204. doi: 10.3390/toxins12030189.

The article was submitted to the journal on 26.12.2023

DOI: 10.15825/1995-1191-2024-2-94-104

FUNCTIONAL EFFICIENCY OF PANCREATIC CELL-ENGINEERED CONSTRUCT IN AN ANIMAL EXPERIMENTAL MODEL FOR TYPE I DIABETES

N.V. Baranova, A.S. Ponomareva, L.A. Kirsanova, A.O. Nikolskaya, G.N. Bubentsova, Yu.B. Basok, V.I. Sevastianov

Shumakov National Medical Research Center of Transplantology and Artificial Organs, Moscow, Russian Federation

The creation of a cell-engineered pancreatic construct (CEPC) from islets of Langerhans and biocompatible matrix carrier (framework/scaffold), which imitates the native microenvironment of pancreatic tissue, is an approach to the treatment of type I diabetes mellitus (T1D). **Objective:** to conduct a comparative analysis of the functional efficacy of CEPC and isolated rat islets of Langerhans after intraperitoneal administration into rats with experimental T1D. **Materials and methods.** T1D was induced in rats by injecting low-dose (15 mg/kg) streptozotocin (STZ) for 5 days. CEPC samples were created using viable and functional allogeneic isolated islets of Langerhans and tissue-specific scaffold obtained by decellularization of human pancreatic fragments. The rats received intraperitoneal injection of allogeneic islets of Langerhans (experimental group 1, n = 4) and CEPC (experimental group 2, n = 4). Control group rats received no treatment (n = 4). Blood glucose levels in the rats were measured, and the pancreas and kidneys of the experimental animals were examined histologically. The follow-up period for all animals continued for 10 weeks. Results. In experimental group 1, on day 7 after injection of Langerhans islets, glycemia decreased significantly from 28.2 ± 4.2 mmol/L to 13.4 ± 2.6 mmol/L. This fall persisted for 7 weeks, following which blood sugar increased to nearly their initial levels (prior to islets administration). In experimental group 2, on day 7 after CEPC administration, there was a more noticeable drop in blood sugar levels from 25.8 ± 5.1 mmol/L to 6.3 ± 2.7 mmol/L compared to experimental group 1. By the 10th week of the experiment, the average glucose level was two times lower than it was at the beginning. Blood glucose levels dropped more sharply in the CEPC group than in the islet group (by 75.6% and 52.5%, respectively). **Conclusion.** In T1D rats, CEPC has a more potent antidiabetic effect than islets of Langerhans. Thus, it has been shown that a tissue-specific scaffold may be used to create bioartificial pancreas in order to increase the functional efficiency of islets.

Keywords: type I diabetes mellitus, islets of Langerhans, cell-engineered construct, pancreas, decellularization, tissue-specific scaffold.

INTRODUCTION

Replacement of damaged beta cells in patients with severe type I diabetes mellitus (T1D) through pancreatic islet transplantation is an effective treatment method that allows to establish long-term stable euglycemia [1], improve the quality of life and reduce secondary complications compared to insulin therapy [2]. However, during pancreatic islet isolation, their functional activity decreases due to a number of damaging factors, such as loss of vascularization, innervation and connections with the extracellular matrix (ECM). After transplantation, the islet revascularization process is completed in 10–14 days. During this period, oxygen and nutrients are delivered to islet cells only by diffusion, which may be insufficient to maintain cell viability in the central part of the islet [3, 4]. Thus, the limited graft functioning time is to some extent connected with islet hypoxia in the posttransplant period [5].

It seems essential to provide the islets of Langerhans with the conditions conducive to maintaining their viability and function *in vitro* and *in vivo*. There is a need to develop new strategies for beta-cell replacement, including the creation of a bioequivalent of pancreas based on insulin-producing cells and a carrier matrix (scaffold) mimicking the pancreatic ECM. Thus, decellularized pancreas with preserved biochemical, spatial and vascular structure of the native ECM can be used as a scaffold for subsequent recellularization with insulin-producing cells and further transplantation [6–9].

Decellularized pancreatic tissue most closely mimics the microenvironment of native pancreatic ECM, i.e. they possess tissue specificity with characteristic features of structure and composition. A significant reduction

Corresponding author: Natalia Baranova. Address: 1, Shchukinskaya str., Moscow, 123182, Russian Federation. Phone: (917) 568-98-22. E-mail: barnats@yandex

in immunogenicity, achieved by removing cellular and nuclear material from decellularized scaffolds, provides an ideal support system for islet cells in transplantation [10, 11]. Successful fabrication and recellularization of scaffold from decellularized pancreatic tissue is an essential component of pancreatic tissue engineering [12].

Previous studies have allowed us to develop protocols for the preparation of tissue-specific scaffolds from decellularized rat [13] and human [14] pancreas. *In vitro* experimental studies have found that culturing islets of Langerhans in the presence of such scaffolds helps preserve their structure, prolongs their viability and insulin-producing function in comparison with islets cultured under standard conditions [6, 13–15]. Some reports [5, 9, 10] have shown that a scaffold from decellularized pancreas also provides islet cells with prolonged survival and functioning *in vivo*.

Decellularized pancreatic tissue scaffolds seeded with islet cells represent a formed cell-engineered pancreatic construct (CEPC), often referred to as bioartificial pancreas. CEPCs appear to be feasible for clinical transplantation to T1D patients to compensate for the endocrine function of the pancreas [8].

The **aim** of the present work was to comparatively analyze the functional efficacy of CEPC and isolated rat islets of Langerhans after intraperitoneal injection in T1D rats.

MATERIALS AND METHODS

Experimental animals

For modeling streptozotocin-induced T1D followed by CEPC implantation (recipient animals) and isolation of islets of Langerhans (donor animals), we used male Wistar rats weighing 300–380 g (n = 30) from a laboratory animal nursery belonging to KrolInfo LLC. Acclimatization and maintenance of the animals was carried out in accordance with interstate standard GOST ISO 10993-2-2009 "Medical Devices. Assessment of the Biological Effect of Medical Devices". Part 2. "Requirements for the Treatment of Animals".

Manipulations with animals were performed in accordance with the European Convention for the Protection of Vertebrate Animals Used for Experimental and other Scientific Purposes (2005) and the Rules of Laboratory Practice approved by Order No. 708 of the Russian Ministry of Health dated August 23, 2010. Approval (Protocol No. 280121-1/1e, dated January 28, 2021) for the experimental studies was obtained from the Local Ethics Committee of Shumakov National Medical Research Center of Transplantology and Artificial Organs.

Modeling of type I diabetes

To induce T1D, the rats were intermittently injected with streptozotocin (STZ) (Biorbyt, India): 15 mg/kg/day intraperitoneally for 5 consecutive days (total dose 75 mg/kg) [16]. The injection agent was prepared ex tempore by diluting STZ in 0.9% sodium chloride solution and injected into the peritoneal cavity. The dynamics of blood sugar levels was determined daily using an Accu-Chek Active glucometer (Roche, Switzerland).

Testing the stability of an experimental model of type I diabetes

To rule out spontaneous reversion of diabetic status, the animals were monitored for the next 14 days after the last STZ injection. Fasting blood glucose and body weight were monitored weekly, appearance and amount of water consumed by the animals were assessed daily.

T1D was considered stable if blood glucose level in the rats exceeded 20.0 mmol/L two weeks after the last dose of STZ injection.

In rats with glucose concentration of less than 20.0 mmol/L, clinical signs of diabetes were mild. Such animals were not used in the experiment. Animals with glucose levels exceeding the glucose meter limit (33.0 mmol/L) were considered unsuitable for further CEPC implantation.

CEPC preparation technology

To create CEPC, tissue-specific finely dispersed scaffold derived from decellularized human pancreatic fragments (DHP scaffold) was chosen as an ECM biomimetic [13, 14]. Studies have shown that DHP scaffold retains the morphofunctional properties of native ECM of pancreatic tissue, contains basic fibrillar proteins (type I collagen, elastin), has low immunogenicity (≤0.1% DNA) and is not cytotoxic with respect to adhesion and proliferation of cell cultures. Allogeneic isolated rat islets of Langerhans were used as an insulin-producing component of CEPC. Freshly isolated islets were identified by dithizone staining (Sigma-Aldrich, USA) and cultured in complete growth medium containing DMEM (1.0 g/L glucose) (PanEco, Russia), 10% fetal calf serum (FBS) (HyClone, USA), Hepes (Thermo Fisher Scientific, USA), 2 mM alanyl-glutamine (PanEco, Russia), 1% antibiotic/antimycotic (Thermo Fisher Scientific, USA) for 24 hours, under standard conditions at 37 °C, in a CO_2 incubator, in a humidified atmosphere containing 5% CO_2.

The viability of islets cultured for 24 hours was determined using intravital fluorescent acridine orange/propidium iodide stain (AO/PI) (PanEco, Russia).

The functional activity of islets was assessed after 24 hours of cultivation using the Rat Insulin ELISA Kit (Thermo Fisher Scientific, USA) to measure insulin levels under the load of hormone secretion stimulant (glucose).

A concentrated suspension of islets was obtained by centrifugation in complete growth medium for 2 minutes at 1200 rpm, then washed from the growth medium in

Hanks' Balanced Salt Solution (HBSS) under the same regime.

For each CEPC sample, 2000 islets obtained from 1–2 rat pancreas were selected, resuspended in 1.0–1.2 mL of Hanks' solution, and mixed with finely dispersed sterile DHP scaffold (10.0 ± 0.1 mg in 100 μL of HBSS) from human pancreas. The resulting CEPC samples were placed into 2-mL syringes with a 23 G needle size.

Intraperitoneal injection of CEPC to rats with experimental type I diabetes

The functional efficacy of CEPC was studied in rats with severe and stable T1D induced by daily intermittent injection of low-dose STZ.

The animals selected for the experiment were categorized into groups:

1) Control group (4 rats, untreated, no administration of islets of Langerhans or CEPC);
2) Experimental group 1 (4 rats, intraperitoneal injection of 2000 allogeneic islets of Langerhans in the form of a suspension);
3) Experimental group 2 (4 rats, intraperitoneal injection of CEPC created from 2000 allogeneic islets of Langerhans and tissue-specific scaffold (DHP scaffold) from decellularized human pancreas).

Follow-up period continued for 10 weeks. Blood glucose levels in the animals were measured on an empty stomach weekly, 12 hours after the last meal.

Histological examination

A morphological study identified some structural disorders in the parenchyma of the pancreas and kidneys. Extracted organs of the experimental animals were fixed in 10% buffered formalin for 24 hours, then dehydrated in alcohols of ascending concentration, kept in a mixture of ethanol and chloroform, pure chloroform, and then embedded in paraffin.

Using a microtome RM2245 (Leica, Germany), 5 μm thick slices were obtained and stained with hematoxylin and eosin and for total collagen using Masson's method. The cellular composition of pancreatic islets in the pancreas of rats from the control and experimental groups was assessed by immunohistochemical staining of the main types of islet cells using antibodies to insulin and glucagon (Abcam, UK) and Rabbit Specific HRP/DAB (ABC) Detection IHC kit visualization system (Abcam, UK).

Detection and assessment of the degree of structural disorders in the kidneys of experimental animals was performed by staining the sections with hematoxylin and eosin.

Statistical analysis

Statistical data processing was done using Microsoft Excel (2016) software. Differences were considered statistically significant if the significance level of p did not exceed the threshold value of 0.05.

RESULTS

Experimental type I diabetes

Rats (n = 13) with fasting blood glucose levels ranging from 20.4 mmol/L to 32.6 mmol/L two weeks after the end of STZ administration were used for experiments to investigate the functional efficacy of CEPC (Table 1). Clinically, these animals showed hypodynamia, a tendency to form wounds and pustules, polyuria, significant

Table 1

Changes in glucose levels and body weight in T1D rats

	Glucose level (mmol/L)			Body weight (g)		
Days after the last STZ dose	1	7	14	1	7	14
Norm (n = 4)	5.5 ± 0.7	5.9 ± 0.3	5.8 ± 0.9	345 ± 15	350 ± 18	365 ± 24
T1D (n = 13)	17.8 ± 3.3	19.1 ± 3.5	26.5 ± 6.1	310 ± 25	295 ± 27	280 ± 23

Note. $p < 0.05$ compared with the values of similar indicators of the norm (intact rats).

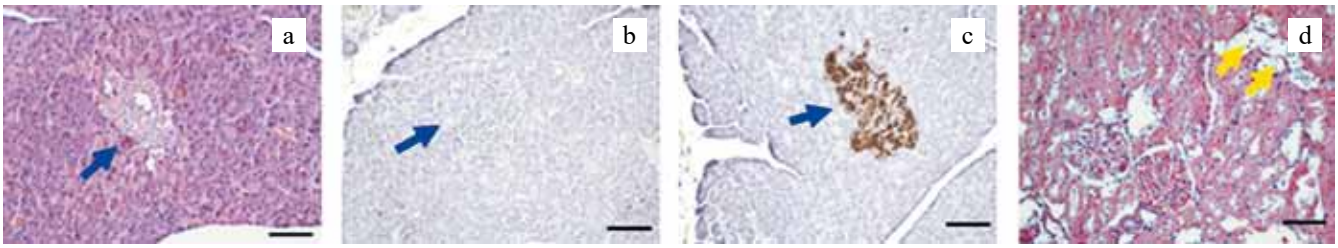

Fig. 1. Pancreas (a–c) and kidney (d) of a rat with experimental T1D; H&E stain (a, d); immunohistochemical staining for insulin (b); immunohistochemical staining for glucagon (c). Blue arrows indicate islets of Langerhans. Yellow arrows indicate tubular epithelial Armanni–Ebstein cells. Scale bar: 100 μm

polydipsia and decreased body weight compared to the intact animals.

To confirm the development of T1D, histologic examination of the pancreas of rats with a blood glucose level of 25.3 mmol/L was performed two weeks after the last STC injection. It was revealed that the exocrine parenchyma was generally preserved; moderate focal lymphoid-cell infiltration was noted only in some lobules. Vacuolated cells (probably beta cells) were detected in few irregularly shaped islets of Langerhans (Fig. 1, a). When stained with antibodies against insulin, a negative reaction was observed, which indicated the death of beta cells (Fig. 1, b). At the same time, glucagon-positive alpha-cells were found not only in the periphery, but also in the central part of the islets and in a much larger number than in healthy rats (Fig. 1, c). Histological examination of rat kidneys with clinical signs of T1D revealed pronounced changes, including the presence of multiple vacuolated tubular epithelial cells (Armanni–Ebstein cells, which are pathognomonic for diabetes) (Fig. 1, d). Foci of inflammatory infiltration (lymphoid cellular with admixture of plasmacytes) were observed. Protein cylinders were occasionally detected in the tubule lumen.

In order to create an experimental model of type 1 diabetes, intermittent injections of STZ were used since this method prevented animal death and spontaneous remission of diabetes while maintaining a stable diabetic state in the animals [16]. The obtained T1D was characterized by stable hyperglycemic indicators (from 20 mmol/L to 33 mmol/L) in the blood of experimental animals and other signs of diabetes: polydipsia, polyuria.

Morphofunctional analysis of isolated rat islets of Langerhans before CEPC creation

Freshly isolated islets of Langerhans of predominantly rounded shape mostly retained the integrity of the macrostructure intact during islet isolation (Fig. 2, a). Pancreatic islets selectively acquired red-orange color when stained with dithizone, while acinar cells remained unstained (Fig. 2, b).

To determine the viability of rat pancreatic islets cultured for 24 hours, staining with vital acridine orange/propidium iodide stain (AO/PI) was performed. Islet viability was found to be higher than 96% (Fig. 2, c).

In the culture medium samples taken after 24 hours of islets culturing, basal insulin level was 178.6 ± 13.3 μIU/mL; after stimulation with "hyperglycemic" glucose

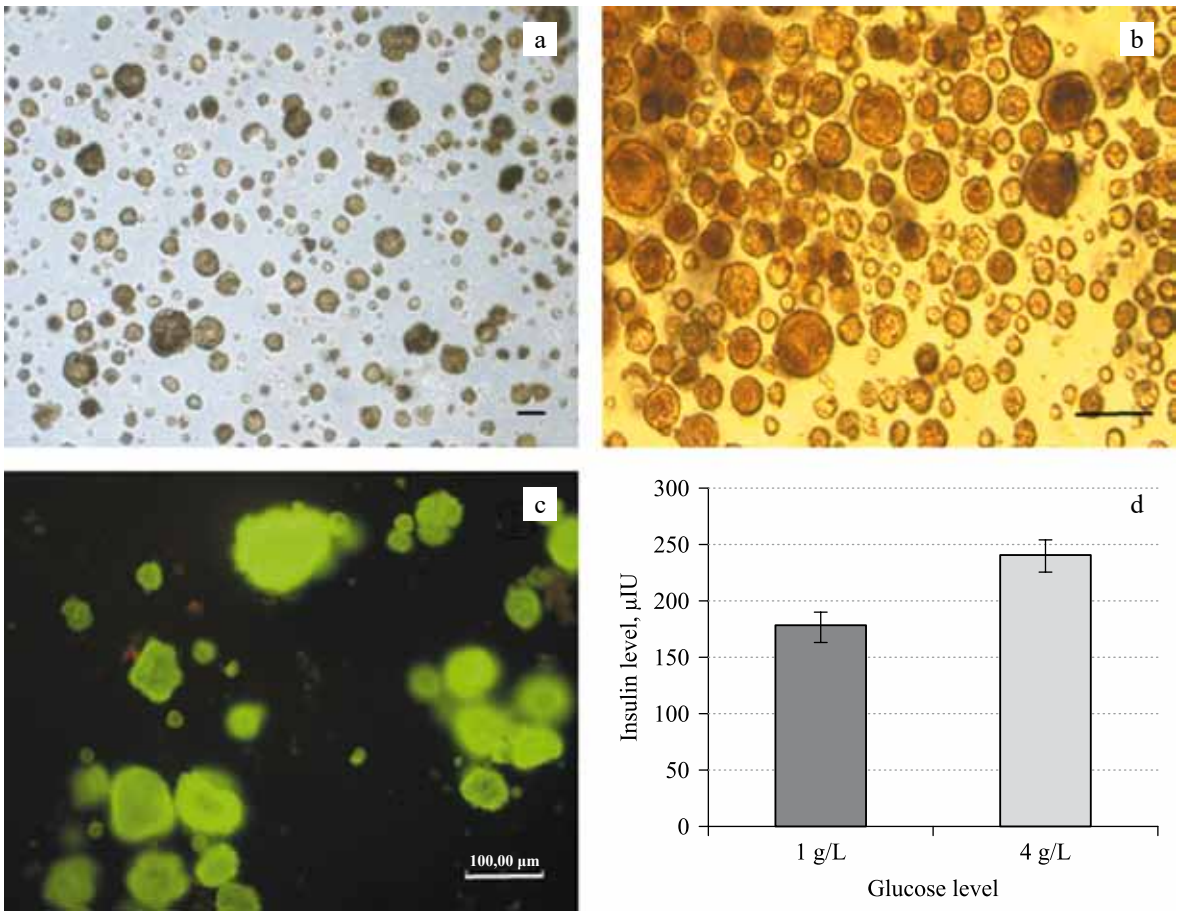

Fig. 2. Isolated islets of Langerhans of a healthy rat. a, phase-contrast microscopy; b, dithizone staining; c, islets cultured for 24 hours, acridine orange and propidium iodide (AO/PI) fluorescent staining; d, functional activity of isolated islets of Langerhans of a healthy rat cultured for 24 hours. Scale bar: 100 μm

level of 4.5 g/L (25 mmol/L), it increased by 35.4% (241.8 ± 14.2 μIU/mL), which confirmed the functional activity of isolated islets (Fig. 2, d).

Thus, it was found that isolated rat islets of Langerhans by their morphofunctional state (level of viability and functional activity) can be used as a cellular insulin-producing component for the creation of CEPC.

Comparative analysis of the functional efficiency of CEPC and islets of Langerhans in rats with experimental type I diabetes

The functional efficacy of CEPC, formed from allogeneic islets of Langerhans and tissue-specific scaffold from decellularized human pancreas, was assessed for 10 weeks in relation to its ability to restore physiological blood glucose levels in rats with STZ-induced T1D.

Control group

All animals in the control group maintained pronounced clinical signs of T1D throughout the follow-up period, and the general condition of the rats worsened. Polydipsia, polyuria, diminished strength, non-healing purulent wounds on tails, further loss of body weight (from 280 ± 23 g to 170 ± 35 g) were noted in the animals. The level of hyperglycemia in the blood in the control group (n = 4) increased during the follow-up period (Table 2). Of the four control rats, two died at 3 and 8 weeks.

In histological samples of the pancreas of rats in control group after withdrawal from the experiment (10 weeks), few irregularly shaped islets of Langerhans were found, with almost complete absence of insulin-positive beta cells and numerous glucagon-positive alpha-cells (Fig. 3, a–c). Rats in the control group had their kidneys examined histologically, and the results showed changes in the organ's morphology, as well as the presence of many Armanni–Ebstein cells and foci of inflammatory infiltration. These findings are indicative of diabetic nephropathy developing on the backdrop of T1D without treatment (Fig. 3, d). In addition, deposits of dense material – protein cylinders – were detected in the lumen of individual tubules.

Experimental group 1 (injection of islets of Langerhans)

In rats from experimental group 1 (n = 4), after intraperitoneal injection of islets of Langerhans, characteristic clinical signs of T1D slowed down within a week, weight gain was noted (from 280 ± 23 g to 305 ± 15 g). Moreover, three days following islets administration, hyperglycemia levels in all recipient rats decreased significantly by 12.5 ± 3.2 mmol/L (Table 3). Thereafter, blood glucose levels in three rats stabilized at a level that was on average 2.5 times lower compared to the level before islet administration. However, after 7 weeks of follow-up, glucose levels in experimental group 1 began to rise. By week 10, it had reached the level above the initial level (before islets administration) in two rats, and had dropped by 7.3 mmol/l below the initial level in one rat (Fig. 4, a). At week 6, the rat with blood glucose level of 27.3 mmol/L died, even though after islet administration, there was a stable decrease in hyperglycemia.

The histological picture of the pancreas of rats from experimental group 1 revealed good preservation of endocrine parenchyma without signs of inflammation and irregularly shaped islets, as in the pancreas of rats from control group, with rare vacuolated cells, probably beta

Table 2

Dynamics of blood glucose level in control group rats without treatment

Day	Blood glucose (mmol/L)			
	Rat 1	Rat 2	Rat 3	Rat 4
0	22.1	20.7	29.5	32.2
4	20.2	22.0	≥33.0	31.5
7	22.7	19.3	30.7	≥33.0
14	27.8	18.8	28.8	24.3
21	25.3	25.5	dead	28.0
28	28.0	26.3	–	≥33.0
35	30.4	28.0	–	≥33.0
42	≥33.0	26.8	–	≥33.0
49	≥33.0	28.4	–	≥33.0
56	dead	26.5	–	≥33.0
63	–	31.2	–	≥33.0
70	–	32.5	–	≥33.0

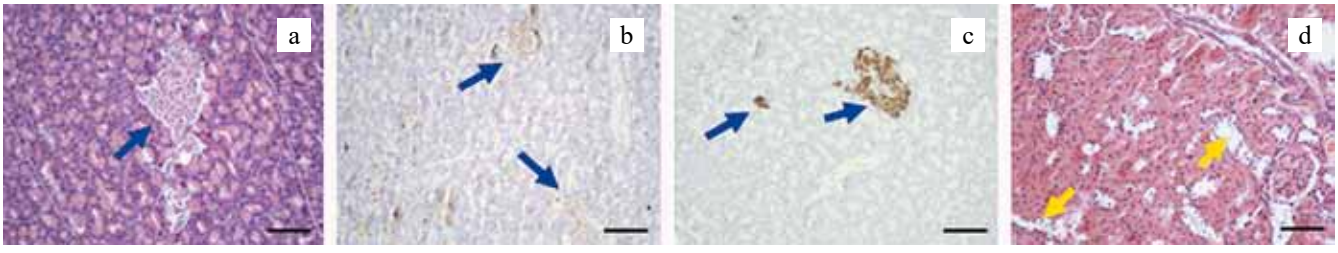

Fig. 3. Pancreas (a–c) and kidney (d) of control group rats with experimental T1D; H&E stain (a, d); immunohistochemical staining for insulin (b); immunohistochemical staining for glucagon (c). Blue arrows indicate islets of Langerhans. Yellow arrows indicate tubular epithelial Armanni–Ebstein cells. Scale bar: 100 μm

cells (Fig. 4, a–c). In two rats (rat 2 and rat 4), immunohistochemical staining revealed no insulin-positive beta cells, while numerous glucagon-positive alpha-cells were present in the islets. In one rat (rat 3), there were single beta cells in the islets (Fig. 4, d). Morphological study of the kidneys of rats from experimental group 1 did not reveal severe degenerative changes in the vascular and tubular apparatus; however, numerous vacuolated cells – Armanni–Ebstein cells – were detected in the tubular epithelium (Fig. 4, e). Flaky material was visualized in the lumen of some tubules.

Table 3

Changes in blood glucose levels in T1D rats of experimental group 1 after injection of islets of Langerhans

Day	Blood glucose (mmol/L)			
	Rat 1	Rat 2	Rat 3	Rat 4
0	26.7	30.7	23.0	32.5
4	11.6	15.3	12.9	23.1
7	13.0	13.5	9.5	18.8
14	11.5	16.0	15.3	10.9
21	15.8	22.3	14.8	12.3
28	23.0	20.9	15.7	14.9
35	27.3	22.6	12.4	14.1
42	dead	18.9	12.1	16.3
49	–	19.1	14.8	15.9
56	–	26.1	23.0	18.7
63	–	25.4	22.3	21.7
70	–	33.0	27.6	25.2

Experimental group 2 (CEPC injection)

Similar to the animals in the experimental group, a slowdown in the clinical manifestations of T1D was seen in rats of experimental group 2 (n = 4) one week following intraperitoneal injection of CEPC based on allogeneic islets of Langerhans with DHP scaffold. T1D signs, including polydipsia and polyuria, virtually vanished in rat 3, and by week 10, the rats gained body weight dramatically from 303 g at the time of CEPC injection to 555 g. In recipient rats 3 and 4, there was a prolonged decrease in blood glucose levels (BGLs) by more than 3-fold compared to baseline, along with individual measurements reaching normoglycemic values of up to 7.5 mmol/L (Table 4). By the end of the experiment (10 weeks of follow-up), BGLs of 9.5 and 7.9 mmol/L, respectively, were recorded in the above rats, which was much lower than the initial average level (25.8 ± 5.1 mmol/L). Rat 1 had no persistent reduction in hyperglycemia: after CEPC injection, blood glucose level ranged from 4.9 to 17.3 mmol/L. At the time of withdrawal from the experiment (70 days), blood glucose in rat 1 was 17.0 mmol/L, not exceeding the baseline value.

In week 4 of follow-up, rat 2 with a glucose level of 5.9 mmol/L died.

Histological examination of the pancreas of rats from experimental group 2 revealed that the exocrine parenchyma was preserved without inflammation signs and with no infiltrates (Fig. 5, a, d). Few vacuolated cells were observed in both round and irregularly shaped is-

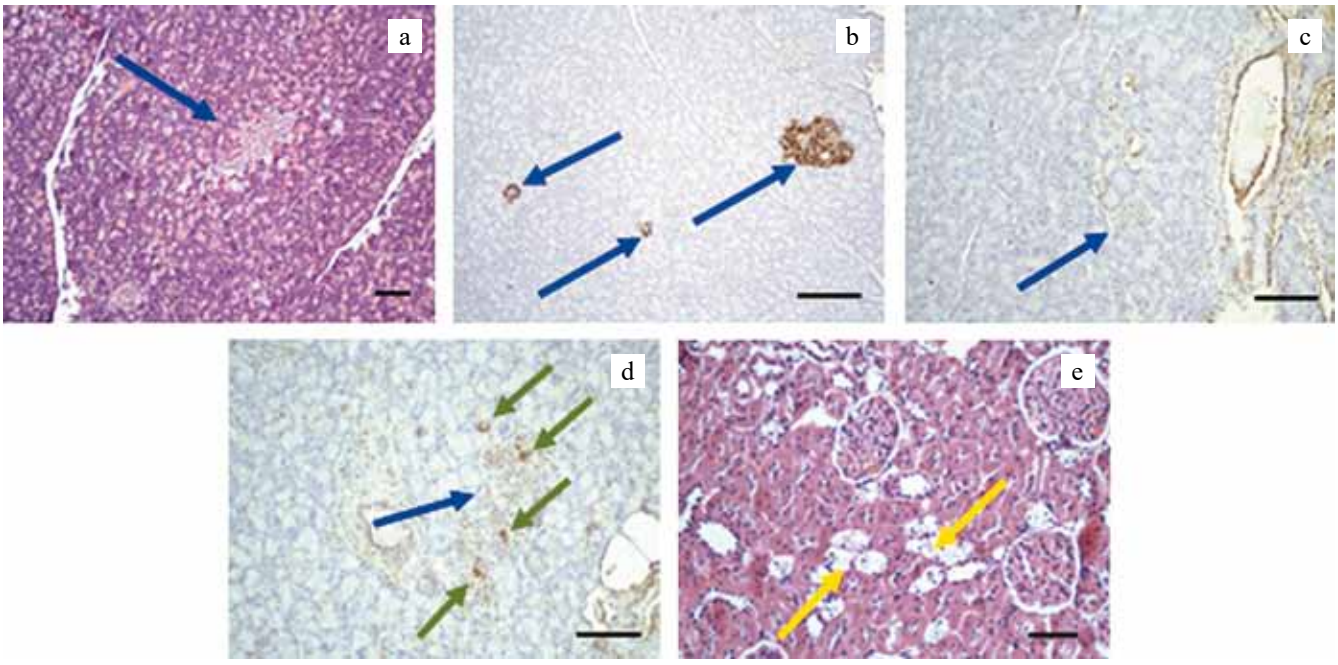

Fig. 4. Pancreas (a–d) and kidney (e) of experimental group 1 rats with T1D after intraperitoneal injection of islets of Langerhans; H&E stain (a, e); immunohistochemical staining for glucagon (b); immunohistochemical staining for insulin (c, d). Blue arrows indicate islets of Langerhans. Yellow arrows indicate tubular epithelial Armanni–Ebstein cells. Scale bar: 100 μm

lets. Immunohistochemical staining for insulin revealed the presence of few beta cells in the pancreatic islets of rats 1 and 4 (Fig. 5, b); in rat 3, the increase in the count of insulin-positive cells turned out to be more significant (Fig. 5, e), while there was lower count of glucagon-positive cells in the islets (Fig. 5, e, f). Experimental data [16] suggest that in addition to its direct antidiabetic effect, CEPC implantation can have a positive effect on the processes of restoring the pool of actively functioning beta cells of the recipientю This has been confirmed by our histological study. Rat kidneys from experimental group 2 showed a different morphological picture in contrast to kidneys from the control group and experimental group 1, showing fewer Armanni–Ebstein cells and no protein cylinders in the tubular lumen (Fig. 5, g).

Fig. 6 shows a comparative diagram of the dynamics of changes in BGLs in animals of the control and experimental groups. The graph of glycemic indicators of the control group is given by the BGLs of one rat, not exceeding the limit value of the glucometer – 33.0 mmol/L, throughout the entire follow-up period. In the control group, hyperglycemia indicators steadily increased throughout the experiment.

After injection of islets of Langerhans in experimental group 1, there was a marked decrease in BGLs from 28.2 ± 4.2 mmol/L to 13.4 ± 2.6 mmol/L, which persisted for 7 weeks, after which it increased to levels close to the initial values (before islets administration).

Table 4

Changes in blood glucose levels in T1D rats of group 2 after CEPC injection

Day	Blood glucose (mmol/L)			
	Rat 1	Rat 2	Rat 3	Rat 4
0	20.4	25.6	24.7	32.6
4	17.9	23.0	5.7	19.5
7	4.9	3.9	10.0	6.5
14	9.0	7.4	3.6	7.9
21	10.8	5.9	6.9	9.2
28	13.2	dead	10.7	10.7
35	17.3	–	13.9	7.2
42	15.6	–	9.6	8.5
49	11.8	–	12.4	10.3
56	12	–	10.6	6.8
63	11.1	–	6.5	8.9
70	17.0	–	9.5	7.9

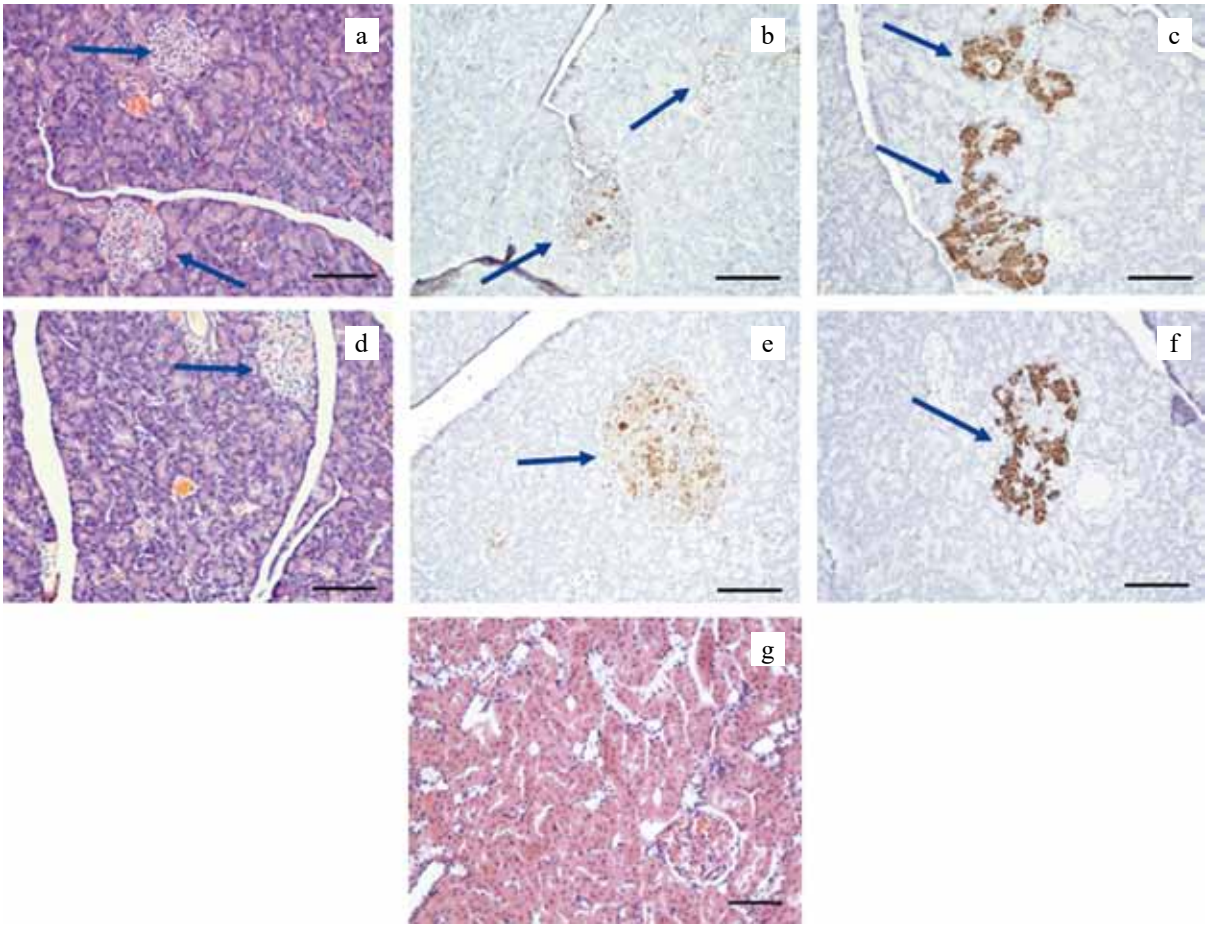

Fig. 5. Pancreas (a–f) and kidney (g) of rats of experimental group 2 with T1D after intraperitoneal injection of CEPC; (a, d, g), H&E; (b, e), immunohistochemical staining for insulin; (c, f), immunohistochemical staining for glucagon. Arrows indicate islets of Langerhans. Scale bar: 100 μm

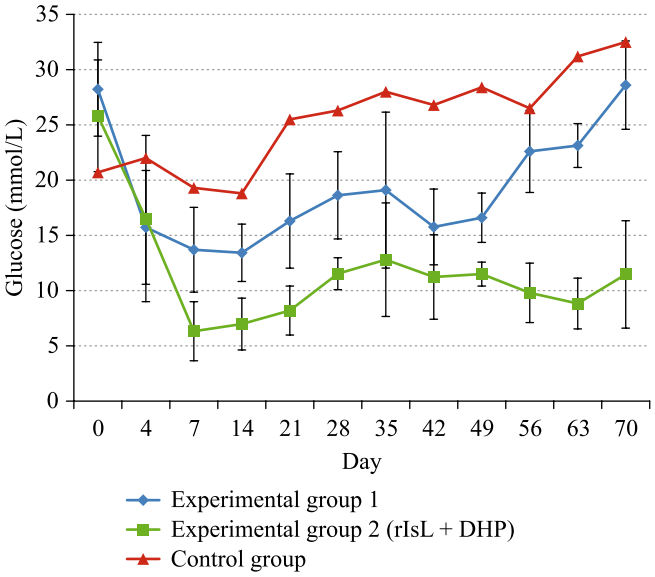

Fig. 6. Changes in blood glucose levels in T1D rats of the control group (without treatment) and experimental groups after intraperitoneal injection of CEPC (islets of Langerhans (rIsL) + decellularized human pancreas (DHP)) or suspension of islets of Langerhans (rIsL). Glycemic indicators of the control group are presented according to blood glucose levels of one rat. Glycemic indicators of experimental group 1 are presented by blood glucose levels of four rats up to 42 days, and then due to the death of one animal, the indicators of three rats were considered. Glycemic indicators of experimental group 2 are presented by blood glucose levels of four rats up to 28 days, and then due to the death of one animal, the indicators of three rats were considered

Experimental group 2 showed a more pronounced decrease in glucose levels from 25.8 ± 5.1 mmol/L to 6.3 ± 2.7 mmol/L compared to experimental group 1. Such concentrations were maintained throughout the follow-up period. The glucose level by week 10 of the experiment was on average 2 times lower than the initial one.

In rats of experimental group 2, after CEPC injection, the maximum decrease in BGLs relative to initial hyperglycemic parameters was by 75.6%; in experimental group 1, it was by 52.5% after administration of islet suspension.

Thus, the studies have shown the *in vivo* functional efficiency of allogeneic islets of Langerhans injected without scaffold and as a part of the human cell-engineered pancreatic construct. There was a more pronounced decrease in blood glucose concentration in recipient rats after administration of experimental CEPC samples compared to the level in recipient rats after administration of islets without scaffold (by 75.6% and 52.5%, respectively).

The obtained results correlate with reports from a preliminary study [17], where, with intraperitoneal CEPC injection, tissue-specific scaffolds provided pancreatic islets with longer survival and effective functioning *in vivo*.

Thus, the important role of tissue-specific scaffold in the creation of a bioartificial pancreas has been demonstrated. The optimal scaffold obtained from decellularized pancreatic tissue for CEPC formation should 1) meet the criteria for effective decellularization, 2) preserve the native structure as much as possible, 3) provide sites necessary for cell adhesion and proliferation, and 4) be evenly populated by insulin-producing cells [6, 14]. Synthetic artificial scaffolds may not meet some of these requirements and, hence, may not positively influence the survival and functioning of islets *in vivo*. The presence of native proteins (various types of collagen, elastin, fibronectin and laminin) in the decellularized pancreatic scaffold, as well as cell adhesion factors, allows to create conditions for prolonged viability of islet cells, thus maintaining the critical mass of islets necessary for transplantation to T1D patients [18].

CONCLUSION

The study found that intraperitoneal administration of CEPC samples in experimental T1D rats resulted in a significant, sustained reduction in fasting blood glucose levels that persisted for 10 weeks. Thus, administration of CEPC revealed a more pronounced antidiabetic effect in T1D rats compared to administration of a suspension of islets of Langerhans. This suggests that in order to improve the functional efficiency of islets, a tissue-specific scaffold could be used to create a bioartificial pancreas. This work lays the groundwork for research on the development of human endocrine cell-engineered pancreatic constructs based on tissue-specific scaffolds made from decellularized human pancreatic tissue and islets of Langerhans of deceased donors in order to partially or completely replace the lost endocrine function of the pancreas in patients with severe T1D.

The authors declare no conflict of interest.

REFERENCES

1. *Shapiro AM, Pokrywczynska AM, Ricordi C.* Clinical pancreatic islet transplantation. *Nat Rev Endocrinol.* 2017; 13 (5): 268–277. doi: 10.1038/nrendo.2016.178.
2. *Cayabyab F, Nih LR, Yoshihara E.* Advances in Pancreatic Islet Transplantation Sites for the Treatment of Diabetes. *Front Endocrinol (Lausanne).* 2021; 12: 732431. doi: 10.3389/fendo.2021.732431.
3. *Reid L, Faye Baxter F, Forbes S.* Effects of islet transplantation on microvascular and macrovascular complications in type 1 diabetes. *Diabet Med.* 2021; 38 (7): e14570. doi: 10.1111/dme.14570.
4. *Eguchi N, Damyar K, Alexander M, Dafoe D, Lakey JRT, Ichii H.* Anti-Oxidative Therapy in Islet Cell Transplantation. *Antioxidants (Basel).* 2022; 11 (6): 1038. doi: 10.3390/antiox11061038.

5. *Amer LD, Mahoney MJ, Bryant SJ.* Tissue engineering approaches to cell-based type 1 diabetes therapy. *Tissue Eng Part B Rev*. 2014; 20 (5): 455–467. doi: 10.1089/ten.TEB.2013.0462.
6. *Mirmalek-Sani S-H, Orlando G, McQuilling JP, Pareta R, Mack DL, Salvatori M et al.* Porcine pancreas extracellular matrix as a platform for endocrine pancreas bioengineering. *Biomaterials.* 2013; 34 (22): 5488–5495. doi: 10.1016/j.biomaterials.2013.03.054.
7. *Abualhassan N, Sapozhnikov L, Pawlick RL, Kahana M, Pepper AR, Bruni A et al.* Lung-derived microscaffolds facilitate diabetes reversal after mouse and human intraperitoneal islet transplantation. *PLoS One.* 2016; 11 (5): e0156053. doi: 10.1371/journal.pone.0156053.
8. *Damodaran G, Vermette P.* Decellularized pancreas as a native extracellular matrix scaffold for pancreatic islet seeding and culture. *J Tissue Eng Regen Med.* 2018; 12 (5): 1230–1237; doi: 10.1002/term.2655.
9. *Lim LY, Ding SSL, Muthukumaran P, Teoh SH, Koh Y, Teo AKK.* Tissue engineering of decellularized pancreas scaffolds for regenerative medicine in diabetes. *Acta Biomater.* 2023; 157: 49–66. doi: 10.1016/j.actbio.2022.11.032.
10. *Wu D, Wan J, Huang Y, Guo Y, Xu T, Zhu M et al.* 3d Culture of MIN-6 Cells on Decellularized Pancreatic Scaffold: *In Vitro* and *In Vivo* Study. *Biomed Res Int*. 2015; 2015: 432645. doi: 10.1155/2015/432645.
11. *Goh S-K, Bertera S, Olsen P, Candiello JE, Halfter W, Uechi G et al.* Perfusion-Decellularized Pancreas As A Natural 3d Scaffold For Pancreatic Tissue And Whole Organ Engineering. *Biomaterials*. 2013; 34 (28): 6760–6772. doi: 10.1016/J.Biomaterials.2013.05.066.
12. *Sabetkish S, Kajbafzadeh AM.* The Most Ideal Pancreas Extracellular Matrix as a Platform for Pancreas Bioengineering: Decellularization/Recellularization Protocols. *Adv Exp Med Biol.* 2021; 1345: 61–70. doi: 10.1007/978-3-030-82735-9_6.
13. Biomimetics of Extracellular Matrices for Cell and Tissue Engineered Medical Products / Eds. Victor I. Sevastianov and Yulia B. Basok. – Newcastle upon Tyne, UK: Cambridge Scholars Publishing, 2023; 339.
14. *Sevastianov VI, Ponomareva AS, Baranova NV, Kirsanova LA, Basok YuB, Nemets EA et al.* Decellularization of Human Pancreatic Fragments with Pronounced Signs of Structural Changes. *Int J Mol Sci.* 2023; 24 (1): 119. doi: 10.3390/ijms24010119.28.
15. *Napierala H, Hillebrandt K-H, Haep N, Tang P, Tintemann M, Gassner J et al*. Engineering an endocrine neopancreas by repopulation of a decellularized rat pancreas with islets of Langerhans. *Sci Rep*. 2017 Feb 2; 7: 41777. doi: 10.1038/srep41777.
16. *Skaletskaya GN, Skaletskiy NN, Kirsanova LA, Bubentsova GN, Volkova EA, Sevastyanov VI.* Experimental implantation of tissue-engineering pancreatic construct. *Russian Journal of Transplantology and Artificial Organs*. 2019; 21 (2): 104–111. (In Russ.). doi: 10.15825/1995-1191-2019-2-104-111.
17. *Ponomareva AS, Baranova NV, Nikolskaya AO, Kirsanova LA, Onishchenko NA, Gonikova ZZ et al.* Intraperitoneal injection of cell-engineered pancreas in rats with experimental type I diabetes (preliminary results). *Russian Journal of Transplantology and Artificial Organs*. 2023; 25 (2): 107–117. doi: 10.15825/1995-1191-2023-2-107-117.
18. *Smink AM, de Vos P.* Therapeutic strategies for modulating the extracellular matrix to improve pancreatic islet function and survival after transplantation. *Curr Diab Rep*. 2018; 18 (7): 39. doi: 10.1007/s11892-018-1014-4.

The article was submitted to the journal on 04.03.2024

DOI: 10.15825/1995-1191-2024-2-105-118

HISTOLOGIC AND GENETIC FEATURES OF REMODELING OF TISSUE-ENGINEERED SMALL-DIAMETER VASCULAR GRAFTS: OUTCOMES OF SIX-MONTH IMPLANTATION IN A SHEEP MODEL

E.A. Senokosova, E.O. Krivkina, E.A. Velikanova, A.V. Sinitskaya, A.V. Mironov, A.R. Shabaev, M.Yu. Khanova, E.A. Torgunakova, L.V. Antonova

Research Institute for Complex Issues of Cardiovascular Diseases, Kemerovo, Russian Federation

Surface modification of polymeric scaffolds with drugs to avoid thrombus formation and infection is a promising area in tissue engineering, which also makes it possible to accelerate the remodeling of such scaffolds and improve long-term patency. **Objective:** to study the histologic and genetic features of remodeling of tissue-engineered small-diameter vascular grafts (SDVGs) with antithrombogenic drug-coated and reinforced external scaffolds, implanted into a sheep carotid artery. **Materials and methods**. Poly(ε-caprolactone) (PCL) matrices, ∅4 mm in diameter, were fabricated via electrospinning, followed by creation of a reinforcing spiral PCL scaffold on their outer surface by extrusion. To prevent thrombus formation and infection, the fabricated grafts were modified with iloprost and cationic amphiphile by complexation through polyvinylpyrrolidone (PVP). The work was carried out to evaluate, by infrared spectroscopy, the formation of PVP-based coating, to study the physical and mechanical properties of the grafts in longitudinal and transverse directions, and to implant the vascular grafts (VGs) into a sheep carotid artery. To assess and control the patency of the implanted grafts, Doppler ultrasound was performed at days 1 and 5, then at 1, 3 and 6 months. The explanted samples were studied via histological and immunofluorescent analyses; gene expression profile was evaluated. **Results.** Ultrasound on days 1 and 5 after implantation showed the patency of vascular grafts to be 100%. At 1 month, the patency decreased to 83.3%; patency was 50% by the end of the implantation period (6 months), without aneurysm formation and detachment of the reinforcing scaffold. Histological and immunofluorescence studies of patent grafts showed the formation of a newly formed three-layer vascular tissue structure on their basis, without signs of inflammation and calcification. However, despite the structural similarity between the newly formed vascular tissue and the native tissue of a sheep carotid artery, analysis of the gene expression profile revealed some differences in terms of genetic profile: *CNN* and *SNA12* expression levels in the neotissue decreased, and those of *CTSB*, *TNFa*, and *TGFb* increased. **Conclusion.** Modified polymeric vascular scaffolds showed good remodeling of the prosthetic wall, without aneurysm formation. The identified genetic differences between newly formed tissue and native tissue are logical in view of formation on the basis of the artificial polymeric scaffold. Further research on reinforced polymeric scaffolds will be aimed at improving the inner surface in order to improve their thromboresistance.

Keywords: vascular grafts; antithrombogenic treatment; antimicrobial treatment; iloprost; cationic amphiphiles.

INTRODUCTION

The increasing cases of cardiovascular diseases every year is the most common cause of death globally [1, 2]. Autologous grafts are the preferred material for restoring blood flow in the affected vascular area. However, accessibility of patients' arteries and veins is limited due to vascular quality associated with comorbidities (high blood pressure, diabetes, and others) [1].

An alternative to autografts are clinically approved synthetic vascular grafts (VGs) made from polytetrafluoroethylene (PTFE) and polyethylene terephthalate (PET, Dacron). They demonstrate high efficiency in replacing large vessels with an internal diameter of more than 6 mm. However, when replacing a vessel segment with a diameter of less than 5 mm, these prostheses become ineffective and have a propensity to cause thrombus formation, stenosis, occlusion of the vascular lumen and infection [2, 3]. Based on various tactics for handling biocompatible and biodegradable polymers, tissue engineering (TE) is a pertinent method for producing small-diameter vascular grafts (SDVGs). Artificial tissue-like matrices and tissues with the required structural and mechanical qualities can be designed using a variety of TE methods [4–6]. A vascular prosthesis made of such material can undergo synchronous biodegradation and remodeling of its wall, allowing body cells to participate in the development of a three-layer native blood vessel structure [7–9]. However, this is a lengthy process and is accompanied by such risks as thrombosis, aneurysm formation and microbial contamination [10–12].

Corresponding author: Evgeniya Krivkina. Address: 6, Sosnovy Bul'var, Kemerovo, 650002, Russian Federation. Phone: (908) 946-66-39. E-mail: leonora92@mail.ru

Highly porous tissue-engineered constructs in contact with blood can provoke thrombus formation. Therefore, when developing products for cardiovascular surgery, these features should be considered. Surface modification of prostheses with antithrombogenic drugs can prevent thrombosis of the lumen of implanted vascular prostheses both in the early postoperative period and in the process of long-term bioresorption of the main scaffold of the prosthesis [11, 13].

Although various approaches to modifying VGs to prevent their infection and thrombus formation have been developed over the years, none of them has been able to demonstrate any significant benefits [14–16].

Apart from the above challenges, if biodegradable VGs are used as prostheses, there should be a clear understanding of the level of synchronization of remodeling with biodegradation processes. There are already works that have analyzed in detail the outcomes of long-term implantation of biodegradable VGs using a large animal model [6, 8, 12, 17]. It has been demonstrated that tissue-engineered vascular prostheses are replaced by newly formed vascular tissue, becoming similar to autologous vessels. This shows the ability of biodegradable prostheses to adaptive growth. Preclinical tests for small-diameter biodegradable VGs on a large laboratory animal model revealed that, despite all encouraging developments and successful testing on a small animal model, the main outcome was aneurysm formation due to accelerated bioresorption of the main scaffold of the vascular prosthesis [6, 17].

Therefore, creation of an external reinforced scaffold would prevent aneurysm formation and other deformational changes in the prosthetic walls during its long-term functioning in the vascular bed. Furthermore, the use of drugs, for surface modification, that can prevent both thrombosis and infection will make highly porous tissue-engineered constructs developed for cardiovascular surgery more effective over the long run.

The **aim** of this study was to investigate the histologic and genetic features of remodeling of tissue-engineered SDVGs that were implanted into a sheep carotid artery and included antithrombogenic and antimicrobial drug-coated and reinforced external scaffolds.

MATERIALS AND METHODS

Fabrication of biodegradable vascular prostheses

Small (4 mm) diameter VGs were fabricated by electrospinning from 12% PCL (Sigma-Aldrich, USA) in trichloromethane. Electrospinning was performed on a Nanon-01A device (MECC, Japan) with the following parameters: voltage at the end of the needle, 22 kV; polymer solution feed rate, 0.5 ml/h; manifold rotation speed, 200 rpm; distance from the needle to the winding manifold, 150 mm; 22 G needle.

Creation of an external reinforcement layer of vascular prostheses

To prevent aneurysm formation on the outer surface of VGs, a reinforcement spiral scaffold was created, which was fabricated from PCL of molecular weight 90,000 Da (Sigma Aldrich, USA) using an original machine consisting of a carriage with an extruder and a rotating shaft, in the following mode: shaft rotation speed, 1 rev/s; carriage speed, 1 mm/s; plastic feed rate, 0.5 mm/s (extruder nozzle 0.5 mm); fiber feed temperature, 160 °C [13].

Formation of drug coating on the surface of vascular prostheses

The VG surface was modified with drugs to prevent thrombosis and infection. In the first step, a hydrogel coating was formed from 10% PVP (PanReac AppliChem, Spain) in 25% ethanol. Afterwards, the prostheses in glass tubes filled with argon were irradiated with ionizing radiation with a total absorbed dose of 15 kGy using pulsed linear gas pedal ILU-10 with a beam of 5 MeV 50 kW (manufacturer – Budker Institute of Nuclear Physics, Russia). This procedure grafted PVP onto the PCL surface through radiation-chemical crosslinking of polymers. Radical centers appear on the PCL surface and in the structure of the applied PVP layer because of ionizing effect, which leads to three-dimensional crosslinking of PVP and its binding to the surface of the polymer graft [18]. Alongside with PVP grafting, the tubular prosthetic scaffolds were sterilized.

At the second stage, using the method of complexation with PVP, antiplatelet agent iloprost (Ilo, Berlimed Sa, Spain) and cationic amphiphile 1,5-bis-(4-tetradecyl-1,4-diazoniabicyclo [2.2.2]octan-1-yl) pentane tetrabromide (A, Nanotech-s LLC, Novosibirsk), which has antimicrobial and antiviral properties, were introduced [5].

The quality of grafting was evaluated earlier by infrared spectroscopy, analyzing the attenuated total reflectance (ATR) spectra of the inner surface of modified prostheses on a Bruker Vertex 80v instrument (Germany) with an ATR attachment (Germany) in the spectral region of 4000–5000 cm^{-1} [19]. Studies have been conducted previously to confirm the formation of PVP coating on prosthetic surfaces and to assess the kinetics of drug release from compounds connected by complexation to the PVP layer [19].

Evaluation of physical and mechanical properties of biodegradable vascular prostheses

The physical and mechanical properties of PCL/PVP/Ilo/A vascular grafts with an external reinforcing scaffold were evaluated under uniaxial tensile conditions in accordance with GOST 270-75. Similar grafts without a reinforcing scaffold were used as a comparison group. The tests were performed on a Z-series universal testing

machine (Zwick/Roell, Germany), using a load cell with 50 N rated load with a permissible error limit of ±1%; a traverse lifting speed of 50 mm/min was used during testing, at an ambient temperature of 37 °C, maintained by a thermal chamber. The ultimate tensile strength of the material was evaluated as the maximum uniaxial tensile stress (MPa) before failure. The stress-strain properties of the material were evaluated using Young's modulus (MPa). The obtained data were exported as the ratio of relative elongation (mm) to stress (MPa) undergone by the sample.

Implantation of biodegradable vascular prostheses into a sheep carotid artery

The study was approved on June 10, 2020 by the local ethics committee of the Research Institute for Complex Issues of Cardiovascular Diseases via minutes No. 12. The handling of animals complied with the requirements of order No. 1179 of the USSR Ministry of Health dated October 10, 1983, order No. 267 of the Russian Ministry of Health dated June 19, 2003, "Rules for carrying out works using experimental animals", the principles of the European Convention for the Protection of Vertebrate Animals used for Experimental and other Scientific Purposes (Strasbourg, 1986), the World Medical Association Declaration of Helsinki on humane treatment of animals (1996) and the Guide for the Care and Use of Laboratory Animals (1996).

PCL/PVP/Ilo/A vascular grafts (n = 12) with an external reinforcing scaffold were implanted into the carotid artery of Edilbay sheep (also known as Edilbaev sheep) using the "end-to-end" method according to the '1 animal – 1 prosthesis' scheme. The diameter and length of the prostheses were 4 mm and 40 mm, respectively. Implantation period was 6 months. Implantation of grafts and anesthetic therapy were carried out according to the scheme given below.

Large laboratory animals were premedicated with xylazine (Xylanite) 0.05–0.25 ml per 10 kg of animal weight and were intramuscularly injected with 1 mg of atropine. Injection anesthesia was performed with 5–7 mg propofol per 1 kg of animal weight, for 90 seconds, then atracurium besylate (Ridelat) was injected intravenously at a dosage of 0.5–0.6 mg per 1 kg of animal weight. Tracheal intubation was performed with a 9.0-diameter endotracheal tube. In the process of manipulations on implantation of VGs into the sheep carotid artery, anesthesia was maintained on sevoran 2–4 vol% and ridelat by continuous infusion at a rate of 0.3–0.6 mg/kg/h. Alongside with that, the following vital signs of the animal were monitored: blood pressure (BP), heart rate (HR), and blood oxygen level (SpO_2). The following parameters were recorded during artificial ventilation (ALV): respiratory rate (RR), 12–15/min; positive end-expiratory pressure (PEEP), 7–9 mbar; respiratory volume (RV), 6–8 ml/kg; fraction of inspired oxygen (FiO_2); 40–60%.

To access the sheep carotid artery, intravenous systemic heparinization was performed – 5000 units, with carotid artery clamping. Then a 40 mm longitudinal incision of the carotid artery was made. The VGs were immediately implanted by separate knotted sutures using Prolene 6/0 thread (Ethicon, USA). After the clamps were removed from the carotid artery, the standard air embolism prophylaxis protocol was followed with subsequent initiation of blood flow and suturing of the wound with Vicril 2.0 thread (Ethicon, USA). At the conclusion of the operation, the suture was treated with BF-6 glue, subcutaneous injection of enoxaparin sodium at a concentration of 4000 anti-Xa IU/0.4 ml was performed and the animal was extubated.

To assess the patency of the implanted prostheses, Doppler ultrasound was performed using an M 7 Premium apparatus (Mindray, China) on the following dates: day 1, day 5, and at 1, 3 and 6 months.

Histological examination

The explanted VG samples were fixed in 10% buffered formalin (BioVitrum, Russia) for 24 hours, then dehydrated in 6 portions of IsoPrep (BioVitrum, Russia) and impregnated with paraffin (3 portions) at 56 °C for 60 minutes in each portion. The impregnated samples were embedded in refractory paraffin HISTOMICS (BioVitrum, Russia). From the obtained samples, 8 μm thick slices were made using an HM 325 microtome (Thermo Scientific, USA). Then they were dried in a thermostat overnight at 37 °C, then dewaxed in 3 o-xylene portions for 1–2 minutes each and dehydrated in 3 portions of 96% alcohol for 1–2 minutes each. The dewaxed slices were then stained with hematoxylin-eosin, van Gieson, and alizarin red S in accordance with previously established staining protocols [19]. The resulting preparations of vascular graft slices were examined using light and fluorescence microscopy on an AXIO Imager A1 microscope (Carl Zeiss, Germany) with ×50 objective lens magnification.

Immunofluorescence test

Explanted VGs were frozen at –140 °C for immunofluorescence staining. Next, frozen samples were fixed in Tissue-Tek cryo-medium (Sakura, Japan) and 8 μm thick slices were made on a CryoStar NX50 cryostat (Thermo Scientific, USA). Then indirect fluorescence staining of the slices was performed using specific antibodies to CD31, von Willebrand factor (vWF), alpha-smooth muscle actin (α-SMA), collagen type III, IV (Abcam, England). Cell nuclei were contrasted with DAPI (Sigma, USA). Control samples were prepared similarly to experimental samples, but 1% bovine serum albumin was used instead of primary antibodies. The preparations were encapsulated in ProLong mounting medium (Life Technologies, USA) under a coverslip and analyzed using a laser scanning microscope LSM 700 (Zeiss, Germany).

Determination of mRNA level

To obtain endothelial lysate from explanted sections of native arteries and patent VGs, the inner endothelial layer was washed with lysing reagent TRIzol (Invitrogen, USA). Samples were placed in TRIzol reagent followed by homogenization (FastPrep-24 Instrument and Lysing Matrix S, MP Biomedicals, USA). The quality and quantity of isolated RNA was determined on a Qubit 4 instrument (Invitrogen, USA) by measuring the RNA Integrity and Quality (RIQ) index using the Qubit RNA IQ Assay Kit (Invitrogen, USA). Based on the isolated RNA, cDNA was synthesized using High-Capacity cDNA Reverse Transcription Kit (Thermo Fisher Scientific, USA). Gene expression was determined by quantitative PCR (qPCR) using BioMaster UDG HS-qPCR Lo-ROX SYBR (2×) master mix (MHR033-2040, Biolabmix, Russia) and primers synthesized by Eurogen on a CFX96 amplifier (BioRad, USA). Characteristics of the genes included in the study are presented in Table 1. The results of qPCR were normalized using three reference genes ACTB, GAPDH, B2M according to available guidelines. Expression of the studied genes was calcula-

Table 1

Characteristics of primers

Gene	Forward primer	Reverse primer
IL1B	5’-TGCTGAAGGCTCTCCACCTC-3’	5’-ACCCAAGGCCACAGGAATCTT-3’
IL6	5’-TGTCATGGAGTTGCAGAGCAGT-3’	5’-CCAGCATGTCAGTGTGTGTGG-3’
IL10	5’-ATGCCACAGGCTGAGAACCA-3’	5’-TCGCAGGGCAGAAAACGATG-3’
IL12A	5’-GCAGAAGGCCAGACAAACCC-3’	5’-TGGAAGCCAGGCAACTCTCA-3’
IL12B	5’-AGAGCCTGCCCATTGAGGTC-3’	5’-GGTTCTTGGGTGGGTCTGGT-3’
CXCR4	5’-CTGGAGAGCAAGCGGTTACCA-3’	5’-ACAGTGGGCAGGAAGATCCG-3’
CXCL8	5’-CTTCCAAGCTGGCTGTTGCTC-3’	5’-ATTTGGGGTGGAAAGGTGTGG-3’
IFNG	5’-TGAACGGCAGCTCTGAGAAAC-3’	5’-TGGCGACAGGTCATTCATCA-3’
TNF	5’-CTTCTGCCTGCTGCACTTCG-3’	5’-TGGCTACAACGTGGGCTACC-3’
ICAM1	5’-GTCACGGGGAACAGATTGTAGC-3’	5’-TGAGTTCTTCACCCACAGGCT-3’
NOS3	5’-CTTCCGTGGTTGGGCAAAGG-3’	5’-CGTTTCCAGCTCCGTTTGGG-3’
FGF2	5’-AGAGCGACCCTCACATCAAACT-3’	5’-TCAGTGCCACATACCAACTGGA-3’
VEGFA	5’-GCTTCTGCCGTCCCATTGAG-3’	5’-ATGTGCTGGCTTTGGTGAGG-3’
TGFB1	5’-TGAGCCAGAGGCGGACTACT-3’	5’-ACACAGGTTCAGGCACTGCT-3’
KDR	5’-ACAGAACCAAGTTAGCCCCATC-3’	5’-TCGCTGGAGTACACAGTGGTG-3’
MMP2	5’-ACCCCGCTACGGTTTTCTCG-3’	5’-ATGAGCCAGGAGCCCGTCTT-3’
NR2F2	5’-GCAAGCGGTTTGGGACCTT-3’	5’-GGACAGGTAGGAGTGGCAGTTG-3’
SNAI2	5’-ACCCTGGTTACTGCAAGGACA-3’	5’-GAGCCCTCAGATTGGACCTG-3’
YAP1	5’-TGCTTCGGCAGGAATTAGCTCT-3’	5’-GCTCATGCTCAGTCCGCTGT-3’
CXCL1	5’-AACATGCAGAGCGTGAAGGTG-3’	5’-CGGGGTTGAGACACACTTCCT-3’
CD14	5’-AATCAAGGCTCTGCGCGTTC-3’	5’-CGTTGGGCCAGTTACCTCCA-3’
CD40LD	5’-ACTGAGAGCTGCAAACACCCA-3’	5’-AAACACCGAAGCACCCTGTT-3’
CNN	5’-CCAACCACACGCAAGTGCAG-3’	5’-TCCTGCTTCTCCGCGTATTTCA-3’
CTSB	5’-AGTGTGGGGACGGCTGTAAC-3’	5’-AGGGAGGGATGGAGTACGGT-3’
CXCL1	5’-AACATGCAGAGCGTGAAGGTG-3’	5’-CGGGGTTGAGACACACTTCCT-3’
CXCL10	5’-AGTACCTTCAGTTGCAGCACCA-3’	5’-TGGGCAGGATTGACTTGCAG-3’
EDN1	5’-GCGACAGTCCACAGGAAGAGA-3’	5’-GGTTGTCCCAGGCTTTCTCC-3’
EDNRA	5’-AGGAACGGCAGCCTGAGAAT-3’	5’-AGGGAACCAGCACAGAGCAA-3’
IL1A	5’-TGACCTGGAAGCCATTGCCA-3’	5’-TGAGGGCGTCGTTCAGGATG-3’
IL4	5’-GGCGTATCTACAGGAGCCACA-3’	5’-ACTCGTCTTGGCTTCATTCACA-3’
IL18	5’-AGGAAGCTATTGAGCACAGGCAT-3’	5’-CTGATTCCAGGTCTTCGCCAT-3’
KLF4	5’-AGGACGGCCACTCACACTTG-3’	5’-ACTTCCACCCACAGCCATCC-3’
MIF	5’-TGCCGATGTTCGTGGTGAAC-3’	5’-GGTCATGAGCTGGTCTGGGA-3’
SELE	5’-CACTGGACCCCAGCACTTACA-3’	5’-GCTGATGGCTGCACAGGTTAC-3’
SELP	5’-TTCCACTGCGCTGAAGGGTA-3’	5’-TGGACTGGTGCTGGAATGCT-3’
PAI	5’-GCAGTGGCAGCAGGAACAAA-3’	5’-TGGTGCTGGTAGGAGGCAGA-3’
SMAD4	5’-TCTGGAGGAGATCGCTTTTGCT-3’	5’-TTCCAACTGCACACCTTTGCC-3’
B2M	5’-CCTTCTGTCCCACGCTGAGT-3’	5’-TGGTGCTGCTTAGAGGTCTCG-3’
ACTB	5’-AGCAAGAGAGGCATCCTGACC-3’	5’-GGCAGGGGTGTTGAAGGTCT-3’
GAPDH	5’-TGGTGAAGGTCGGAGTGAACG-3’	5’-AGGGGTCATTGATGGCAACG-3’

ted using the $2^{-\Delta\Delta Ct}$ method and expressed as a multiple change relative to native carotid arteries.

RESULTS

Physical and mechanical properties of prostheses

A comparative evaluation of physical and mechanical properties of the PCL/PVP/Ilo/A vascular grafts was carried out before and after formation of an outer reinforcing layer in longitudinal and transverse directions. Indices obtained in the longitudinal direction were also compared with similar indices of the sheep carotid artery. It has been proved that the formation of a reinforcing layer in the form of a polycaprolactone spiral on the outer surface of PCL/PVP/Ilo/A grafts helped to increase the strength of VGs in longitudinal and transverse directions, but at the same time the stiffness of grafts in transverse direction increased 2 times, which is an undesirable moment for such products (Table 2). Nevertheless, the critical difference between polymeric VGs and the parameters of the sheep carotid artery was only in Young's modulus, which in PCL/PVP/Iloo/A vascular grafts with and without a reinforcing external spiral exceeded the Young's modulus values of the sheep carotid artery (in the longitudinal direction) by 13.3 and 17.4 times, respectively, $p < 0.05$.

In our previous studies, it was shown that in contrast to unmodified PCL-based VGs, the spectrum of modified PVP-based grafts contained a band at 1654 cm^{-1} corresponding to the $–CONH_2$ group of the pyrrolidine ring, which confirms PVP grafting onto the surface of vascular prosthesis [19].

The kinetics of drug release combined with complexation with grafted PVP provided indirect proof of the stability of PVP grafted to the surface upon its interaction with the aqueous phase. In particular, iloprost has been shown to be able to be released into phosphate-buffered saline within three months. Cationic amphiphile in the form of phosphate salt of molecular ion C41H84Br3N4+ was also co-preserved on the surface of prostheses incubated for 3 months in phosphate-buffered saline [19]. At the same time, cationic amphiphile was determined unchanged on the surface of prostheses stored for 6 months at –20 °C [19].

Results of implantation of PCL/PVP/Ilo/A prostheses

The original protocol of layer-by-layer fusion method used to form the PCL external reinforcement scaffold prevented the vascular graft's visual and surgical properties from deteriorating. As shown in Fig. 1, a, the surrounding polymer fiber did not deform the product wall and did not peel off from it, allowing the outermost reinforcing threads to be captured in a continuous microsurgical suture during prosthesis implantation into the sheep carotid artery using the end-to-end method. This ensured the robustness of the "prosthesis + artery" complex and prevented the reinforcing scaffold from peeling off the base of the product (Fig. 1, b).

Ultrasound results

According to ultrasound results, 100% patency was noted on days 1 and 5 after implantation of PCL/PVP/Ilo/A grafts. Blood flow velocity during this period ranged from 120.35 cm/s to 153.43 cm/s. At 1 month after implantation, patency was 83.3%, but by the third month, it decreased to 50.0% with this figure remaining after 6 months of implantation, until the 6-month follow-up deadline. Ultrasound did not reveal any aneurysm formation and stenosis in the prosthetic walls, neither did it detect any detachment of the external reinforcing scaffold (Fig. 2).

Results of the study of explanted vascular prostheses

Upon examining the implanted prosthesis site after 6 months of the experiment, it was observed that each of them had developed a moderately vascularized connective tissue capsule that clearly showed an intact exterior PCL scaffold. There were no stenoses, aneurysms, or any

Table 2

Mechanical properties of PCL/PVP/Ilo/A tubular polymeric scaffolds before and after creation of an outer reinforcing layer (longitudinal and transverse direction)

	n	Stress (MPa)	Relative elongation (%)	Young's modulus (MPa)
		Longitudinal direction (Me (25–75%))		
PCL/PVP/Ilo/A	6	0.98 (0.79–1.13)	285.0 (166.2–392.9)**	8.54 (6.04–15.87)**
PCL/PVP/Ilo/A with an outer reinforcing layer	6	1.35 (1.29–1.39)*	201.2 (128.1–232.3)*	6.5 (5.54–11.09)**
Sheep carotid artery		1.2 (1.06–1.9)	158.5 126.0–169.5)	0.49 (0.39–0.66)
		Transverse direction (Me (25–75%))		
PCL/PVP/Ilo/A	6	1.24 (1.13–1.31)	28.43 (20.64–38.45)	9.62 (8.84–10.49)
PCL/PVP/Ilo/A with an outer reinforcing layer	6	2.43 (2.2–2.87)*	30.83 (28.66–34.60)	20.62 (17.58–23.04)*

Note: *, $p < 0.05$ relative to PCL/PVP/Ilo/A vascular grafts with no outer reinforcing layer; **, $p < 0.05$ relative to sheep carotid artery (longitudinal direction).

significant prosthetic deformities found. There were no foci of inflammation (Fig. 3).

Based on the outcomes of explantation and further transverse dissection of the PCL/PVP/Ilo/A grafts, it was determined that 50% of the explanted prosthesis had no thrombus in the lumen. Occluded prostheses contained grayish thrombus over the entire area and length of the product (Fig. 3, b). Patent prostheses were elastic, no parietal thrombi were found, and the anastomoses were a smooth connection between the prosthesis and the artery, maintaining the blood vessel diameter (Fig. 3, c). After six months of functioning as a component of the vascular bed, visually patent prostheses matched the native sheep artery: the middle of the prosthesis and the "prosthesis + artery" complex maintained a round vascular lumen;

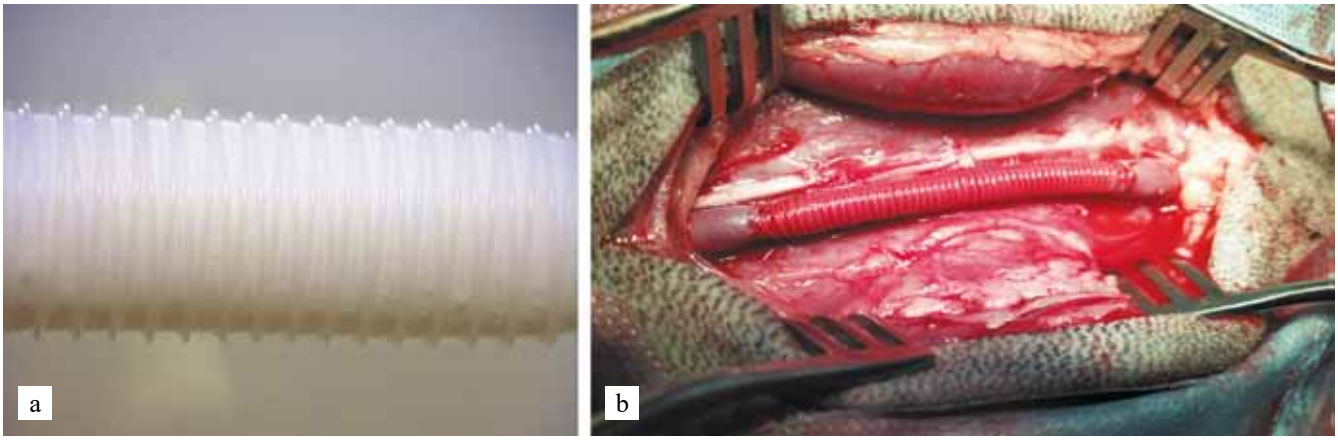

Fig. 1. PCL/PVP/Ilo/A vascular graft. a, prosthesis stereomicroscopy with an anti-aneurysmal scaffold, magnification 10×; b, prosthesis implanted in a sheep carotid artery

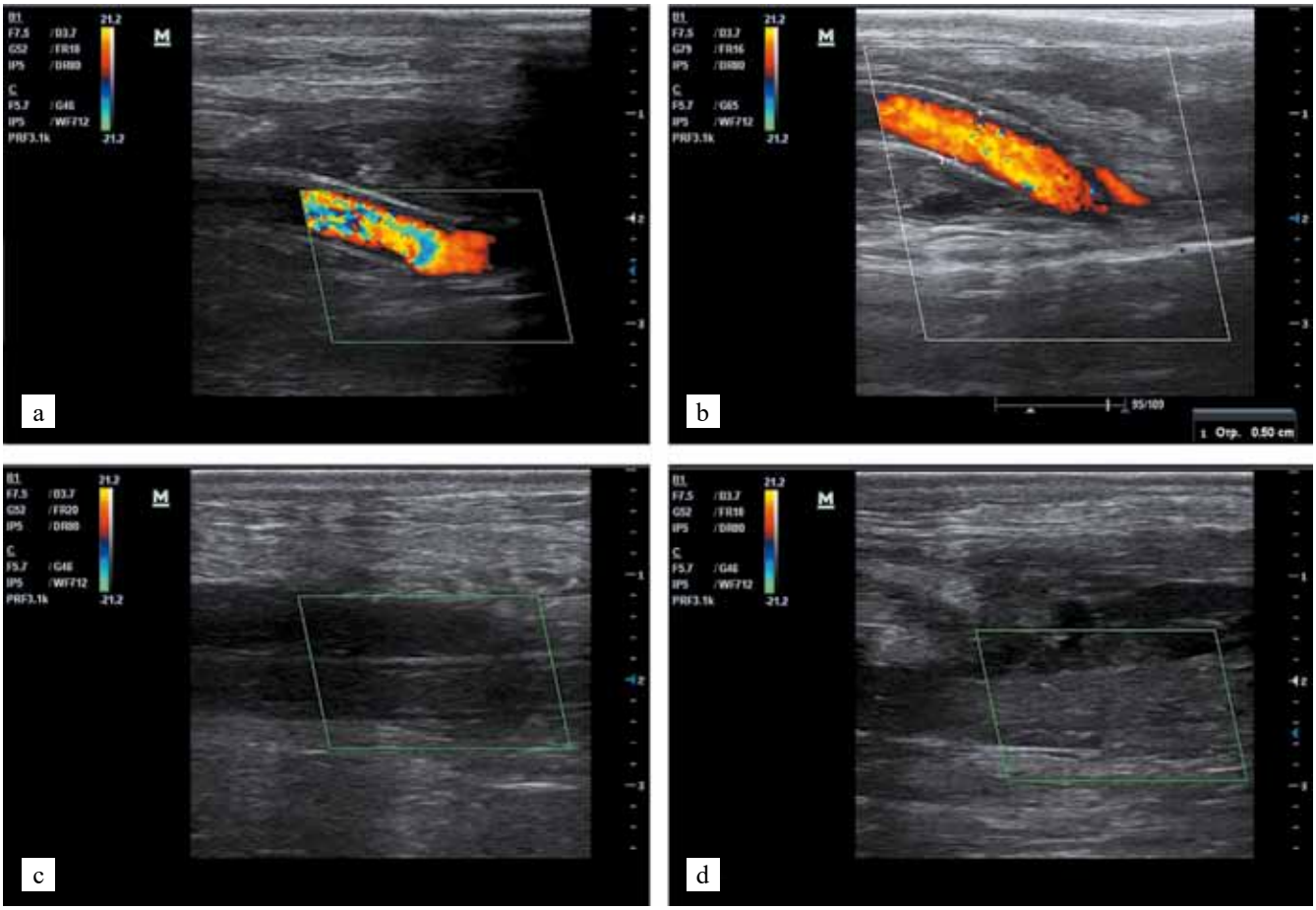

Fig. 2. Results of ultrasound monitoring of the patency of PCL/PVP/Ilo/A vascular grafts at different periods of implantation in a sheep carotid artery. Patent grafts: a, 5 days; b, 6 months. Thrombosed grafts: c, 5 days; d, 6 months

the thickness of the remodeled wall of the product was comparable to that of the artery wall (Fig. 3, c, d).

Results of histological examination

Based on the results of histological study of patent PCL/PVP/Ilo/A vascular grafts after 6 months of implantation into a sheep carotid artery, it was revealed that the tubular polymer base of the product almost completely biodegraded with the formation of newly formed three-layer vascular tissue on its base (Fig. 4). The newly created vascular wall consisted of a neointima with a thickness of 81 to 146 μm, neomedia with a thickness of 198 to 232 μm, and neoadventitia with a thickness of 144 to 217 μm. In the combined measurements, the wall of the remodeled vessel was 423 to 595 μm, which is comparable to thickness values for native sheep carotid artery (320 to 430 μm). On the side of the vascular lumen, the neointima was covered by a monolayer of elongated endothelium-like cells. The structural basis of neomedia was represented by cells similar in morphology to smooth muscle cells (see Fig. 4). The cell clusters were framed by collagen fibers. Scattered small clusters of structureless polymeric masses surrounded by single multinucleated foreign body giant cells, macrophages and fibroblast-like cells were also found in this layer. Vasa vasorum was predominantly detected along the border with the neoadventitia. The latter was the outer layer of the newly formed tissue, which resembled the structure of sheep artery adventitia and was formed by collagen bundles with partial filling with fibroblast-like and multinucleated giant cells (see Fig. 4). There were no signs of inflammation and calcification of the wall of the patent prosthesis.

The polymer base of the thrombosed PCL/PVP/Ilo/A grafts was also almost completely degraded 6 months after implantation without calcium deposits and inflammatory infiltration. These prostheses were distinguished by the presence of a thickened vascularized connective tissue capsule (see Fig. 4).

It is important to note the high preservation of the external wraparound scaffold in both occluded and patent prostheses: non-fibered round-shaped PCL filaments, surrounded by a collagen capsule without signs of calcification, were visualized in the transverse projection (see Fig. 4).

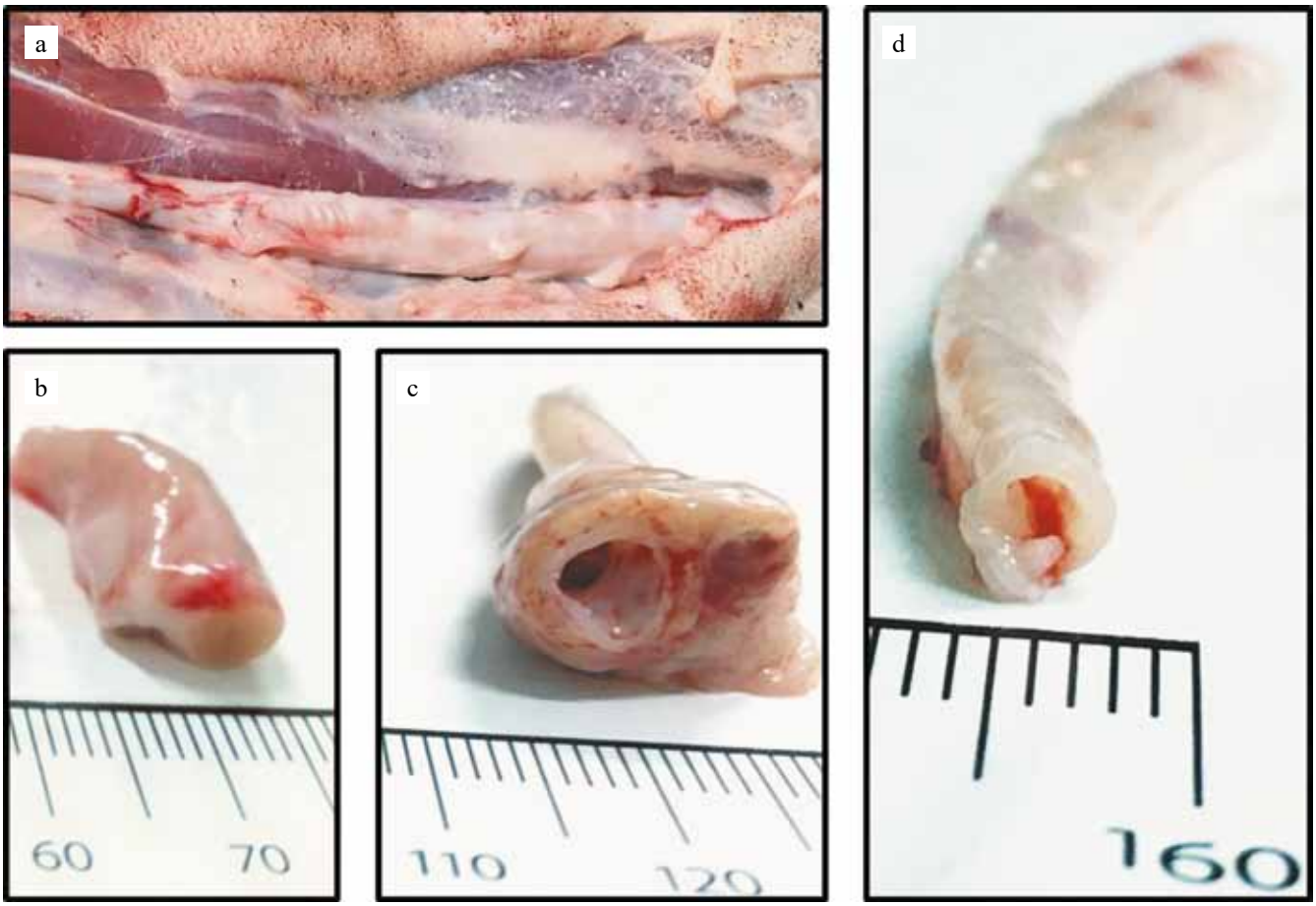

Fig. 3. Macrophotograph of explanted PCL/PVP/Ilo/A vascular grafts: a, macrophotograph of a PCL/PVP/Ilo/A graft at the moment of explantation; b, thrombosed graft; c, patent graft; d, intact sheep carotid artery

Immunofluorescence test results

The results of immunofluorescence study of explanted patent PCL/PVP/Ilo/A prostheses are consistent with those of histological study, confirming the formation of a continuous endothelial layer on the inner surface of the prosthesis (Fig. 5). The functionality of endothelial cells was demonstrated by the presence of vWF. A neointima of typical structure was formed on the graft wall, which consisted of α-SMA-positive cells and contained types III and IV collagens. A large amount of collagen types III and IV was also detected in the subendothelial layer. The prosthesis wall was actively populated with cells. Small complexes of $CD31^+$, α-$actin^+$, and vWF^+ cells were present in the wall thickness, which may indicate the formation of capillaries in the prosthesis wall. Also, large amounts of type III and IV collagens were found in the prosthesis wall (see Fig. 5).

Results of gene expression profiling

A comparative analysis of mRNA levels in the endothelial lysate and homogenate of patent remodeled PCL/PVP/Ilo/A grafts after 6 months of implantation showed that the newly formed vascular tissue at the site of the biodegradable vascular graft had differences from the genetic characteristics of native sheep carotid artery tissue. Genes found in the endothelial lysate were categorized into three groups according to the level of changes in expression: increased level (*IL6* (4.93-fold), *TNFA* (5.52-fold), *CTSB* (2.40-fold), *SMAD4* (2.63-fold)); decreased level (*ICAM1, FGF2, TGFB, MIF1, IL18, CNN, CXCL1, CXCL10, IL4, SELP, KLF4*); unchanged level (*IL1B, IL10, IL8, IL12A, VEGF, CXCR4, NR2F2, SNAI2, YAP1, KDR, MMP2, CD14*, *CD40L, EDN, PAI, SELE*).

For newly formed tissue, overexpression of the following genes in the homogenate was noted: *IL10* (2.83-

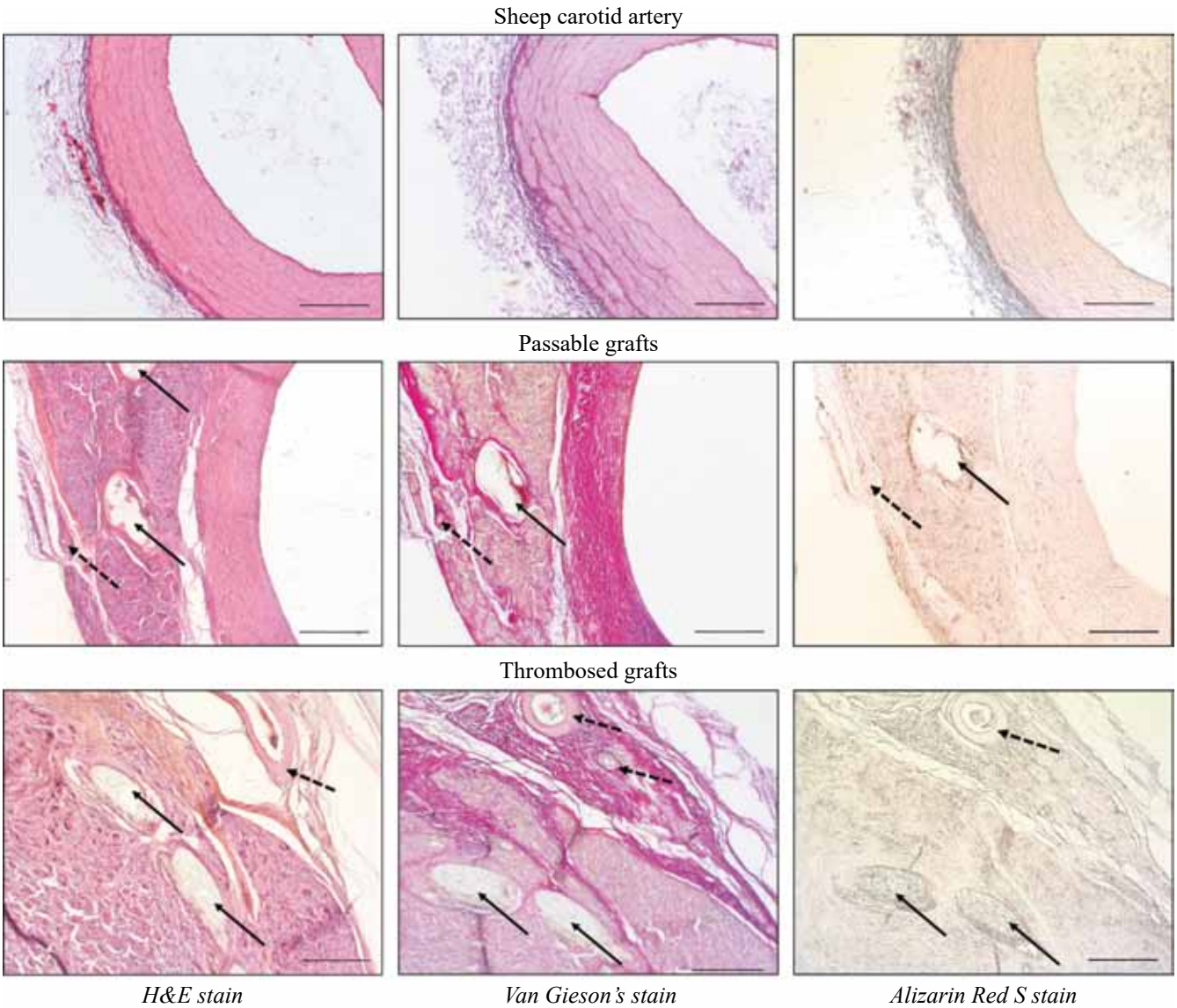

Fig. 4. Results of histological examination of explanted samples of PCL/PVP/Ilo/A vascular grafts at 6 months of implantation: solid arrow, PCL-strands of reinforced scaffold; dotted arrow, vasa vasorum. Scale bar 500 μm

fold), *CXCL 8* (4.56-fold), *TNF* (17.95-fold), *CXCR4* (13.42-fold), *TGFB* (6.06-fold), and *CTSB* (2.05-fold). Decreased mRNA levels compared to native sheep carotid artery tissue were noted for the following genes: *IL6, VEGF, NR2F2, SNAI2, ICAM1, YAP1, FGF2, MIF1, IL18, CD14, CD40L, EDN, EDN, IL4, SELE, SELP, SMAD4, KLF4, EDNRA* (Table 3).

Remodeling of patent PCL/PVP/Ilo/A grafts over 6 months of implantation was characterized by expression of genes with significant changes in mRNA levels, which are key markers from the position of endothelial biology processes such as inflammation (*IL6, IL4, CXCL8, IL10, TNFa, CD40L, CXCL1, CXCL10, MIF1*), endothelial to mesenchymal transition (*SNAI2*), endothelial differentiation (*VEGF*) and endothelial mechanotransduction (*YAP1, KLF4*), and leukocyte adhesion (*SELE, SELP*). It is worth noting that some important tissue remodeling markers were also associated with pronounced changes in mRNA levels: intercellular adhesion molecule (*ICAM*), smooth muscle cell marker (*CNN*), *TGFb* signaling pathway molecule (*SMAD4, TGFb*), and fibroblast growth factor (*FGF2*); (see Table 3).

DISCUSSION

High clinical demand is directing research efforts towards development of alternative small-caliber vascular shunts. The design of such artificial functionally active vascular prostheses should be based on the characteristics of the target native blood vessels in terms of implantation locus. The design of such a product should support the required blood flow, withstanding blood current pressure without experiencing mechanical damage. In addition, the structure of the inner surface of the prosthesis must prevent thrombus formation. Many functions of blood vessels are conditioned by structural components of different vascular layers at the biomolecular level. Therefore, it is necessary to ensure proper remodeling of the artificial scaffold of the vascular graft to fully reproduce the vascular tissue on its basis. Particular attention should be directed towards solving the problem of microbial contamination of the porous structure of a vascular graft. So, inclusion of an effective local antibacterial agent is necessary to prevent infection.

Formation of anti-aneurysmatic protection on the outer surface of polycaprolactone VGs contributed to higher prosthesis strength in longitudinal and transverse directions but caused a twofold increase in stiffness in the transverse direction, which is a standard but an undesirable moment for polymeric products.

The results of our own study of PCL/PVP/Ilo/A vascular grafts with antimicrobial coating and external reinforcing spiral implanted into a sheep carotid artery demonstrated 50% patency 6 months after implantation. When explanted, these prostheses were visually similar to the native sheep artery; There were no aneurysms, inflammation or other deformities. The exterior PCL spiral was highly preserved, indicating that its scaffolding function to prevent aneurysm formation at even

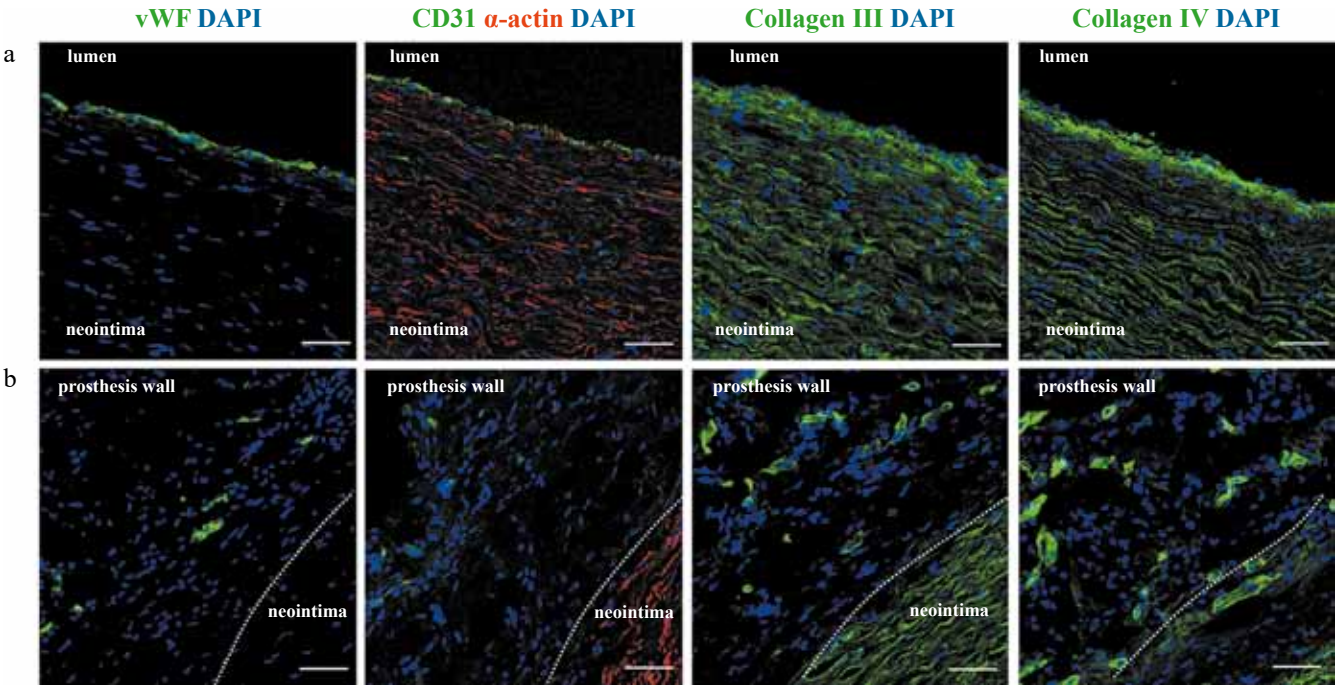

Fig. 5. Confocal microscopy of PCL/PVP/Ilo/A vascular grafts with anti-aneurysmal winding at 6 months of implantation: staining with specific fluorescent antibodies for von Willebrand factor (vWF, green), CD31 (endothelial cells, green), α-actin of smooth muscle cells (α-actin, red), collagen type III (green), collagen type IV (green). Cell nuclei were contrasted with DAPI (blue); a, prosthesis neointima and lumen; b, prosthesis wall. Scale bar 50 μm

longer implantation durations was successfully fulfilled. After implanting a nanocomposite vascular graft into a sheep carotid artery for 9 months, Ahmed et al. observed similar outcomes in terms of patency and development of prosthetic wall failure [20].

We were able to determine the features of the surrounding tissues and the degree to which the wall of the patent VGs had been successfully remodeled using histological methods. The explanted specimens had a neointima on their inner surface, which was covered in a continuous layer of mature, functionally active endothelial cells. Collagen fibers, smooth muscle-like cells, and vasa vasorum made up the middle layer. Neoadventitia was a representation of the outer layer. The newly formed tissue showed no signs of inflammation and calcification. These prostheses had morphological synchronization of the processes of biodegradation and remodeling of their wall.

Despite structural similarity between the newly formed vascular and native tissue, which was revealed by histological and immunofluorescent staining, a comparative analysis of gene expression profile showed some differences in their genetic profile. The CNN gene, which encodes the calponin protein and is a marker of smooth muscle cells, is of particular note in the results obtained. We found a significant decrease in gene expression for this gene in the neointima of remodeled prostheses, which is consistent with the proteomic profiling data we had previously obtained [19]. Furthermore, there was elevated expression of the CTSB gene encoding the lysosomal protein cathepsin B, in both endothelium lysate and homogenate. This finding could suggest chronic inflammation [21].

The process of reticulo-histiocytic cells biodegrading the polymer scaffold may be linked to an increase in inflammatory transcripts (TNFa) and transforming growth factor (TGFb) in homogenates of remodeled grafts. This

Table 3

Multiplicity of gene expression changes in endothelial lysate and homogenate of patent vascular grafts relative to intact sheep carotid arteries

Gene	Encoded protein	Homogenate	Endothelial cell lysate
IL1B	Interleukin-1 beta	0.58	0.65
IL4	Interleukin-4	0.11	0.37
IL6	Interleukin-6	0.27	4.93
IL10	Interleukin-10	2.83	0.71
CXCL8	Interleukin-8	4.56	1.99
IL12A	Interleukin-12A	0.97	1.57
IL18	Interleukin-18	0.2	0.5
TNF	Tumor necrosis factor	17.95	5.52
CXCL1	Growth-regulated alpha protein	0.88	0.06
CXCL10	C-X-C motif chemokine	0.08	0.16
VEGF	Vascular endothelial growth factor A	0.27	1.17
CXCR4	C-X-C chemokine receptor type 4	13.42	1.41
NR2F2	Nuclear receptor subfamily 2 group F member 2	0.14	0.75
SNAI2	Snai2	0.22	1.71
ICAM1	Intercellular adhesion molecule 1	0.36	0.35
YAP1	Yes-associated protein 1	0.005	0.68
KDR	Vascular endothelial growth factor receptor 2	0.84	1.06
FGF2	Fibroblast growth factor 2	0.014	0.18
MMP2	Matrix metallopeptidase 2	1.71	1.82
TGFB	Transforming growth factor beta-1	6.06	0.45
MIF1	Macrophage migration inhibitory factor	0.43	0.27
CTSB	Cathepsin B	2.05	2.40
CD14	Monocyte differentiation antigen CD14	0.41	1.35
CD40L	CD40 ligand	0.21	1.24
CNN	Calponin-1	0.03	0.42
EDN1	Endothelin-1	0.24	1.12
PAI1	Plasminogen activator inhibitor type 1	0.56	0.64
SELE	Selectin E	0.33	0.55
SELP	P-selectin	0.45	0.29
SMAD4	Mothers against decapentaplegic homolog 4	0.30	2.63
KLF4	Krueppel-like factor 4	0.40	0.09

is a known mechanism for resorption of biodegradable polymers. In addition, it is important to acknowledge the significant decrease in SNAI2 gene expression. This gene encodes a particular transcription factor that guarantees a modification in endothelial phenotype.

CONCLUSION

After being implanted into a sheep's carotid artery for six months, tissue-engineered SDVGs with an antithrombogenic drug-coated and reinforced external scaffold showed harmonious remodeling of the graft wall. Given that the newly formed vascular tissue was created entirely from scratch using an artificial matrix, the genetic discrepancies between it and the native one should not be surprising. This histological similarity indicates that the resulting graft wall remodeling rate is appropriate for the developed product to successfully function as part of the bloodstream. To enhance thromboresistance, more research is needed to improve the inner surface of the vascular graft.

The study was performed within the framework of the fundamental theme (No 0419-2022-0001) of the Research Institute for Complex Issues of Cardiovascular Diseases – "Molecular, Cellular and Biomechanical Mechanisms of the Pathogenesis of Cardiovascular Diseases in the Development of New Methods of Treatment of Cardiovascular Diseases based on personalized pharmacotherapy, introduction of Minimally Invasive Medical Devices, Biomaterials and Tissue-Engineered Implants".

The authors declare no conflict of interest.

REFERENCES

1. *Stowell CET, Li X, Matsunaga MH, Cockreham CB, Kelly KM, Cheetham J et al*. Resorbable vascular grafts show rapid cellularization and degradation in the ovine carotid. *J Tissue Eng Regen Med.* 2020; 14 (11): 1673–1684. doi: 10.1002/term.3128. PMID: 32893492.
2. *Diener H, Hellwinklel O, Carpenter S, Avellaneda AL, Debus ES*. Homografts and extra-anatomical reconstructions for infected vascular grafts. *J Cardiovasc Surg.* 2014; 55: 217–223. PMID: 24796916.
3. *Gordon TN, Kornmuller A, Soni Y, Flynn LE, Gillies ER*. Polyesters Based on Aspartic Acid and Poly(Ethylene Glycol): Functional Polymers for Hydrogel Preparation. *Eur Polym J.* 2021; 152: 110456. doi: 10.1016/j.eurpolymj.2021.110456.
4. *Guan G, Yu C, Xing M, Wu Y, Hu X, Wang H et al*. Hydrogel Small-Diameter Vascular Graft Reinforced with a Braided Fiber Strut with Improved Mechanical Properties. *Polymers (Basel)*. 2019; 11 (5): 810. doi: 10.3390/polym11050810.
5. *Hasan A, Memic A, Annabi N, Hossain M, Paul A, Dokmeci M et al*. Electrospun scaffolds for tissue engineering of vascular grafts. *Acta Biomater*. 2014; 10 (1): 11–25. doi: 10.1016/j.actbio.2013.08.022.
6. *Matsuzaki Y, Iwaki R, Reinhardt JW, Chang Yu-Ch, Miyamoto S, Kelly J et al*. The effect of pore diameter on neo-tissue formation in electrospun biodegradable tissue-engineered arterial grafts in a large animal model. *Acta Biomater*. 2020; 115: 176–184. doi: 10.1016/j.actbio.2020.08.011.
7. *Montini-Ballarina F, Calvo D, Caracciolo PC, Rojo F, Frontini PM, Abraham GA et al*. Mechanical behavior of bilayered small-diameter nanofibrous structures as biomimetic vascular grafts. 2016. *J Mech Behav Biomed Mater*. 2016; 60: 220–233. doi: 10.1016/j.jmbbm.2016.01.025.
8. *Blum KM, Zbinden JC, Ramachandra AB, Lindsey SE, Szafron JM, Reinhardt JW et al*. Tissue engineered vascular grafts transform into autologous neovessels capable of native function and growth. *Commun Med (Lond).* 2022; 2: 3. doi: 10.1038/s43856-021-00063-7.
9. *Mrówczyński W, Mugnai D, de Valence S, Tille JC, Khabiri E, Cikirikcioglu M et al*. Porcine carotid artery replacement with biodegradable electrospun poly-e-caprolactone vascular prosthesis. *J Vasc Surg*. 2014; 59 (1): 210–219. doi: 10.1016/j.jvs.2013.03.004. PMID: 23707057.
10. *Zhao L, Li X, Yang L, Sun L, Mu S, Zong H et al*. Evaluation of remodeling and regeneration of electrospun PCL/fibrin vascular grafts *in vivo*. *Mater Sci Eng C Mater Biol Appl.* 2021; 118: 111441. doi: 10.1016/j.msec.2020.111441. PMID: 33255034.
11. *Matsuzaki Y, Miyamoto Sh, Miyachi H, Iwaki R, Shoji T, Blum K et al*. Improvement of a Novel Small-diameter Tissue-engineered Arterial Graft With Heparin Conjugation. *Ann Thorac Surg.* 2021; 111 (4): 1234–1241. doi: 10.1016/j.athoracsur.2020.06.112.
12. *Matsuzaki Y, Ulziibayar A, Shoji T, Shinoka T.* Heparin-Eluting Tissue-Engineered Bioabsorbable Vascular Grafts. *Appl Sci.* 2021; 11: 4563. doi: 10.3390/app11104563.
13. *Fang Z, Xiao Y, Geng X, Jia L, Xing Y, Ye L et al*. Fabrication of heparinized small diameter TPU/PCL bi-layered artificial blood vessels and *in vivo* assessment in a rabbit carotid artery replacement model. *Biomater Adv.* 2022; 133: 112628. doi: 10.1016/j.msec.2021.112628. PMID: 35527159.
14. *Berard X, Puges M, Pinaquy JB, Cazanave C, Stecken L, Bordenave L et al*. *In vitro* evidence of improved antimicrobial efficacy of silver and triclosan containing vascular grafts compared with rifampicin soaked grafts. *Eur J Vasc Endovasc Surg*. 2019; 57 (3): 424–432. doi: 10.1016/j.ejvs.2018.08.053. PMID: 30301647.
15. *Clarke J, Shalhoub J, Das SK*. Ceramic gentamicin beads in vascular graft infection – a cautionary note. *Vasc Endovascular Surg*. 2013; 47 (1): 76–77. doi: 10.1177/1538574412465970. PMID: 23154662.
16. *Bisdas T, Beckmann E, Marsch G, Burgwitz K, Wilhelmi M, Kuehn C et al*. Prevention of vascular graft infections with antibiotic graft impregnation prior to implantation: *in vitro* comparison between daptomycin, rifampin and nebacetin. *Eur J Vasc Endovasc Surg*. 2012; 43 (4): 448–456. doi: 10.1016/j.ejvs.2011.12.029. PMID: 22264589.

17. *Krivkina EO, Mironov AV, Shabaev AR, Velikanova EA, Khanova MYu, Sinitskaya AV et al*. Features of remodeling of newly formed vascular tissue based on biodegradable vascular prostheses implanted in the carotid artery of sheep: morphogenetic analysis. *The Siberian Journal of Clinical and Experimental Medicine.* 2023; 38 (1): 151–159. [In Russ.] doi: 10.29001/2073-8552-2023-38-1-151-159.
18. *Burkert S, Schmidt T, Gohs U, Dorschner H, Arndt K-F.* Cross-linking of poly(N-vinyl pyrrolidone) films by electron beam irradiation. *Radiation Physics and Chemistry*. 2007; 76: 1324–1328. doi: 10.1016/j.radphyschem.2007.02.024.
19. *Antonova L, Kutikhin A, Sevostianova V, Lobov A, Repkin E, Krivkina E et al.* Controlled and Synchronised Vascular Regeneration upon the Implantation of Iloprost and Cationic Amphiphilic Drugs-Conjugated Tissue-Engineered Vascular Grafts into the Ovine Carotid Artery: A Proteomics-Empowered Study. *Polymers.* 2022; 14: 5149. doi: 10.3390/polym14235149. PMID: 36501545.
20. *Ahmed M, Hamilton G, Seifalian AM.* The performance of a small-calibre graft for vascular reconstructions in a senescent sheep model. *Biomaterials.* 2014; 35 (33): 9033–9040. doi: 10.1016/j.biomaterials.2014.07.008. PMID: 25106769.
21. *Fan Y, Pei J, Li X, Qin Y, Xu Y, Ke M et al.* Construction of tissue-engineered vascular grafts with high patency by mimicking immune stealth and blocking TGF-β mediated endothelial-to-mesenchymal transition. *Composites Part B: Engineering.* 2023; (251): 110487. doi: 10.1016/j.compositesb.

The article was submitted to the journal on 09.12.2023

DOI: 10.15825/1995-1191-2024-2-119-125

OBTAINING A MOUSE MODEL OF STREPTOZOTOCIN-INDUCED TYPE 1 DIABETES MELLITUS

G.N. Skaletskaya, N.N. Skaletskiy, G.N. Bubentsova, L.A. Kirsanova, Yu.B. Basok, V.I. Sevastianov

Shumakov National Medical Research Center of Transplantology and Artificial Organs, Moscow, Russian Federation

Objective: to obtain a stable mouse model of type 1 diabetes mellitus (T1DM) using streptozotocin (STZ), which has a toxic effect on pancreatic beta cells. **Materials and methods.** Experiments were performed on 30 white non-diabetic male mice of the SHK colony, which were injected intraperitoneally with STZ at a dose of 200 mg/kg by two methods: 15 animals (group 1) once and 15 animals (group 2) intermittently – 5 consecutive days at 40 mg/kg per day. **Results.** In group 1, one mouse died after 2 days due to hypoglycemic coma, 4 mice developed hyperosmolar hyperglycemia (>33.3 mmol/l), 3 mice had spontaneous remission of diabetes, and 7 mice had stabilized hyperglycemia at levels close to 20 mmol/l. In group 2, only one mouse showed spontaneous remission of diabetes, while the remaining 14 animals showed stable diabetes with average hyperglycemia levels moderately above 20 mmol/L until the end of the 4-week follow-up. A histological study of the pancreas of these animals confirmed the destructive effect of STZ on islets in the form of mass death of insulin-producing β-cells. **Conclusion.** Split-dose intraperitoneal injection of STZ provides a stable experimental T1DM in 93% of laboratory mice.

Keywords: diabetes mellitus, streptozotocin, glycemia.

INTRODUCTION

Diabetes mellitus (DM) remains one of the major challenges of modern medicine and public health due to its high prevalence and steadily increasing incidence. Inadequate prevention and treatment of specific complications leads to reduced work capacity and to premature death among patients with DM. Therefore, development of new, more effective approaches to antidiabetic treatment is highly important. New DM therapies should typically undergo a required cycle of preclinical trials, primarily laboratory animal experiments. In this regard, the use of laboratory models that are adequate for DM in humans becomes crucial. At the same time, it is essential to determine the etiopathogenetically appropriate type of diabetes – type 1 diabetes (T1DM) or type 2 diabetes (T2DM) – for a given experimental model [1–3]. The most commonly used diabetic models are mice and rats.

T1DM in mice can be broadly divided into two main types: spontaneous and induced. A characteristic example of spontaneous T1DM is its experimental model in non-obese diabetic (NOD) mice [4]. About 1 month after birth, signs of pancreatic islet inflammation occur in these animals. This is accompanied by destruction of pancreatic insulin-producing beta cells. Such a destructive process happens most intensively at the age of 11–14 weeks against the background of infiltration of the pancreatic islets by immune cells. Mass death of beta cells leads to absolute insulin deficiency and formation of a characteristic diabetic syndrome. However, the use of this model, as well as other mice with spontaneous T1DM, has shown to be inadequate, as many drugs successfully used in NOD mice were ineffective in clinical trials. Since achieving stable diabetes in mice with spontaneous β-cell destruction is often impossible to guarantee, extrapolation of antidiabetic treatment results using such experimental DM models in the preparation of clinical trials is problematic [5–8].

Since insulin insufficiency is a hallmark of T1DM, it can be achieved experimentally by administering chemicals that kill beta cells. With the development of different protocols for injection of beta-cytotoxic drugs, it is possible to obtain T1DM models that meet the criteria for the experimental studies performed. The most widely used agent that can induce β-cell destruction is streptozotocin (STZ).

STZ was originally isolated from actinobacteria Streptomyces achromogenes in 1960 as an antibiotic with a putative antitumor effect. In preclinical tests in laboratory animals, the diabetogenic property of STZ was discovered and described in 1963 [9]. In subsequent years, it was shown [10] that the occurrence of a characteristic diabetes after STZ injection is due to selective destruction of pancreatic beta cells and development of absolute insulin deficiency, characteristic of insulin-dependent (type I) DM in humans. This finding has been

Corresponding author: Galina Skaletskaya. Address: 1, Shchukinskaya str., Moscow, 123182, Russian Federation. Phone: (903) 771-18-13. E-mail: Skalink@mail.ru

successfully used in the development of experimental models of DM using STZ, primarily in rats and mice, which have natural endurance and good tolerance to even severe diabetes. An argument in favor of the induced DM model (in addition to STZ, alloxan, a mesoxalic acid ureide, is sometimes used, but it is less cytospecific and more toxic), compared with expensive races of rats and mice with spontaneous DM, is its much lower cost, especially since these drugs can be successfully administered even to outbred animals.

In our earlier article [11], we outlined two basic protocols for creating an STZ model of stable DM in laboratory rats. STZ was administered by a simple and safe method – intraperitoneal – which is not inferior to intravenous injection in terms of diabetogenic efficacy [12]. It was shown that a single injection of STZ at a dose of 70 mg per 1 kg body weight in Wistar rats produced a mixed diabetogenic effect, ranging from a slight increase and spontaneous reversal of hyperglycemia to a very high level of hyperglycemia and the death of some rats. Moreover, split-dose injection of STZ in the same dose (70 mg/kg) but divided into 5 consecutive days (14 mg/kg each), did not lead to animal death and there were almost no cases of spontaneous reversion of experimental DM, ensuring its stable course.

For several reasons (lower cost of animals, including their maintenance, saving diabetogenic drug and tested antidiabetic agent, etc.) it is reasonable to use laboratory mice as a diabetic model. In this regard, we decided to determine the STZ administration regimen that would ensure stable diabetes in these animals, considering the experience of obtaining experimental DM in rats, but using an STZ dose that is more accepted when dealing with mice (200 mg/kg) [13].

MATERIALS AND METHODS

Experiments were performed on 30 SHK white non-diabetic male mice with an initial weight of 25–30 g. The animals were obtained from a specialized nursery at the Research Center for Biomedical Technologies, Federal Biomedical Agency (Russia).

All animal manipulations were performed in compliance with the bioethical principles approved by the European Convention for the Protection of Vertebrate Animals Used for Experimental and other Scientific Purposes, 2005 and in accordance with the Rules of Laboratory Practice (Order 7080 approved by the Russian Ministry of Health, dated August 23, 2010.

STZ from Sigma (USA) was used as a diabetogenic agent. The agent was dissolved ex tempore in saline and injected in the animals intraperitoneally at the rate of 200 mg per 1 kg body weight by two methods: as a single injection in 15 mice (group 1) and intermittently in the remaining 15 mice, for five consecutive days, at a dose of 40 mg/kg each day (group 2). Glycemia in mice was determined at 12:00–12:30 noon in fasting capillary blood using test strips by Accu-Chek Performa glucometer (Roche), measuring range 0.6–33.3 mmol/L. To assess the nature and degree of morphological lesion of islets by STZ, we performed histological examination of the pancreas of mice with DM euthanized at the end of the experiment, as well as intact animals (control). Paraffin blocks were prepared from formalin-fixed pancreatic tissue samples, and 4–5 μm thick sections were stained with hematoxylin and eosin, and immunohistochemically for insulin and glucagon to detect islet beta cells and alpha cells.

Statistical data processing was performed using Microsoft Excel (2016) software. Descriptive statistics indicators – number of observations, arithmetic mean and standard deviation – were calculated. Student's t-test was used to determine the statistical significance of differences between means. Differences were considered statistically significant if significance level p did not exceed 0.05.

RESULTS AND DISCUSSION

The first visible signs of change in condition among the majority of the experimental animals were noted after 3–4 days of follow-up: thirst (increased volume of water intake) and polyuria appeared. In both groups, diabetes was confirmed by determination of hyperglycemia (Fig. 1); however, its magnitude and dynamics differed significantly depending on how STZ was administered – once or intermittently.

In group 1 (single injection at a dose of 200 mg/kg), one mouse died on day 2, apparently from hypoglycemic coma (glycemia of 1.3 mmol/L). Four of the remaining 14 mice had a rise in blood glucose, from moderate to

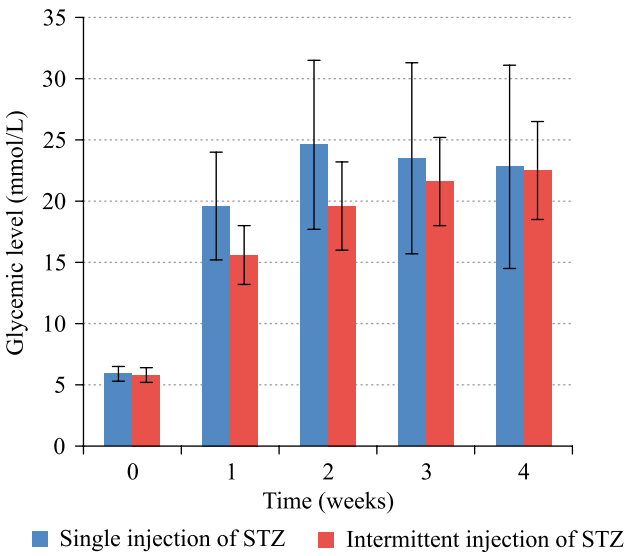

Fig. 1. Changes in glycemia after single and split-dose injection of streptozotocin in non-diabetic mice over a 4-week follow-up period

hyperosmolar hyperglycemia (>33.3 mmol/L) within 1–2 weeks. Three of them had a moderate rise in glycemia in the first 2 weeks after STZ injection (up to 12.8–17.9 mmol/L, mean 15.3 mmol/L); in the next 2 weeks, it spontaneously mean to subnormal (not fasting) levels, and by the end of follow-up it ranged from 8.9 to 12.8 mmol/L (average 11.0 mmol/L). In the remaining 7 group 1 mice, hyperglycemia was quite severe and persistent, ranging from 19.1 to 24.8 mmol/L (mean 22.3 mmol/L) at the end of follow-up.

So, 1 out of 15 experimental mice had fatal hypoglycemia following a single (200 mg/kg) intraperitoneal injection of STZ. The most likely explanation of this was the massive amounts of insulin released into the bloodstream following the mass death of islet beta cells as a result of the cytotoxic action of STZ. The remaining 14 mice also experienced hyperglycemia, but its height and dynamics of changes were ambiguous, and their features made it possible to identify three variants of STZ-induced DM after a single STZ injection. The first of them can be attributed to the maximum diabetogenic effect noted in 4 animals, where hyperglycemia reached an exceedingly elevated level (>33.3 mmol/l), which persisted practically until the end of a 4-week follow-up.

At the same time, the animals' overall health was not terrible, confirming that mice can tolerate induced DM relatively well, even in cases where very high glycemia is reached. However, the use of animals with prohibitive levels of hyperglycemia is hardly advisable because this makes it impossible to accurately assess the dynamics of glycemic changes during studies of a specific sugar-lowering medication.

The second variant of the course of STZ-induced DM can be attributed to changes in glycemia in 3 other mice. Following a period of moderate hyperglycemia, there was a gradual but significant drop in blood sugar levels, accompanied by disappearance of severe clinical signs of diabetes. This may be considered a spontaneous reversion of T1DM which appears to have occurred because the animals' pancreatic β-cells are not sensitive enough to the toxic effect of STZ.

In the remaining 7 mice from group 1, fairly severe hyperglycemia was stable and most often exceeded 20 mmol/L. The proportion of these variants of hyperglycemia dynamics in mice from this group was 29%, 21%, and 50%, respectively (Fig. 2).

Significantly more favorable results were obtained in group 2 mice, where STZ was injected into the peritoneal cavity also at 200 mg/kg, but in small equal doses (40 mg/kg/day) for 5 consecutive days.

Firstly, there was no case of animal death, which can be primarily down to exclusion of hypoglycemic coma due to split-dose administration of less toxic doses of STZ. For the same reason, there was no rise in glycemia to an ultra-high level. Secondly, only in one case was there a tendency to spontaneous reversal of hyperglycemia, most likely due to individual low sensitivity of pancreatic β-cells in this animal to STZ. Finally, an overwhelming number of mice in group 2 (14 out of 15) showed chronic hyperglycemia, which most often exceeded 20 mmol/L, but did not reach a very high level, averaging 23.4 mmol/L at the end of follow-up. Such stability of diabetes in split-dose STZ injection is quite probably facilitated by the development of an autoimmune process in the pancreatic islets of the experimental mice, leading to irreversible death of beta cells; this process has been identified by several researchers [7, 8, 10, 12, 13].

Thus, in 14 of the 15 experimental mice, or 93% of the cases, split-dose STZ stabilized experimental T1DM without causing extreme elevations in hyperglycemia; just one mouse had a spontaneous reversion of its diabetic status (Fig. 3).

Upon completion of the experiments, histological examinations of the experimental animals' pancreas de-

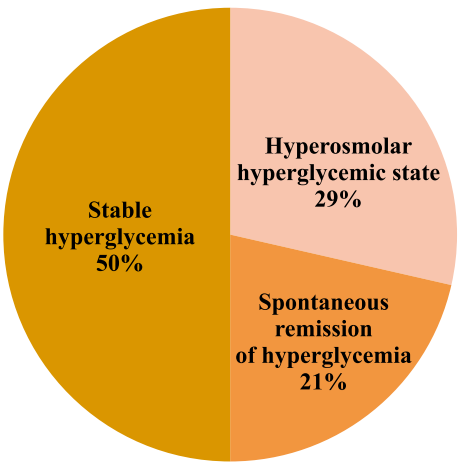

Fig. 2. Different degrees and dynamics of hyperglycemia in mice after a single intraperitoneal injection of streptozotocin at a dose of 200 mg/kg

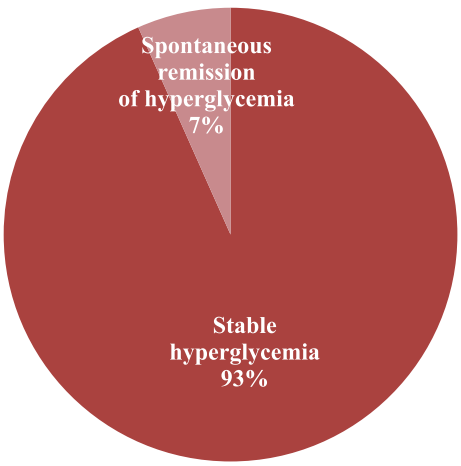

Fig. 3. Different degrees and dynamics of hyperglycemia in laboratory mice after split-dose intraperitoneal injection of streptozotocin at a total dose of 200 mg/kg

monstrated some structural alterations typical of STZ-induced T1DM. When compared to the morphologic image of the pancreas of intact nondiabetic mice (Fig. 4, a, 5), the destructive changes in the islets (Fig. 4, b, 6) were particularly noticeable in group 2 rats with stable diabetes. At the same time, almost all insulin-producing islet beta cells died after split-dose STZ injection (Fig. 6, a), while glucagon-producing alpha cells were not exposed to toxic effects and remained in the form of compact groups (Fig. 6, b), as if filling the vacant spaces occupied by β-cells earlier. Preservation of α-cells in STZ-induced DM mice has also been reported in a number of relevant studies [12, 13].

CONCLUSION

Both single and split-dose injections of STZ can stabilize a T1DM model in mice. However, split-dose injection is considerably more rational. Although after a single intraperitoneal STZ injection at a dose of 200 mg/kg, the proportion of mice with marked hyperglycemia was quite high (78.6%), but a significant proportion of them (28.6%) had unacceptably high (>33.3 mmol/L) blood glucose levels. At the same time, 21.4% of animals in this group showed signs of spontaneous reversion of diabetes. After a 4-week follow-up of group 1 mice, only half of them could be selected as experimental animals with experimental DM.

Since no experimental animals died and a significantly higher proportion of them had stable experimental T1DM in the absence of excessive hyperglycemia, the induction of T1DM by split-dose STZ injection should be viewed as more significant. The number of cases of spontaneous reversion of diabetic status was negligible. This type of STZ-induced DM is the one that can be suggested for use in an objective assessment of the out-

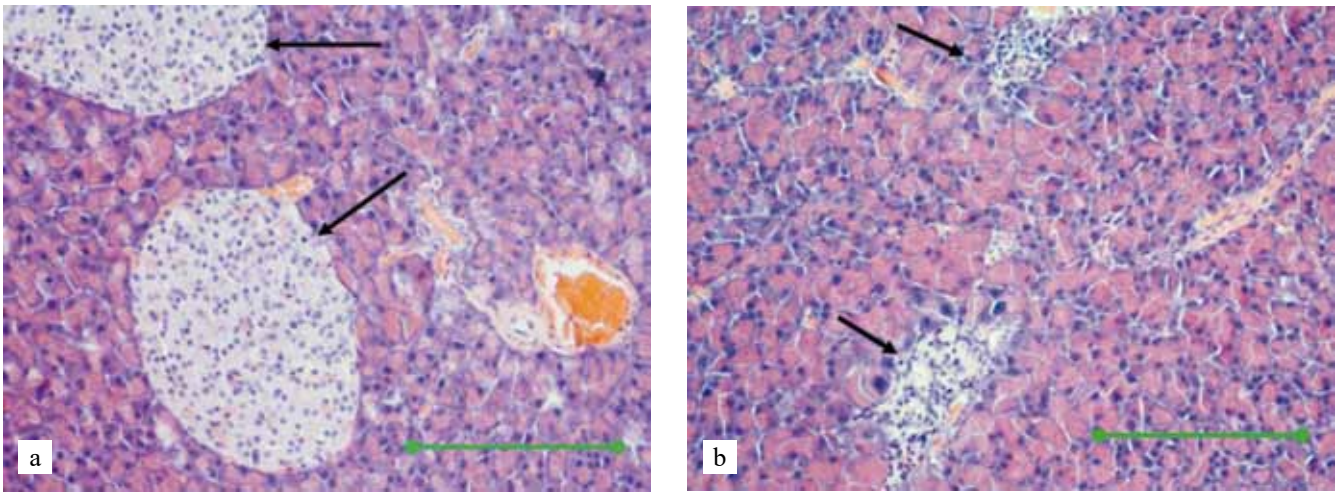

Fig. 4. Morphological pictures. a, islets in the pancreas of an intact non-diabetic mouse; b, pancreas of a mouse with streptozotocin-induced T1DM – severe destruction of islets. H&E stain. Scale bar, 200 μm

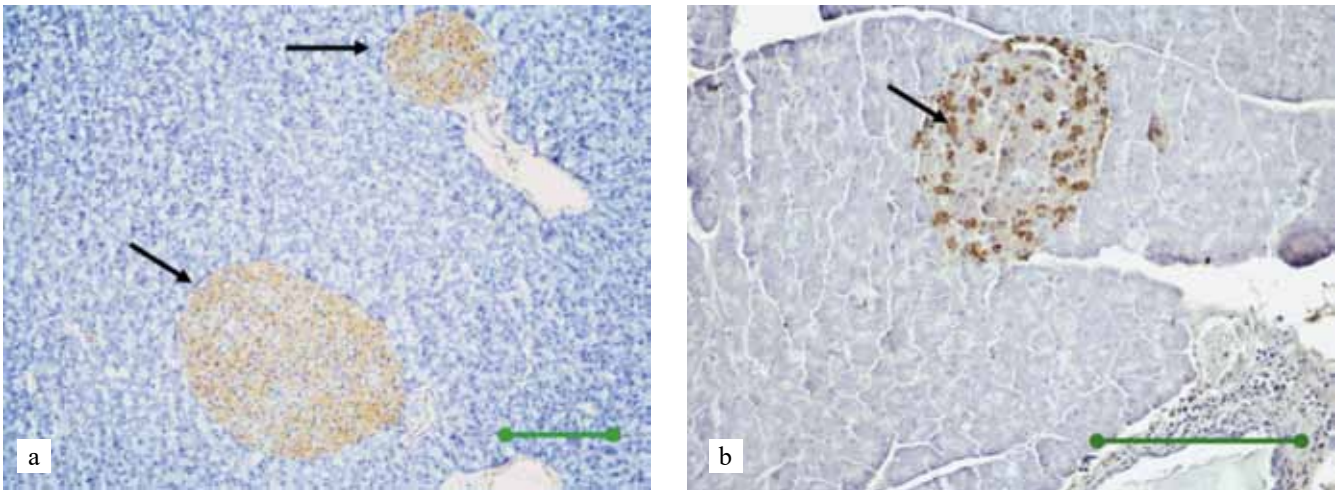

Fig. 5. Pancreas of an intact nondiabetic mouse. a, identification of beta cells in the islets. Immunohistochemical staining for insulin. Scale bar, 100 μm; b, identification of alpha cells in the islets. Immunohistochemical staining for glucagon. Scale bar, 200 μm

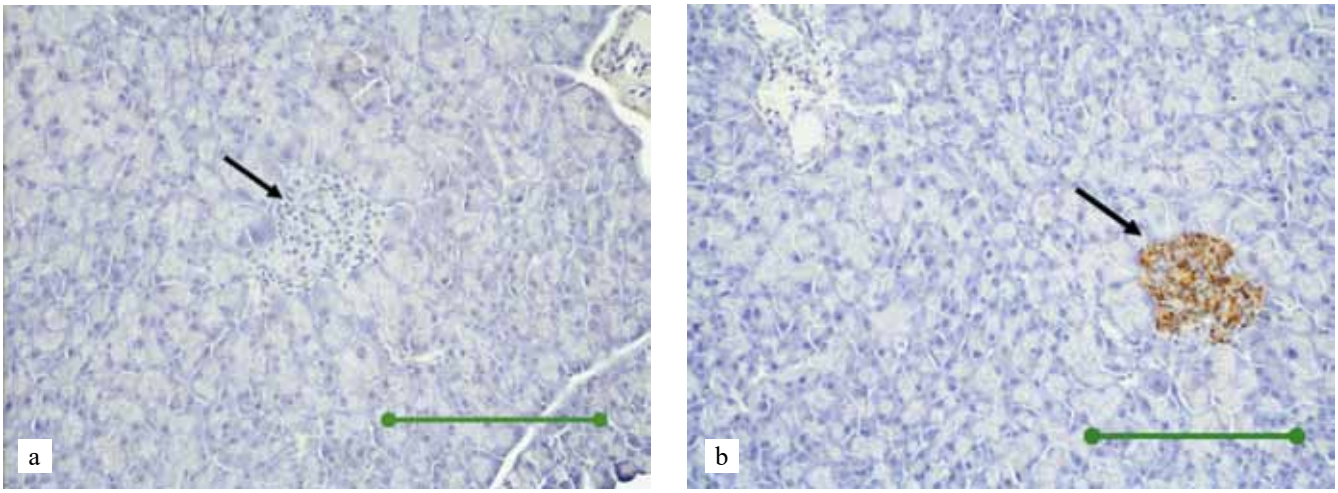

Fig. 6. Pancreas of a mouse with streptozotocin-induced T1DM. a, no beta cells in the islet. immunohistochemical staining for insulin; b, compactly located alpha cells in the islet. Immunohistochemical staining for glucagon. Scale bar, 200 μm

comes of various islet cell transplantation choices and other antidiabetic treatment methods.

The authors declare no conflict of interest.

REFERENCES

1. *Lenzen S.* Animal models of human type 1 diabetes for evaluating combination therapies and successful translation to the patient with type 1 diabetes. *Diabetes Metab Res Rev*. 2017; 33 (7). doi: 10.1002/dmrr.2915.
2. *Athmuri DN, Shiekh PA*. Experimental diabetic animal models to study diabetes and diabetic complications. *Methods X.* 2023 Nov 4; 11: 102474. doi: 10.1016/j.mex.2023.102474.
3. *Pandey S, Chmelir T, Chottova Dvorakova M.* Animal Models in Diabetic Research-History, Presence, and Future Perspectives. *Biomedicines.* 2023 Oct 20; 11 (10): 2852. doi: 10.3390/biomedicines11102852. PMID: 37893225.
4. *Makino S, Kunimoto K, Muraoka Y, Mizushima Y, Katagiri K, Tochino Y.* Breeding of a Non-Obese, Diabetic Strain of Mice. *Jikken Dobutsu.* 1980; 29: 1–13.
5. *Rothbauer M, Rosser JM, Zirath H, Ertl P*. Tomorrow today: organ-on-a-chip advances towards clinically relevant pharmaceutical and medical *in vitro* models. *Curr Opin Biotechnol.* 2019; 55: 81–86. doi: 10.1016/j.copbio.2018.08.009].
6. *Furman BL, Candasamy M, Bhattamisra SK, Veettil SK*. Reduction of blood glucose by plant extracts and their use in the treatment of diabetes mellitus; discrepancies in effectiveness between animal and human studies. *J Ethnopharmacol*. 2020; 247: 112264. doi: 10.1016/j.jep.2019.112264.
7. *Pandey S, Dvorakova MC*. Future Perspective of Diabetic Animal Models. *Endocr Metab Immune Disord Drug Targets.* 2020; 20 (1): 25–38. doi: 10.2174/1871530319666190626143832.
8. *Kottaisamy CPD, Raj DS, Prasanth Kumar V, Sankaran U.* Experimental animal models for diabetes and its related complications – a review. *Lab Anim Res*. 2021; 37 (1): 23. doi: 10.1186/s42826-021-00101-4.
9. *Rakieten N, Rakieten ML, Nadkarni MV.* Studies on the diabetogenic action of streptozotocin. *Cancer Chemother Rep. Part 1*. 1963; 29: 91–98.
10. *Junod A, Lambert AE, Stauffacher W, Renold AE.* Diabetogenic action of streptozotocin: Relationship of dose to metabolic response. *J Clin Invest*. 1969; 48: 2129–2139. doi: 10.1172/JCI106180.
11. *Skaletskaya GN, Skaletskiy NN, Volkova EA, Sevastyanov VI.* Streptozotocin model of stable diabetes mellitus. *Russian Journal of Transplantology and Artificial organs.* 2018; 20 (4): 83–88. [In Russ, English abstract]. doi: 10.115825/1995-1191-2018-4-83-88.
12. *Like AA, Rossini AA.* Streptozotocin-induced pancreatic insulitis: New model of diabetes mellitus. *Science*. 1976; 193 (4251): 415–417. doi: 10.1126/science.180605.
13. *Furman BL.* Streptozotocin-Induced Diabetic Models in Mice and Rats. *Curr Protoc.* 2021 Apr; 1 (4): e78. doi: 10.1002/cpz1.78.

The article was submitted to the journal on 05.02.2024

DOI: 10.15825/1995-1191-2024-2-126-134

EFFECT OF THE DELIVERY ROUTE AND DOSE OF MULTIPOTENT MESENCHYMAL STEM CELLS ON THE EFFICACY OF CELL THERAPY (REVIEW)

N.V. Pak, E.V. Murzina, N.V. Aksenova, T.G. Krylova, V.N. Aleksandrov
Kirov Military Medical Academy, St. Petersburg, Russian Federation

Multipotent mesenchymal stem cells (MMSCs) are known to be excellent therapeutic agents. Apart from their ability to differentiate into various cell types, and thus participate in the repair of injured tissues and organs, they can influence the regeneration process through secretion of paracrine factors. Thus, MMSC therapy represents a special type of medical intervention that has both a systemic range of therapeutic efficacy and local activity on individual sites of an organ. Over the past decades, MMSC therapy has continuously been in a cautious transition from research development to clinically approved therapies. Clinical trial data has shown that this therapy is rarely associated with severe adverse events, is well tolerated and quite safe in the short-term period. However, it has a number of limitations for use, mainly due to the risk of malignant transformation. The success of stem cell transplantation in the treatment of various diseases has been confirmed both in preclinical studies and in clinical practice. The main issues that arise when assessing the therapeutic efficacy of MMSC-associated therapy are the type of cells (adipogenic, bone marrow, etc.), delivery route, number of cells injected, and the optimal number of injections. There is a growing body of experimental and clinical evidence suggesting that both an adequate delivery route and an adequate dose can increase the likelihood of success of MMSC-associated. Each cell delivery route has costs and benefits. However, there is generally contradictory evidence on the comparative efficacy of different cell delivery routes. The optimal dose of transplanted cells is also debated, as high MMSC doses may increase the risks of complications and may not have the proper effect both when administered systemically and locally. These aspects require further systematization of available data to maximize the effect of cell therapy by selecting the safest and most appropriate approaches.

Keywords: multipotent mesenchymal stem cells, cell therapy, transplantation, delivery route, delivery dose.

INTRODUCTION

Modern breakthroughs in biotechnology, molecular and cellular biology have made stem cells one of the means for treating numerous diseases. Multipotent mesenchymal stem cells (MMSCs) have three main therapeutic effects: they differentiate and replace damaged tissue cells, they produce bioactive molecules, and they engage in intercellular communication and interact with immune cells [1–3].

MMSC-based therapy is generally considered a safe procedure with some limitations. The main risks associated with MMSC use are their possible oncogenicity (transformation into tumors, stimulation of tumor growth) [4, 5] and induction of severe pro-inflammatory processes [4] and fibrosis (transformation into myofibroblasts) [4, 6, 7]. Many studies have proposed algorithms to improve engraftment and differentiation of transplanted cells. While some strategies focus on increasing cell resistance to the microenvironment in recipient tissues, others try to increase cell survival after transplantation. These strategies can range from simple modification of culture conditions, known as cell preconditioning, to genetic modification of cells to avoid cellular senescence [8]. An essential element in improving the efficacy of cell therapy and reducing the risk of adverse events is the search for optimal delivery routes and doses for MMSCs. Despite many preclinical and clinical studies, the safety and efficacy of MMSC-related therapies remain problematic for clinical application [9, 10].

The **aim** of this work is to conduct an informational and analytical study of experimental and clinical data on the efficacy of various stem cell delivery routes and doses as a means of therapy for various diseases.

RESULTS AND DISCUSSION

MMSCs are typically administered intravenously or intra-arterially to achieve systemic effects on the body. When administered systemically, they can migrate directly (homing) to the site of injury in response to chemokine and cytokine secretions [11]. Although the exact mechanism of how MMSC home to sites of injury has not been fully understood, it is known that it is a multistep process in which chemotactic factors play a significant role [8]. Chemoattraction of MMSCs to the target tissue seems

Corresponding author: Natalya Pak. Address: 6, Akademika Lebedeva str., St. Petersburg, 194044, Russian Federation. Phone: (812) 292-32-63. E-mail: natalya_pak@mail.ru

to be mainly mediated by stromal factor SDF-1/CXCR4 axis, but monocyte chemoattractant protein/CCR2 and hepatocyte protein as well as cytokines such as TGF-β1, IL-1β, TNF-α or G-CSF may also be involved in MMSC migration [12–14]. It is obvious that intravascular administration is the least invasive delivery route and, therefore, the most preferable from a clinical standpoint. However, this route has significant drawbacks. The major one is that a large number of injected cells can linger in the capillary network of lungs (first passage effect) and other organs, such as liver and kidneys. Considering that during transmigration, MMSCs should traverse membranes between vascular endothelial cells and the target tissue, it is obvious that delivering cells to target tissues through systemic infusion in the most efficient manner is rather difficult. At the same time, MMSCs can form microemboli, which create major consequences for organ function, given that the estimated cell diameter is 20–30 μm [8, 15]. There are serious concerns about the safety of this delivery method because studies on mice models have shown that in the intra-arterial delivery route, micro-occlusions are created, whose number was directly correlated with cell count [16]. Following intravenous injection, the presence of MMSCs or their detritus in the pulmonary capillary network is not just a temporary delay – macrophage phagocytosis occurs there, and the MMSC detritus is then further carried with blood to other organs [17]. One way to improve cell diffusion homing is the preconditioning of target tissues. For example, several studies have shown that administration of a number of hormones, chemokines, growth factors, and enzymes in experimental animals, as well as exposure to physical factors (ultrasound, irradiation), enhances MMSC migration to the injury site [8].

It should be noted that the injection procedure may be complicated by resuspension of cells in solutions that have low osmotic pressure, since mechanical stress can destroy cell membranes and lead to a significant proportion of the cell population dying [18].

It is established that the half-life of MMSCs after systemic administration is about 12 hours. However, as noted earlier, most of the cells are retained in the lungs, where they are utilized or, from where they migrate within 24 hours [2, 6, 8, 19]. After cells are injected directly into tissues against the background of venous blockade, detritus enters the bloodstream much later in smaller amounts. The main part of implanted MMSCs is found in other organs and tissues (liver, spleen, etc.) within 7 days [2, 20]. There is evidence that MMSCs can survive for 30 days after subcutaneous implantation [2, 21], but after that, they are undetectable in the liver, kidney and spleen [17]. After intravenous injection, cells can be detected in the lungs for 150 days [20].

Administration of MMSCs by surgical implantation or transendocardial injection has resulted in the retention of only 16% and 11% of MMSCs in the myocardium, respectively [5]. Intracoronary infusion also caused retention of 11% of MMSCs. Overall, approximately 0.1–2.7% of injected stem cells actually reach the target tissues [22]. Other implanted MMSCs mainly exert remote effects on regenerative processes via cytokines, exosomes and microvesicles, and exhibit mainly anti-inflammatory, immunomodulatory and anti-apoptotic effects [23]. It should be mentioned that less than 1% of cells are detected in the target organ in both animal research and some clinical trials using MMSCs for the therapy of osteogenesis imperfecta [15].

There are reports indicating that MMSCs, when delivered locally, mobilize progenitor cells to the injury site, thereby enhancing regenerative activity [5, 20, 21]. In doing so, they improve wound healing and skin graft survival. However, experimental studies have shown that MMSCs do not stay long in the injection site – most of them migrate into the surrounding tissues within 1 hour and are no longer detected in the injection site after 2 days [2, 21].

In a comparative study of three different MMSC delivery routes (intraperitoneal, intravenous and anal) in a mouse model of colitis, intraperitoneal delivery was shown to provide a higher MMSC content in organs and faster recovery of experimental animals [15]. The efficacy of therapy was evaluated by histological index, total body weight of animals and their survival rate.

Distribution and engraftment of MMSCs in organs were analyzed and quantified through isolation of the cells from green fluorescent protein (GFP+), as well as using near-infrared fluorescence imaging. There is evidence that intraperitoneally injected MMSCs aggregate with macrophages and lymphocytes in the abdominal cavity and secrete TSG-6 (tumor necrosis factor-inducible gene 6 protein), which is likely the main anti-inflammatory mechanism of MMSCs. Increased serum TSG-6 level was detected after MMSC transplantation, with the highest levels detected after intraperitoneal delivery.

It should be noted that the abdominal cavity contains many immune cells that can become components of MMSC aggregates. Such close intercellular cross-linking between MMSCs and immune cells may be another factor contributing to improved therapeutic effects [15]. It has also been observed that intraperitoneal injection provided better mucosal repair and higher cell engraftment in inflamed colon.

Intraperitoneal injection of MMSCs had a positive effect on recovery of mice with experimental spinal cord compression injury (SCI) [24]. The evaluation criterion was the effect of MMSC transplantation on white matter preservation. It was shown that experimental groups of animals that received MMSCs at a dose of 8×10^5 cells/mouse had a greater number of preserved fibers. In addition, these groups were characterized by higher levels of trophic factors (brain-derived neurotrophic factor, nerve growth factor, neurotrophin-3 and neurotrophin-4) in the

spinal cord, which improved motor activity. So, intraperitoneal or intravenous injections of MMSCs promoted favorable outcomes as a treatment for SCI without a significant statistical difference between the two. This supports the idea that these cells do not replace damaged spinal cord cells but act through local paracrine effects.

F. Yousefi et al. (2013) showed that intraperitoneal injection of MMSCs can reduce the number of inflammatory aggressor cells in the brain and improve clinical parameters in mice with experimental autoimmune encephalomyelitis [25].

There is evidence that intraperitoneal injection of MMSCs can suppress peritoneal inflammation by restoring the mesothelial layer and reducing complement activation in fungal or yeast peritonitis in rats; it almost completely prevents experimental autoimmune uveitis in mice by suppressing Th1/Th7 immune responses, protecting the retina against immune-mediated injury [24].

Wang et al. (2016) showed that the best outcomes in the treatment of experimental colitis were achieved by intraperitoneal transplantation of MMSCs [15]. It was found that GFP+ MMSCs migrated into inflamed colon and even traveled through the entire intestinal wall, reaching the luminal side. This finding is consistent with the results that show MMSCs injected intraperitoneally migrate and take root in an inflammatory colon [26]. Although the precise processes underlying this phenomenon are still unknown, it can be hypothesized that cytokines are involved in the process. It is known that genetic modification of MMSCs to increase CXCR4 expression enhances cell migration into the intestine in radiation enteritis, and consequently, improves condition. Experimental studies by Yang et al. (2019) showed that a single intraperitoneal injection of MMSCs (2×10^6 cells/mouse) dramatically improved clinical parameters of body weight and colon length, as well as ulcer size and histologic parameters in mice with colitis compared to those without [27].

Nevertheless, in some cases, intravenous injection has been found to be more successful than intraperitoneal injection [28]. This discrepancy may be due to different types of adipose tissue- and bone marrow-derived MMSCs that differ in proliferation rate, differentiation ability, cytokine secretome and chemokine receptor expression, which may affect migration, engraftment and even local function [29, 30]. There is evidence that bone marrow MMSCs-based therapies demonstrate the highest osteogenic potential in bone regeneration compared to MMSCs derived from other tissues [8]. Furthermore, the therapeutic effects of various MMSC sources and delivery methods on lung and cardiovascular injuries vary [31]. Therefore, while evaluating study findings and making specific therapeutic application choices, it is important to consider the biological differences between MMSCs and other sources. Meanwhile, there is a report that claims that because the immunophenotypes of bone marrow and adipose tissue stem cells are more than 90% identical, it is impossible to determine which stem cell source – adipose tissue or bone marrow – will yield the best outcomes for cell therapy [9]. Besides, when assessing efficacy, it is important to consider that MMSCs may exert their therapeutic effects distally through modulatory cytokines [32].

Intramuscular injection of MMSCs has been proposed as a better alternative to intravenous administration [33]. Braid et al. (2018) report that while cells injected intravenously were undetectable as early as a few days after injection, and cells delivered intraperitoneally and subcutaneously were detectable within 3–4 weeks, MMSCs injected intramuscularly survived *in situ* for more than 5 months. Allogeneic single intramuscular transplantation of umbilical cord-derived MMSCs to rats with simulated hind limb ischemia promoted functional and morphological recovery of ischemic skeletal muscle tissue [34]. At the same time, the cells injected into experimental animals stimulated angiogenesis in the injury site.

In general, quite numerous experimental studies have shown MMSCs to improve functional recovery in ischemic stroke; this is attributed to the ability of MMSCs to enhance the endogenous regenerative potential of nervous tissue [35, 36]. This is due to the action of bioactive substances released by the cells, which activate and stimulate other cell types [37]. The choice of an optimal delivery route for MMSCs in cerebral ischemia depends on the type of central nervous system (CNS) injury (focal or multifocal). The peculiarities of focal CNS injury suggest that the most appropriate way may be intracerebral cell transplantation directly into the injury site, and in case of multiple lesion areas – systemic intravascular or endolumbar injection [37].

It has been shown that intraportal and intravenous administration of MMSCs in experimental liver cirrhosis promotes faster recovery of liver function. Moreover, liver weight decreased the most with intraportal injection of stem cells [38]. Administration of acridine orange-labeled MMSCs intravenously, intraperitoneally, into the hepatic artery or portal vein at a dose of 4×10^6 cells/kg body weight showed a significant increase in cell count in the liver after its subtotal resection regardless of the injection method [39]. At the same time, intraperitoneal delivery was characterized as the least effective.

When correcting diabetes in an experiment, intravenous injection of bone marrow-derived MMSCs statistically significantly reduced glucose levels in mice of the experimental group compared to the control group [40].

It was found that MMSC implantation promotes neurological recovery in a rat model of traumatic brain injury (TBI) [41]. Intravenous injection of cells into rats reduced the number of microglia and other inflammatory cells and production of proinflammatory cytokines. It also stimulated the synthesis of anti-inflammatory

cytokines leading to inhibition of inflammatory reactions caused by TBI [42].

In clinical practice, the multipotent and secretory potential of MMSCs finds application in the field of regenerative medicine for restoration of tissue structures of the body that were damaged by injuries or that developed pathology (combustiology, traumatology, dentistry, etc.). Here, introduction of stem cells in the patient is usually done intravenously to provide a systemic effect on the patient's body [2, 23]. Direct comparison of delivery methods is often absent here due to logistical problems [5]. An adequate dose of MMSCs administered once has been shown to have a positive clinical effect in 3–6 months (and beyond). In certain cases, however, a repeat course of treatment in 1–2 weeks (4–6 months) is necessary to reach the desired therapeutic outcome [2, 43–46].

The experience of intravenous injection of MMSCs in patients with chronic heart failure (CHF) against the background of ischemic heart disease is presented. It was shown that intravenous administration of autologous MMSCs at a dose of 50×10^6 cells in combination with standard drug therapy improves basic hemodynamic parameters and reduces the level of biochemical markers of CHF [47]. In addition, there is evidence showing the successful application of intracoronary and intramyocardial delivery routes in the treatment of ischemic conditions in clinical practice [48].

To date, 125 clinical trials have been conducted using MMSCs in neurologic diseases [31], including the treatment of TBI. Injection of autologous bone marrow-derived MMSCs in patients in the subacute phase of TBI improved neurological function in 40% of patients [49, 50], promoted recovery of consciousness, motor and cognitive functions [51]. Intravenous delivery is used for TBI therapy, since MMSC delivery via the intracerebral route is considered to be the most effective, but also the most invasive [31].

The outcomes of clinical trials on cirrhosis therapy using MMSCs are contradictory and occasionally inconsistent with the results of experimental studies [52]. Nevertheless, uncontrolled clinical studies have demonstrated that introduction of autologous MMSCs into the hepatic arterial bed through endovascular surgery is safe, well tolerated, and provides a positive effect in patients with cirrhosis of various etiologies [53].

For the treatment of patients with knee joint conditions, delivery of autologous MMSCs was via intraarticular injection of cell culture isolated from different sources [9, 54]. It was noted that long-term follow-up parameters were significantly superior to those in the control group receiving conventional treatment [54].

The use of intraperitoneal cell transplantation in clinical practice has significant limitations due to possible complications. These complications include catheter infection and mechanical damage to intraperitoneal structures [15]. At the same time, it should be noted that high peritoneal vascularization allows a greater number of transplanted cells to simultaneously gain access to the lymphatic and circulatory systems, which certainly promotes engraftment in the injury and inflammation sites [24]. It is obvious that the trend to expand the use of intraperitoneal injections in cell therapy applications will increase and will influence the intensification of innovative developments aimed at preventing complications.

Another crucial factor influencing the therapeutic efficacy of MMSCs is the number of cells injected. The quantity of cells that reach the damage site increases with an increase in the initial dose of cells delivered. Various MMSC dosages have been found to be effective in experimental investigations. Doses from 3×10^5 cells/mouse to 2×10^6 cells/mouse appear in the protocols of experimental studies [15, 24, 25]. Sometimes, to observe any effect, larger doses, up to 5×10^6 cells/mouse, are used [37, 55]. However, the researchers conclude that intravenous injection of MMSCs at a high dose (up to 1×10^7 cells/mouse) can increase mortality in mice due to potential pulmonary embolism.

Usually, MMSC doses in the range of 5×10^5 to 5×10^6 cells/mouse are used to achieve therapeutic effect in experimental rats [55, 56]. At the same time, cell survival after transplantation into recipient tissue depends not only on dose, but also on duration and conditions of cultivation, such as presence of serum or oxygen, mechanical stress during implantation or cell death due to lack of fixation [56, 57]. There is an opinion that regional injection (endolumbar, intraperitoneal, intramuscular) results in a tenfold decrease in the therapeutic dose of cells [2].

A significant challenge lies with translating the experimental dosage of the cell product for use in clinical practice. As mentioned above, the commonly used cell dose is 1×10^6 cells/mouse (body weight 30 g), which is equivalent to 33×10^6 cells/kg or approximately 2.3 billion cells for a 70 kg adult [14]. Researchers have suggested that high cell doses may increase the risks of complications, including alloimmunization when using allogeneic MMSCs, and may not have the proper effect when injected both intravenously and topically [2, 22, 58]. Nonetheless, the concept of "optimal dose" of systemically injected MMSCs in clinical practice does not exist yet since there is no clear dose-effect correlation [8]. Today, the standard dose is 1–2 million cells per kg of weight [2, 58]. Moreover, compared to standard doses, 5–10 higher doses of cells are used during the cell therapy process for newborns – but usually just once [2, 43].

Using autologous MMSCs, experimental and clinical simulations were used to examine the efficacy of various cell delivery methods in the treatment of Parkinson's disease [59]. When compared to baseline data, an intravenous injection of 160,000 cells/kg weight (low dose) resulted in a statistically significant decrease in motor disorders. At the same time, transnasal injection

in a similar dose in patients of the other group had a similar effect. These findings suggested that while designing long-term maintenance therapy for Parkinson's disease, the efficacy of minimally invasive techniques for delivering low-dose MMSCs should be taken into account.

CONCLUSION

Most preclinical and clinical studies have shown that MMSC implantation is effective, safe and well tolerated. Analysis of data from scholarly publications indicates that there is ongoing research being done to find the best cell delivery dosages and routes. It should be noted that attempts are now being undertaken to develop the option of using exosomes and extracellular vesicles as a cell-free means to realize the features of MMSCs, with the goal of removing any potential side effects. It is obvious that application of a cellular product in practical healthcare requires maximum adaptation to the type of disease or injury in terms of the choice of implantable MMSC doses and their delivery routes given the need to ground the therapeutic strategy with a clear and thorough understanding of the disease mechanisms. In general, research findings and the opinions of different authors on this issue are far from being ambiguous and sometimes contradictory. As such, a versatile study of the therapeutic potential of MMSCs remains pertinent.

The authors declare no conflict of interest.

REFERENCES

1. *Caplan AI*. Mesenchymal stem cells: time to change the name! *Stem cells. Transl Med.* 2017; 6 (6): 1445–1451. doi: 10.1002/sctm.17-0051.
2. *Potapnev MP.* Ways to improve the efficiency of cell therapy based on multipotent mesenchymal stromal cells. *Genes and cells*. 2021; 16 (4): 22–28. [In Russ, English abstract]. doi: 10.23868/202112003.
3. *Moskalev AV, Gumilevsky BYu, Apchel AV, Tsygan VN.* Stem cells and their physiological effects. *Bulletin of the Russian Military Medical Academy.* 2019; 68 (4): 172–180. [In Russ, English abstract].
4. *Han Y, Li X, Zhang Y, Han Y, Chang F, Ding J.* Mesenchymal stem cells for regenerative medicine. *Cells.* 2019; 8 (8): 886. doi: 10.3390/cells8080886.
5. *Caplan H, Olson SD, Kumar A, George M, Prabhakara KS, Wenzel P et al.* Mesenchymal stromal cell therapeutic delivery: translational challenges to clinical application. *Front Immunol*. 2019; 10: 1645. doi: 10.3389/fimmu.2019.01645.
6. *Payushina OV, Tsomartova R, Chereshneva EV, Ivanova MYu, Kuznetsov SL.* Regulatory influence of mesenchymal stromal cells on the development of liver fibrosis: cellular and molecular mechanisms and prospects for clinical application. *Journal of General Biology*. 2020; 81 (2): 83–95. [In Russ, English abstract]. doi: 10.31857/S0044459620020062.
7. *Popova AP, Bozyk PD, Goldsmith AM, Linn MJ, Lei J, Bentley JK, Hershenson MB*. Autocrine production of TGF-β1 promotes myofibroblastic differentiation of neonatal lung mesenchymal stem cells. *Am J Physiol: Lung Cell Mol Physiol*. 2010; 298: 735–743. doi: 10.1152/ajplung.00347.2009.
8. *García-Sánchez D, Fernández D, Rodríguez-Rey JC, Pérez-Campo FM.* Enhancing survival, engraftment, and osteogenic potential of mesenchymal stem cells *World J Stem Cells*. 2019; 11 (10): 748–763. doi: 10.4252/wjsc.v11.i10.748.
9. *Di Matteo B, Vandenbulcke F, Vitale ND, Iacono F, Ashmore K, Marcacci M, Kon E.* Minimally manipulated mesenchymal stem cells for the treatment of knee osteoarthritis: A systematic review of clinical evidence. *Stem Cells Int.* 2019; 2019: 1735242. doi: 10.1155/2019/1735242.
10. *Wang Z, Wang L, Su X, Pu J, Jiang M, He B.* Rational transplant timing and dose of mesenchymal stromal cells in patients with acute myocardial infarction: a meta-analysis of randomized controlled trials. *Stem Cell Res Ther.* 2017; 8 (1): 1–10. doi: 10.1186/s13287-016-0450-9.
11. *Zhidkova OV.* Vzaimodejstvie mezenhimal'nyh stromal'nyh i endotelial'nyh kletok v usloviyah ponizhennogo soderzhaniya kisloroda i provospalitel'noj aktivacii. [Dissertation]. Moscow, 2020; 24.
12. *De Becker A, Riet IV.* Homing and migration of mesenchymal stromal cells: How to improve the efficacy of cell therapy? *World Stem Cells*. 2016; 8 (3): 73–87. doi: 10.4252/wjsc.v8.i3.73.
13. *Heirani-Tabasi A, Toosi S, Mirahmadi M, Mishan MA, Bidkhori HR, Bahrami AR et al.* Chemokine receptors expression in MSCs: Comparative analysis in different sources and passages. *Tissue Eng Regen Med.* 2017; 14 (5): 605–615. doi: 10.1007/s13770-017-0069-7.
14. *Lin W, Xu L, Zwingenberger S.* Mesenchymal stem cells homing to improve bone healing. *J Orthop Translat.* 2017; 9: 19–27. doi: 10.1016/j.jot.2017.03.002.
15. *Wang M, Liang C, Hu H, Zhou L, Xu B, Wang X et al.* Intraperitoneal injection (IP), Intravenous injection (IV) or anal injection (AI)? Best way for mesenchymal stem cells transplantation for colitis. *Sci Rep*. 2016; 6 (1): 30696. doi: 10.1038/srep30696.
16. *Cui LL, Kerkelä E, Bakreen A, Nitzsche F, Andrzejewska A, Nowakowski A et al.* The cerebral embolism evoked by intra-arterial delivery of allogeneic bone marrow mesenchymal stem cells in rats is related to cell dose and infusion velocity. *Stem Cell Res Ther.* 2015; 6 (1): 11. doi: 10.1186/scrt544.
17. *Maiborodin IV, Maslov RN, Mikheeva TV, Khomenyuk SV, Maiborodina VI, Morozov VV et al.* Distribution of multipotent mesenchymal stromal cells and their detritus throughout the body after subcutaneous injection. *Journal of General Biology.* 2020; 81 (2): 96–107. [In Russ, English abstract]. doi: 10.31857/S0044459620020050.
18. *Aguado BA, Mulyasasmita W, Su J, Lampe KJ, Heilshorn SC.* Improving viability of stem cells during syringe needle flow through the design of hydrogel cell carriers. *Tissue Eng Part A.* 2012; 18 (7–8): 806–815. doi: 10.1089/ten.tea.2011.0391.
19. *Weiss AR, Dahlke MN.* Immunomodulation by mesenchymal stem cells (MSCs): mechanisms of action of li-

ving, apoptotic, and dead MSCs. *Front Immunol.* 2019; 10: 1191. doi: 10.3389/fimmu.2019.01191.
20. *Zhuang WZ, Lin YH, Su LJ, Wu MS, Jeng HY, Chang HC et al.* Mesenchymal stem/stromal cell-based therapy: mechanism, systemic safety and biodistribution for precision clinical application. *J Biomed Sci.* 2021; 28 (1): 28. doi: 10.1186/s12929-021-00725-7.
21. *Levy O, Kuai R, Siren EM, Bhere D, Milton Y, Nissar N et al.* Shattering barriers toward clinically meaningful MSC therapies. *Sci Adv.* 2020; 6 (30): eaba6884. doi: 10.1126/sciadv.aba6884.
22. *Kouroupis D, Sanjurjo-Rodriguez C, Jones E, Correa D.* Mesenchymal stem cell functionalization for enhanced therapeutic applications. *Tissue Eng Part B Rev*. 2019; 25 (1): 55–77. doi: 10.1089/ten.teb.2018.0118.
23. *Kabat M, Bobkov I, Kumar S, Grumet M.* Trends in mesenchymal stem cell clinical trials 2004–2018: Is efficacy optimal in narrow dose range? *Stem cells Transl Med*. 2020; 9 (1): 17–27. doi: 10.1002/sctm.19-0202.
24. *Ramalho BS, de Almeida FM, Sales CM, de Lima S, Martinez AMB.* Injection of bone marrow mesenchymal stem cells by intravenous or intraperitoneal routes is a viable alternative to spinal cord injury treatment in mice. *Neural Regen Res.* 2018; 13 (6): 1046–1053. doi: 10.4103/1673-5374.233448.
25. *Yousefi F, Ebtekar M, Soleimani M, Soudi S, Hashemi SM.* Comparison of *in vivo* immunomodulatory effects of intravenous and intraperitoneal administration of adipose-tissue mesenchymal stem cells in experimental autoimmune encephalomyelitis (EAE). *Int Immunopharmacol.* 2013; 17 (3): 608–616. doi: 10.1016/j.intimp.2013.07.016.
26. *Castelo-Branco MT, Soares ID, Lopes DV, Buongusto F, Martinusso CA, do Rosario A Jr et al.* Intraperitoneal but not intravenous cryopreserved mesenchymal stromal cells home to the inflamed colon and ameliorate experimental colitis. *PloS One.* 2012; 7 (3): e33360. doi: 10.1371/journal.pone.0033360.
27. *Yang H, Feng F, Fu Q, Xu S, Hao X, Qiu Y et al.* Human induced pluripotent stem cell-derived mesenchymal stem cells promote healing via TNF-α-stimulated gene-6 in inflammatory bowel disease models. *Cell Death Dis*. 2019; 10 (10): 718. doi: 10.1038/s41419-019-1957-7.
28. *Gonçalves FC, Schneider N, Pinto FO, Meyer FS, Visioli F, Pfaffenseller B et al.* Intravenous vs intraperitoneal mesenchymal stem cells administration: what is the best route for treating experimental colitis? *World J Gastroenterol*. 2014; 20 (48): 18228–18239. doi: 10.3748/wjg.v20.i48.18228.
29. *Li C, Wu X, Tong J, Yang X, Zhao J, Zheng Q et al.* Comparative analysis of human mesenchymal stem cells from bone marrow and adipose tissue under xeno-free conditions for cell therapy. *Stem Cell Res Ther*. 2015; 6 (1): 55. doi: 10.1186/s13287-015-0066-5.
30. *Heo JS, Choi Y, Kim HS, Kim HO.* Comparison of molecular profiles of human mesenchymal stem cells derived from bone marrow, umbilical cord blood, placenta and adipose tissue. *Int J Mol Med*. 2016; 37 (1): 115–125. doi: 10.3892/ijmm.2015.2413.
31. *Zhang K, Jiang IY, Wang B, Li T, Shang D, Zhang X.* Mesenchymal stem cell therapy: a potential treatment targeting pathological manifestations of traumatic brain injury. *Oxid Med Cell Longev*. 2022; 2022: 4645021. doi: 10.1155/2022/4645021.
32. *Sala E, Genua M, Petti L, Arena V.* Mesenchymal stem cells reduce colitis in mice via release of TSG6, independently of their localization to the intestine. *Gastroenterol.* 2015; 149 (1): 163–176. doi: 10.1053/j.gastro.2015.03.013.
33. *Braid LR, Wood CA, Wiese DM, Ford BN.* Intramuscular administration potentiates extended dwell time of mesenchymal stromal cells compared to other routes. *Cytotherapy.* 2018; 20 (2): 232–244. doi: 10.1016/j.jcyt.2017.09.
34. *Arutyunyan IV, Fatkhudinov TK, Elchaninov FV, Makarov AV, Vasyukova OA, Usman NYu et al.* Investigation of the mechanisms of therapeutic activity of allogeneic multipotent mesenchymal umbilical cord stromal cells in a rat hind limb ischemia model. *Genes and Cells.* 2018; 13 (1): 82–89. [In Russ, English abstract]. doi: 10.23868/201805010.
35. *Fu Y, Karbaat L, Wu L, Leijten J, Both SK, Karperien M.* Trophic effects of mesenchymal stem cells in tissue regeneration. *Tissue Eng Part B Rev*. 2017; 23 (6): 515–528. doi: 10.1089/ten.teb.2016.0365.
36. *Kalinina YuA, Gilerovich EG, Korzhevsky DE.* Astrocytes and their involvement in the mechanisms of therapeutic action of multipotent mesenchymal stromal cells in ischemic brain injury. *Genes and Cells.* 2019; 14 (1): 33–40. [In Russ, English abstract]. doi: 10.23868/201903004.
37. A*leksandrov VN, Kamilova TA, Martynov BV, Kalyuzhnaya LI.* Kletochnaya terapiya pri ishemicheskom insul'te. *Bulletin of the Russian Military Medical Academy*. 2013; 43 (3): 199–205. [In Russ].
38. *Kotkas IE, Zemlyanoy VP.* The effectiveness of the use of stem cells in the treatment of liver cirrhosis (experimental study). *Tavrichesky medico-biological bulletin.* 2020; 23 (1): 54–61. [In Russ, English abstract]. doi: 10.37279/2070-8092-2020-23-1-54-61.
39. *Maklakova IYu, Grebnev DYu, Yusupova VCh, Primakova EA.* Study of MMSC homing after liver resection. *Pathological Physiology and Experimental Therapy*. 2019; 63 (1): 40–45. [In Russ, English abstract]. doi: 10.25557/0031-2991.2019.01.40-45.
40. *Doroshenko OS, Prokopova AV, Gostyukhina AA.* Biochemical parameters of blood serum in rats with alloxan-induced diabetes and its correction by bone marrow cells. *Current issues of fundamental and clinical medicine: abstracts of the report of a scientific conference*. Tomsk, 2020: 480–483.
41. *Chen Y, Li J, Ma B, Li N, Wang S, Sun Z et al.* MSC-derived exosomes promote recovery from traumatic brain injury via microglia/macrophages in rat. *Aging.* 2020; 12 (18): 18274–18296. doi: 10.18632/aging.103692.
42. *Matthay MA, Pati S, Lee JW.* Concise review: mesenchymal stem (stromal) cells: biology and preclinical evidence for therapeutic potential for organ dysfunction

following trauma or sepsis. *Stem Cells*. 2017; 35 (2): 316–324. doi: 10.1002/stem.2551.

43. *Nitkin CR, Rajasingh J, Pisano C, Besner GE, Thébaud B, Sampath V.* Stem cell therapy for preventing neonatal diseases in the 21th century: current understanding and challenges. *Pediatr Res.* 2019; 87 (2): 265–276. doi: 10.1038/s41390-019-0425-5.
44. *Hlebokazov F, Dakukina T, Potapnev M, Kosmacheva S, Moroz L, Misiuk N et al.* Clinical benefits of single vs repeated courses of mesenchymal stem cell therapy in epilepsy patients. *Clin Neurol Neurosurg.* 2021; 207: 106736. doi: 10.1016/j.clineuro.2021.106736.
45. *Grégoire C, Lechanteur C, Briquet A, Baudoux É, Baron F, Louis E, Beguin Y.* Review article: mesenchymal stromal cell therapy for inflammatory bowel diseases. *Aliment Pharmacol Ther*. 2017; 45 (2): 205–221. doi: 10.1111/apt.13864.
46. *Elgaz S, Kuçi Z, Kuçi S, Bönig H, Bader P.* Clinical use of mesenchymal stromal cells in the treatment of acute graft-versus-host disease. *Transf Med Hemother.* 2019; 46 (1): 27–34. doi: 10.1159/000496809.
47. *Sergienko NV, Naletova EN.* Vliyanie kletochnoj terapii na biohimicheskie markery serdechnoj nedostatochnosti u pacientov s ishemicheskoj bolezn'yu serdca. *Nauchno-prakticheskij vestnik "Chelovek i ego zdorov'e"*. 2016; (1): 50–56. [In Russ].
48. *Smolyaninov AB, Ivolgin DA, Aizenshtadt AA.* Mesenchymal stem cells: perspectives of cardiologic application. *Cardiological Bulletin*. 2013; 8 (2): 5–11. [In Russ, English abstract].
49. *Andrzejewska A, Dabrowska S, Lukomska B, Janowski M.* Mesenchymal stem cells for neurological disorders. *Adv Sci*. 2021; 8 (7): 2002944. doi: 10.1002/advs.202002944.
50. *Tian C, Wang X, Wang X, Wang L, Wang X, Wu S, Wan Z.* Autologous bone marrow mesenchymal stem cell therapy in the subacute stage of traumatic brain injury by lumbar puncture. *Exp Clin Transplant.* 2013; 11 (2): 176–181. doi: 10.6002/ect.2012.0053.
51. *Viet QHN, Nguyen VQ, Le Hoang DM, Thi THP, Tran HP, Thi CHC.* Ability to regulate immunity of mesenchymal stem cells in the treatment of traumatic brain injury. *Neurol Sci.* 2022; 43 (3): 2157–2164. doi: 10.1007/s10072-021-05529-z.
52. *Zhang Z, Wang FS.* Stem cell therapies for liver failure and cirrhosis. *J Hepatol.* 2013; 59 (1): 183–185. doi: 10.1016/j.jhep.2013.01.018.
53. *Kotkas IE, Enukashvili NI, Asadulayev SM, Chubar AV*. Autologous mesenchymal stem cells in treatment of liver cirrhosis: evaluation of effectiveness and visualization method. *Science & Innovations in Medicine*. 2020; 5 (3): 197–203. [In Russ, English abstract]. doi: 10.35693/2500-1388-2020-5-3-197-203.
54. *Konev VA, Labutin DV, Bozhkova SA.* Experimental justification for clinical application of bone growth stimulators in traumatology and orthopaedics (a review). *Siberian Medical Review*. 2021; 4 (130): 5–17. [In Russ, English abstract]. doi: 10.20333/25000136-2021-4-5-17.
55. *Chebotareva AA.* Influence of intact and apoptosis-induced mesenchymal stem cells on the dynamics of apoptosis in the renal tissue in experimental acute kidney injury. *Bulletin of new medical technologies*. 2016; 23 (4): 88–93. [In Russ, English abstract]. doi: 10.12737/23855.
56. *Demyanenko EV, Glukhov AI, Gryzunova GK.* Effect of mesenchymal stem cells on apoptosis rates in the renal parenchyma under experimental stress. *Acta Biomedica Scientifica*. 2019; 4 (1): 138–142. [In Russ, English abstract]. doi: 10.29413/ABS.2019-4.1.21.
57. *Shakouri-Motlagh A, O'Connor AJ, Brennecke SP, Kalionis B, Heath DE.* Native and solubilized decellularized extracellular matrix: A critical assessment of their potential for improving the expansion of mesenchymal stem cells. *Acta Biomater.* 2017; 55: 1–12. doi: 10.1016/j.actbio.2017.04.014.
58. *Galipeau J, Sensebe L.* Mesenchymal stromal cells: clinical challenges and therapeutic opportunities. *Cell Stem Cell*. 2018; 22: 824–833. doi: 10.1016/j.stem.2018.05.004.
59. *Aleinikova NE, Chizhik VA, Boyko AV, Nizhegorodova DB, Zafranskaya MM, Ponomarev VV.* Experience in the use of cell therapy for Parkinson's disease: the effectiveness of minimally invasive transplantation methods. *Science and Health*. 2021; 23 (2): 81–91. [In Russ, English abstract]. doi: 10.34689/SH.2021.23.2.008.

The article was submitted to the journal on 29.08.2023

DOI: 10.15825/1995-1191-2024-2-135-144

CHALLENGES OF OBTAINING CULTURED CORNEAL ENDOTHELIAL CELLS FOR REGENERATIVE PURPOSES

D.S. Ostrovskiy[1], S.A. Borzenok[1, 2], B.E. Malyugin[1, 2], O.P. Antonova[1], M.Kh. Khubetsova[1], T.Z. Kerimov[1, 2]

[1] Fyodorov Eye Microsurgery Complex, Moscow, Russian Federation
[2] Moscow State University of Medicine and Dentistry, Moscow, Russian Federation

Human posterior corneal epithelium (corneal endothelium) has limited proliferative activity both *in vivo* and *in vitro*. Disease or dysfunction in these cells leads to impaired corneal transparency of varying degrees of severity, up to blindness. Currently, the only effective standard treatment for corneal endothelial dysfunction is transplantation of donor cornea that contains a pool of healthy and functionally active cells. However, there is a global shortage of donor corneas, which has led to an unmet clinical need and the fact that only 1 patient out of 10 in need receives surgical treatment. Therefore, creation of cellular constructs and artificial human corneas containing healthy endothelium is a very urgent challenge facing modern ophthalmic transplantology. This review presents the current state of affairs, challenges and prospects for obtaining cultured corneal endothelial cells (CECs) *in vitro* for transplantation purposes.

Keywords: cornea, endothelium, posterior epithelium, transplantation, cells.

INTRODUCTION

The human cornea is a transparent, avascular tissue that is nourished primarily through the anterior chamber moisture from corneal posterior epithelial cells (otherwise known as the endothelium). The corneal endothelium is a monolayer of hexagonal cells, lying on a specialized basement membrane called Descemet's membrane. Its main function is to maintain the cornea in a transparent, relatively dehydrated state by an important layer of metabolic pumps mediated through Na/K-ATPase [1], as well as barrier function through ZO-1 tight contact proteins [2].

It is known that human endothelial cell density is approximately 6000 cells/mm^2 during the first month of life, but gradually decreases with age, with an annual loss of approximately 0.6% of the total cell population per year [3]. In healthy individuals, this natural decrease in density does not result in any clinically significant impairment of corneal structure and function. In case of more active endothelial cell loss, for example, due to surgical interventions or ocular trauma, there may be partial restoration of the functional integrity of the endothelial layer due to cell migration and increased area of healthy cells [3].

When the CEC density falls below the critical threshold of approximately 500 cells per mm^2, the endothelium loses its ability to regulate corneal stromal hydration, which leads to clouding and, consequently, to reduced visual acuity [3]. According to the World Health Organization, corneal diseases in 2020 were the cause of reduced vision in 7% of the world's population, and the third leading cause of blindness and low vision [4]. Penetrating keratoplasty was the gold standard for treating corneal endothelial diseases for a long time. However, taking the first place today are selective methods of lamellar keratoplasty, namely posterior lamellar keratoplasty (PLK), in which the donor graft includes a stromal layer in addition to the endothelium and Descemet's membrane, and Descemet's membrane endothelial keratoplasty (DMEK), in which only the endothelium is transplanted with the underlying Descemet's membrane [5–7]. These techniques today give good clinical and functional outcomes, while surgical methods of obtaining grafts for lamellar keratoplasty continue to improve [8, 9]. However, organizational and medical and legal problems related to donation are still an issue in many countries around the world, which explains the shortage of donor material. On the other hand, postoperative endothelial cell loss after PLK and DMEK reaches 35% or more per year [10] and that leads to the need for repeat keratoplasty [11]. Repeat keratoplasty is the second leading indication for corneal transplantation in some developed countries of the world [12].

Thus, there is a real need to study alternative therapeutic pathways that would help to reduce dependence on donor material in the treatment of corneal endothelial diseases, as well as increase the viability of transplanted endothelial cells, both donor and recipient.

Corresponding author: Dmitriy Ostrovskiy. Address: 59a, Beskudnikovsky Bul'var, Moscow, 127486, Russian Federation. Phone: (499) 488-85-58. E-mail: dmitriy.ostrovskiy@gmail.com

PREPARATION AND *IN VITRO* CULTIVATION OF CORNEAL ENDOTHELIAL CELLS

One of the ways to solve the problem of corneal endothelial dysfunction is the use of cell culture [13]. However, these cells proliferate weakly, due to their origin from neural crest progenitor cells and contact inhibition and expression of TGF-b factor in the anterior chamber moisture, endothelial cells are overwhelmingly in the G1 phase of the cell cycle [14].

Despite this, there is ongoing global effort to obtain cultured CECs. Mannagh J. et al. published the first report on a successful endothelium culture in 1965. They suggested immersing isolated corneoscleral discs in 0.06% pronase, incubating them at 37 °C for 2 hours, and then scraping the endothelium cells. Cultivation was carried out in an Eagle medium with addition of 6 g/L glucose and 20% fetal bovine serum under standard conditions. Corneas of donors aged 28 and 70 years were used in the experiment. The authors visualized attached rounded conglomerates of cells after 48 hours, which took on a characteristic epithelial morphology after 72 hours. However, on day 10, the cells acquired a mesenchyme-like morphology, which indicated an epithelial-mesenchymal transition (EMT) [15].

It is important to note that there has never been a single protocol for isolation and cultivation, nor a standard formula for the nutrient medium and required additives. This is because the criteria for choosing donor material have been controversial since the first culture of endothelial cells was obtained. In this review, we present protocols that made it easier to produce CEC cultures that did not undergo EMT at least up to passages 2.

DONOR CHARACTERISTICS

Joyce and Zhu conducted a comparative analysis of the possibility of obtaining cultured CECs. They were able to present the donor selection criteria (Table) [16].

In addition, exclusion criteria included the presence of diabetes mellitus, glaucoma, generalized infection (sepsis), and chemotherapy in the donor [17]. However, according to several Russian authors, diabetes and cancer (without the intoxication stage) are the preferred choice of donor as they can drive endothelial cells to mitosis [18, 19].

Table

Donor selection criteria for corneal endothelial cell culture

Donor age	2–79 years
Endothelial cell density	1,800–3,891 cells/mm^2
Average time from death to corneal preservation	≤12 hours
Average time from death to introduction into experiment	≤7 days

Parekh and Ahmad also showed that endothelial cell culture could be obtained from donors with mean ages greater than 75 years and mean endothelial cell densities of 1943.75 ± 222.02 kl/mm^2. In order to force cell conglomerates to adhere to one another during cultivation, the scientists employed Rho-associated kinase (ROCK) inhibitors and viscoelastic [17].

CELL ISOLATION METHODS

All currently available corneal endothelium isolation methods can be divided into 4 groups: mechanical, mechanical with the use of enzymes; enzymatic and based on organ culturing.

In the first of these isolation methods, the endothelium is mechanically separated from Descemet's membrane and then transferred to the culture surface. Obtaining a uniform CEC culture is this method's undeniable advantage. However, the culture obtained by this technique has a very low cellular activity, and most of the obtained cells express markers of early apoptosis [20].

The enzymatic isolation method involves incubation of the corneoscleral disc with collagenase, dispase, ethylenediaminetetraacetic acid (EDTA) or trypsin solution, which inevitably leads to a heterogeneous cell culture containing corneal stromal fibroblast admixtures. Subsequent application of selective culture media does not yield the expected homogeneous CEC culture [21–23].

Combined use of mechanical and enzymatic methods provides a gentler isolation of CECs, but the use of enzymes requires a long incubation time, which leads to increased cellular injury [21–24].

Obtaining a heterogeneous cell culture due to the presence of underlying stromal layers is one of the drawbacks of the method of organ culture of Descemet's membrane with an adjacent endothelial layer. Furthermore, this technique yields a culture with incredibly low mitotic activity [21].

COMPOSITION OF NUTRIENT MEDIUM

A comparative analysis of basic nutrient media for obtaining cultured CECs was carried out by Peh G. et al. [25]. Such nutrient media as DMEM [26], OptiMEM [27], DMEM/F12 [28], and Ham's F12/M199 [29] were investigated. It was shown that when DMEM and DMEM/F12 were used, the cell culture lost mitotic activity after the second passage, the cells became larger and underwent apoptosis. In turn, the use of OptiMEM and Ham's F12/M199 promoted culture maintenance up to the third passage with preservation of mitotic activity and expression of specific epithelial markers, such as ZO-1 and Na/K ATP-ase. However, despite the presence of a typical immunocytochemical pattern, the cells lost their characteristic morphologic shape. According to Zhu et al., these changes are caused by the presence of the main fibroblast growth factor in the composition of the nutrient media, which helps stimulate EMT [30].

Today, the most effective CEC culture scheme involves the step-by-step use of different nutrient media, the so-called "two media method". The first one is a medium containing the basic serum-free endothelial medium Human Endothelial SFM, which is necessary for stabilization of the cell culture and maintenance of the characteristic phenotype. To activate the proliferative activity of cells, the culture is placed in the second medium, Ham's F12/M199. The use of this approach allows obtaining a more homogeneous cell culture with a characteristic morphology and preventing the occurrence of EMT [31]. Despite the advantages of this method, currently available preclinical and clinical trials are based on the use of DMEM/F12 [32] and OptiMEM [33] media.

CULTURE ADDITIVES

In addition to the choice of the basic nutrient medium, selection of factors that support CEC culture is highly relevant. Factors such as bFGF [35], LIF [36], EGF [36], NGF [37], endothelial cell growth supplement [38] and L-Ascorbic acid 2-phosphate [39] have been reported to promote endothelial growth. The use of LIF is thought to delay contact inhibition and, together with bFGF in a serum-free medium, promote endothelial cell proliferation with preservation of the characteristic phenotype [35].

In scholarly publications, there are reports on the production of a non-transformable CEC cell line brought to passage 224 [39]. In this study, the cells were maintained in a DMEM/F12-based nutrient medium supplemented with 20% fetal bovine serum, antibiotics, basic fibroblast growth factor (bFGF), epidermal growth factor (EGF), N-acetylglucosamine hydrochloride, glucosamine hydrochloride, chondroitin sulfate, oxidation and degradation products of chondroitin sulfate, carboxymethyl chitosan, bovine eye extract and culture supernatant of human corneal stromal cells in logarithmic phase. The presented result, as stated by the authors, was achieved due to the use of conditioned medium. Zhu et al. reported that the use of conditioned keratocyte medium in the logarithmic growth phase stimulates CEC proliferation better than the use of bone marrow-derived mesenchymal stem cells [40]. The presented data possibly show the potential of using conditioned media to stimulate CEC proliferation.

There is a known pharmacological approach to endothelial repair using ROCK inhibitor Y-27632 [41]. The use of ROCK in culturing helps to regulate cell shape and movement by affecting the cytoskeleton [42]. ROCK inhibitor Y-27632 has been shown to promote better cell adhesion, inhibit apoptosis, is non-toxic and does not alter the morphology of human corneal endothelium [43, 44]. ROCK has been proposed as an active agent for restoring endothelial cell loss *in vivo* in animal models [8].

According to a number of publications, EMT can be inhibited using low molecular weight inhibitors RhoA and ROCK inhibitor Y-27632. EMT may be triggered by destruction of intercellular junctions during culture and culture passing [40].

Consequently, further research into the peculiarities of production and long-term cultivation of endothelial cells are needed in order to optimize and standardize conditions for their cultivation with confirmation of functional properties and to further translate these studies into clinical practice.

SEEDING DENSITY OF ENDOTHELIAL CELLS

A very important factor is the initial seeding density of cells required to preserve their hexagonal morphology and expression of all markers. It has been shown in studies that such a density is 1×10^4 cells per cm^2 [45].

SUBSTRATE FOR CORNEAL ENDOTHELIAL CELLS CULTURE

In addition to selecting the proper composition of the nutrient medium, another unresolved issue is the choice of an optimal culture surface [45]. Many research teams use coatings such as type I collagen [46] and fibronectin [16], type IV collagen [48], chondroitin sulfate and laminin [49], matrigel [50], and FNC coating mix [27] to obtain 2D cultured CECs. It is worth noting that the use of type IV collagen as well as laminin-511 E8 [51], as components of the corneal Descemet's membrane, seems to be the best solution to obtain homogeneous CEC culture [40]. Silk fibroin is also well established. It has been shown that its use can support CEC growth with characteristic morphology and expression of specific markers [52].

3D CULTURE OF CORNEAL ENDOTHELIAL CELLS

Several authors use 3D cultured CECs because of its undeniable advantage in terms of introducing cell culture into the anterior chamber of the eye. The use of 3D spheroids has been shown to preserve expression of ZO-1 and Na/K ATPase. This culturing option helps to overcome EMT [53, 54].

CRYOPRESERVATION

It should be noted that cultured CECs are unique, and their production is an expensive procedure. Therefore, it is important to prevent the loss of valuable cell cultures by cryopreservation. The possibility of using the following media for CEC cryopreservation has been shown: Opti-MEM + 10% DMSO + 10% FBS; Cellbanker 2; Bambanker; KM Banker; Stem-Cellbanker; Bambanker hRM; ReproCryo DMSO Free RM. Among them, only the use of Bambanker hRM, which does not contain xeno additives, complies with the requirements of good manufacturing practice (GMP) [55].

CELL CHARACTERIZATION

Cell characterization is one of the main points of culturing. It involves both determination of the functional

properties of the culture and confirmation of its authenticity. Studying morphology is the simplest and most obvious method of cell identification.

Peh et al. [45] proposed the use of the cell circularity index to evaluate the shape of CECs in order to distinguish them from elongated fibroblasts.

$$\text{Cell circularity} = \frac{4\pi \cdot \text{Area}}{\text{Perimeter}^2}$$

where a value approaching 1.0 indicates a circular profile.

Currently, the main standard procedures for cell culture identification are techniques for studying their genotype and the markers specific to the cells under study.

GENOTYPE OF CORNEAL ENDOTHELIAL CELLS

To assess the genotype of CECs obtained *in vitro*, reverse transcription-polymerase chain reaction (RT-PCR) is used to study mRNA expression. It should be noted that at present, there is no clear set of investigated genes necessary to confirm endothelial cell species-specificity. The most frequently investigated genes in primary human CEC culture are Na+/K+ ATPase (ATPA1), ZO-1 (TJP1), collagen type 8 (COL8) and transporter family (SLC4). The study of the following genes is also sporadically reported: Vimentin, N-cadherin, CD166, Nestin, OCT 3/4, Snail, p27, a-SMA, and Laminin [56–58].

PHENOTYPE OF CORNEAL ENDOTHELIAL CELLS

To study the phenotype of CECs obtained *in vitro*, the immunocytochemical method of staining for the following markers – Na+/K+ ATP-ase, ZO-1, Ki67 – found in almost all scientific reports, is mainly used. These markers are accepted by many researchers as basic and characteristic for human CECs [59]. In addition, N- and E-cadherin, Actin, CD 166, CD44, CD77, nestin, vimentin, type IV and VIII collagen, cytokeratin 3, a-SMA, and GFAP are also determined.

CLINICAL MARKERS FOR TESTING THE HOMOGENEITY OF CULTURED CORNEAL ENDOTHELIAL CELLS

The first clinical panel of CD markers was proposed by Kinoshita et al[33]. In their study, it was shown that endothelial cells expressing CD166+ and not expressing CD44- CD133- CD105- CD24- CD26- have unaltered genotype and phenotype and can be used for cell therapy. The absence of CD44, CD24, and CD26 indicates the exclusion of aneuploid cells, thus linking phenotypic analysis to cellular karyotype [60, 61].

It is worth noting a number of studies that report that functioning endothelial cells express CD166, CD200, GPC4, HLA-ABC and PD-L1 [57, 62–64] and do not express a-SMA, CD9, CD24, CD24, CD26, CD44, CD73, CD90, CD105, CD133, SNAIL, ZEB1 and vimentin [64–66].

RUSSIAN INNOVATIONS IN OBTAINING ENDOTHELIAL CELLS

Today the process of procurement and transplantation of posterior corneal epithelial cells in the Russian Federation is limited by Federal Law No. 180 “On Biomedical Cell Products”. However, the use of suspension of uncultured CECs is a legitimate method of using these cells and does not conflict with the above Law. According to some reports, corneal endothelial transplantation can be considered as a variant of selective endothelial keratoplasty [24].

Up until now, a comparison of different methods of endothelial cell isolation in an *ex vivo* experiment has been carried out in Russia. It has been found that the modified enzymatic approach of isolating endothelial cells is more efficient and desirable than the modified mechanical isolation method: a statistically significant difference ($p < 0.05$) in the number of isolated cells and particle size was found via analysis of flow cytometry data. At the same time, there were no statistically significant differences in the viability of endothelial cells isolated using the modified enzymatic method compared to the modified mechanical method. Development of endothelial cell isolation protocols has fundamental and clinical significance, as demonstrated by the authors of this study [24].

APPLICATIONS OF IPS CELLS

In 2006, a group of scientists from Kyoto University led by Takahashi and Yamanaka first obtained induced pluripotent stem (iPS) cells, which were isolated from fibroblasts by epigenetic reprogramming [67].

Currently, development of protocols for obtaining corneal epithelial cells from iPS cells is still ongoing. For instance, Martínez et al. investigated the optimal time to start cultivating so that iPS cells may start differentiating into the phenotypes of corneal epithelial precursors – limbal epithelial stem cells [68]. Several methods for producing CECs from iPS cells have been published so far [69].

There are ongoing studies aimed at deriving keratocytes from iPS cells. For instance, well-known protocols outline a step-by-step keratocyte production scheme, where it is suggested to synthesize keratocytes through the stage of obtaining neural crest cells to prevent iPS cells from transitioning into fibroblast-like cells [70].

It is established that iPS techniques can be used to derive CECs from embryonic stem cells [21, 66, 71–73] and umbilical cord blood stem cells [74].

ANIMAL TESTING MODELS

When modeling cultured CEC transplantation, the choice of an animal model must be carefully considered.

It is not possible to use animals belonging to the rodent or hare groups since their corneal endothelium is capable of regeneration and proliferation in contrast to human CECs [75]. For effective evaluation of endothelial cell transplantation, it is possible to use other animal models, such as cats [76], pigs or primates [77], as there are similar morphofunctional features between the endothelial cells of these animals and humans. However, it should be noted that these animals are expensive to maintain and care for, obtaining all permits and ethical approvals is not easy either.

CLINICAL APPLICATIONS

Today, there are two known studies on the clinical application of cultured human CECs [32, 33]. It is worth noting that in both studies, patients with bullous keratopathy were treated. These works were confirmed by preclinical studies *in vivo*, as well as on cadaveric eye in an *ex vivo* model. In the work of Kinoshita et al., cells were administered by injection in combination with ROCK inhibitor at a 1×10^6 kL/mL concentration; Parikumar et al. [32] used a nanocomposite gel in the form of a sheet with cultured cells on its surface at 5×10^5 cl/mL.

However, the researchers did not evaluate the migration of the injected cells, which led to much debate about the efficacy and precise role of cell culture in favorable outcomes. It is also worth noting that neither group reported side effects in patients. Kinoshita et al. stated the theoretical possibility of the cell culture entering the trabecular meshwork and the development of glaucoma, but no patient was found to have this pathology during a two-year follow-up [33].

Kinoshita et al. also published the results of a five-year follow-up of 11 patients. Normal corneal transparency was restored in 10 out of 11 patients. In the study of the final endothelial cell density after 5 years, 1000 cells per mm^2 and 2000 cells per mm^2 were obtained in 8 and 2 patients, respectively. Central corneal thickness returned to normal in 10 of 11 patients (<630 μm) within 5 years [78].

CONCLUSION

Transplanted cultured CEC has the potential to quickly restore vision and lessen the requirement for donor tissue, which could drastically alter how corneal endothelial diseases are treated. Results from different research groups show that CEC transplantation can be used in the treatment of corneal endothelial disorders. However, there are a few challenges that must be resolved before this technology can be used in a clinical setting. One of these issues is optimizing the CEC culture isolation and cultivation protocols. In addition, it is necessary to develop experimental methods that would allow tracking and mapping transplanted cells to assess the success of cell therapy. There is also a need to establish objective methods for assessing corneal transparency. Currently, macrophotography using a slit lamp is accepted, but interpretation of resulting images is subjective and varies significantly from author to author.

The only work published to date on human endothelial cell transplantation is by Kinoshita et al. (2018). It was carried out with 8% fetal bovine serum used in endothelial cell culturing. The existence of xenogeneic products, however, poses a serious obstacle to the continued mass use of cell products. It is important to note that, as of right now, no data on the development of a protocol for obtaining and culturing endothelial cells without the use of xenogenic products have been published.

In our view, it is best to take into account progressive techniques of using cell cultures, namely 3D spheroids, since the introduction of cell suspension makes it difficult to trace the point cell engraftment and to assess its efficiency. Because biocompatible substrate carriers require a somewhat larger surgical incision than that required for injecting a cell culture, they may technically complicate surgery in the hospital due to the increased traumatic nature of the intervention. In addition, using various matrices may need their removal later on, which could lead to side effects and complications. Thus, in the aspect of the aforementioned, the complex of issues surrounding endothelial keratoplasty is highly relevant, although it has not been well investigated and calls for more investigation.

This work was supported by a grant (No. 22-25-00356) from the Russian Science Foundation.

The authors declare no conflict of interest.

REFERENCES

1. *Clausen MV, Hilbers F, Poulsen H*. The structure and function of the Na,K-ATPase isoforms in health and disease. *Front Physiol*. 2017; 8: 371.
2. *Hutcheon AEK, Zieske JD, Guo X*. 3D *in vitro* model for human corneal endothelial cell maturation. *Exp Eye Res*. 2019; 184: 183–191. doi: 10.1016/j.exer.2019.04.003.
3. *Yamamoto A, Tanaka H, Toda M, Sotozono C, Hamuro J, Kinoshita S et al*. A physical biomarker of the quality of cultured corneal endothelial cells and of the long-term prognosis of corneal restoration in patients. *Nat Biomed Eng*. 2019; 3 (12): 953–960. doi: 10.1038/s41551-019-0429-9.
4. *Robaei D, Watson S*. Corneal blindness: a global problem. *Clin Exp Ophthalmol*. 2014; Apr; 42 (3): 213–214. doi: 10.1111/ceo.12330.
5. *Malyugin BE, Moroz ZI, Borzenok SA, Drozdov IV, Ayba EE, Pashtaev AN*. Pervyy opyt i klinicheskie rezul'taty zadney avtomatizirovannoy posloynoy keratoplastiki (ZAPK) s ispol'zovaniem predvaritel'no vykroennykh konservirovannykh ul'tratonkikh rogovichnykh transplantatov. *Oftal'mokhirurgiya*. 2013; 3: 12–16.
6. *Malyugin BE, Shilova NF, Antonova OP, Anisimova NS, Shormaz IN*. Sravnitel'nyy analiz kliniko-

funktsional'nykh rezul'tatov zadney posloynoy keratoplastiki s ispol'zovaniem femtosekundnogo lazera i mikrokeratoma. *Oftal'mokhirurgiya*. 2019; 1: 20–26.
7. *Maliugin BÉ, Shilova NF, Anisimova NS, Antonova OP*. Transplantation of endothelium and Descemet's membrane. *Vestnik Oftalmologii*. 2019; 135 (1): 98–103. (In Russ.). https://doi.org/10.17116/oftalma201913501198.
8. *Rajan MS*. Surgical strategies to improve visual outcomes in corneal transplantation. [e-journal]. *Eye*. 2014; 28 (2): 196.
9. *Kalinnikov YuYu, Dinh THA, Zolotarevskiy AV, Kalinnikova SYu*. A new surgical approach to pre-Descemet's endothelial keratoplasty. *Vestnik Oftalmologii*. 2023; 139 (1): 55–66. (In Russ., In Engl.). doi: 10.17116/oftalma202313901155.
10. *Baydoun L, Tong CM, Tse WW*. Endothelial cell density after Descemet membrane endothelial keratoplasty: 1 to 5-year follow-up. *Am J Ophthalmol*. 2012; 154: 762–763.
11. *Tarantino-Scherrer JN, Kaufmann C, Bochmann F, Bachmann LM, Thiel MA.* Visual recovery and endothelial cell survival after Descemet stripping automated endothelial keratoplasty for failed penetrating keratoplasty grafts: A cohort study. *Cornea*. 2015; 34: 1024–1029.
12. Eye Bank Assotiation of America (EBAA). Eye banking statistical report. Washington, D.C., 2019. 110 p.
13. *Malyugin BE, Borzenok SA, Komakh YuA, Arbukhanova PM, Zheltonozhko AA, Saburina IN et al.* Modern possibilities of cell technologies in biological equivalent of artificial cornea constructing. Byulleten' SO RAMN. 2014; 34 (5): 43–47.
14. *Joyce NC, Navon SE, Roy S, Zieske JD.* Expression of cell cycle-associated proteins in human and rabbit corneal endothelium *in situ*. [e-journal]. *Investig Ophthalmol Vis Sci*. 1996; 37 (8): 1566.
15. *Mannagh JJ, Irving A*. Human corneal endothelium: Growth in tissue cultures. *Arch Ophthalmol*. 1965; 74: 847–849.
16. *Joyce NC, Zhu CC.* Human corneal endothelial cell proliferation: potential for use in regenerative medicine. *Cornea*. 2004; 23: S8–S19.
17. *Parekh M, Ahmad S, Ruzza A, Ferrari S*. Human Corneal Endothelial Cell Cultivation From Old Donor Corneas With Forced Attachment. *Sci Rep*. 2017; 7 (1): 142. doi: 10.1038/s41598-017-00209-5.
18. *Ronkina TI.* Zakonomernosti vozrastnyh izmenenij endoteliya rogovicy cheloveka v norme i patologii, vozmozhnosti aktivacii proliferacii endoteliya i ih znachenie v oftal'mologii. [Dissertation]. M., 1994; 50.
19. *Yavisheva TM.* Morfo-funkcional'nye osobennosti endoteliya rogovicy cheloveka v norme i patologii i otbor donorskogo materiala dlya keratoplastiki. [Dissertation]. M., 1990; 198.
20. *Bartakova A, Kuzmenko O, Alvarez-Delfin K, Kunzevitzky NJ, Goldberg JL.* A Cell Culture Approach to Optimized Human Corneal Endothelial Cell Function. *Invest Ophthalmol Vis Sci*. 2018; 59 (3): 1617–1629. doi: 10.1167/iovs.17-23637.
21. *Parekh M, Ferrari S, Sheridan C, Kaye S, Ahmad S.* Concise Review: An Update on the Culture of Human Corneal Endothelial Cells for Transplantation. *Stem Cells Transl Med*. 2016; 5 (2): 258–264. doi: 10.5966/sctm.2015-0181.
22. *Kazantsev AD, Ostrovskiy DS, Borzenok SA*. Experience of a new method of isolation and cultivation of human corneal endothelial cells *ex vivo*. *Vestnik Soveta molodykh uchenykh i spetsialistov Chelyabinskoy oblasti.* 2017; 3 (4 (19)): 50–52.
23. *Kazantsev AD, Ostrovskiy DS, Gerasimov MYu, Borzenok SA*. Izuchenie eksperimental'nykh metodov vydeleniya i kul'tivirovaniya kletok endoteliya rogovitsy cheloveka. *Sovremennye tekhnologii v oftal'mologii*. 2017; 4: 105–108.
24. *Malyugin BE, Borzenok SA, Ostrovskiy DS, Antonova OP, Hubetsova MH, Tsikarishvili NR.* Development of a method for obtaining a suspension of human corneal endothelial cells and its subsequent transplantation in an *ex vivo* experiment. *Fyodorov Journal of Ophthalmic Surgery*. 2022; 4: 56–64. doi: 10.25276/0235-4160-2022-4-56-64.
25. *Peh GS, Toh KP, Wu FY, Tan DT, Mehta JS*. Cultivation of human corneal endothelial cells isolated from paired donor corneas. *PLoS One*. 2011; 6 (12): e28310. doi: 10.1371/journal.pone.0028310.
26. *Ishino Y, Sano Y, Nakamura T, Connon CJ, Rigby H, Fullwood NJ, Kinoshita S.* Amniotic membrane as a carrier for cultivated human corneal endothelial cell transplantation. *Invest Ophthalmol Vis Sci*. 2004; 45: 800–806.
27. *Zhu C, Joyce NC*. Proliferative response of corneal endothelial cells from young and older donors. *Invest Ophthalmol Vis Sci*. 2004; 45: 1743–1751.
28. *Li W, Sabater AL, Chen YT, Hayashida Y, Chen SY, He H, Tseng SC.* A novel method of isolation, preservation, and expansion of human corneal endothelial cells. *Invest Ophthalmol Vis Sci*. 2007; 48: 614–620.
29. *Engelmann K, Friedl P*. Optimization of culture conditions for human corneal endothelial cells. *In Vitro Cell Dev Biol*. 1989; 25: 1065–1072.
30. *Zhu YT, Chen HC, Chen SY, Tseng SC.* Nuclear p120 catenin unlocks mitotic block of contact-inhibited human corneal endothelial monolayers without disrupting adherent junctions. *J Cell Sci*. 2012; 125 (Pt 15): 3636–3648.
31. *Peh GS, Chng Z, Ang HP, Cheng TY, Adnan K, Seah XY et al.* Propagation of human corneal endothelial cells: a novel dual media approach. *Cell Transplant*. 2015; 24 (2): 287–304. doi: 10.3727/096368913X675719.
32. *Parikumar P, Haraguchi K, Senthilkumar R.* Human corneal endothelial cell transplantation using nanocomposite gel sheet in bullous keratopathy. *Am J Stem Cells*. 2018; 7 (1): 18–24.
33. *Kinoshita S, Koizumi N, Ueno M, Okumura N, Imai K, Tanaka H et al*. Injection of cultured cells with a ROCK inhibitor for bullous keratopathy. *N Engl J Med*. 2018; 995–1003.
34. *Lee JG, Kay EP*. FGF-2-mediated signal transduction during endothelial mesenchymal transformation in corneal endothelial cells. *Exp Eye Res*. 2006; 83 (6): 1309–1316.
35. *Liu X, Tseng SC, Zhang MC, Chen SY, Tighe S, Lu WJ, Zhu YT*. LIF-JAK1-STAT3 signaling de-

lays contact inhibition of human corneal endothelial cells. *Cell Cycle*. 2015; 14 (8): 1197–1206. doi: 10.1080/15384101.2015.1013667.
36. *Zhu YT, Chen HC, Chen SY, Tseng SC.* Nuclear p120 catenin unlocks mitotic block of contact-inhibited human corneal endothelial monolayers without disrupting adherent junctions. *J Cell Sci*. 2012; 125: 3636–3648.
37. *Chen KH, Azar D, Joyce NC.* Transplantation of adult human corneal endothelium *ex vivo*: a morphologic study. *Cornea*. 2001; 20 (7): 731–737.
38. *Liu Y, Sun H, Hu M, Zhu M, Tighe S, Chen S et al*. Human Corneal Endothelial Cells Expanded *In Vitro* Are a Powerful Resource for Tissue Engineering. *Int J Med Sci*. 2017; 14 (2): 128–135. doi: 10.7150/ijms.17624.
39. *Yokoi T, Seko Y, Yokoi T, Makino H, Hatou S, Yamada M et al*. Establishment of functioning human corneal endothelial cell line with high growth potential. *PLoS One*. 2012; 7 (1): e29677. doi: 10.1371/journal.pone.0029677.
40. *Zhu YT, Tighe S, Chen SL, John T, Kao WY, Tseng SC.* Engineering of Human Corneal Endothelial Grafts. *Curr Ophthalmol Rep*. 2015; 3 (3): 207–217.
41. *Koizumi N, Okumura N, Ueno M.* Rho-associated kinase inhibitoreye drop treatment as a possiblemedicaltreatment for Fuchs corneal dystrophy. *Cornea*. 2013; 32 (8): 1167–1170. doi: 10.1097/ico.0b013e318285475d.
42. *Okumura N, Kinoshita S, Koizumi N.* The Role of Rho Kinase Inhibitors in Corneal Endothelial Dysfunction. *Curr Pharm Des*. 2017; 23 (4): 660–666. doi: 10.2174/1381612822666161205110027.
43. *Galvis V, Tello A, Fuquen JP, Rodríguez-Barrientos CA, Grice JM*. ROCK Inhibitor (Ripasudil) as Co-adjuvant After Descemetorhexis Without an Endothelial Graft. *Cornea*. 2017; 36 (12): e38–e40. doi: 10.1097/ICO.0000000000001381.
44. *Bi YL, Zhou Q, Du F, Wu MF, Xu GT, Sui GQ.* Regulation of functional corneal endothelial cells isolated from sphere colonies by Rho associated protein kinase inhibitor. *Exp Ther Med*. 2013; 5: 433–437.
45. *Peh GS, Toh KP, Ang HP, Seah XY, George BL, Mehta JS.* Optimization of human corneal endothelial cell culture: density dependency of successful cultures *in vitro*. *BMC Research Notes.* 2013; 6: 176.
46. *Ostrovskiy DS, Gerasimov MYu, Khubetsova MKh, Kazantsev AD, Borzenok SA.* Kul'tivirovanie kletok zadnego epiteliya rogovitsy cheloveka s ispol'zovaniem biopokrytiya kollagena I tipa. *Geny i kletki*. 2019; 14 (S): 174.
47. *Malyugin BE, Borzenok SA, Saburina IN, Repin VS, Kosheleva NV, Kolokol'tsova TD i dr.* Razrabotka bioinzhenernoy konstruktsii iskusstvennoy rogovitsy na osnove plenochnogo matriksa iz spidroina i kul'tivirovannykh kletok limbal'noy zony glaznogo yabloka. *Oftal'mokhirurgiya*. 2013; 4: 89–97.
48. *Zhu YT, Hayashida Y, Kheirkhah A, He H, Chen SY, Tseng SC.* Characterization and comparison of intercellular adherent junctions expressed by human corneal endothelial cells *in vivo* and *in vitro*. *Invest Ophthalmol Vis Sci*. 2008; 49 (9): 3879–3886.
49. *Engelmann K, Böhnke M, Friedl P.* Isolation and long-term cultivation of human corneal endothelial cells. *Invest Ophthalmol Vis Sci*. 1988; 29 (11): 1656–1662.
50. *Miyata K, Drake J, Osakabe Y, Hosokawa Y, Hwang D, Soya K et al*. Effect of donor age on morphologic variation of cultured human corneal endothelial cells. *Cornea*. 2001; 20 (1): 59–63.
51. *Okumura N, Kakutani K, Numata R, Nakahara M, Schlötzer-Schrehardt U, Kruse F et al*. Laminin-511 and -521 enable efficient *in vitro* expansion of human corneal endothelial cells. *Invest Ophthalmol Vis Sci*. 2015; 56 (5): 2933–2942.
52. *Vázquez N, Rodríguez-Barrientos CA, Aznar-Cervantes SD, Chacón M, Cenis JL, Riestra AC et al*. Silk Fibroin Films for Corneal Endothelial Regeneration: Transplant in a Rabbit Descemet Membrane Endothelial Keratoplasty. *Invest Ophthalmol Vis Sci*. 2017; 58 (9): 3357–3365. doi: 10.1167/iovs.17-21797.
53. *Audrey EK, Hutcheon James D, Xiaoqing G.* 3D *In Vitro* Model for Human Corneal Endothelial Cell Maturation. *Exp Eye Res*. 2019; 184: 183–191.
54. *Ostrovskiy DS, Kazantsev AD, Komakh YuA, Malyugin BE, Borzenok SA.* Poluchenie kul'tury kletok zadnego epiteliya rogovitsy cheloveka dlya transplantatsii. *Russian Journal of Transplantology and Artificial Organs*. 2018; 20 (S1): 157.
55. *Okumura N, Kagami T, Watanabe K, Kadoya S, Sato M, Koizumi N.* Feasibility of a cryopreservation of cultured human corneal endothelial cells. *PLoS One*. 2019; 14 (6): e0218431. doi: 10.1371/journal.pone.0218431.
56. *Chen Y, Huang K, Nakatsu MN, Xue Z, Deng SX, Fan G.* Identification of novel molecular markers through transcriptomic analysis in human fetal and adult corneal endothelial cells. *Hum Mol Genet*. 2013; 22: 1271–1279.
57. *Dorfmueller S, Tan HC, Ngoh ZX, Toh KY, Peh G, Ang HP et al*. Isolation of a recombinant antibody specific for a surface marker of the corneal endothelium by phage display. *Nat Publ Gr*. 2016; 6: 1–12.
58. *Bartakova A, Alvarez-Delfin K, Weisman AD, Salero E, Raffa GA, Merkhofer RM et al*. Novel identity and functional markers for human corneal endothelial cells. *Invest Ophthalmol Vis Sci*. 2016; 57: 2749–2762.
59. *Kazantsev AD, Ostrovskiy DS, Gerasimov MYu, Borzenok SA*. Razrabotka protokola fenotipirovaniya kletok zadnego epiteliya rogovitsy kadavernykh glaz cheloveka. *Sovremennye tekhnologii v oftal'mologii*. 2018; 4: 158–162.
60. *Hamuro J, Ueno M, Toda M, Sotozono C, Montoya M, Kinoshita S.* Cultured human corneal endothelial cell aneuploidy dependence on the presence of heterogeneous subpopulations with distinct differentiation phenotypes. *Invest Ophthalmol Vis Sci*. 2016; 57: 4385–4392.
61. *Toda M, Ueno M, Hiraga A, Asada K, Montoya M, Sotozono C et al*. Production of homogeneous cultured human corneal endothelial cells indispensable for innovative cell therapy. *Invest Ophthalmol Vis Sci*. 2017; 58: 2011–2020.
62. *Cheong YK, Ngoh ZX, Peh GS, Ang HP, Seah XY, Chng Z et al*. Identification of cell surface markers glypican-4 and CD200 that differentiate human corneal endotheli-

um from stromal fibroblasts. *Invest Ophthalmol Vis Sci*. 2013; 54: 4538–4547.
63. *Okumura N, Hirano H, Numata R, Nakahara M, Ueno M, Hamuro J et al*. Cell surface markers of functional phenotypic corneal endothelial cells. *Invest Ophthalmol Vis Sci.* 2014; 55: 7610–7618.
64. *Ueno M, Asada K, Toda M, Hiraga A, Montoya M, Sotozono C et al*. Micro RNA profiles qualify phenotypic features of cultured human corneal endothelial cells. *Invest Opthalmol Vis Sci*. 2016; 57: 5509.
65. *Ueno M, Asada K, Toda M, Nagata K, Sotozono C, Kosaka N et al*. Concomitant evaluation of a panel of exosome proteins and MIRS for qualification of cultured human corneal endothelial cells. *Invest Ophthalmol Vis Sci*. 2016; 57: 4393–4402.
66. *Wei Z, Batagov AO, Carter DRF, Krichevsky AM*. Fetal bovine serum RNA interferes with the cell culture derived extracellular RNA. *Sci Rep*. 2016; 6: 31175.
67. *Takahashi K, Yamanaka S.* Induction of pluripotent stem cells from mouse embryonic and adult fibroblast cultures by defined factors. *Cell*. 2006 Aug 25; 126 (4): 663–676. doi: 10.1016/j.cell.2006.07.024. Epub 2006 Aug 10. PMID: 16904174.
68. *Martínez García de la Torre RA, Nieto-Nicolau N, Morales-Pastor A, Casaroli-Marano RP*. Determination of the Culture Time Point to Induce Corneal Epithelial Differentiation in Induced Pluripotent Stem Cells. *Transplant Proc*. 2017; 49 (10): 2292–2295.
69. *Chakrabarty K, Shetty R, Ghosh A.* Corneal cell therapy: with iPSCs, it is no more a far-sight. *Stem Cell Res Ther*. 2018 Oct 25; 9 (1): 287.
70. *Naylor RW, McGhee CN, Cowan CA, Davidson AJ, Holm TM, Sherwin T.* Derivation of Corneal Keratocyte-Like Cells from Human Induced Pluripotent Stem Cells. *PLoS One*. 2016 Oct 28; 11 (10): e0165464.
71. *Lee JB, Song JM, Lee JE, Park JH, Kim SJ, Kang SM et al*. Available human feeder cells for the maintenance of human embryonic stem cells. *Reproduction*. 2004; 128 (6): 727–735.
72. *Chen P, Chen JZ, Shao CY, Li CY, Zhang YD, Lu WJ et al*. Treatment with retinoic acid and lens epithelial cell-conditioned medium *in vitro* directed the differentiation of pluripotent stem cells towards corneal endothelial cell-like cells. *Exp Ther Med*. 2015; 9 (2): 351–360.
73. *Zhang K, Pang K, Wu X.* Isolation and transplantation of corneal endothelial cell-like cells derived from in-vitro-differentiated human embryonic stem cells. *Stem Cells Dev*. 2014; 23 (12): 1340–1354.
74. *Joyce NC, Harris DL, Markov V, Zhang Z, Saitta B.* Potential of human umbilical cord blood mesenchymal stem cells to heal damaged corneal endothelium. *Mol Vis*. 2012; 18: 547–564.
75. *Mimura T, Yamagami S, Yokoo S, Araie M, Amano S.* Comparison of rabbit corneal endothelial cell precursors in the central and peripheral cornea. *Invest Ophthalmol Vis Sci*. 2005; 46 (10): 3645–3648. doi: 10.1167/iovs.05-0630.
76. *Van Horn DL, Sendele DD, Seideman S, Buco PJ.* Regenerative capacity of the corneal endothelium in rabbit and cat. *Invest Ophthalmol Vis Sci*. 1977; 16 (7): 597–613.
77. *Van Horn DL, Hyndiuk RA.* Endothelial wound repair in primate cornea. *Exp Eye Res*. 1975; 21 (2): 113–124. doi: 10.1016/0014-4835(75)90076-7.
78. *Numa K, Imai K, Ueno M, Kitazawa K, Tanaka H, Bush JD et al*. Five-Year Follow-up of First 11 Patients Undergoing Injection of Cultured Corneal Endothelial Cells for Corneal Endothelial Failure. *Ophthalmology*. 2021; 128 (4): 504–514. doi: 10.1016/j.ophtha.2020.09.002.

The article was submitted to the journal on 24.11.2023

DOI: 10.15825/1995-1191-2024-2-145-155

BIOMIMETIC APPROACH TO THE DESIGN OF ARTIFICIAL SMALL-DIAMETER BLOOD VESSELS

E.A. Nemets[1], Yu.V. Belov[1, 2], K.S. Kiryakov[1], N.V. Grudinin[1], V.K. Bogdanov[1], K.S. Filippov[1], A.O. Nikolskaya[1], I.Yu. Tyunyaeva[1], A.A. Vypryshko[1], V.M. Zaxarevich[1], Yu.B. Basok[1], V.I. Sevastianov[1, 2]

[1] Shumakov National Medical Research Center of Transplantology and Artificial Organs, Moscow, Russian Federation

[2] Institute of Biomedical Research and Technology, Moscow, Russian Federation

Objective: to create 2-mm diameter multilayer porous tubular scaffolds (PTS) with characteristics that resemble small-diameter native blood vessels in terms of characteristics. **Materials and methods.** PTS made of polycaprolactone (PCL, MM 80000) with a PCL-made sealing coat/layer with gelatin addition (PCL-gelatin) with a diameter of 2 mm were created by electrospinning (NANON-01A). Bioactive coating was applied to the PTS surface by sequential incubation in solutions of bovine serum albumin, heparin (Hp), and platelet lysate (PL). Cytotoxicity was investigated under conditions of direct contact of PTS with a monolayer of NIH/3T3 mouse fibroblasts. Viability of human umbilical vein endothelial cells (EA.hy926) was evaluated using Live/Dead® Viability/Cytotoxicity Kit. Permeability and blood flow parameters of the PTS implanted in the infrarenal section of the rat aorta were recorded using Doppler imaging. **Results.** A three-layer PTS construct with an inner diameter of 2 mm was developed. Its inner and outer layers were formed from 0.2 mL of PCL solution, and the middle sealing coat/layer was from 0.5 mL of PCL with addition of 30% (by weight of polymer) gelatin. Introduction of the sealing coat/layer reduced surgical porosity (SP) from 56.2 ± 8.7 mL/(cm^2·min) for a single-layer PTS made of pure PCL to 8.9 ± 2.6 mL/(cm^2·min) for a three-layer PTS. The resulting PTS demonstrated physicomechanical characteristics similar to those of native blood vessels; it also showed no cytotoxicity. Application of a bioactive coating of Hp and PL allowed for increased *in vitro* adhesion and proliferation of endothelial cells. The technique of implantation of 10 mm long fragments of three-layer PTS into the infrarenal section of a rat aorta was corrected, thus minimizing blood loss and narrowing the anastomosis site. In an acute experiment, it was proven that the prostheses were patent and that blood flow parameters (systolic and diastolic velocity, resistivity index) were close to the corresponding indicators of native rat aorta. **Conclusion.** The developed three-layer PTS constructs have low SP and physicomechanical properties close to those of native blood vessels. Bioactive coating improves the *in vitro* matrix properties of PTS relative to human endothelial cells. At short-term implantation into the aorta of experimental animals, PTS showed no early thrombosis, while blood flow parameters were close to those of native rat aorta. Thus, three-layer PTS with bioactive coating can be used as a scaffold for creation of *in situ* tissue-engineered construct of a small-diameter blood vessel.

Keywords: vascular prosthesis, electrospinning, tubular porous scaffold, polycaprolactone, gelatin, heparin, platelet lysate, endothelial cells, cytotoxicity, implantation, rat aorta.

INTRODUCTION

Biomimetic materials, which are biocompatible composite materials that mimic the structure and basic characteristics of various human tissues and/or organs, are widely used in regenerative medicine [1]. Recently, prostheses – biomimetic vascular grafts, including those with a diameter of less than 5 mm – have been quite often developed using additive technologies, mainly electrospinning and bioprinting [2].

When developing blood vessel prostheses (BVPs), it is necessary to maintain a certain balance between sufficiently high biological porosity, which is provided by the presence of pores with a pore size large enough to allow tissue sprouting due to cell migration into the BVP, and low surgical porosity (SP), which is a criterion for blood loss through the walls of the vascular prosthesis after its incorporation into the bloodstream. A water permeability of BVPs of more than 50 mL/(cm^2·min) at a pressure of 120 mmHg is a criterion that determines the need for additional efforts to reduce SP [3, 4].

A study on textile BVPs made of polyethylene terephthalate showed that regardless of pore size (20 μm to 100 μm), there is a correlation ($R^2 > 0.9$) between water permeability and blood loss, with blood loss being

Corresponding author: Evgeniy Nemets. Address: 1, Shchukinskaya str., Moscow, 123182, Russian Federation. Phone: (968) 840-47-45. E-mail: evgnemets@yandex.ru

about 10 times less than water permeability because of the higher viscosity and presence of formed elements [5].

Hydrogel coatings made of collagen or gelatin [6, 7], chondroitin sulfate [8], silk fibroin [9], sodium alginate [10], dextran derivatives [11], chitosan [12] and a number of others are actively used to reduce SP.

One of the significant problems of the sealing coat/layer for hydrogel-based vascular grafts is the insufficiently long functional life amidst contact with body media, which makes it necessary to apply additional crosslinking [13–15]. The crosslinking agents used in this approach, which belong to the class of aldehydes, epoxy compounds, isocyanates, etc. are toxic substances that are difficult to remove entirely from the coating volume. Their unpredictable behavior in the body makes it undesirable for them to enter the bloodstream.

In addition, a comparative study of BVPs fabricated using different techniques has shown that applying a coating that allows reducing SP is associated with undesirable changes in the physicomechanical properties of vascular grafts, in particular, an increase in Young's modulus [16].

Multilayer BVPs with highly porous outer and inner layers and a sealing layer located between them can be an alternative to hydrogel coatings. To form the sealing coat, they were dipped in aqueous solutions of gelatin [17] or a mixture of albumin and alginate [18]. The middle layer was also formed from densely packed fibers by electrospinning [19, 20].

Using the electrospinning method, we had previously developed a biocompatible highly porous scaffold made of polycaprolactone (PCL) in the form of tubes, with a diameter of 3 mm, which has physicomechanical properties that comparable to those of natural blood vessels [21]. Nonetheless, the minimal surgical porosity that was attained was close to the maximum permissible.

The aim of this work was to develop 2 mm diameter multilayer porous tubular scaffolds (PTSs) that would resemble small natural blood arteries in terms of characteristics.

MATERIALS AND METHODS

Fabrication of samples of porous tubular scaffolds

PTSs were obtained using a NANON-01A electrospinning machine (MECC CO, Japan) at 25 kV. The distance between the 18 G needle and the 2 mm diameter cylindrical electrode was 10 cm, the rod was rotated at 1000 rpm, and solutions were applied at a rate of 4 mL/h. The outer and inner PTS layers were formed with 0.2 mL of a 10% PCL solution (MM 80000, Sigma-Aldrich, USA) in methylene chloride (JSC ECOS-1, Russia), and the middle sealing coat/layer was formed with 0.5 mL of a 5% PCL-gelatin solution. The obtained scaffolds were dried at 37 °C for 2 hours and vacuumized at 20 mmHg and 37 °C for 24 hours.

Application of modifying coating

The PTS sample was sequentially treated with aqueous solutions of bovine serum albumin (1 mg/mL, 1.5–2 hours at 37 °C), heparin (Hp, 1 mg/mL, 1.5–2 hours at 37 °C), glutaraldehyde (1%, 18 hours at room temperature), then again with heparin (1 mg/mL, 1.5–2 hours, 37 °C). Between stages and at the end of coating, the PTS was washed three times in 100 mL of distilled water. The heparinized scaffold (PTS-Hp) was dried at 37 °C, vacuumized (10–20 mmHg at room temperature), and sterilized by gamma radiation at a 1.5 MRad dose.

Human platelet lysate (PL) solution was obtained by diluting a lyophilized preparation (Renam, Russia) with Hanks' Balanced Salt Solution (HBSS) containing no Ca^{2+} and Mg^{2+} ions (HBSS, Gibco® by Life Technologies™, SC) in the ratio of 1:9 followed by sterilization by filtration through a filter with a pore diameter of 0.22 μm.

Sterile PTS-Hp samples were treated with PL solution under aseptic conditions for 1 hour at 37 °C (PTS-PL) immediately before the experiment.

Surface morphology of blood vessel prostheses

A scanning electron microscope (SEM) JSM-6360LA (JEOL, Japan) was used to analyze the surface morphology of PTSs. The accelerating voltage was 5 kV. The conductive coating on the surface of the studied samples was formed by gold sputtering on the JFC-1600 unit (JEOL, Japan) for 40 seconds at a constant current of 5–7 mA.

Physicomechanical properties of blood vessel prostheses

To investigate the physical and mechanical properties of PTSs, tensile tester Shimadzu EZ Test EZ-SX (Shimadzu Corporation, Japan) was used at a tensile speed of 5 mm/min. The results obtained were processed in the TrapeziumX program, version 1.2.6, which allows calculating the elongation at break (%), tensile strength (N) and Young's modulus (MPa).

Cytotoxicity study

The cytotoxic effect of laboratory PTS samples was evaluated in accordance with the requirements of the

interstate standard GOST ISO 10993-5-2023 "Studies on cytotoxicity" [22].

Mouse fibroblast cell line NIH3T3 (American Type Culture Collection) was cultured in a CO_2 incubator at 37 °C, in a humidified atmosphere containing (5 ± 1) % CO_2 in culture vials (CELLSTAR® Greiner Bio-One, Germany) with complete growth medium DMEM containing high glucose (PanEco, Russia) and 10% fetal bovine serum (Biosera, Germany), antibiotic and antimycotic Anti-Anti (Gibco® by Life Technologies™, USA) and 2 mM glutamine (PanEco, Russia). Cells were suspended using TrypLE™ Express Enzyme dissociation reagent (Gibco® by Life Technologies™, UK). Cell count in the suspension was determined using a Goryaev chamber (MiniMed®, Russia). Fibroblasts were then seeded into flat-bottomed 24-well culture plates (CELLSTAR® Greiner Bio-One, Germany) at a seeding density of 7–12 × 10^4 cells per well and incubated for 24 hours at 37 °C in a humidified atmosphere containing (5 ± 1) % CO_2 until formation of (80 ± 10) % monolayer. The test PTS samples were placed directly on the surface of the fibroblast monolayer. At the end of incubation, the test samples were removed from the wells, washed with phosphate buffered saline (PBS), and 0.1% trypan blue solution (PanEco, Russia), which stains lysed cells and cells with damaged cell membranes, was added for 1–2 minutes. After removal of the dye and washing with PBS, the culture was assessed for morphological changes and decreased cell density using a fluorescence microscope.

To analyze the results, the following scale of the degree of cell reaction to direct contact with PTS was used:

0 means no lysis (no reaction);

1 means ≤20% of cells lysed (minor reaction);

2 means ≤50% of cells lysed (mild reaction);

3 means ≤70% of cells lysed (moderate reaction);

4 means >70% of cells lysed (strong reaction).

A non-cytotoxic material should have a reaction grade of "0".

Study of PTS interaction with endothelial cells

Immortalized human umbilical vein cell line, EA.hy926 (ATCC®CRL-2922™), from the American Type Culture Collection (ATCC), which have similarity with primary cultures [23, 24], were selected for *in vitro* study.

Sterile samples of unmodified and modified PTSs were placed on the bottom of a flat-bottomed 24-well culture plate (CELLSTAR® Greiner Bio-One, Germany), human endothelial cells (ECs) were plated at a seeding density of 5 × 10^4 cells/cm^2 under aseptic conditions and cultured in a CO_2 incubator under standard conditions for a selected time interval.

Human EC viability was assessed using Live/Dead® Viability/Cytotoxicity Kit (Molecular Probes® by Life Technologies™, USA): Dulbecco′s PBS containing 2 μM calcein AM and 4 μM EthD-1 was added to the wells of the plate after 15 minutes. The staining results were visualized using a Nikon Eclipse TS100 inverted fluorescence microscope (Japan), equipped with a Digital Sight DS-Vil digital camera (Nikon, Japan).

Metabolic activity of human ECs on the surface of PTS was evaluated using PrestoBlue™ HS Cell Viability Reagent (Invitrogen™ by Thermo Fisher Scientific, USA): 10% PrestoBlue™ Cell Viability Reagent was added to wells with the test samples and control (cell-free medium), after which the plate was incubated for 3 hours at 37 °C in a humidified atmosphere containing (5 ± 1) % CO_2. Changes in absorbance of the medium were recorded using a microplate reader as previously described at 570 nm and 600 nm wavelengths. The percentage of reduced PrestoBlue™ was calculated using formula (1):

$$\frac{117{,}216 \cdot A_{570\ Samp} - 80{,}586 \cdot A_{600\ Samp}}{155{,}677 \cdot A'_{600} - 14{,}652 \cdot A'_{570}} \times 100\%, \quad (1)$$

where 117,216 and 80,586 are the molar extinction coefficients for the oxidized form of PrestoBlue™ Vital Reagent at λ = 600 nm and λ = 570 nm, respectively; 155,677 and 14,652 are the molar extinction coefficients for the reduced form of the reagent at λ = 600 nm and λ = 570 nm, respectively; $A_{570\ Samp}$ and $A_{600\ Samp}$ are the absorbance of the test sample at λ = 600 nm and λ = 570 nm, respectively; A'_{570} and A'_{600} are the absorbance of the cell-free control sample at λ = 600 nm and λ = 570 nm, respectively.

Human EC count on the PTS surface was estimated using a calibration curve, linear in semi-logarithmic coordinates up to a concentration of human ECs of 0.8 × 10^5.

Implantation of a PTS fragment into the infrarenal aorta of a rat

Three-layer PTS with a diameter of 2 mm and length of 10 mm were implanted into the abdominal aorta of rats using the end-to-end technique. The anesthetized animal was fixed on the operating table in the supine position. Hair was removed from the anterior abdominal wall with a razor, the surgical field was treated with an antiseptic. Access to the abdominal aorta was performed by midline laparotomy. Next, the infrarenal aorta was isolated and the proximal part of the vessel was clamped below the renal arteries. The distal part was clamped above the trifurcation of the abdominal aorta. After clamping, the

infrarenal aorta was resected, proximal and then distal anastomoses with PTS were formed using atraumatic polypropylene suture 8-0. After initiating blood flow, hemostasis was monitored. At the final stage, layer-by-layer suturing of the surgical wound was performed with subsequent treatment of the sutures with antiseptic agent and anesthetic solution. After the surgery, the animals were kept in vivarium conditions with free access to food and water.

To confirm the patency of the implanted PTS, the study was performed on a Vivid E9 ultrasound machine (General Electric, USA) with WindowBlinds™ software (M OCX© Stardock) using sector (1.5–5 mHz) and linear (2.5–12 mHz) transducers and conductive gel Mediagel (Geltek, Russia). Zoletil (Virbac Sante Animale, France) was used for sedation of the test animals before dopplerometry, followed by shaving of the abdominal region with a veterinary trimmer. Aortic lumen diameter or PTS (d, cm), peak systolic velocity (Vps, m/s) and maximum end diastolic velocity (Ved, m/s) were measured, after which resistivity index was calculated according to formula (2).

$$RI = (Vps - Ved)/Vps \quad (2)$$

Statistical processing

Quantitative and statistical processing of data obtained was performed using Microsoft Excel 2007 application. All results are presented as mean value ± standard deviation. Differences were considered significant at $p < 0.05$ when the number of samples (n) ranged from 3 to 5.

RESULTS AND DISCUSSION

The lowest water permeability of our previously developed 3 mm diameter PCL-based PTS was quite high at 30.4 ± 1.5 mL/(cm^2·min) [20], which was still below the maximum permissible value of 50 mL/(cm^2·min). When switching to 2 mm diameter PTS, the water permeability of PCL-based PTS could not be reduced to satisfactory values, which determined the need for additional efforts to reduce SP. To address this problem, we proposed to form multilayer PTSs incorporating an inner sealing coat/layer made of PCL with gelatin addition.

Fig. 1 summarizes the results of the study of the effect of gelatin concentration in the sealing coat/layer on the water permeability of a 2 mm diameter three-layer PTS.

As can be seen from Fig. 1, water permeability decreased with increasing gelatin concentration, reaching values less than 10 mL/(cm^2·min) at 30% protein concentration. Attempts to increase the gelatin level above 30% resulted in a jump in the risk of delamination of the multilayer structure upon contact with water. As a result, a gelatin level of 30% (by weight relative to PCL) was chosen as the optimal concentration for formation of the sealing coat/layer.

Both surfaces of the triple-layer PTS exhibit a highly porous structure formed by fibers, several micrometers in diameter, with pores large enough to allow cell migration into the matrix (Fig. 2).

Table summarizes the physicomechanical characterization of small-diameter three-layer PTS with bioactive coating.

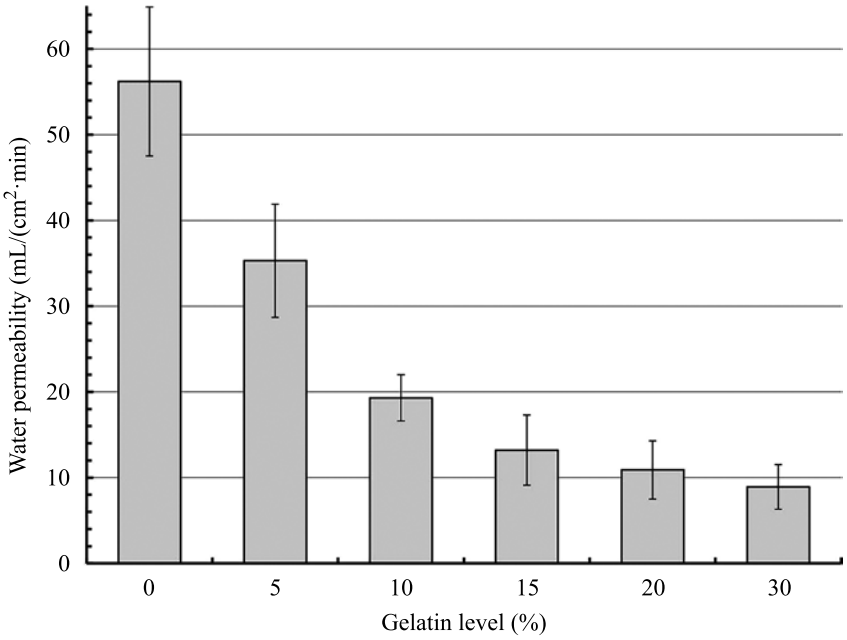

Fig. 1. Effect of gelatin levels in the sealing coat/layer on the water permeability of a 2 mm diameter three-layer PTS. Inner and outer layers are made from 0.2 mL of PCL, the middle sealing coat/layer is made from 0.5 mL of PCL-gelatin solution

As can be seen from Table, the three-layer PTS has physicomechanical properties comparable to the mechanical properties of blood vessels of similar diameter.

In the cytotoxicity test, a three-layer PTS with bioactive coating showed a level of "0" – no cytotoxicity.

Fig. 3 shows photographs of human EC culture of the EA.hy926 line 24 hours and 168 hours after seeding on the surface of culture plastic (CP) and the inner surface of PTS without modifying coating, modified with heparin only (PTS-Hp), and with bioactive coating from Hp and PL (PTS-PL). The CP surface was used to control the morphology and adequate growth of the investigated cell cultures.

At 24 hours after seeding, the inner surface of PTS-PL samples showed the highest number of adhered and spread ECs, compared to samples from unmodified PCL and PTS-Hp, which had substantially less number of adhered endothelial cells. It is important to note that a large number of non-spread and dead cells was observed on the inner surface of unmodified PTS; this finding appears to be connected to PCL's hydrophobic nature [13, 25, 26]. After 168 hours of culturing, an EC monolayer was formed on the CP surface and on the PTS-PL sample. In contrast, no EC monolayer was formed on the surface of either the heparinized sample or the unmodified control, no proliferation occurred, and there was a significant number of non-viable cells. Note that, despite hydrophilization of the surface of PCL-based PTS under the conditions of this experiment, heparin modification does not promote scaffold endothelialization *in vitro*.

Fig. 4 presents the results of the quantitative study of EC proliferation on the inner surface of the original and modified PTS.

As shown in Fig. 4, after 24 hours, EC count on the inner surface of the original, modified scaffolds differs slightly ($10.1 \pm 1.3 \times 10^3$ kL, $13.2 \pm 1.4 \times 10^3$ kL, and $16.7 \pm 1.1 \times 10^3$ kL for PCL, PCL-Hp, and PCL-PL, respectively). After 96 hours of cultivation, cell count on each scaffold variant uniformly increased approximately 2-fold. By the end of the period, PCL-PL increases 3.6-fold (to $60.4 \pm 1.8 \times 10^3$ kL), while EC count on the outer surface of the original and PCL-Hp increases 2.9-fold (to $29.1 \pm 1.9 \times 10^3$ kL and $32.0 \pm 1.4 \times 10^3$ kL, respectively). The difference in cell count on the inner

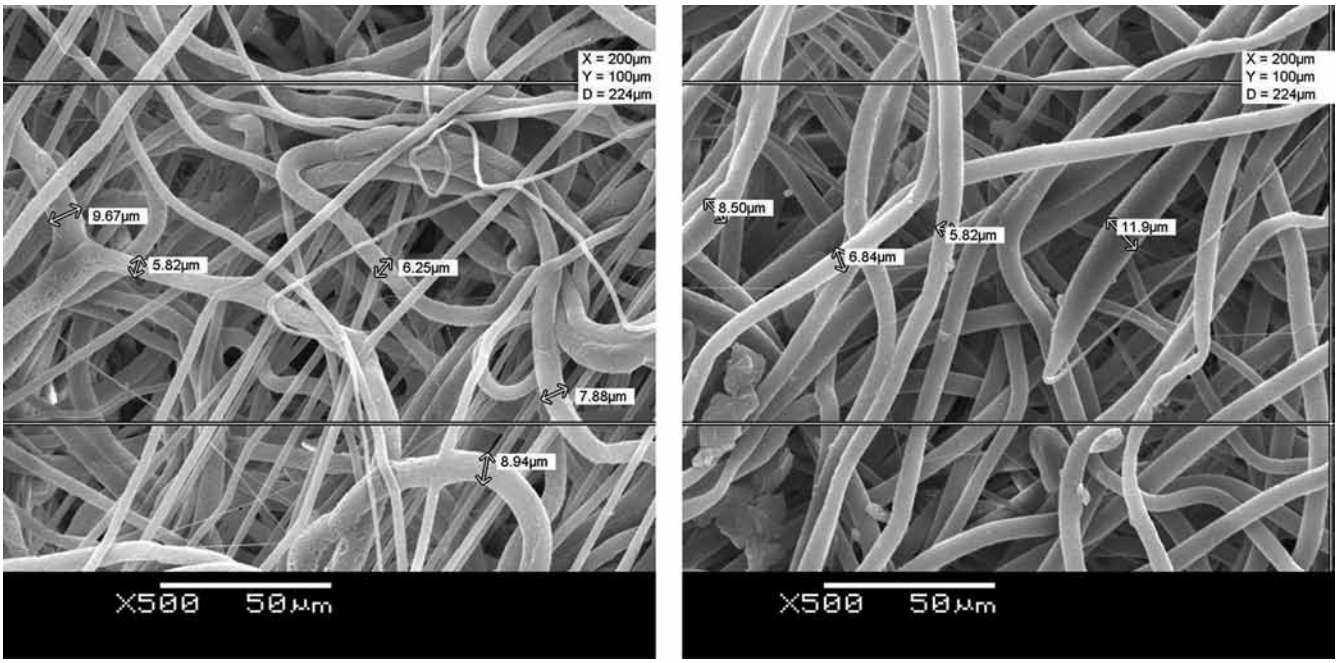

Inner surface **Outer surface**

Fig. 2. Surface microstructure of a three-layer PTS. Inner and outer layers are made from 0.2 mL of PCL, the middle sealing coat/layer is from 0.5 mL of PCL-gelatin solution

Table

Physicomechanical characteristics of three-layer scaffolds

	Young's modulus (MPa)	Tensile strength (N)	Elongation at break (%)
PTS, diameter 2 mm	6.6 ± 0.3	12.6 ± 3.2	412 ± 30
Rat aorta, diameter 2 mm	8.5 ± 2.2	2.0 ± 0.3	93 ± 16

surface of unmodified PCL and PCL-Hp is insignificant despite hydrophilization of the surface due to heparin immobilization.

Thus, the presence of PL in the modifying coating under the *in vitro* conditions of the experiment is a key factor in promoting adhesion, spreading and stimulating proliferation of endothelial cells (EA.hy926) on the inner surface of the scaffolds, increasing their matrix properties.

An *in vivo* study of the functional properties of small-diameter vascular grafts was conducted by prosthetizing the infrarenal section of the rat abdominal aorta with three-layer PTS that had a 2 mm inner diameter and a 10 mm length.

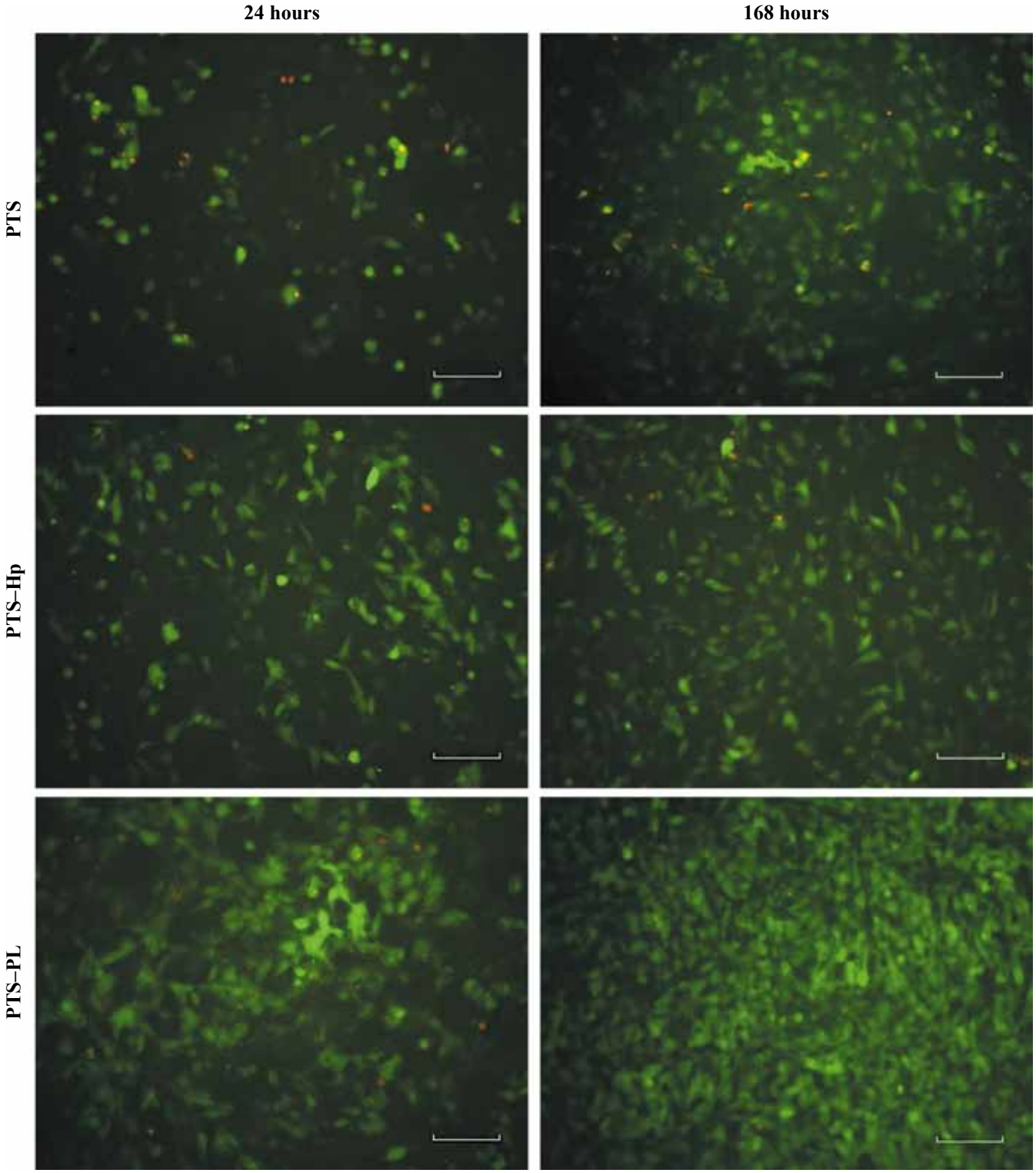

Fig. 3. Endothelial cell growth on the inner surface of PTS. Seeding density of 5×10^4 cells/cm^2. Live/Dead® Viability/Cytotoxicity Kit staining. Magnification 20×. Scale bar: 100 μm

The implantation technique was corrected. Initially, the artery was transected after clamping, and 6–8 interrupted sutures were used to produce direct anastomoses with the PTS. In order to minimize blood loss and narrow the anastomosis area, we tried to create oblique slices of the proximal and distal ends of the aorta with the formation of anastomoses by continuous locking sutures. As a result, we were able to optimize hemostasis and maintain ideal anastomosis diameter.

Doppler ultrasound was carried out to confirm PTS patency shortly after implantation (Fig. 5).

Fig. 6 shows Doppler ultrasound results for the implanted PTS. Implanted modified and unmodified PTS demonstrated similar blood flow parameters that were no different from those obtained for rat aorta.

Future *in vivo* studies are to be continued for up to 1 year with a detailed study of the neointima formation process involving histologic methods.

CONCLUSION

The three-layer PCL-based PTS constructs that were created, with a PCL-gelatin sealing coat/layer, have low SP and demonstrate physicomechanical properties that are close to those of native blood vessels. Application of bioactive coating based on Hp and PL improves the *in vitro* interaction of PTS with ECs. When implanted into the aorta of an experimental animal, PTS demonstrated

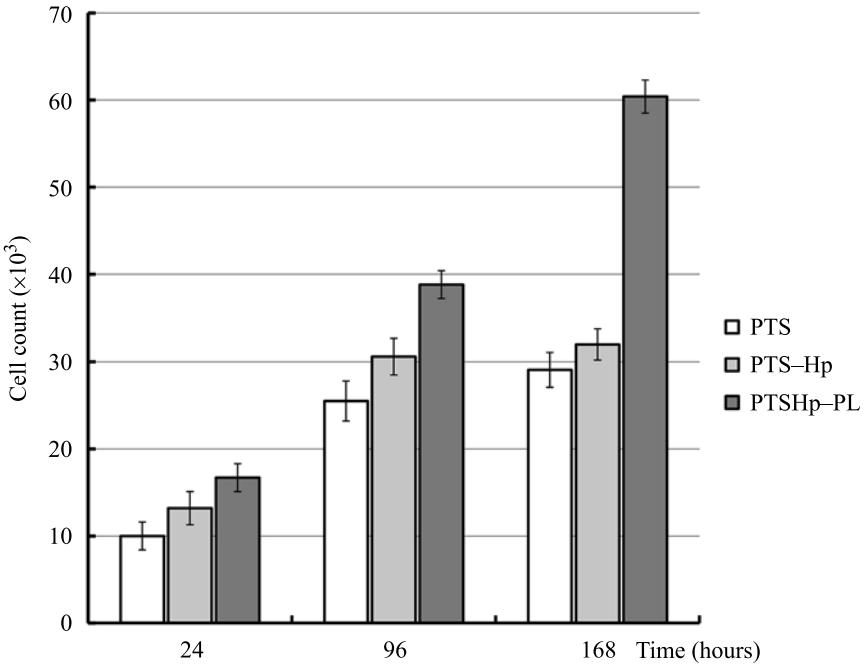

Fig. 4. Endothelial cell proliferation in the inner surface of PTS. Seeding density 5×10^4 cells/cm^2

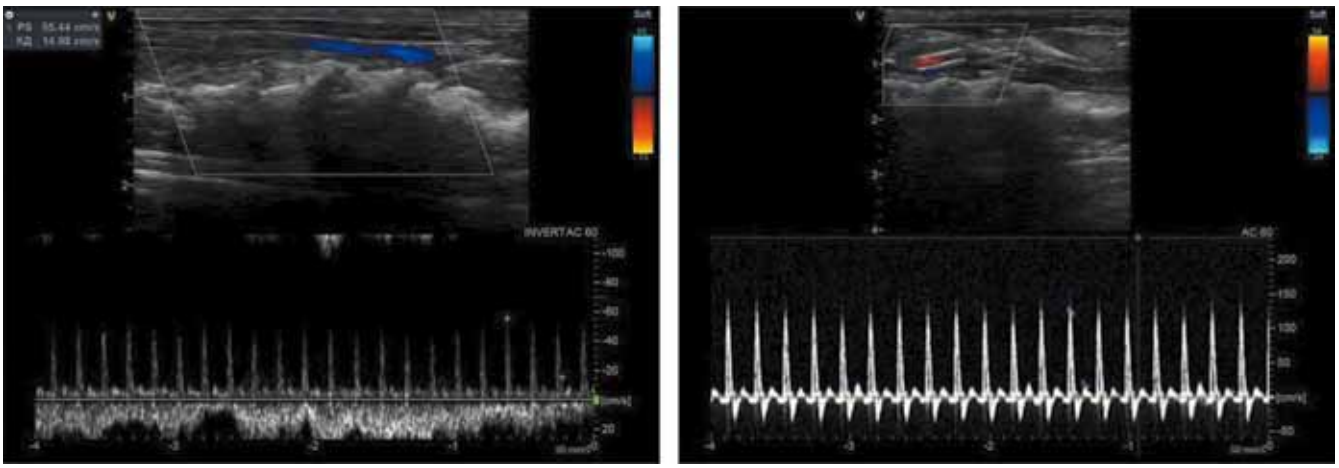

Unoperated rat (control) **PTS, 4 weeks after implantation**

Fig. 5. Doppler ultrasound of implanted coated PTS 4 weeks after implantation (typical measurement)

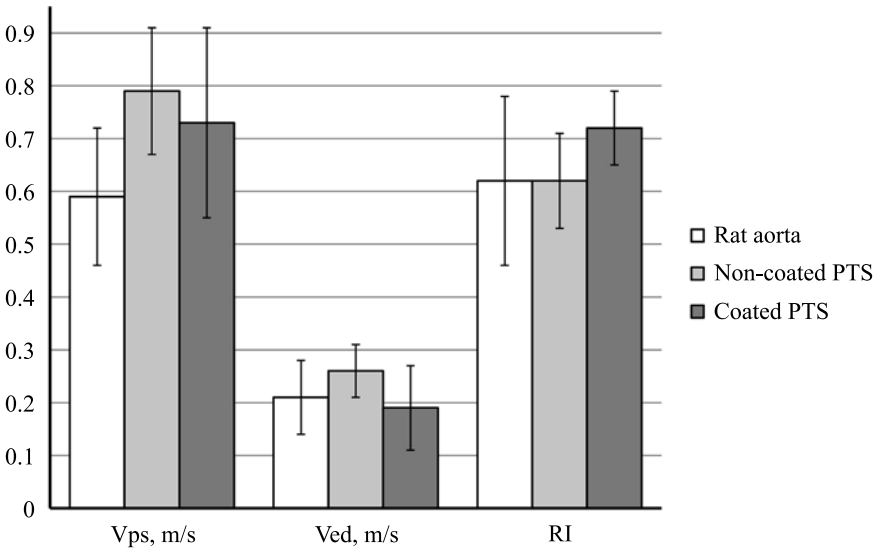

Fig. 6. Peak systolic velocity (Vps), diastolic velocity (Ved) and resistive index (RI) 4 weeks after PTS implantation (n = 6)

no early thrombosis, while blood flow parameters were close to those of the rat aorta. Thus, three-layer PTS with bioactive coating can be used as a scaffold to produce *in situ* tissue-engineered constructs of small-diameter blood vessels.

The authors are grateful to V.A. Surguchenko for participation in experiments with cell cultures, and to V.A. Ryzhikova for assistance in conducting Doppler ultrasound.

The authors declare no conflict of interest.

REFERENCES

1. *Das D, Noh I.* Overviews of Biomimetic Medical Materials. *Adv Exp Med Biol*. 2018; 1064: 3–24. doi: 10.1007/978-981-13-0445-3_1.
2. *Weekes A, Bartnikowski N, Pinto N, Jenkins J, Meinert C, Klein TJ.* Biofabrication of small diameter tissue-engineered vascular grafts. *Acta Biomater*. 2022 Jan 15; 138: 92–111. doi: 10.1016/j.actbio.2021.11.012.
3. *Wesolowski SA, Fries CC, Karlson KE, De Bakey M, Sawyer PN.* Porosity: primary determinant of ultimate fate of synthetic vascular grafts. *Surgery*. 1961; 50: 91–96.
4. *Lebedev LV, Plotnik LL, Smirnov AD.* Protezy krovenosnykh sosudov. L.: Meditsina, 1981; 192.
5. *Guan G, Yu C, Fang X, Guidoin R, King MW, Wang H, Wang L.* Exploration into practical significance of integral water permeability of textile vascular grafts. *J Appl Biomater Funct Mater.* 2021; 22808000211014007. doi: 10.1177/22808000211014007.
6. *Copes F, Pien N, Van Vlierberghe S, Boccafoschi F, Mantovani D.* Collagen-Based Tissue Engineering Strategies for Vascular Medicine. *Front Bioeng Biotechnol.* 2019; 7: 166. doi: 10.3389/fbioe.2019.00166.
7. *Fortin W, Bouchet M, Therasse E, Maire M, Héon H, Ajji A et al.* Negative *In Vivo* Results Despite Promising *In Vitro* Data With a Coated Compliant Electrospun Polyurethane Vascular Graft. *J Surg Res.* 2022; 279: 491–504. doi: 10.1016/j.jss.2022.05.032.
8. *Huang F, Sun L, Zheng J. In vitro* and *in vivo* characterization of a silk fibroin-coated polyester vascular prosthesis. *Artif Organs.* 2008; 12: 932–941. doi: 10.1111/j.1525-1594.2008.00655.x.
9. *Lee JH, Kim WG, Kim SS, Lee JH, Lee HB.* Development and characterization of an alginate-impregnated polyester vascular graft. *J Biomed Mater Res.* 1997; 36: 200–208. doi: 10.1002/(sici)1097-4636(199708)36:2<200::aid-jbm8>3.0.co;2-o.
10. *Lisman A, Butruk B, Wasiak I, Ciach T.* Dextran/Albumin hydrogel sealant for Dacron(R) vascular prosthesis. *J Biomater Appl.* 2014; 28: 1386–1396. doi: 10.1177/0885328213509676.
11. *Madhavan K, Elliott WH, Bonani W, Monnet E, Tan W.* Mechanical and biocompatible characterizations of a readily available multilayer vascular graft. *J Biomed Mater Res B Appl Biomater*. 2013; 101: 506–519. doi: 10.1002/jbm.b.32851.
12. *Nemets EA, Pankina AP, Surguchenko VA, Sevastianov VI.* Bistability and cytotoxicity of medical devices based on cross-linked biopolymers. *Russian Journal of Transplantology and Artificial Organs*. 2018; 20 (1): 79–85. (In Russ.). doi: 10.15825/1995-1191-2018-1-79-85.
13. *Glushkova TV, Ovcharenko EA, Rogulina NV, Klyshnikov KYu, Kudryavtseva YuA, Barbarash LS.* Dysfunction Patterns of Epoxy-Treated Tissue Heart Valves. *Kardiologiia*. 2019; 59 (10): 49–59. (In Russ.). doi: 10.18087/cardio.2019.10.n327.

14. *Hennink WE, van Nostrum CF.* Novel crosslinking methods to design hydrogels. *Adv Drug Deliv Rev.* 2002; 54: 13–36. doi: 10.1016/s0169-409x(01)00240-x.
15. *Novikova SP, Salokhedinova RR, Loseva SV, Nikolashina LN, Levkina AYu*. Analysis of physico-mechanical and structural characteristics of vascular prostheses. *Grudnaya i serdechno-sosudistaya khirurgiya*. 2012; 54 (4): 27–33.
16. *Popova IV, Stepanova AO, Sergeevichev DS, Akulov AE, Zakharova IS, Pokushalov AA et al.* Comparative study of three vascular grafts produced by electrospinning *in vitro* and *in vivo*. *Patologiya krovoobrashcheniya i kardiokhirurgiya*. 2015; 19 (4): 63–71.
17. *Chen X, Yao Y, Liu S, Hu Q.* An integrated strategy for designing and fabricating triple-layer vascular graft with oriented microgrooves to promote endothelialization. *J Biomater Appl*. 2021; 36: 297–310. doi: 10.1177/08853282211001006.
18. *Huang R, Gao X, Wang J, Chen H, Tong C, Tan Y, Tan Z.* Triple-Layer Vascular Grafts Fabricated by Combined E-Jet 3D Printing and Electrospinning. *Ann Biomed Eng*. 2018; 46 (9): 1254–1266. doi: 10.1007/s10439-018-2065-z.
19. *Liu K, Wang N, Wang W, Shi L, Li H, Guo F et al.* A bioinspired high strength three-layer nanofiber vascular graft with structure guided cell growth. *J Mater Chem B*. 2017; 5 (20): 3758–3764. doi: 10.1039/c7tb00465f.
20. *Nemets EA, Surguchenko VA, Belov VYu, Xajrullina AI, Sevastyanov VI.* Porous Tubular Scaffolds for Tissue Engineering Structures of Small Diameter Blood Vessels. *Inorganic Materials: Applied Research.* 2023; 14: 400–407. doi: 10.1134/S2075113323020338.
21. Izdeliya meditsinskie. Otsenka biologicheskogo deystviya meditsinskikh izdeliy. Chast' 5. Issledovanie na tsitotoksichnost': metody *in vitro*: GOST ISO 10993-5-2023. M.: Rossiyskiy institut standartizatsii, 2023.
22. *Blache U, Guerrero J, Güven S, Klar AS, Scherberich A.* Microvascular networks and models: *in vitro* formation. *W. Holnthoner, A. Banfi, J. Kirkpatrick, H. Redleds*. Vascularization for tissue engineering and regenerative medicine. Reference series in biomedical engineering. Springer, Cham. 2021: 345–383. doi: 10.1007/978-3-319-54586-8.
23. *Grigoriev AM, Basok YuB, Kirillova AD, Surguchenko VA, Shmerko NP, Kulakova VK et al*. Cryogenically structured gelatin-based hydrogel as a resorbable macroporous matrix for biomedical technologies. *Russian Journal of Transplantology and Artificial Organs*. 2022; 24 (2): 83–93. doi: 10.15825/1995-1191-2022-2-83-93.
24. *Rampersad SN.* Multiple applications of alamar blue as an indicator of metabolic function and cellular health in cell viability bioassays. *Sensors*. 2012; 12: 12347–12360. doi: 10.3390/s120912347.
25. *Wang Z, Liu S, Guidoin R, Kodama M.* Polyurethane vascular grafts with thorough porosity: does an internal or an external membrane wrapping improve their *in vivo* blood compatibility and biofunctionality? *Artif Cells Blood Substit Immobil Biotechnol*. 2004; 32 (3): 463–484. doi: 10.1081/bio-200027524.
26. *Tara S, Kurobe H, Rocco KA, Maxfield MW*, *Best CA, Yi T et al.* Well-organized neointima of large-pore poly(L-lactic acid) vascular graft coated with poly(L-lactic-co-ε-caprolactone) prevents calcific deposition compared to small-pore electrospun poly(L-lactic acid) graft in a mouse aortic implantation model. *Atherosclerosis*. 2014; 237 (2): 684–691. doi: 10.1016/j.atherosclerosis.2014.09.030.

The article was submitted to the journal on 29.03.2024

INSTRUCTIONS TO AUTHORS

Articles should contain original information that has not been previously published and is not considered for publication in other editions. Fee for publication of manuscripts will not be charged.

The manuscript should be presented in Microsoft Word format A4, 1.5 spacing, and Times New Roman font size 12. Submit your article to the online submission system in accordance with the instructions on the journal's website https://journal.transpl.ru.

Structure of the article

The Title page should include:

- Initials (first name and patronymic) of the authors of the article should be specified before their respective last names.
- Author names (list the author's initials before listing his or her last name as when registering for ORCID, or Open Researcher and Contributor ID – a non-proprietary alphanumeric code that uniquely identifies scientific authors).
- Full official name of the institution, city and country.
- If authors from different institutions participated in writing of the manuscript, it is necessary to correlate those with the names of the authors by adding a digital index uppercase after last name, and right before the name of the institution.

Information about the authors

For each author fully specify the last and the first name, patronymic and position in the relevant department/institution.

For correspondence

Fully specify the last and the first name, patronymic of the author, who will be holding correspondence, address (including postal code), telephone, fax number, e-mail.

Abstract

Each article must be accompanied by an abstract. The amount of text for the abstract of the original article should be of no more than 300 words, for a literature review, clinical observation – no more than 200 words. The abstract must fully comply with the content of the work. The abstract should not use abbreviations without prior expansion.

Abstract of ***the original article*** should contain the following sections: ***Objective***, ***Materials and methods***, ***Results***, ***Conclusion***. The abstract should present the most important results of the research.

Do not write: "*A comparative analysis of the sensitivity and specificity was conducted …*"

Should write: "*The sensitivity was ... % and ...%, p = , specificity, respectively ...% and ...%, p =* ".

Keywords

At the end of the abstract keywords must be given. To select the keywords a thesaurus of U.S. National Library of Medicine should be used – Medical Subject Headings (MeSH) at http://www.ncbi.nlm.nih.gov/mesh.

Conflict of interest

The author should inform the editor about the factual or potential conflict of interest have included the information about such conflict into the respective section of an article.

If there is no conflict of interest, the author should say so in the form like the following: "Author declares unawareness of the conflict of interest".

This information is supposed to be placed before the article text.

Text of article

Original article should include the following sections:

- Introduction
- Materials and methods
- Results
- Discussion
- Conclusion
- References

Review article should include an analysis of the literature with the presentation of modern sources (mainly in the last 5 years).

Clinical observation should be well illustrated (to reflect the essence of the problem) and include discussion with the use of literature data.

References in the text are indicated by number in square brackets: [1], [2, 5], [14–18] and ***in the references section are presented in order of their appearance in the text.*** All values given in the article should be expressed or duplicated in **SI** units.

References

The author is solely responsible for the accuracy of the data included in the references section of the article. References to unpublished papers or papers in print works are not allowed.

References are presented on a separate page.

The names of journals can be contracted in accordance with an embodiment of reduction adopted by the specific journal.

If the article quoted has DOI (a digital object identifier) or/and PMID (Pub Med identifier) they must be specified after the description of the article. To compile descriptions in References section NLM bibliographic reference citation standard is used – U.S. National Library of Medicine (http://www.nlm.nih.gov/bsd/uniform_requirements.html). If the number of authors does not exceed 6, the bibliographic description includes all the authors. If the number of authors is more, only the first six authors should be indicated and then add et al.

Requirements for tables and figures

Tables should be placed into the text; they should have numbered heading and clearly labeled graphs, convenient and simple to read. Table's data must comply with the numbers in the text, but should not duplicate the information therein. Table references in the text are required.

Illustrations and drawings should be submitted in electronic format (JPEG or TIFF format with a resolution of at least 300 dpi and no smaller than 6 × 9 cm), in a volume of close to 1 MB. Drawings must include all copyright symbols – arrows, numbers, signs, etc. Figure captions should be submitted in a separate file with the extension *.doc. First, the name is given, then all arithmetic and alphabetical symbols (lettering) are explained.

Articles should be addressed
to the Russian Journal of Transplantology and Artificial Organs website:
https://journal.transpl.ru/vtio
E-mail: vestniktranspl@gmail.com

Издание зарегистрировано в Госкомпечати РФ, № 018616 от 23.03.99 г.

Подписано к печати 21.06.24.

Тираж 1000 экз.

ООО «Издательство «Триада».
ИД № 06059 от 16.10.01 г.
170034, г. Тверь, пр. Чайковского, 9, оф. 514,
тел.: +7 (915) 730-10-37, +7 (910) 647-49-85
E-mail: triadatver@yandex.ru
http://www.triada.tver.ru

Заказ 25211